Sedimentology of Narji Limestone in the Neoproterozoic Kurnool Group of rocks, Cuddapah Basin, India

THESIS SUBMITTED FOR THE DEGREE OF
DOCTOR OF PHILOSOPHY (SCIENCE),
JADAVPUR UNIVERSITY

ADRIKA ROY
INDEX NO- 86/16/ Geol.Sc./24

DEPARTMENT OF GEOLOGICAL SCIENCES
JADAVPUR UNIVERSITY
KOLKATA – 700032, INDIA

2023

CERTIFICATE FROM THE SUPERVISOR(S)

This is to certify that the thesis entitled **"Sedimentology of Narji Limestone in the Neoproterozoic Kurnool Group of rocks, Cuddapah Basin, India"** submitted by **Smt. Adrika Roy** who got her name registered on 04.05.2016 for the award of **Ph.D. (Science) degree** of **Jadavpur University**, is absolutely based upon her own work under the supervision of **Dr. Debasish Shome (Retd.), Dr. Gopal Chakrabarti and Dr. Soumik Mukhopadhyay** and that neither this thesis nor any part of it has been submitted for either any degree/diploma or any other academic award anywhere before.

Debasish Shome 24.1.23

DR. DEBASISH SHOME
Professor (Retd.)
Dept. of Geological Sciences
Jadavpur University, Kolkata-700 032

24.1.23

DR. GOPAL CHAKRABARTI, WBES
Joint Director of Public Instruction
Scholarship and Stipend
Government of West Bengal

24/1/23

Soumik Mukhopadhyay
Associate Professor
Department of Geological Sciences
Jadavpur University
Kolkata-700032,W.B.

(Signature of the Supervisor(s) date with office seal)

DEDICATED

TO MY

GRANDPARENTS

Geologists have a saying rock remember.

-Neil Armstrong

ACKNOWLEDGEMENTS

Firstly, I am deeply thankful to my supervisors Prof. (Retd.) Debasish Shome, Department of Geological Sciences, Jadavpur University and Dr. Gopal Chakrabarti, Associate Professor of Geology, WBES (officiating as Joint Director of Public Instruction (S&S), Education Directorate, Govt. of West Bengal) and Dr. Soumik Mukhopadhyay, Department of Geological Sciences, Jadavpur University for their tireless academic and mental support during my Ph.D. study and related research works. I would like to thank UGC (University Grant Commission) of Govt. of India and State Govt. for providing the financial support vide UGC Non-Net and State Fellowship scheme. I would also like to thank Department of Science and Technology (DST), Govt. of India for the grant to do the chemical analysis vide PURSE (Phase-II) program (No. F4/SC/20/15). I would like to express my gratefulness to Dr. C. Manikyamba, Senior Principal Scientist, NGRI and Mr. Arijit Pahari, Research Scholar, NGRI for their assistance during the sample analysis days in NGRI. Sincere thanks to all the reviewers for their constructive comments during the review of my research articles related with the Ph.D. work. I am also grateful to the head of the department along with all the faculty members of the department as well as the non-teaching staffs of department of Geological Sciences, Jadavpur University and to my fellow lab mates for their continuous support. I would like to extend a big thank to Mr. Shekar and Mr. Shaik Masum Basha for their unconditional assistance during my field days. Lastly, I would like to thank my parents, for their support, love and blessings. Without their support this thesis would not have been possible.

ABSTRACT

The sedimentological and geochemical study on carbonate-dominated Narji Formation of the Kurnool Group belonging to the crescent-shaped, westwardly convex epicratonic Proterozoic Cuddapah Basin, India is based on three chosen sections (Section-A :15°18′ 45.00″ N, 78°07′ 35.76″ E; Section- B:15°25′18.49″ N, 78°05′6.20″ E; Section-C:15°27′36.68″ N, 78°08′34.30″ E) from northern part of the exposed outcrops of the aforesaid formation. Since there is little available geochronological data on this formation, it may be inferred from other evidence that the age of Narji Formation is early Neoproterozoic. The studied area is mapped, logged and sampled systematically. Measured sections provide crucial information on the spatial and vertical variation of lithofacies. Carbonate samples collected from section (A) (15°18′ 45.00″ N, 78°07′ 35.76″ E) of Patapadu-Yaganti hills are used for geochemical analysis (Major, Trace and REE analysis). Within the major oxides, a wide range of CaO (31.45 to 72.03 wt.%) and SiO2 (14.27 to 45.92 wt%) is recorded. Relatively higher concentration of SiO_2 within limestones suggests clastic input**.** PAAS normalized REE + Y pattern shows seawater like REE + Y pattern (depleted LREE and enriched to flat HREE) with negative Eu anomaly. The Er/Nd ratio varies from 0.06 to 0.22 with an average 0.17 and this points terrigenous input within the limestones. The Y/Ho ratios vary in between 30.05 and 45.45, and this also suggests that the limestones were deposited in a marine environment but due to the terrigenous input or contamination, the Y/Ho ratio is slightly decreased. Positive Ce anomaly, high U/Th (> 1.25), and V/ (V + Ni) (>0.5) ratios of Narji limestones clearly indicate that their deposition was in a suboxic to anoxic condition. A total number of six facies arranged into 2 facies associations like intertidal and subtidal are deposited in a carbonate dominated platform over the Banganapalle

Quartzite. Intertidal facies association consisting of laminated limestone and heterolithic facies is considered as the shallowest facies association. The facies which developed within the subtidal facies association are Quartzite-bearing massive purple limestone facies, Calcareous shale facies, Massive whitish grey limestone facies, Intra-formational conglomerate facies and all these point to the deposition of Narji Formation lithology in a subtidal-intertidal carbonate dominated platform with suboxic to anoxic condition. Most of the coeval successions of Narji Formation rocks throughout the globe also indicate a similar type of depositional pattern during this time interval (early Neoproterozoic) especially during the breaking and amalgamation of Rodinia.

Table of Contents

1. CHAPTER-1: INTRODUCTION

1.1	INTRODUCTION	1
1.2	PROTEROZOIC SEDIMENTARY BASINS OF INDIA	2
1.3	INTRODUCING THE CUDDAPAH BASIN	2
1.4	INTRODUCING THE KURNOOL SUB-BASIN WITHIN CUDDAPAH BASIN	10
1.5	PREVIOUS WORK	13
1.6	PRESENT STATUS IN RESPECT OF SEDIMENTOLOGY OF KURNOOL SUB-BASIN	19
1.7	PRESENT STATUS IN RESPECT OF GEOCHEMISTRY OF KURNOOL SUB-BASIN	22
1.8	AGE OF KURNOOL GROUP OF ROCKS; PARTICULARLY OF NARJI LIMESTONE	24
1.9	STATEMENT OF THE PROBLEM	26
1.10	STUDY AREA	29
1.11	METHODOLOGY	30
1.8	FIGURES AND TABLES	33

2. CHAPTER-2: GEOLOGICAL SETTINGS AND STRATIGRAPHY

2.1	REGIONAL GEOLOGY AND STRATIGRAPHY	47
2.2	BASEMENT ROCKS	53
2.3	LITHOLOGICAL DESCRIPTION	54
2.3.1	ARENITES	54
2.3.2	ARGILLITES	55
2.3.3	CARBONATES	55

2.4	GEOLOGY AND STRATIGRAPHIC SEQUENCE OF THE STUDY AREA	56
2.5	MAFIC IGNEOUS ACTIVITY AFFECTING THE CUDDAPAH	57
2.6	MAFIC DYKE SWARMS	61
2.7	STRUCTURAL SETTING	62
2.8	GEOCHRONOLOGICAL CONSTRAINTS ON STRATIGRAPHIC DEVELOPMENT	65
2.9	FIGURES AND TABLES	68

3. CHAPTER-3: FACIES ANALYSIS

3.1	INTRODUCTION	78
3.2	FACIES ANALYSIS	78
3.3	KARST FEATURES IN THE NARJI LIMESTONE	84
3.4	DEPOSITIONAL ENVIRONMENTS AND PLATFORM DEVELOPMENT	84
3.5	FIGURES AND TABLES	90

4. CHAPTER-4: PRESSURE SOLUTION STRUCTURE- STYLOLITE

4.1	INTRODUCTION	100
4.2	ORIGIN OF MICROSTYLOLITES	101
4.3	OCCURRENCE OF STYLOLITE	103
4.4	CLASSIFICATION OF MACROSTYLOLITE	104
4.5	CLASSIFICATION OF MICROSTYLOLITES	107
4.6	MICROSTYLOLITE AND HOST ROCK RELATIONSHIP	110
4.7	FIGURES AND TABLES	111

5. CHAPTER-5: GEOCHEMISTRY OF CARBONATES

5.1	INTRODUCTION	123
5.2	PETROGRAPHY OF THE NARJI LIMESTONE	123
5.3	GEOCHEMISTRY OF THE NARJI LIMESTONE	125
5.3.1	RESULTS	125
5.3.1.1	MAJOR OXIDES	125
5.3.1.2	TRACE ELEMENTS	126
5.3.1.3	RARE EARTH ELEMENTS	127
5.4	DISCUSSION	128
5.4.1	SOURCE OF REE	128
5.4.2	BEHAVIOUR OF EUROPIUM	129
5.4.3	Y/HO RATIO AND SEAWATER CHEMISTRY	130
5.4.4	CE ANOMALY–REFLECTION ON PALEO REDOX CONDITION	130
5.4.5	ELEMENTAL RATIOS IN NARJI LIMESTONES–REFLECTION ON PALE REDOX CONDITION	131
5.5	CONCLUSION	132
5.6	FIGURES AND TABLES	133

6. INTERGRATION

6.1	INTRODUCTION	148
6.2	CLUES FROM FACIES ANALYSIS	148
6.3	CLUES FROM STYLOLITE	149
6.4	CLUES FROM PETROGRAPHIC ANALYSIS	150

6.5	CLUES FROM GEOCHEMICAL ANALYSIS	151
6.6	DISCUSSION	152
6.6.1	EVOLUTION OF KURNOOL SUB-BASIN DURING THE DEPOSITION OF THE NARJI FORMATION LITHOLOGY	152
6.6.2	COMPARISON OF NARJI FORMATION WITH OTHER COEVAL SUCCESSIONS	153
6.7	CONCLUSION	155

7.BIBLIOGRAPHY

	REFERENCES	157

8.SUPPLEMENTARY MATERIALS

9.PHOTO GALLERY

10. PUBLICATIONS

10.1	Geochemistry of the Neoproterozoic Narji limestone, Cuddapah Basin, Andhra Pradesh, India: implication on paleoenvironment	
10.2	Neoproterozoic sedimentation and depositional environment: an example from Narji Formation, Cuddapah Basin, India	
10.3	Study of Micro-Stylolite based on Geometry and Bedding Relationship Pattern in Neoproterozoic Narji Limestone from Betamcherla – Banganapalle Area of Kurnool Sub-Basin, Andhra Pradesh, South India	

List of Figures

1. CHAPTER-1: INTRODUCTION

1.1	Generalized geological map of Peninsular India showing the major cratons and various dyke swarms intruding those cratons (modified after **Meert et al., 2011**). CITZ- Central Indian tectonic zone, NS- Narmada-Son lineament, GR- Godavari rift, C- Cuddapah Basin, V- Vindhyan Basin, Ch- Chhattisgarh Basin	34
1.2	Generalized tectonic map of the Indian subcontinent including Purana basins, cratonic regions and fold belts (modified after **Meert and Pandit, 2015**). VB- Vindhyan Basin, PG- Prahnita-Godavari Basin, ChB- Chhattisgarh Basin, CuB- Cuddapah Basin, KBB- Kaladgi-Bhima Basin, MB- Marwar Basin, IB- Indravati Basin, EDD- Eastern Dharwar Craton, WDD- Western Dharwar Craton, MR- Mahandi Rift, R- Rajmahal trap, CG-Closepet Granite, SIB- South Indian Block, NIB-North Indian Block, AFB- Aravalli Fold Belt, DFB- Delhi Fold Belt, EGMB- Eastern Ghat Mobile Belt, SMB- Satpura Mobile Belt, NSL- Normada-Son lineament, CIS- Central Indian Suture, PCSZ- Palghat-Cauvery Shear Zone	35
1.3	Illustrations showing the processes of amalgamation and breakup of Rodinia (modified after Li et al. 2008; Li 2011) (a) ca. 1100 Ma; (b) ca. 825 Ma; (c) ca. 750 Ma; (d) ca. 440 Ma.	36
1.4	Inferred Cuddapah Basin Limits. The great similarities for the crescent shaped boundaries of all the Formations of Cuddapah Basin have resulted from a land-locked condition of the basins with a probable connection to the open sea in the North East (after **Murthy, 1981**)	37
1.5	(a) Impending collision between two continents; (b) Postulated geometry produced by collision;	38

	and (c) Theoretical Bouguer anomaly calculated for such crustal structure (modified after **Singh and Mishra, 2002**)	
1.6	Configuration of an Archaean–Paleoproterozoic supercontinent "SIWA", with the Napier Complex located at the position of the Cuddapah basin of India and the Yilgarn craton at the eastern coast of India. Representative basic dykes of the Napier Complex, South India (SI), and the Western Australia (WA) are shown by red colour. Arrows marked as $N_{Yilarn,}$ N_{Napier} and $N_{Dharwar}$ are north directions for ~2400 Ma for the Yilgarn craton, the Napier complex and the Dharwar craton, respectively (modified after **Mohanty, 2011**)	39
1.7	Panel diagrams showing geodynamic evolution of the Cuddapah basin. Stage (a): Opening of Papaghni sub-basin as a back arc basin at ~2 Ga, as a result of westerly directed subduction along eastern Indian continental margin. The newly opened basin received detritus from Dharwar craton during the initial stage of Gulcheru sedimentation and during later stages (Vempalle Formation and Chitravati Group) received detritus and dissolved load also from a magmatic arc situated southeast of depositional basins. Stage (b): Extinction of magmatic arc and change of subduction polarity at ~1.85 92 Ga, possibly because of plume activity. Sedimentation in Papaghni sub-basin probably ceased after this episode. Stage (c): The intervening oceanic plates are consumed and possibly Napier block of Antarctica collided with eastern Dharwar craton at ~1.6 Ga, giving rise to Krishna orogeny (The Cuddapah basin evolved as a foreland basin and post-Papaghni sedimentation received detritus mainly from the evolved orogen (modified after **Absar et al., 2016**)	40
1.8	Simplified geological map of the Cuddapah Basin (modified after **Saha and Tripathy, 2012**). Western margin of the basin is convex and developed over the Eastern Dharwar; whereas the	41

	eastern margin is concave and has a contact with Nellore schist belt and Eastern Ghat Belt	
1.9	Palaeogeographical cartoons interpreting the tectonic situation of the three main stages of basin formation. Initially, the Cuddapah Basin formed as a Paleoproterozoic rift-passive margin on the edge of the Eastern Dharwar Craton **(Collins et al 2015**). By the end of the Paleoproterozoic, the Ongole Domain (and Ender by Land in Antarctica) collided with the passive margin, whence it evolved into a foreland basin in front of the resulting Krishna Orogen. After a period of erosion, the latest Mesoproterozoic to Neoproterozoic Kurnool Group reflects small-scale tectonic movements' craton ward of the Tonian Eastern Ghats Orogen and erosion of the Eastern Dharwar Craton.	42
1.10	Geological maps of the study area (a) Generalized geological map of the Cuddapah Basin (modified after Geological survey of India 1:2 million scale map, 1998); (b) Detail of the north-western Cuddapah Basin showing locations of the measured sections investigated in this study (modified after Survey of India Quadrangle map number 57E, 1:250000 scale	43

2. CHAPTER-2: GEOLOGICAL SETTINGS AND STRATIGRAPHY

2.1a	Lithostratigraphy of the Papaghni and Chitravati groups, Cuddapah Basin. MDA- maximum depositional age (after **Kumar et al., 2015**)	69
2.1b	Lithostratigraphy of the Srisailam and Kurnool groups, Cuddapah Basin. MDA- maximum depositional age (after **S. Patranabis-deb et al., 2012**)	70

2.2	Geological map of the Cuddapah Basin (modified after **Nagaraja Rao and Ramalingaswamy, 1976**)	71
2.3	The Paleo-Mesoproterozoic dyke swarms and rifts within the Indian Craton. NIB-North Indian Block, SIB- south Indian Block, CTZ- Central tectonic zone, C- Cuddapah Basin, G- Godavari Basin, S- Singhbhum Basin, c- Dykes around Cuddapah Basin, D- Dharmapuri dykes, T-Tiruvannamalai dykes, NK- North Kerala dykes, SK- South Kerala dykes (after **Hou et al., 2008**)	72
2.4	Detailed geology of the Dharwar craton and the Cuddapah basin, showing truncation of mafic dykes and lineaments along the boundary of the Dharwar craton and the Cuddapah basin (after **Mohanty, 2011**)	73
2.5	Tectonic map of Cuddapah Basin showing overall structural pattern on either side of Rudravaram line (after **Meijerink et al., 1984**)	74
2.6	Geological map of the Cudddaph Basin showing the sub-basins, boundary thrusts of the Nallamalai Fold Belt (NFB) and Nellore Schist Belt (NSB). The Udaygiri and Vinjamuru groups represent two distinct domains within the NSB. In the western part of the basin the lower Cuddapah rock groups (Papaghni and Chitravati Groups), the younger Kurnool Group, and the Srisailam Formation are outcropped. The Palnad subbasin is in the northeastern part. Gani–Kalva Fault (GKF), Atmakur Fault (AF) and Kona Fault (KF) are the main transverse faults within Cuddapah Basins (after **Saha and Patranabish-Deb, 2014**)	75

3. CHAPTER-3: FACIES ANALYSIS

3.1	Litholog of the studied sections from Narji Formation, Cuddapah Basin, India	91
3.2	Field photograph of comparatively coarse-grained Quartzite-bearing massive purple limestone (N1) (15°18’45.00’’N, 78°07’35.76’’E), recorded from the Patapadu section Cuddapah Basin, India. Scale: Diameter of the coin- 2.40 cm	92
3.3	Field photograph of coarse-grained Quartzite-bearing massive purple limestone facies (N1) (15°18’45.00’’N, 78°07’35.76’’E), with bifurcating Symmetrical ripple mark (R.I. = 5–8) in plan view and recorded from Kottala section, Cuddapah Basin, India. Length of the diagonal scale- 15.20 cm	92
3.4	Field photograph of straight to wavy laminated limestone facies (N2) characterized by irregularly undulated layers, recorded from Betamcherla section, Cuddapah Basin, India. Scale: Diameter of the coin- 2.70 cm.	93
3.5	Field photograph of lamination of dark grey and light streaks of clay within laminated limestone facies (N2) (15°18’45.00’’N, 78°07’35.76’’E). Note the elephant skin weathering structure, recorded at the top surface in the Betamcherla section, Cuddapah Basin, India. Scale: Length of the hammer- 31.80 cm	93
3.6	Field photograph of calcareous shale facies (N3) with well-defined fissility plane, recorded within the lowermost part of Patapadu Section, Narji Formation Patapadu section, Cuddapah Basin, India. Scale: Length of the hammer- 31.80 cm	94
3.7	Field photograph of clay and mud layer within heterolithic facies (N4), recorded in the Patapadu Section Cuddapah Basin, India. Note the discontinuous value of lamination and also	94

	intermixing of clay and mud with distortion. Scale: Length of the hammer- 31.80 cm	
3.8	Field photograph of top surface of the heterolithic facies(N4) from Patapadu section, Cuddapah Basin, India. Note the intermixing of clay and mud. Scale: Length of the hammer- 31.80 cm	95
3.9	Field photograph of Massive white grey limestone(N5) (15°18’45.00’’N, 78°07’35.76’’E) showing macro stylolite and iron leaching from Patapadu section, Cuddapah Basin, India. Scale: Length of the hammer- 31.80 cm	95
3.10	Field photograph of occurrence of lenticular type chert nodules and bands of chert within massive limestone facies(N5), recorded from Betamcherla Section, Cuddapah Basin, India. Scale: Diameter of the coin- 2.70 cm	96
3.11	Field photograph of Intraformational conglomerate facies(N6). Note the tabular and sub rounded micritic clasts within poorly sorted siliceous matrix, recorded from Patapadu Section, Cuddapah Basin, India. Length of the diagonal scale- 15.20 cm	96
3.12	Paleoenvironmental reconstruction of the Neoproterozoic Narji Formation carbonate platform showing the distribution of facies	97

4. CHAPTER-4: PRESSURE SOLUTION STRUCTURE- STYLOLITE

4.1	Photomicrograph showing inclined microstylolite of massive limestone facies of Patapadu Section, Cuddapah Basin, India. Note also branching of microstylolite	112
4.2	Photomicrograph showing dolomite grains along stylolite, recorded from Patapadu Section, Cuddapah Basin, India	112

4.3	Photomicrograph showing micro fault cross cutting the stylolite, from Patapadu Section, Cuddapah Basin, India.	113
4.4	Macro stylolite– (Simple wavy type) noticed in Narji Limestone recorded from from Patapadu Section, Cuddapah Basin, India. Length of the hammer- 31.80 cm	113
4.5	Macro stylolite – Suture type stylolite structure noticed in Narji Limestone from Patapadu Section, Cuddapah Basin. Scale: Length of the diagonal scale- 15.20 cm	114
4.6	Macro stylolite– Undulatory type stylolite structure noticed in Narji Limestone from Patapadu Section, Cuddapah Basin. Scale: Length of the hammer- 31.80 cm	114
4.7	Photomicrograph showing small and gentle undulatory type micro stylolite from Patapadu Section, Cuddapah Basin.	115
4.8	Photomicrograph showing simple isolated micro stylolite with large sparite grains from Patapadu Section, Cuddapah Basin.	115
4.9	Photomicrograph showing smooth crest and trough micro stylolite from from Betamcherla Section, Cuddapah Basin	116
4.10	Photomicrograph showing stylolite running bedding parallel, irregular and anastomosing across the laminated limestone unit near Betamcherla area, Narji Formation, Cuddapah Basin, Andhra Pradesh from Betamcherla Section, Cuddapah Basin.	116
4.11	Photomicrograph showing simple suture type resembling like ammonoid suture pattern from Patapadu Section, Cuddapah Basin.	117

4.12	Photomicrograph showing horizontal micro stylolite developed parallel to bedding plane from Patapadu Section, Cuddapah Basin.	117
4.13	Photomicrograph showing microstylolite formed perpendicular to the bedding from Patapadu Section, Cuddapah Basin.	118
4.14	Photomicrograph of inclined microstylolite within a micrite dominant matrix from Patapadu Section, Cuddapah Basin	118
4.15	Photomicrograph of micro stylolite with inclined branching from Patapadu Section, Cuddapah Basin.	119
4.16	Photomicrograph of Vertical-Horizontal cross cutting type micro stylolite from Patapadu Section, Cuddapah Basin.	119
4.17	Photomicrograph of interconnecting network type stylolite from Kottala Section, Cuddapah Basin.	120

5. CHAPTER-5: GEOCHEMISTRY OF CARBONATES

5.1	Field photograph of sinuous crested ripple resembling like tuning fork within quartzite bearing massive limestone (15°18’45.00’’N, 78°07’35.76’’E) from Cuddapah Basin. (Length of diagonal scale- 15.20 cm)	134
5.2	Photomicrograph of patchy distribution of quartzite within micrite dominated limestone in quartzite bearing massive limestone facies (15°18’45.00’’N, 78°07’35.76’’E) from Cuddapah Basin, India.	134
5.3	Photomicrograph of calcite cementation in the pore spaces in between the quartz grains (15°18’45.00’’N, 78°07’35.76’’E) from Cuddapah Basin	135
5.4	Photograph of massive whitish limestone of Narji Formation. (Length of the hammer- 31.80	135

	cm) (15°18’45.00’’N, 78°07’35.76’’E) from Cuddapah Basin	
5.5	Photomicrograph of different types of stylolites within massive whitish limestone (15°18’45.00’’N, 78°07’35.76’’E) from Cuddapah Basin	136
5.6	Photomicrograph of scattered crystals of pyrite within limestone, the margins of the pyrite are surrounded by sparite that probably formed as a residue after the replacement of pyrite by calcite, (15°18’45.00’’N, 78°07’35.76’’E) from Cuddapah Basin	136
5.7	Photograph of straight and wavy laminated limestone characterized by irregular undulated layers (15°18’45.00’’N, 78°07’35.76’’E) from Cuddapah Basin**. (**Length of the hammer- 31.80 cm**)**	137
5.8	Photomicrograph of dark streaks of clay within limestone interlaminated with light coloured coarse sparite crystal (15°18’45.00’’N, 78°07’35.76’’E) from Cuddapah Basin	137
5.9	Photomicrograph of lowermost part of the calcareous shale facies (15°18’45.00’’N, 78°07’35.76’’E) from Cuddapah Basin. Note green colour glauconite sand. Most glauconite grains within the micritic matrix are replaced by Fe-calcite.	138
5.10	Bivariate plots of SiO_2, TiO_2, Al_2O_3, against CaO, and TiO_2, Al_2O_3, MgO, Fe_2O_3, against SiO_2 in Narji limestones	139
5.11	Distribution of PAAS normalized trace elements of Narji limestones. PAAS value is defined from **Taylor and McLennan,1985**	140
5.12	Distribution of PAAS normalized REE+Y patterns of Narji limestones. PAAS value is defined from **Taylor and McLennan, 1985**	140
5.13	Litholog of the measured stratigraphic section with the positions of the limestone samples collection. Er/Nd, Y/Ho and U/Th ratios of the	141

	Narji limestones are also plotted, showing their vertical variations within the studied section	
5.14	Bivariate plots of major oxide (%) and trace elements (in ppm) of Narji limestones against ∑REE	142

List of Tables

1. CHAPTER-1: INTRODUCTION

1.1	Detailed stratigraphy of the Cuddapah Basin (modified after **Saha and Patranabis-Deb, 2014)**	44
1.2	A brief summary on the ages of different Formations from Kurnool Group	45

2. CHAPTER-2: GEOLOGICAL SETTINGS AND STRATIGRAPHY

2.1	Lithostratigraphic classification of Kadapah Formation (Cuddapah Supergroup) (Proposed by **King, 1872**)	76
2.2	Stratigraphy of the Cuddapah Basin (Proposed by **Rao et al., 1987**).	77

3. CHAPTER-3: FACIES ANALYSIS

3.1	Summarized table of the facies recognized in the studied sections of the Narji Formation, Kurnool Basin, India	98
3.2	Summarized table of the facies associations with their constituent facies and depositional	99

	environment, recognized in the studied sections of the Narji Formation, Kurnool Basin, India	

4. CHAPTER-4: PRESSURE SOLUTION STRUCTURE- STYLOLITE

4.1	Classification of macrostylolite recorded in Narji Formation	121
4.2	Classification of microstylolite recorded in Narji Formation	122

5. CHAPTER-5: GEOCHEMISTRY OF CARBONATES

5.1	Lithology of the geochemically analyzed Narji Limestone samples	143
5.2	Major oxides (wt. %) content in the Narji limestones, Cuddapah Basin with the average value of PAAS **(Taylor and McLennan, 1985)**	144
5.3	Trace elements (in ppm) concentrations in the Narji limestones, Cuddapah Basin with the average value of PAAS **(Taylor and McLennan, 1985)** and obtained values for the standard, JLS-1.	145
5.4	REE concentration (in ppm) in the studied Narji limestones, Cuddapah Basin with the average value of PAAS (**Taylor and McLennan, 1985**) and obtained values for the standard, JLS-1.	146
5.5	Elemental ratios and anomalies of the studied Narji limestones. $Ce/Ce^* = Ce_{SN}/ (La_{SN} \times Pr_{SN})^{0.5}$; $Eu/Eu^* = Eu_{SN}/ (Sm_{SN} \times Gd_{SN})^{0.5}$; $Pr/Pr^* = [Pr/ (0.5Ce + 0.5Nd)]_{SN}$	147
5.6	Average geochemical values of the Narji Limestones compared to the other Proterozoic carbonate rocks of India showing seawater like REE patterns	147

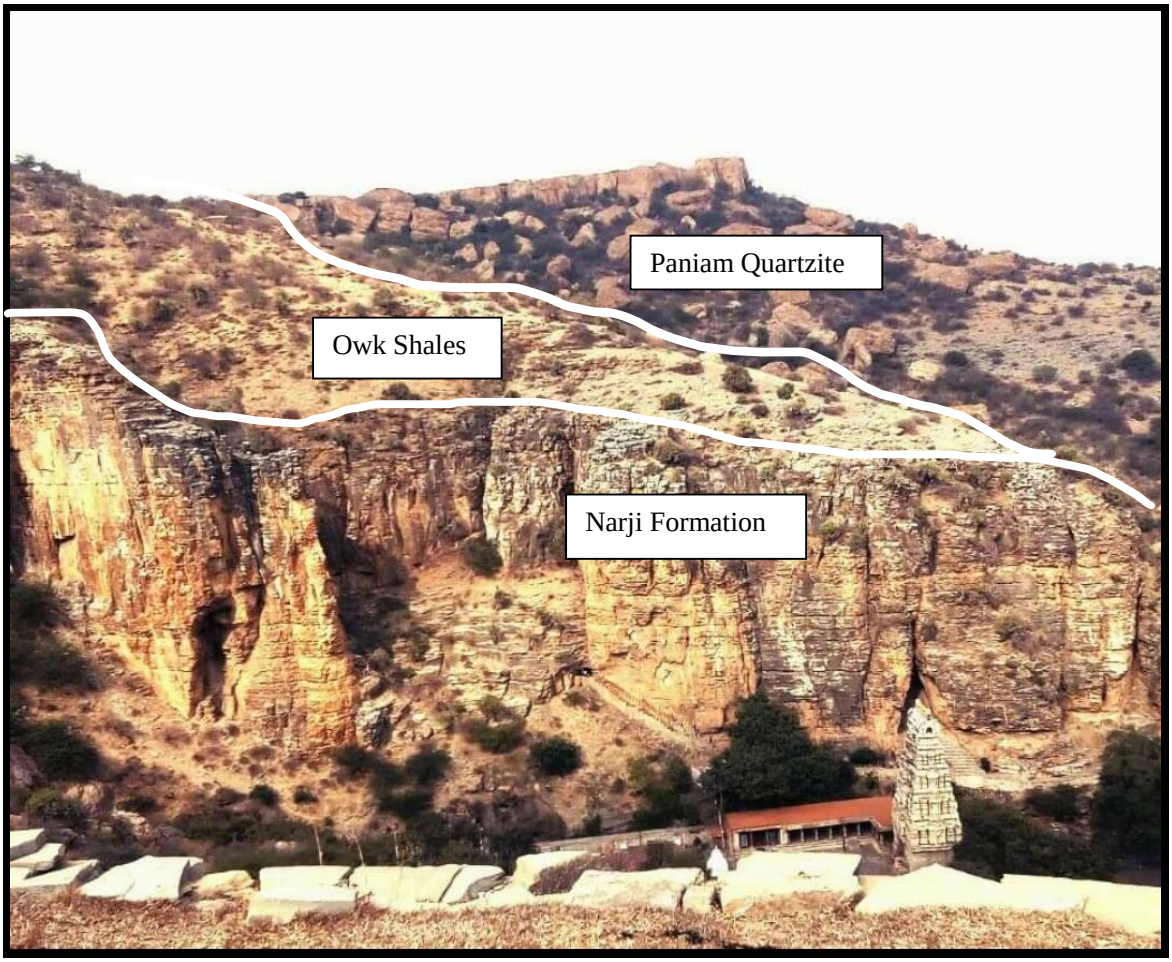

Panoramic view of Narji Formation of Cuddapah Basin, Andhra Pradesh, India. A field photograph where the Narji Formation grades upward into the Owk Shales then Paniam Quartzite. The photograph has been captured near about the Patapadu-Yagantipalle road cut section of Andhra Pradesh, India.

CHAPTER-1
INTRODUCTION

1.1 INTRODUCTION

The Indian subcontinent covering approximately 5,000,000 km^2 make up a distinct lithospheric plate with Himalayan Sectors **(Meert et al, 2010).** About~3.0 billion years of geological history of Peninsular India includes the constituent the Archean Cratonic Nuclei **(**ACN), their bordering orogenic belt, intrusive and extrusive cover and the sedimentary basins. The ACN that collectively form Peninsular India contains Aravalli -Bundelkhand craton, Singhbhum and the Baster craton, the Western and the Eastern Dharwar craton **(**WDC and EDC) and the Southern Granulitic Province **(Fig 1.1**). Each craton experiences the progressive stabilisation of the block with intrusive events including mafic dyke swarms and initiation and gradual filling of the Proterozoic sedimentary basin developed within the cratons. Mafic dyke points to the central extension process and can represent supercontinent assembly and/or dispersal, subduction, large igneous province emplacement, and crust mantle interaction.

The Dharwar Craton is an Archean continental fragment with a continuously- exposed crustal section from low grade gneisses and greenstone basins in the north to the granulite in the south. At the surface, the craton is divided into the Western Dharwar Craton **(**WDC) and the Eastern Dharwar Craton **(**EDC) by the 2.5 Ga Clospet granite. The central part of the WDC hosts 3.4 Ga greenstone belt while the northern part constituents the 2.6 Ga Dharwar Basins **(Taylor et al, 1984**).

The EDC crusts **consists** largely consists of granitoid rocks, all the juvenile additions to the continental crusts from 2.6-2.5 Ga. To the east the EDC, is wrapped by the Proterozoic Cuddapah Basin **(**CB) and the Eastern Ghat granulite terrain. The northern part of the EDC and the Bastar Craton is separated by the Proterozoic Godavari Graben. The 65 Ma flood basalt province of the Deccan Volcanic Province **(**DVP) covers the NW part of the Dharwar

craton. It is not clear whether of the WDC or EDC form the basement of the flood basalt province.

In this thesis we are presenting sedimentological and geochemical studies from a Proterozoic sedimentary basin on the Eastern Dharwar craton from the Peninsular India located in the Indian subcontinent.

1.2 PROTEROZOIC SEDIMENTARY BASINS OF INDIA

Each of the aforementioned cratonic elements contains Precambrian -Early Palaeozoic sedimentary **(**or metasedimentary) basin fills of the Peninsular India **(Fig 1.2**). Among the best-preserved sedimentary successions are the so called 'Purana' or the ancient basins **(Chakraborty,2000)**. These include the really extensive Cuddapah, Chhattisgarh and Vindhyan basins along with smaller regional basins known as Indravati, Khariar, Pranhita - Godavari, Bhima, Kunigal, Kurnool and Marwar. There appear to be several key intervals of basin developments **(**and closure) within Peninsular India. Purana -I basins began development in the Paleoproterozoic **(**2.5-1.6 Ga); Purana -II basin formed during Mesoproterozoic **(**1.6-1.0 Ga); and the development of the Purana -III basins is confined to the Ediacaran-Cambrian interval. Basin closure and developments may be temporary and may be related to the formation/break-up of the supercontinents Columbia **(Fig1.3**, Purana-I), Rodina **(Fig 1.3**, Purana-II) and Gondwana **(Fig1.3**, Purana-III). The basin closure is may be related to the creation of tectonic barriers of sedimentation, burial by younger **(**and now eroded) sedimentary sequences, sea level changes and many other factors.

1.3 INTRODUCING THE CUDDAPAH BASIN

The Cuddapah Basin in southern India is one of the largest depositaries developed in the mid Proterozoic times. They resemble as the product of crustal extension with red-

coloured, arenaceous –pelitic lithology with local carbonate and volcanic rocks.

The Cuddapah basin is developed in the south –central part of the Peninsular India, and covering an area of 45000 km^2.It has a crescent shape, convex to the west, with the length of 400 km and a maximum width of 145 km **(Nagaraja Rao et al ,1987).** The total thickness of the basin is about 6000km unconformably overlying the peninsular gneiss. Whereas the sediment in the western part of the basin is generally unfolded and dipping towards the center of the basin, the eastern part of the basin in contrast is 50km wide arcuate zone of steeply dipping, isoclinically folded, inverted strata forming the Nallamalai hills. The Cuddapah basin tectonically overlies to the east by an Archean thrust mass, which include the Dharwar type Nellore schist belt. Deep seismic sounding indicates that this thrust and several other small imbrications within this basin are steeply inclined and penetrate to the base of the crust. Crustal shortening associated with the eastern thrust is at least 5km but taken together with the other associated feature it may increase **(Drury et al, 1984**). The Cuddapah may be said that is the remnant of the original depositary that extends to the considerable distance to the east.

Geochronological studies carried out in these intracratonic basins indicate that the deposition may have started nearly 2700 Ma **(**Cuddapah Basin) ago and completed by nearly 750 Ma **(Rasmussen et al, 2002; Ray et al, 2002; Ray et al, 2003; Patranabis-Deb et al, 2007; Malone et al, 2008; Das et al, 2009; Conrad et al, 2011; Saha and Patranabis-Deb, 2014; Collins et al, 2015; Khelen et al, 2020**).

The Cuddapah basin shows a composite structure divided by the three-separate group of deposition, each forming a stratigraphic group **(Meijerink et al, 1984).**

- The Cuddapah **(**2000-1470 Ma)
- The Nallamalai **(**1470-1000 Ma)

- The Kurnool **(**1000-500 Ma)

The lithostratigraphy of the Cuddapah Basin consists of

1. Cuddapah Supergroup
2. Kurnool Group

The Cuddapah exposed in the south-western part of the basin. The Nallamalai in the east north eastern part and the Kurnool in the central-north-western and extreme north western portion. The strata are being deposited in rhythmic transgression separated by tectonic breaks. Each rhythm is characterized by lower sandstone with conglomerate followed upward by clay shales and phyllites, carbonates and local volcanic rocks. Some of the common features are red colours, crossbedding, sun cracks and other shallow water features **(Kinsman,1969).** Dolomites and certain unicellular organism are also found **(Schopf and Prasad, 1978).**

Cuddapah Supergroup consists of Papaghni, Chitravati, Nallamalai Groups, and Srisailam Formation from base to top **(Table 1.1**). Each of the group is interrupted by basin wide unconformities and is composed of clastic **(**argillaceous and arenaceous) as well as non-clastic **(**carbonate) group of rocks, reflects a fining upward succession which further suggests a shallow marine shelfal condition during deposition of the sediments **(Patranabis-Deb et al, 2012; Saha and Tripathy, 2012; Chakrabarti et al, 2014**). The Papaghni Group consists of the Gulcheru, and Vempalle Formation **(Table 1.1**). Similarly, the Chitravati Group is composed of the Pulivendla, Tadpatri, Gandikota Formation, and the Nallamalai Group consists of the Bairenkonda, and Cumbum Formation **(Table 1.1**). The Papaghni, and the Chitravati are considered as the two oldest groups of this basin, mainly exposed in the western part of the basin and are relatively undeformed in nature **(Nagaraja Rao et al, 1987; Saha and Tripathy, 2012**). The Nallamalai Group is exposed in the eastern part of the Cuddapah Basin. Characteristically this Nallamalai Group is highly deformed, thrust

bounded, and unconformable on Chitravati group **(Chaudhuri et al, 2002; Saha and Tripathy, 2012; Sheppard et al, 2017**). The ditto sediment assemblage **(**sandstone-shale-carbonate with variable proportions of sediment types) of these three groups indicates similar depositional environment with syn-sedimentation tectonic activity (**Dasgupta,2006**). The Srisailam Formation may be unconformably **(Patranabis-Deb et al, 2012**) or disconformable **(Collins et al, 2015**) overlies the Chitravati Group, and shows a tectonic contact with Nallamalai Group in the south, and east **(Collins et al, 2015; Sheppard et al, 2017**). Within Cuddapah Supergroup, the sedimentary strata of Papaghni, and Chitravati Group are frequently interrupted by numerous mafic-ultramafic sills, and dykes. The relatively younger Kurnool Group is unconformable on the Papaghni, Chitravati Groups, and Srisailam Formation **(Collins et al, 2015; Sheppard et al, 2017**).

To account for the evolution of Cuddapah Basin several theories are proposed by various workers like **(Murthy, 1981); (Bhattacharji and Singh, 1984); (Drury et al, 1984); (Bhattacharji, 1987); (Nagaraja Rao et al, 1987); (Chaudhuri et al, 2002); (Singh and Mishra, 2002); (Anand et al, 2003); (Chetty, 2011); (Mishra, 2011); (Mohanty, 2011); (Basu and Bickford, 2015)**; **(Absar et al, 2016); (Sesha Sai et al, 2014) and (Kale et al, 2020)**.

Based on the lithostratigraphy, rock types, and structural distribution **(Nagaraja Rao et al, 1987)** propose that the evolution of Cuddapah Basin involved with the development of four sub-basins, as follows-

I. The Papaghni Sub-basin in the western part of the basin; composed of the Papaghni, and Chitravati Group of rocks;
II. The Nallamalai Sub-basin in the eastern part of the basin; composed of the Nallamalai Group of rocks;

III. The Srisailam Sub-basin in the north-western part of the basin; composed of the rocks of Srisailam Formation;

IV. The Kurnool, and Palnad Sub-basin in the central part of the basin; composed of the Kurnool Group of rocks.

On the basis of aeromagnetic mapping of the Cuddapah Basin **(Murthy, 1981)** proposes a paleogeographic model for this basin **(Fig. 1.4**). The great similarities for the crescent shaped boundaries of all the formations have resulted from a land-locked condition of the basin with a probable connection to the open sea in the North East **(Murthy, 1981; Fig. 1.4**).

For the evolution of Cuddapah Basin a thermo-mechanical model related with crustal doming, erosion, and subsidence is suggested by **(Bhattacharji and Singh, 1984), (Drury et al ,1984) and (Bhattacharji, 1987)**.Based on magmatism in the western part of the basin **(Rao et al., 1987)** propose that the initiation of Cuddapah Basin is under a thermal regime, and on the basis of profound deformation in the eastern part,**(Rao et al., 1987)** also infer that the eastern part suffer a stress which is related with up thrusting. On the basis of geophysical investigation **(Singh and Mishra, 2002)** showed the development of Cuddapah Basin as a peripheral foreland basin, formed through Proterozoic continent-continent collision **(Fig. 1.5**). Based on sedimentological aspects **(Chaudhuri et al, 2002)** propose formation of the Cuddapah Basin as an intracratonic rift basin with the presence of open sea in the eastern direction of the South India cratonic Provenance. In a similar way, geochemical analysis and subsidence modelling by **(Anand et al., 2003)** proposed a passive rifting with the formation of this intracratonic basin. **(Mishra, 2011)** also explains the formation of Cuddapah Supergroup in relation with rifting phase which is further followed by a plate convergence event leading to the formation of Kurnool Group of rocks. Based on low angle dipped detachment faults and kinematic history **(Chetty, 2011)** infers that the development of

Cuddapah Basin is connected with the Proterozoic collision process and the probable evolution stages are as follows:

Stage 1: Collisional processes lead to the development of mobile belts and thrust zones in the adjoin basement underneath the Cuddapah Basin within 2600 to 2000 Ma.

Stage 2: The initiation of Cuddapah Basin starts soon with the freeze of the collisional processes and related with the development of extensional tectonic regime. Magmatism is associated with this stage leads to the formation of sills and dykes within the basin at around 1800 Ma.

Stage 3: 'Listric' type of normal fault with N-S trend leads to the development of Papaghni basin and with continuous extensional tectonism 'domino' type of normal fault occurred which finally resulted the development of Nallamalai Basin **(**1600 - 1400 Ma).

Stage 4: Development of imbricate thrusting, and folding in the Nallamalai Basin due to the strong compression phase.

Stage 5: Initiation of extensional regime with the formation of transfer faults **(**1400 – 850 Ma).

Stage 6: Reactivation of transpressional dextral shearing along the mobile belt with post-Kurnool thrust event **(**650 – 450 Ma).

According to **(Mohanty, 2011)**, the morphological fit of the margin of the Napier Complex of East Antarctica at the position of Cuddapah Basin of the Dharwar Craton, together with the matching tectonic trend lines, mafic dykes showing identical composition and orientation, and identical tectonic evolution of the blocks on opposite sides of the matching line indicate juxtaposition of the Napier Complex with "SIWA" **(**SI: South India, WA: Western Australia) during early Paleoproterozoic time **(Mohanty, 2011).** This assembly is separated at ~ 1950 Ma to give rise to the development of Cuddapah Basin **(Fig. 1.6**).

Also, **(Basu and Bickford, 2015)** suggest that during the fragmentation of the earliest supercontinent Kenorland in Paleoproterozoic **(**1900-2000 Ma) Papaghni-Chitravati sub-basin of Cuddapah basin is opened up. This earliest Purana Basin is closed at around 1800 Ma, when the fragments of Kenorland reassemble again to form another supercontinent Columbia **(Basu and Bickford, 2015**). This event is marked by formation of a Large Igneous Province **(**LIP) in the Southern Indian Block **(French et al., 2008**). The mafic igneous activities are probably associated with the breakup of Kenorland, when the Rayner complex separates from India to reside in East Antarctica **(Mohanty, 2011; Basu and Bickford, 2015**).

One of the workers named (**Absar et al, 2016)** has proposed a model **(Fig. 1.7**) for the evolution of Cuddapah Basin and the stages are follows:

Stage 1: Opening of Papaghni sub-basin as a back-arc basin in an around 2000 Ma, due to subduction in western direction along with the eastern Indian continental margin. The newly opened basin received detritus from Dharwar craton during the initial stage of Gulcheru sedimentation and during later stages **(**Vempalle Formation, and Chitravati Group) received detritus and dissolved load also from a magmatic arc situated southeast of depositional basin.

Stage 2: Extinction of magmatic arc with the change in the polarity of subduction in an around 1850 Ma, probably due to plume activity. Sedimentation in the Papaghni sub-basin possibly shut down after this episode.

Stage 3: Dharwar craton collided with Antarctica/Australia craton at 1600 Ma and the rest part of Cuddapah basin evolved as foreland basin behind 'collisional' Krishna Orogen **(Dobmeier and Raith, 2003; Henderson et al, 2014**). Sedimentation of Nallamalai Group, and Srisailam Formation take place in a post collisional foreland basin **(**e.g, **Collins et al., 2015, Joy et al., 2015**).

Stage 1 and Stage 2 of this model is mainly evolved during the fragmentation of Kenorland Supercontinent, and the Stage 3 evolved during the amalgamation of Kenorland fragments. Kenorland breaks up ~ 2.0 Ga **(Ernst et al, 2013**) an event that is preceded by the emplacement of ~2.17 Ga mafic dyke swarms suggesting major rifts on a global scale **(Basu and Bickford, 2015)**. This is about the time when the earliest set of Purana basins **(**e.g., Cuddapah, i.e., Papaghni-Chitravati; Kaladgi; Gwalior-Bijawar-Sonrai) opens. Mafic, and ultramafic intrusions into Lower Cuddapah group of rocks followed as did the eruption of mafic, and felsic pyroclastic **(Kale, 1991,2016; Basu and Bickford, 2015**). The fragments of Kenorland reassembled, and attained maximum packing around 1.6 Ga to form the supercontinent Columbia **(Ernst et al., 2013**), an event that is marked by formation of a Large Igneous Province **(**LIP) in the Southern Indian Block **(**SIB) **(French et al, 2008; Absar et al, 2016**). During this period of amalgamation of Kenorland fragments the Nallamalai Group, and Srisailam Formation evolved as a part of foreland basin. The possible paleo-super continental reconstruction after the break-up and during the amalgamation of Kenorland supercontinent is shown in **(Absar et al., 2016).** They proposed that Andean-type subduction initiated at the eastern margin of Indian continent is synchronous with Glenburgh orogeny, and collision between Pilbara and Yilgarn craton of Australia. The intervening oceanic crust is consumed with the progression of subduction and the Indian craton possibly collided with Napier block of Antarctica, which coincided with the age of peak metamorphism of Ongole domain of the Krishna Orogen **(Absar et al., 2016**). This time frame possibly represents amalgamation event of Kenorland fragments and the formation of the Columbia supercontinent.

Based on the mafic-ultramafic sill bodies configuration as well as the shallow marine non-clastic sequences **(Sesha Sai et al., 2014)** has also proposed a continental arc setting during the development of Papaghini, and Chitravati group of rocks.

Mukherjee et al. (2019) has further proposed that the crescent shape of the Cuddapah basin is mainly due to the thrusting related to the Eastern Ghat Orogeny. Progressive stages of rifting and development of sub-basins are imprinted in the rocks that occur as basin fills. The later phases of deformations have also slightly modified and produced the final shape of the basin.

Recently **(Goswami et al., 2020)** pointed a basin evolution model with the signatures of active rifting. The model presents the mechanism of bimodal volcanism during rifting, and sedimentation. Different sub-basins within the Cuddapah basin indicate a combined mechanism of rifting, and orogenic events.

1.4 INTRODUCING THE KURNOOL SUB-BASIN WITHIN CUDDAPAH BASIN

King, (1872) first proposed a four-fold lithostratigraphic classification of the Cuddapah Basin. **(King, 1872)** classified the litho-units of the Cuddapah Basin is broadly into older Kadapah **(**Cuddapah) and younger Karnul **(**Kurnool) Formation where each formation is further sub-divided into four sub-groups. Thus, the Kadapah Formation consists with Paupugnee **(**Papaghni) beds, Cheyair beds, Nullamullay **(**Nallamalai) beds, Kistnah **(**Kistna) beds **(Table 1.1**) and Karnul Formation consists with Banaganpilly unit, Jummulmudgoo unit, Paneum unit, Khoond-air unit. It lies at the eastern margin of the Dharwar Craton in the south-eastern part of the Indian shield in southern Andhra Pradesh. The arcuate shaped Cuddapah Basin **(North 13º15′ to 17º00′ and East 77º45′ to 80º15′**) covers an outcrop area of 45,000 km^2, includes sediments more than 12-km thick **(Tripathy and Saha, 2013; Fig 1.8).** The maximum length and breadth of the Cuddapah Basin is 300 Km and 150 Km towards NNE-SSW and EW direction respectively **(Mohanty, 2011**). The basin seems to have had a complicated history and was subjected to compressive tectonics. Early phase of basin development to represent initial rifting **(Collins et al., 2015)** and

evolution into a marine passive margin **(Fig. 1.9),** similar to the model proposed by **(Ravikant, 2010).**

The **Cuddapah Supergroup** is mainly consisted of argillaceous and arenaceous sediments with relatively a smaller number of calcareous sediments **(Rao et al., 1987**). This crescent-shaped basin mainly composed of orthoquartzite-carbonate suite and basic-to-acid volcanics and sills in the lower part, and siliceous shales with quartzite in the upper parts. The western margins marked by a profound non-conformity of Cuddapah sediments resting on the Archean Peninsular Granite Gneiss complex. The lithostratigraphy of Cuddapah basin is composed of Cuddapah Supergroup and Kurnool Supergroup. The Cuddapah Supergroup is predominantly composed of arenaceous to argillaceous with subordinate calcareous to dolomite whereas the Kurnool Group mainly composed of carbonate facies with subordinate fine clastics. The western part of the basin is generally undeformed and developed in Papaghni and Srisailam Sub-basins and the Nallamalai fold belt in the east, which resulted due to easterly compression and thrusting related to the Eastern Ghat orogeny. Kurnool Group is developed in the Kurnool and the Palnad sub-basins as half graben due to reactivation of related fractures.

The Papaghni and Kurnool Basin are geographically interlinked, but their deposition took place in different time. The Papaghni contains the older Cuddapah sediments whereas the Kurnool consists of comparatively younger sediments which overlie Cuddapah group with a major unconformity. Srisailam sub-basin contains the younger Cuddapah sediments whereas the Palnad sub-basin exposes the younger Kurnool sequences. The eastern half of the Cuddapah basin is occupied by the Nallamalai fold belt consisting of upper Cuddapah sediments. Nallamalai fold belt is easily demarcated from the undeformed western sub-basin by a prominent fault line known as the Rudravaram line along which the cleavage begins to develop in the Cuddapah sediments, which intensely deformed towards the thrust in the east.

The formation of Kurnool Basin is less disputed compared to Cuddapah basin. The Kurnool Basin was formed due to gravity-induced block faulting that caused the basin to form in a depocenter. During the deposition of Kurnool Group underwent subsidence controlled by deep faults and strong local movements all of which varied during the cycles **(Meijerink, 1984; Chakraborty et al., 2010).** After deposition, there has been eastward thrusting movement of deep faults, epeirogeny movements, folding and metamorphism in the eastern part of the basin **(Chakraborty et al., 2010).**

The Cuddapah basin is situated in the eastern Peninsular India contains about 12km thick stratigraphy, which is deepest at the east of the basin and which overlies over a 40-km thick crust of the Eastern Dharwar Craton **(Naganjaneyulu, K. and Harinarayana, T, 2004).** Sedimentary structures indicate that they have been derived from the south and the west **(Dasgupta et al., 2005; Rao and Gokhale, 1973).** The direction of flow of the ripples is from west to east in Banaganapalle Formation which is consistent with the sediments being sourced from the Dharwar Craton. The western part of the basin the sediments are generally unmetamorphosed except for the parts of Kurnool Group, whereas in the eastern part they show deformation in the form of Nallamalai fold thrust belt **(Chakraborty et al., 2010; Meijerink, 1984).**

The outcrop of rocks of the Neoproterozoic Kurnool Group occurs in two separate areas in the Cuddapah Basin: the Kundair Valley in the west covering parts of Cuddapah and Kurnool districts and the Palnad area in the northeast covering parts of Guntur, Nalgonda and Krishna districts. The lower units of the Kurnool Group lie unconformable over the lower Cuddapah succession **(**Papaghni and Chitravati Groups) in some parts of Cuddapah and Kurnool districts and the basement granite gneisses. In the Palnad area, the Kurnool Group lies unconformable over the basement granite gneisses and the Srisailam formation, the topmost unit belonging to the Nallamalai Group. The maximum age of sedimentation of the Kurnool

Group is constrained by the kimberlite pipes dated 1090 Ma, **(Anil Kumar et al., 1993**) which provided detritus to the diamond-bearing conglomerates at the base of the Kurnool Group. **(King, 1872)** first proposed the lithostratigraphy of Cuddapah Basin with a fourfold classification. After that several workers and institution **(Sen and Narasimha Rao, 1968; Dutt, 1975; Meijerink et al., 1984; Rao et al., 1987; GSI, 1981)** revised the lithostratigraphy of Cuddapah supergroup. All these lithostratigraphic study comes with the conclusion that strata within the Cuddapah Basin **(Saha and Patranabis-Deb, 2014**) include the Cuddapah Supergroup and the unconformably overlying Kurnool Group **(Table 1.1).**

1.5 PREVIOUS WORK

The Cuddapah supergroup of rock is separated by the Kurnool group of rock by an angular unconformity in between them. These sets of rocks belong to upper Proterozoic. The earlier work is carried out by Mackenzie. In 1794 who focused his attention on the lithology of this tract. More emphasis was given mostly on economic evaluation of the area, particularly for diamond and iron by **(Heyne, 1814).** Four other contemporary workers, namely **(Malcolmson, 1840)** and **(Newbold, 1846)** for the first time started describing various rock types of Cuddapah and Kurnool.They have marked the position of Cuddapahs and Kurnool in the geological scale.

The geology of the Cuddapah Basin was revealed through the monumental work carried by **(King, 1872)** published in classic Memoir. His greatest contribution to the geology was the detail stratigraphic study of the entire Kurnool basin.

Prominent work regarding geomorphology of the Kurnool basin was not carried out until 1955. **(Dutt, 1962)** carried out extensive work on geomorphologic features of the Kurnool basin. In the year 1962, 1975 and 1986 the Kurnool basin was mapped with the report of

cement and flux grade limestone. He also marked an unconformity at the base of the Paniam Quartzite and altogether regarded Kurnool as a group.

Saluja et al, (1971) had carried out detailed palynological investigations and were the first to report micro-planktons from the Kurnool shales. He assigned late Precambrian to Cambrian age for these sediments and inferred that the Kurnool sediments are deposited under shallow marine conditions. Later on, few other scientists' **(Sharma and Shukla, 1999, 2012,2016)** inferred carbonaceous mega remain from Owk shales and assigned its age to Neoproterozoic times. Also, **(Crawford and Compston, 1973)** worked on the age factor of Cuddapah and Kurnool Group of rocks.

Work was carried on tectonic framework of sedimentation along with the work on lithological aspects of the Owk and Nandyal shale of the Kurnool sediments in the Western part of Palnad basin by **(Reddy and Vijayam, 1973 & 1976).** The detail study on clay mineral in Owk and Nandyal Shales have been carried out inferring that deposition took place in marine environment. Study of microstylotite and diagenetic aspect in limestone along with the tectonic activity of the area was studied within Narji Limestone.

Natarajan and Rajagopalan Nair, (1977) has interpreted the tectonic history of Kurnool by studying the Kurnool thrust and other structural features **(**primary and secondary) in the north-eastern part of the Palnad basin, Krishna district. Detail work has been carried out on pressure solution structures **(**stylolites) in Narji Limestones from Jaggayyapeta area and described their nature and types, megascopic and microscopic features and tectonic effects on them.

Arya and Rao, (1979) first reported bioturbation unit in Narji Formation in the form of worm burrows belonging to the *Skolithos* and *Glossifungites* assemblages **(Seilacher, 1967**). They were present in dark, pyrite-bearing limestones of euxinic, quiet-water facies indicating wider environmental distribution. These structures confirm that diverse body fossils and

ichnofossils of the *Ediacaran* assemblage **(**700 m.y.) which led to the evolution of simpler, and probably smaller, soft-bodied metazoans later.

Rajurkar, (1977) carried out detail structural work. Cuddapah orogeny of the Pre-Kurnool age suffered severe deformation which is interpreted from the structural patterns and other details whereas during post-Kurnool suffered little deformation with very little folding, and extensive faulting.

Kamal and Vijayam, (1982) carried out detail petrographic studies on the basis of the types of cementing material, authigenic products and replacement texture of Paniam sands. It is inferred that deposition took place in beach to dune environments, subjected to shallow to medium burial and involved in redoximorphic to locomorphic stages of diagenesis. Report and origin of intraformational conglomerate from this group was also carried out by **(Kamal and Vijayam, 1982).**

Dasari, (1989) worked on detailed isotopic variation in Narji and Koilkuntla limestone. He observed a progressive increase of O^{18} values from base to the top horizon. It is due to interaction of various horizons with fresh water in the later geological periods and possible consequent exchange.

Venkatachalapathy et al., (1992) has carried out detailed palynological work with some report on microplanktons from this group. It has been inferred that the deposition of Kurnool Group of sediments took place in shallow marine intertidal depositional during Precambrian-Cambrian times.

Lakshminarayana et al., (1999) studied in detail the Paleocurrent pattern of the Banaganapalle Formation in the Kurnool sub basin and inferred the provenance as mainly the intrabasinal tract occupied by lower Cuddapah sediments, igneous intrusive and the basement located to the west.

Gururaja et al., (2000) identified demarcation strata between Precambrian and Cambrian in the Cuddapah Basin.

Patil DJ et al., (2002) carried out work on geochemistry and Carbon, Oxygen and strontium isotope of carbonate rocks from Kurnool Group. It is inferred the open system diagenetic trends for the carbonate rocks of Narji Formation and for Koilkuntla Formation does not show any definite alteration trends.

Harish et al., (2003) worked on the petrography and fluid inclusion studies on Palnad siliciclastic indicated probable tectonic activity during the deposition of the sediments in the study area of Banaganapalle and Paniam Formation of the Kurnool Basin. He also suggested that the source rock for Palnad siliciclastic is Archaean granites, granitic gneisses and sedimentary formations belonging to Cuddapah Group.

Saha and Chakraborty, (2003) studied the detail deformation pattern of Kurnool and Nallamalai groups in the NE part **(**Palnad basin) of the Cuddapah basin.

Subsequently **(Saha et al, 2006)** did the detailing on sedimentary sequences in Palnad and Kurnool sub-basins. He also interpreted their paleogeographic and tectonic implications.

Scientists worked on the geology of the Julakallu area, Guntur district, Palnad sub-basin. The geological studies have marked the presence of unknown Cumbum shale/phyllite in the Julakallu-pinneliare within the Palnad sub-basin. Cumbum shale/phyllite along with Quartzite found to be resting above Narji Limestone.

Later **(Butchi Babu et al., 2008)** estimated the thickness of limestone formation in Kurnool sub basin by Aeromagnetic anomalies.

Gupta et al., (2010) concluded that Banganapalle formation represents cyclic sedimentation in inter to supratidal flat environment having high Uranium potential.

Some carried out provenance studies by U-Pb-H-L-O isotopic composition of Zircons from the conglomerates and **(Sharma, 2011)** reported Neoproterozoic and Ediacaran

palaeobiological remains in the purana basins of Peninsular India and inferred the age of Kurnool, Bhima and Vindhyan.

Chetty T, (2011) also worked on tectonics and deformation pattern of the Cuddapah basin. The presence of low-dipping detachment faults and shear zones in the lower crust, and their possible linkage with the extensional faults in the upper crust have been inferred. The fault patterns and kinematic history in conjunction with the crustal architecture strongly suggest that the evolution of CB is genetically related to the Proterozoic collisional processes and associated crustal-scale transpressional tectonics in the basement at the eastern margin.

Perrin et al., (2011) studied the process of karstification for groundwater in the carbonate rocks and its implication was done by him to avoid unexpected collapse, reservoir leaks, inaccurate groundwater budgeting etc.

Banerjee et al., (2012) carried out radiometric examination of the stratigraphic boreholes for Uranium exploration. It is unconformity-related, with uranium deposits present in the marginal parts of Srisailam and Palnad Sub-basins, Nalgonda and Guntur districts, Andhra Pradesh. Thick sedimentary columns are exposed in these basins which are composed of c arenaceous, argillaceous and calcareous sediments of Meso- to Neoproterozoic age and are deposited over Neoarchean to Paleoproterozoic basement granitoids and greenstone belt of Archaean age.

Joy et al., (2012) worked on geology of the Banaganapalle conglomerate of Kurnool Group and inferred the diamond provenance for the sequence.

Saha and Tripathy, (2012) worked on Tuff beds in Kurnool sub basin and inferred the felsic volcanism in Proterozoic intracratonic basins.

Sharma and Shukla, (2012) reported and discussed their significance of helically coiled microfossil in the Owk shale and burrow structures in the Narji Limestone and assigned Kurnool Basin of Ediacaran age close to the Cambrian.

According to **(Patranabis-Deb et al., 2012),** the Narji was formed on an extensive carbonate platform. It was formed during the rifting stage of the Kurnool Basin which was rapidly followed by re-establishment of a stable shelf regime representing peripheral foreland basin.

Saha and Tripathy, (2012) first reported Felsic Tuff from the Owk shales in the Proterozoic Kurnool sub-basin in southern India which is derived from low degree melting of continental crust, suggesting intermittent tectnothermal instability which likely to be influenced by basinal topography and cyclic development of the carbonate platforms.

Bickford et al., (2013) inferred the age and the provenance for the Owk Shales by caring out the detail work on U-Pb ages of Zircons in the Owk Shales. The data depicted that the zircons grains derived from the ca. 2.5 Ga granitic/gneissic/greenstone basement of the Dharwar cratons that also host minor older Archean enclaves. A single 1880 Ma grain shows result that derived from a ca. 1.9 Ga LIP. In the absence of any younger magmatic zircon, the absolute age of the Owk Shale remains elusive.

Paul et al., (2013) carried out a detailed study on mineral chemistry of radioactive uranium deposit of Koppunuru area in Palnad basin. The study has revealed the potential for multi-episodic epigenetic U-mineralization in basement granitoids and the overlying Banaganapalle Formation.

Singh et al., (2016) also has reported uranium mineralization in Koppunuru area of Guntur district in Palnad basin. They have reported uranium mineralization in the granitic rocks which forms the basement for Palnad sediments.

Bharani et al., (2015) worked on X-ray diffraction technique which revealed that the carbonate rocks of Kurnool Group contain calcite, dolomite and quartz as dominant mineral

composition. It was inferred that the carbonates are deposited in a gradually deepening ocean as chemical precipitates.

Gopakumar and Waghmare, (2016) indicated presence of apatite, quartz, clinochlore, muscovite and traces of xenotime within the Phosphatic bands within the Owk shales.

Dar et al., (2011) carried Groundwater trace element geochemistry in Narji Limestone. It consists of a range of substituted trace elements in the mineral matrix. Dissolution influenced by pH–Eh, recharge processes and residence time controls Ca^{2+}, Mg^{2+}, Mn, Al, Cd, Ba, Sr, Co, Li, Rb, V, Fe, Pb, As, Si and Cu concentrations, while the weathering of quartzites and shales releases minute quantities of Na^{+}, K^{+}, Cl^{-}, Si and F into groundwater. A significant amount of Na^{+}, K^{+}, Cl^{-}, NO^{3}, SO^{2-} 4, Al, Fe, Cd, As, Pb, Ni, Zn, Mn, Sr, Cl, Br, Sb, Ag, Mo, Co and Cu has leached into groundwater from the use of fertilizers/manures and decayed organic matter in cultivated areas. Urbanization, land-use changes, mining and local industries sewage, waste disposal and industrial and commercial activities effected the composition of groundwater.

1.6 PRESENT STATUS IN RESPECT OF SEDIMENTOLOGY OF KURNOOL SUB-BASIN

Patranabis Deb et al., (2012) divided the Cuddapah Supergroup succession into four unconformity-bound sequences, namely, the Papaghni, Chitravati, Srisailam and Kurnool groups. The formation is represented by four major cycles of sedimentation. Kurnool is represented by the fourth and the last cycle consisting of conglomerates, feldspathic sandstones, super mature quartz arenites, minor shale and carbonates. Banganapalli Quartzite records a major rift succession rapidly followed by re-establishment of a stable shelf regime when an extensive carbonate platform of the Narji was developed. Later on, rhythmite in Koilkuntla limestone and high quartz percentage in the Paniam

Quartzite **(**ca. 89% quartz), suggest that the Kurnool sediments formed in a passive margin basin **(Beukes, 1987).** The major basin-wide unconformity presents at the base of the Kurnool Group **(**Cycle IV) which can be correlated a rifting event and fragmentation of Rodinia.

The Kurnool Group overlies the Papaghni and Chitravati groups and onlaps the gneissic basement with a major unconformity that extends over the entire Papaghni sub basin **(Saha et al., 2009).** The Palnad and Kunderu valley regions are considered as an extension of the Kurnool Basin. The Kurnool Group is more than 500 m thick, and is divided into six formations, comprising two carbonate platform units and two intervals of sandstones and shales.

Banganapalle Quartzite is the basal unit of lower conglomerate bed followed successively by grit, quartzite and shale **(King, 1872).** The sequence of Banganapalle Quartzite in the type area is as follows:

- Quartzite
- Conglomerate
- Shale
- Conglomerate

Conglomerate is oligomictic, consisting of sub-rounded pebbles of chert, jasper and quartzite. Barytes is also noticed as pebbles in the conglomerate **(Rao et al., 1987**). Petrographic as well as geochemical studies of siliciclastic from Banganapalle Formation depict their source from Archean granites, gneisses and lower Cuddapah sediments **(Harish and Basavarajappa, 2000; Kumar et al., 2022**). An integrated study by **(Barkat et al., 2020)** involving facies association analysis, architectural element analysis, paleohydrology and detrital zircon geochronology allowed detail insight of sedimentology and paleogeography of Neoproterozoic Banganapalle Formation **(**BF), Kurnool Group. Detailed process-based

facies and paleoenvironmental analysis have led to the identification of fourteen facies types, grouped under four different facies associations, which record paleoenvironmental settings ranging between mid-alluvial fan to distal fluvial plain. Whereas mass flows, hyper concentrated flows, streamlets and sheet floods dominate the depositional process on the BF fan **(**middle to distal) surface, streams of varied geometry viz. braided and ephemeral meandering occupied the proximal and distal BF alluvial plain.

Narji Formation is resting over the Banganapalle Quartzite conformably and the contact between the two is gradational. The limestone is divided into lower flaggy, middle massive and upper flaggy units. The upper unit have thin glauconitic ferruginous quartzite. The limestone is bluish-grey to dark-grey in colour, hard and compact in the middle horizon and breaks with conchoidal fracture **(Rao et al., 1987).** The Narji Limestone has a thickness ranging from 120 to 180m and accounts for one-third of the total thickness of the Kurnool Group.

Owk Shale in most of the cases is characterized by the presence of yellow and white ochre **(Rao et al., 1987).** This is very well laminated thin bedded unit consisting of silty claystone within thin beds of fine-grained quartzite **(Richards et al., 1968).**

This is essentially quartz arenite, but **(Dutt, 1962)** recorded siliceous shale in the upper part and identified thin conglomerate and grit beds at the base. The upper horizon of the Paniam Quartzite exhibits typical pinnacle nature a feature which distinguish the Paniam quartzite from rest of the quartzite of the Kurnool Group and Cuddapah Supergroup. Petrographic as well as geochemical studies of siliciclastic from Paniam Formation depict their source from Archean granites, gneisses and lower Cuddapah sediments **(Harish and Basavarajappa, 2000)**. The siliciclastic are matured to super-matured quartz arenites.

Koilkuntala limestone is light-grey to dark-grey in colour and flaggy with occasional massive bands **(Rao et al., 1987).** The limestone in the lower horizon has flaggy quartzite intercalation.

Nandyal shale, though basically argillaceous, has calcareous intercalation and shows lower shaly and calcareous flaggy unit and an upper shaly limestone **(Rao et al., 1987).** The shaly flag is purple calcareous shale which is soft and weathers into pencil-like fragments. The shaly limestone is dark-grey and greenish-grey and breaks into sharp edges **(King, 1872).** The thickness of the Nandyal Shale varies from 100 to 300m.

1.7 PRESENT STATUS IN RESPECT OF GEOCHEMISTRY OF KURNOOL SUB-BASIN

Geochemical analysis on siliciclastic from Kurnool subbasin depict **their source from Archean granites, gneisses and lower Cuddapah sediments (Harish and Basavarajappa, 2000). Further an eugeosynclinal passive margin tectonic sedimentation setting has been proposed by Harish and Basavarajappa, (2000).**

Bharani et al., (2015) performed x-ray diffraction technique revealed that the carbonate rocks of Kurnool Group contain calcite, dolomite and quartz as dominant mineral. It was inferred that the carbonates are deposited in a gradually deepening ocean as chemical precipitates.

Dar et al., (2017) discussed the trace element concentration in association with major ions in the Narji Limestone aquifer of Andhra Pradesh, India, to evaluate the origin and contributing factors of elements and their level of pollution in the aquifer. The limestone is constituted dominantly of calcite with small amounts of dolomite, silica, clay and disseminated pyrite. Trace metals are present in small amounts in the rock minerals.

Gopakumar and Waghmare, (2016) examined phosphatic band in the Neoproterozoic Formation in Kurnool basin. Petrographic examination reveals that the phosphatic bands are composed of cryptocrystalline apatite having very low birefringence. Chemical analysis of selected samples of phosphatic bands indicates that the P_2O_5 content ranges from 5–19.8%, whereas, the P_2O_5 content identified by EPMA ranges from 1.76–38.11%. Such P contents indicate that these deposits are true phosphorites. Apatite, quartz, clinochlore, muscovite and traces of xenotime are the mineral constituents of the phosphatic bands identified by XRD. The apatite mineral is identified as carbonate fluorapatite.

Saha and Tripathy, (2012) did geochemistry in Rhyolitic to rhyodacite tuff beds in the upper part of the Owk Shale in the Proterozoic Kurnool subbasin, southern India which included REE and trace element abundances. The rheomorphic features of the tuff beds and textural characters of the altered vesicular glass are interpreted to represent welded as well as unwelded felsic tuff. Association with submarine sediments below and above the tuff beds raises the possibility of contribution from submarine ash flow and ash fall. However, minor admixture with clasts of nonvolcanic origin cannot be excluded altogether, and may explains lightly lower ΣLREE compared to other known rhyolitic/rhyodacite tuffs from the Chhattisgarh and Vindhyan basins in India. There is strong enrichment of incompatible elements Cs, Rb, Ba and Th compared to primordial mantle.

A continental crust source for the parent melt is suggested by **(Hoffman, 1988)**. The tuff samples from the Owk Shale have SLREE/SHREE ratios varying between 14.8 and 22.5, much higher than post-Archean sediments with an average of 9.7 ± 1.8 **(Nance and Taylor, 1976)**. We therefore, argue sediment admixture had minimal influence on the trace and REE geochemistry of the tuff samples from the Owk Shale.

1.8 AGE OF KURNOOL GROUP OF ROCKS; PARTICULARLY OF NARJI LIMESTONE

The Kurnool Group is one of the most debatable sedimentary litho-package within the Cuddapah basin in terms of its depositional age **(**summarized in **Table 1.2**). The group is deposited in presently two spatially different sub-basins viz, Kurnool and Palnad sub-basins. Field evidence suggest the presence of rhyolitic to rhyodacite tuff beds within the Owk Shale **(Saha and Tripathy, 2012**). However, **(Bickford et al., 2013)** based on SHRIMP dating of zircons from the same Owk Shale **(Saha and Tripathy, 2012**) deduced variable age from 1.8 to 3.3 Ga and suggested the tuff beds of the Owk Shale to be volcanoclastic sandy mudstone with zircons being detrital and not magmatic. Based on the available geochronological data two sets of inferences can be drawn for the ages of Kurnool Basin opening. The age of Kurnool sediments has always been constrained based on its maximum age of deposition and bracketed by the thrusting event of the Nallamalai Fold Belt over the Kurnool and Palnad sub-basins. The maximum age limit for Kurnool sedimentations is suggested as mid to late Mesoproterozoic. Earlier, it was suggested that the diamonds found within the conglomeratic beds of the Banganapalle Quartzite are sourced from the kimberlites present within the Eastern Dharwar. These kimberlites have an age of ~1090 Ma **(Kumar et al., 1993., Kumar et al., 2022**). However, **(Joy et al., 2012)** based on the difference between the garnets recovered from Banganapalle diamond old working dumps and with those of the kimberlites found from the Eastern Dharwar **(**such as Wajrakarur kimberlite field) suggested that the source of diamonds is from the lamproites intruded within the Tadpatri Formation. **(Joy et al., 2012)** estimated an age of 1400 -1300 Ma for these lamproites based on the age of zircons recovered from the stream sediment samples. Thus, based on this argument ~1300 Ma is understood to be the maximum age limit for deposition of the Banganapalle Quartzite. (**Kumar et al., 2022)** reported 1.43 Ga age for the Garledinne lamproite intruded within the

Tadpatri shale, exposed in western part of Banganapalle town. However, authors do not support this lamproite to be the primary source of the zircons recovered from Banganapalle conglomerate by **(Joy et al., 2012)**. The presence of sedimentary carbonate xenoliths from the kimberlite of Siddanapalli present in the granite-greenstone terrain of the Gadwal area, Eastern Dharwar craton, presents a contrasting view as proposed by **Dongre et al., (2008),** which suggest the Kurnool sediments to be older than ~1090 Ma. **Based on such observations (Dongre et al., 2008; Chalapathi Rao et al., 2010; Joy et al., 2012) it may be argued that the Kurnool basin must had opened between 1090 to 1300 Ma**. However, the inferences drawn by **(Dongre et al., 2008)** are still open for debate **(Basu and Bickford, 2015**) as the carbonate xenoliths may be of the Kurnool, Bhima or any other sedimentary basin which include schist belts of Eastern Dharwar craton which might have been eroded. Proving the existence of concealed sedimentary sequences equivalent to the Kurnool Group at Siddanapalli and adjoining area in the Gadwal granite-greenstone terrain will substantiate such observations. A Neoproterozoic age for the Kurnool Group **(**Table 1.2) was proposed by **(Crawford and Compston, 1973)** based on the date of a dolerite sill underlying the Kurnool Group. **(Collins et al., 2015)** indicated an early Neoproterozoic age based on the dating of detrital zircon from the Paniam Quartzite that yielded an age of 913±11 Ma**.** Evidences for Neoproterozoic age interpreted on the values of δ13C, δ18O and 87Sr/86Sr of the Palnad sub-basin which are suggested to be similar to those in late Neoproterozoic carbonate succession world-wide **(Craig, 1957; Kumar et al., 1999; Patil et al., 2002**). Based on lithostratigraphic correlation and fossil evidence, a Neoproterozoic age has been assigned to the Kurnool Group **(Kale and Phansalkar, 1991**). Similarly, the micropaleontological studies of the Chuaria and Obruchevella microfossil from the Owk Shale indicate an Ediacaran age close to the Cambrian has been assigned for the Kurnool Basin **(Sharma and Shukla, 2012; Shukla et al., 2020**). It may be noted that the underlying

Narji Limestone **(**100 to 200 m) and Banaganapalle rudaceous-arenaceous sequence **(**10 to 50 m thick) of the Kurnool Group are older than the Owk shale. Considering the Precambrian – Cambrian age of the Obruchevella microfossils **(Sharma and Shukla, 2016; Shukla et al., 2020**) and keeping in view of the combined thickness of the underlying Narji Limestone and Banganapalle Quartzite **(**maximum ~ 250 m) it can be inferred that the deposition of the Kurnool Group of sediments took place during the terminal part of Neoproterozoic between 635 Ma to 541 Ma. **(Goutham et al., 2006)** based on palaeomagnetic studies suggested that the deposition of the Kurnool Group is around Riphean-Vendian boundary **(**~700Ma) which continued up to 590 Ma. A glance at **(Table-1.2**) reveal that various workers indicated a Late Neoproterozoic age for the sedimentary rocks of the Kurnool basin based on the micropaleontological studies. We observe that, owing to the absence of geochronological records of the intrusive magmatic rocks exclusively confined to the Kurnool Group of rocks, radiometric dating of the glauconite from the Banaganapalle quartzite will substantiate the existing knowledge on the depositional age of the Kurnool Group.

1.9 STATEMENT OF THE PROBLEM

The Proterozoic Cuddapah Basin presenting sediments of 1.6 Ga time span evolved chronologically in 3 distinct phases:

i. The evolution of the Paleo-Mesoproterozic segments witnessed sedimentation, magmatism and tectonism in the form of Cuddapah Super Group

ii. The Neoproterozoic segment represented by protracted period of non-deposition and

iii. The Neoproterzoic segment marked by the Kurnool Group of sediments.

However, there is poor geochronological data in support of Neoproterozoic age of Kurnool sediments.

At a very early stage of mantle perturbation, two major trends of lineaments **(**NE-SW and NW-SE) appeared to have been set in the basement which controlled the initiation of the Proterozoic Cuddapah basin of Peninsular India **(Bhattacharji, 1981). Bhattacharji, (1986)** has offered a combined thermo-mechanical model for the same on the argument that a thermal "driving load" is a prerequisite for the basin evolution. **Chatterjee and Bhattacharji, (2001)** clearly demonstrated the Cuddapah basin as rift basin based on their study of the magmatic components of the basin**. Goswami et al., (2020)** also proposes a basin evolution model with signature of active rifting. However, **(Singh and Mishra, 2002)** have offered an alternative model based on geophysical study. To them, the Cuddapah basin may represent a foreland basin. They conclude that the presence of prominent seismic reflectors in the upper mantle under the Cuddapah basin may indicate that some crustal rocks might have subducted towards the west suggesting divergent collision along the middle to late Proterozoic Eastern Ghat Mobile Belt. **Chetty, (2011)** also infers that the development of the Cuddapah Basin is connected with the Proterozoic collision process.

The Cuddapah Basin was formed due to gravity induced block faulting that caused the basin to form in a depocenter. The Kurnool Group underwent subsidence during deposition controlled by deep faults and strong local movements, all of which varies during its evolution **(Chakraborty et al., 2010; Meijerink, 1984**). After deposition, there has been eastern thrusting movement of deep faults, epiorogenic movements, folding and metamorphism in the eon part of the basin **(Chakraborty et al., 2010**).

Globally the late Mesoproterozoic to Neoproterozoic from 1300 to 900 Ma is understood as period of continental assemblage of Rodonia. The opening of Kurnool basin is also directly correlated with the Rodonia supercontinent. Whereas, the period between late Mesoproterozoic to Neoproterozoic is moved by the scarcity of passive margin deposits **(Bardley, 2011; Cawood and Hawkeasworth, 2014**). The Kurnool Group deposition is

understood to be a passive margin deposit with presence of an open sea in the eastern and South-Eastern margin of presently outcropped. Based on facies study **(Saha et al., 2006**) a rift related opening of Cuddapah Basin is envisaged and are also related to deposition of the Kurnool Group along and across the E-W faults present in the western margin of Cuddapah Basin **(**Gani-Kalva and Kona faults; **(Tripathy and Saha, 2013 & 2015**). Such half-graben type oblique normal, wrench/scissor faults may thus act as proxy for opening of the Kurnool basin **(Tripathy and Saha, 2013 & 2015**).

A survey of previous literature indicates that many aspects of the basin are either grossly regional or limited to describe some salient and specific occurrences. As such no attempt had been made to decipher the nature of Kurnool sedimentation within the aforesaid basin evolutionary model as proposed by **(Tripathy and Saha, 2013 & 2015**).

The proposed work tilted as '**Sedimentology of Narji Limestone in the Neoproterozoic Kurnool Group of Rocks, Cuddapah Basin, India**' is an attempt to highlight the sedimentology of the Kurnool basin during the early Neoproteroic time along with petrographic and geochemical attributes within the framework of fault-controlled basin evolutionary model. This thesis has been taken up with the following objectives

I. Identification of key constituent facies of the Narji Formation;

II. Characterization and evaluation of the primary facies and identification of diagenetic changes in three selected sections, west-central part of the Cuddapah Basin;

III. Description of the paleoredox condition, siliciclastic input and seawater chemistry during deposition of the Narji Limestone based on geochemistry;

IV. Construction of a depositional model;

V. The comparative study with other coeval formations from different parts of the world which will assists to throw light on the global variation on the environment of deposition prevailing during the early Neoproterozoic time before the onset of snowball earth.

The detailed sedimentological study of the Narji limestone helps in understanding the media of transportation, depositional environment and provenance. The geochemical studies of shale and limestones help to evaluate the sedimentary environment under which they were deposited and reconstruct the ancient environment conditions. Also, a detailed study of the diagenetic effects on rocks helps to reconstruct the environment of deposition as well as post-depositional textural and mineralogical changes.

1.10 STUDY AREA

The present study on Narji Formation geographically covers the northern part of the Formation and three sections are chosen for the investigation **(Fig. 1.10**). The first section is along the road cut section **(**A) **(**15°18′ 45.00″ N, 78°07′ 35.76″ E) of Patapadu-Yaganti hills, located around 11Km from the town of Banaganapalle in Kurnool District. The second section is around Betamcherla hills **(**B) **(**15°25′18.49″ N, 78°05′6.20″ E) and the third section is the Kottala hills **(**C) **(**15°27′36.68″ N, 78°08′34.30″ E). The limestone quarry of Betamcherla section is about 21 km NW side and the road cut Kottala section is about 18 km NW from the town of Banaganapalle. The studied area is mapped, logged and sampled systematically. Measured sections provide crucial information on the spatial and vertical variation of lithofacies. Carbonate samples are collected from section **(**A) **(**15°18′ 45.00″ N, 78°07′ 35.76″ E) of Patapadu-Yaganti hills for geochemical analysis **(**Major, Trace and REE analysis). These all data are further used to depict the depositional environment of the Narji Formation within the studied region.

1.11 METHODOLOGY

The Narji outcrops are examined by sidewise mapping and vertical logging of sections across two- and three-dimensional exposures of the formations. Identification of suitable section has been determined through the study of quadrangle map **(**57 I), topographic maps **(**57 I/3 and 57 I/4) and google earth.

The study area covers the limestone query **(**15°25'18.49" N, 78°05'6.20" E) and small hillocks in the road cut section **(**15°18’45.00’’N, 78°07’35.76’’E) and **(**15°27'36.68" N, 78°08'34.30" E) having distance about 20km apart from Bagannnapalle –Betamcherla area Kurnool District, Andhra Pradesh.

Methodology widely covers the following parts

I. Identification of lithofacies and sedimentary structures from several dispersed sections.
II. Diagenetic alteration within the various lithotypes;
III. Geometry of stylolite with relationship with bedding plane
IV. Petrographic and geochemical studies of selected samples from chosen section.
V. Construction of 3-D block diagram to incorporate the facies data.

The **field study** typically consists with

I. Identification of base of the Narji Formation.
II. Lateral tracing and logging of individual layers of the Narji Formation along dip direction with a stretch of around 300 m along the strike.
III. Identification of marker bed.
IV. Identification of lithological assemblages and their repetition through time.
V. Record of lateral facies variation of the major lithological units.
VI. Study of limestone including structures, grain size variation etc.

VII. Stratigraphic sequence building which includes establishing boundary, keeping stress on contact relationship; grain size distribution; replacement character etc.

VIII. Organized collection of samples for geochemical **(**fresh sample needed) and petrological analysis.

The **laboratory study** includes:

I. Sorting of representative samples

II. Thin section preparation for petrographic analysis

III. Sample preparation and analysis for geochemical studies

IV. Construction of lithologs and block diagram.

I. Sorting of representative samples: Fresh, unweathered samples are first sorted for preparation of thin sections and geochemical analysis.

II. Thin section preparation: For preparation of thin section samples are reduced into small slices. Section perpendicular to bedding is best suited for this purpose. Each sample is mounted on a glass slide after preliminary grinding. The sample is then further grinded and polished to bring to a thickness of 0.03 mm. The thin section is covered with a cover slip to avoid dust contamination and oxidation

III. Sample preparation and analysis for geochemical studies: -For geochemical analysis to remove the contamination all the samples are cleaned throughout with distilled water. This is followed by subsequent air drying, powdering in a mortar and finally sieved through a 200 ASTM mesh. Major element concentrations are obtained by a Bruker model S4 Pioneer sequential wavelength – dispersive X-ray fluorescence **(**XRF) spectrometer and the trace and rare earth elements are analysed by high resolution inductively coupled plasma mass spectrometer **(**HR-ICP-MS) in which JLS-1 is used as the standard. At first 50 mg of each sample is taken in Savillex vessels and with that 10 ml of 7:3 HF – HNO_3 acid mixture

is added. The vessels are then tightened and placed on the hot plate at 150º C for 50 hours. After that, the vessels are opened and a single drop of $HClO_4$ is added with the mixtures which are further evaporated to near dryness at 160º C. The rest of the residues of each vessel are dissolved by adding 20 ml of 1:1 HNO_3-Milli-Q water and placed on the hot plate for 30 to 45 minutes at 100º C to dissolve all suspended particles. Subsequently, Rhodium solution **(**in an amount 5 ml) is added as an internal standard to each vessel and the volume is raised up to 250 ml by adding Milli-Q water. This solution of each sample is stored in HDPE **(**High Density Polyethylene) bottles. 5 ml of this solution again mixed with 50 ml Milli-Q water **(**1:10 ratio) and stored in Eppendorf tubes for analysis. The analytical precision of the geochemical data is better than 5%RSD.

IV. Construction of lithologs and block diagram: -Lithologs, composite lithologs have been drawn in CorelDRAW software with a purpose to identify the spatial and vertical variations of lithofacies within the study area of Narji Formation. 3D block diagram also draws in CorelDRAW software to elucidate the deposition of Narji Formation.

FIGURES AND TABLES

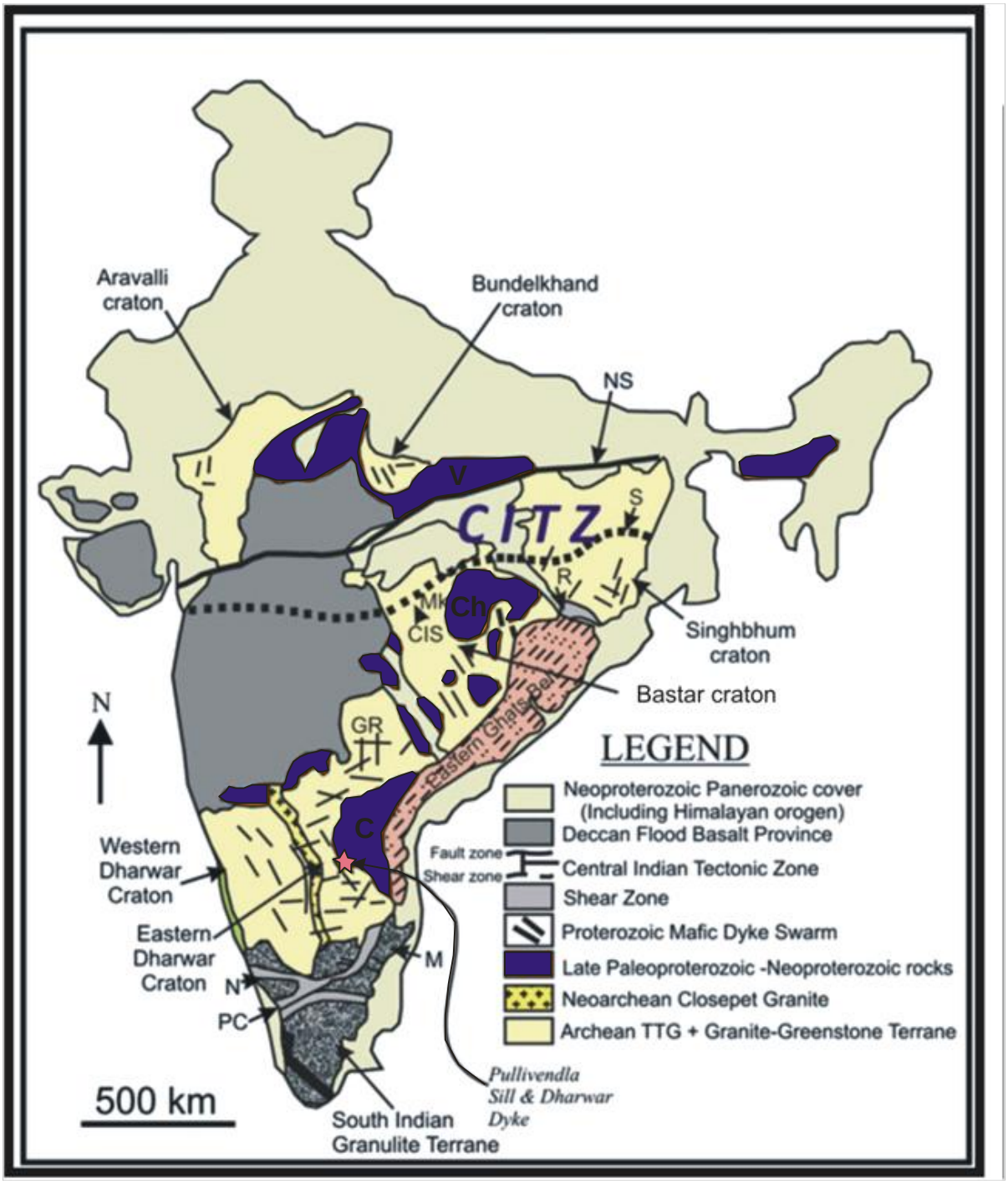

Fig. 1.1 Generalized geological map of Peninsular India showing the major cratons and various dyke swarms intruding those cratons (modified after **Meert et al., 2011**). CITZ- Central Indian tectonic zone, NS- Narmada-Son lineament, GR- Godavari rift, C- Cuddapah Basin, V- Vindhyan Basin, Ch- Chhattisgarh Basin.

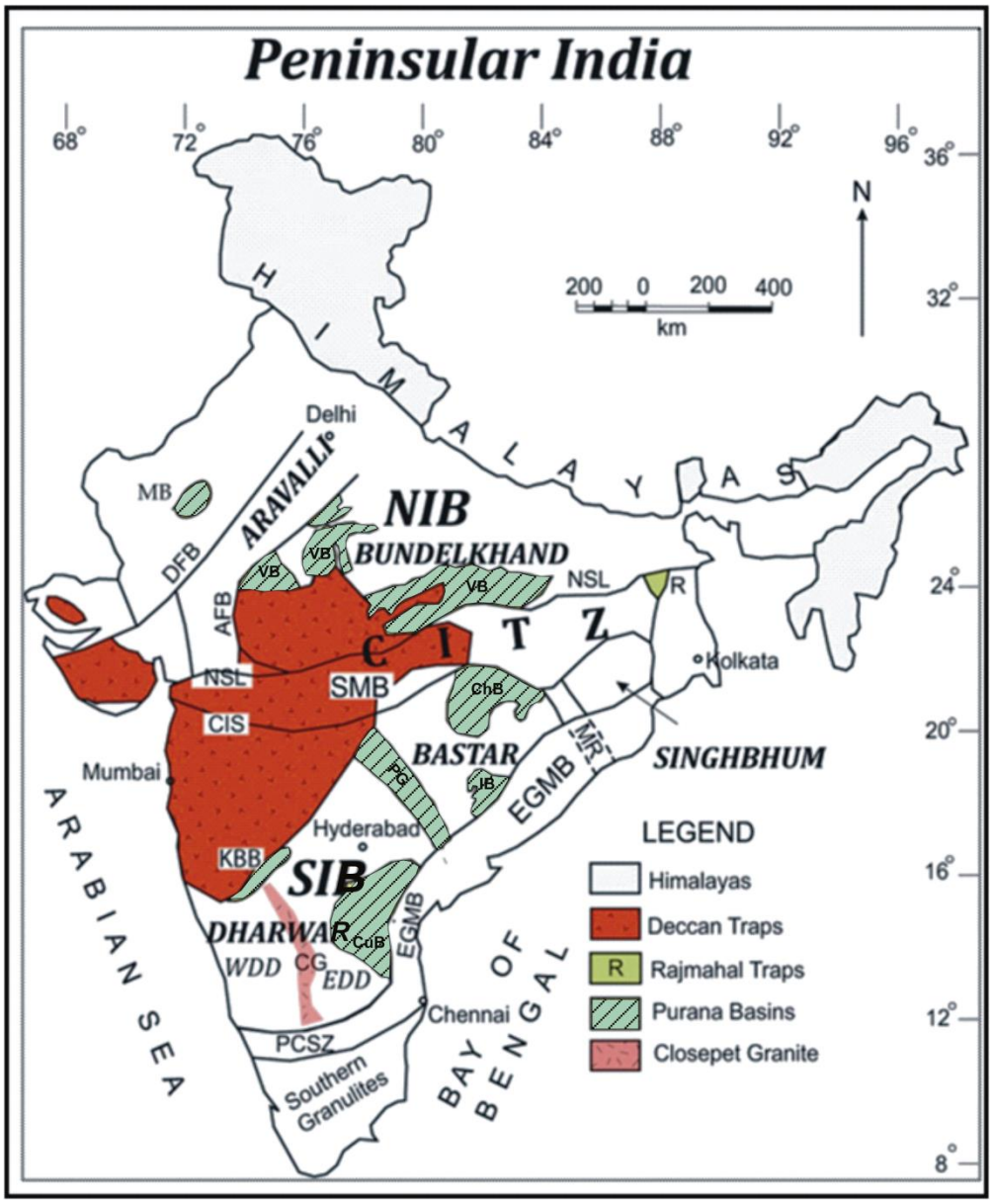

Fig. 1.2 Generalized tectonic map of the Indian subcontinent including Purana basins, cratonic regions and fold belts (modified after **Meert and Pandit, 2015**). VB- Vindhyan Basin, PG- Prahnita-Godavari Basin, ChB- Chhattisgarh Basin, CuB- Cuddapah Basin, KBB- Kaladgi-Bhima Basin, MB- Marwar Basin, IB- Indravati Basin, EDD- Eastern Dharwar Craton, WDD- Western Dharwar Craton, MR- Mahandi Rift, R- Rajmahal trap, CG-Closepet Granite, SIB- South Indian Block, NIB-North Indian Block, AFB- Aravalli Fold Belt, DFB- Delhi Fold Belt, EGMB- Eastern Ghat Mobile Belt, SMB- Satpura Mobile Belt, NSL- Normada-Son lineament, CIS- Central Indian Suture, PCSZ- Palghat-Cauvery Shear Zone

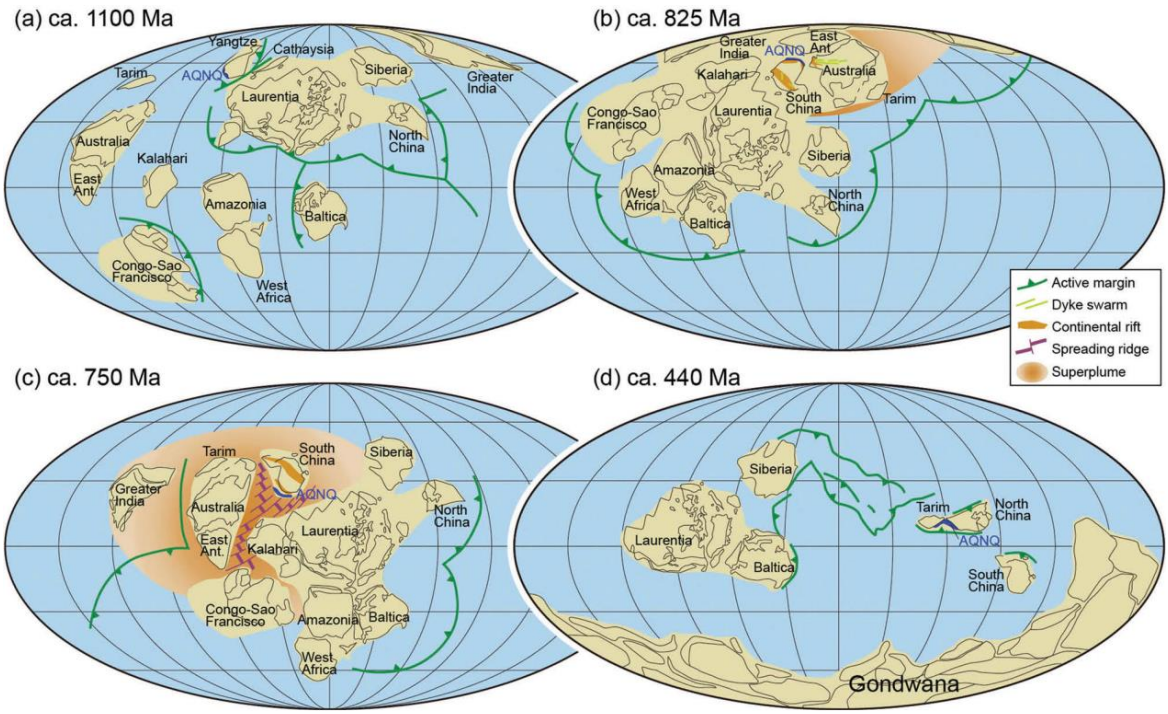

Fig. 1.3 Illustrations showing the processes of amalgamation and breakup of Rodinia (modified after Li et al., 2008; Li, 2011) (a) ca. 1100 Ma; (b) ca. 825 Ma; (c) ca. 750 Ma; (d) ca. 440 Ma.

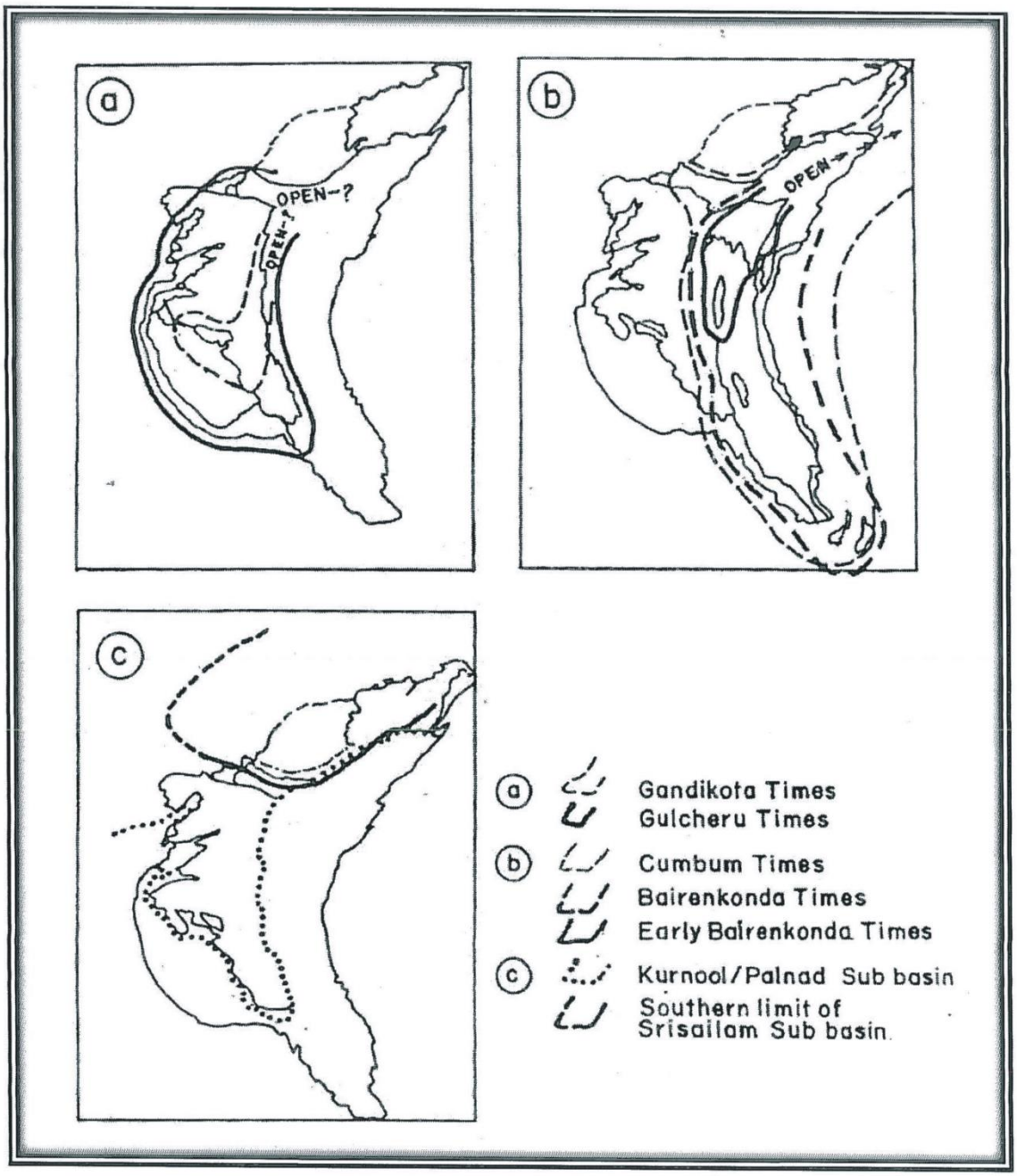

Fig. 1.4 Inferred Cuddapah Basin Limits. The great similarities for the crescent shaped boundaries of all the Formations of Cuddapah Basin have resulted from a land-locked condition of the basin with a probable connection to the open sea in the North East (after **Murthy, 1981**)

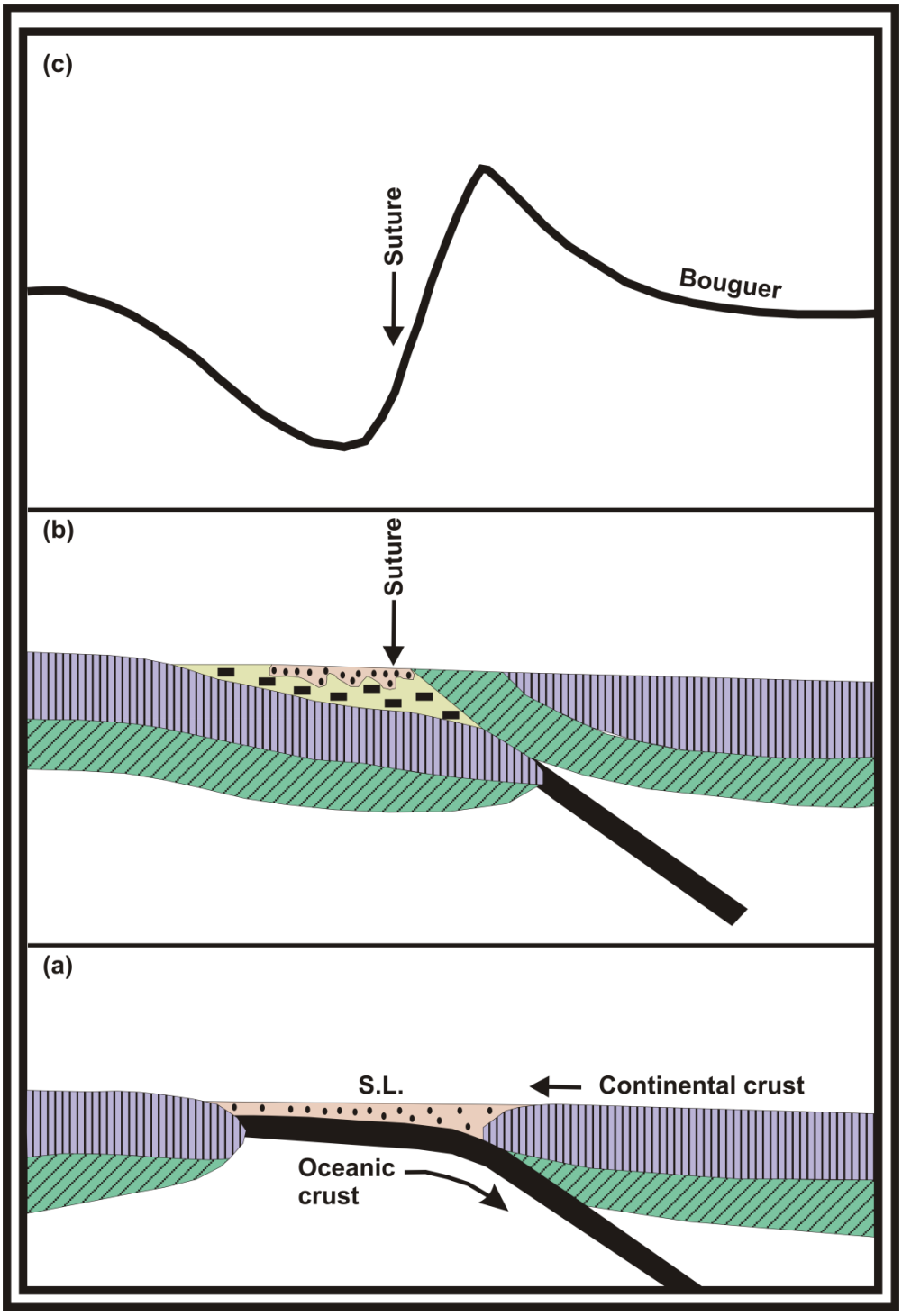

Fig. 1.5 (a) Impending collision between two continents; (b) Postulated geometry produced by collision; and (c) Theoretical Bouguer anomaly calculated for such crustal structure (modified after **Singh and Mishra, 2002**)

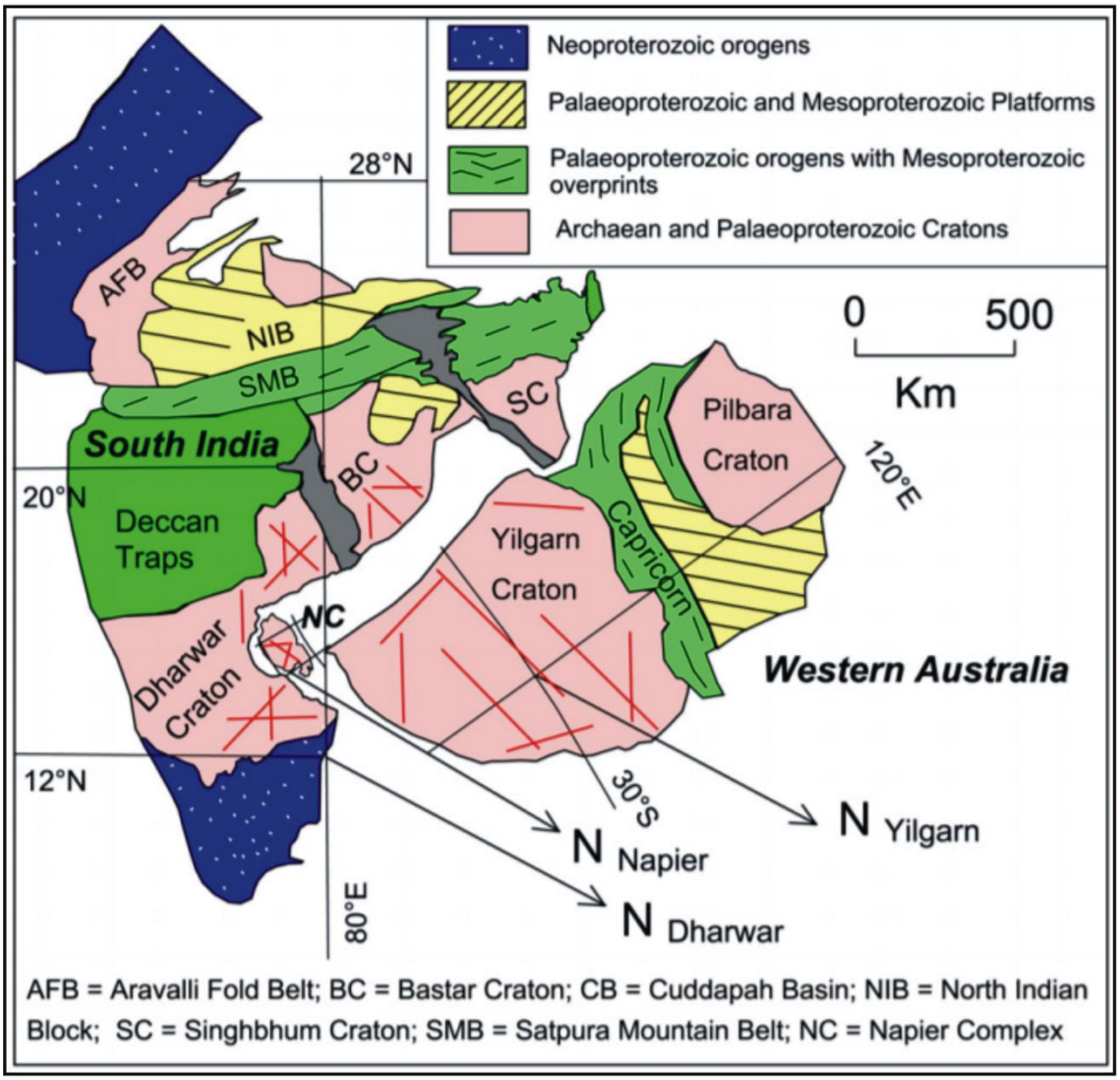

Fig. 1.6 Configuration of an Archaean–Paleoproterozoic supercontinent "SIWA", with the Napier Complex located at the position of the Cuddapah basin of India and the Yilgarn craton at the eastern coast of India. Representative basic dykes of the Napier Complex, South India (SI), and the Western Australia (WA) are shown by red colour. Arrows marked as N_{Yilarn}, N_{Napier} and $N_{Dharwar}$ are north directions for ~2400 Ma for the Yilgarn craton, the Napier complex and the Dharwar craton, respectively (modified after **Mohanty, 2011**)

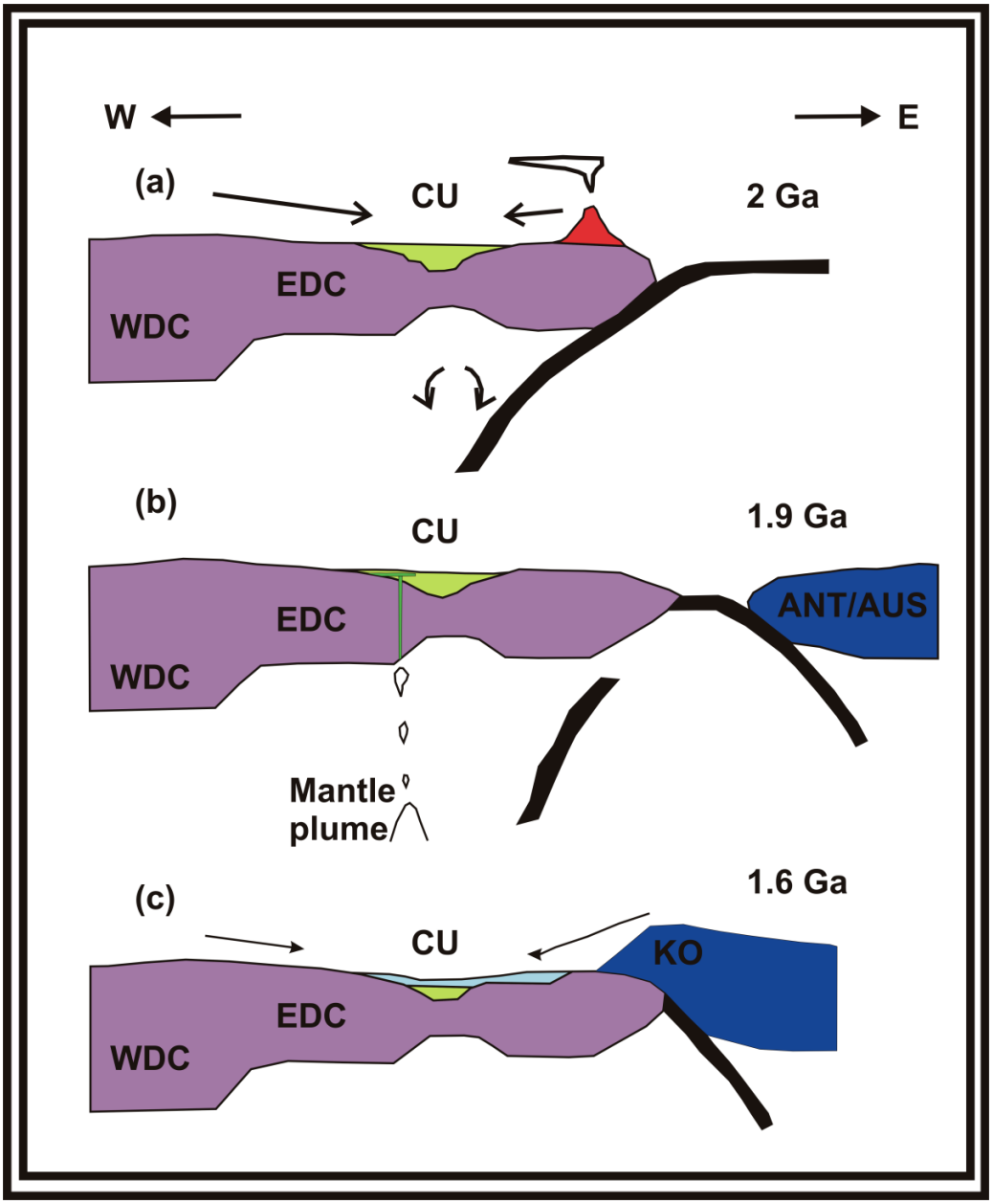

Fig. 1.7 Panel diagrams showing geodynamic evolution of the Cuddapah basin. Stage (a): Opening of Papaghni sub-basin as a back arc basin at ~2 Ga, as a result of westerly directed subduction along eastern Indian continental margin. The newly opened basin received detritus from Dharwar craton during the initial stage of Gulcheru sedimentation and during later stages (Vempalle Formation and Chitravati Group) received detritus and dissolved load also from a magmatic arc situated southeast of depositional basin. Stage (b): Extinction of magmatic arc and change of subduction polarity at ~1.85 Ga, possibly because of plume activity. Sedimentation in Papaghni sub-basin probably ceased after this episode. Stage (c): The intervening oceanic plates are consumed and possibly Napier block of Antarctica collided with eastern Dharwar craton at ~1.6 Ga, giving rise to Krishna orogeny (The Cuddapah basin evolved as a foreland basin and post-Papaghni sedimentation received detritus mainly from the evolved orogen (modified after **Absar et al., 2016**)

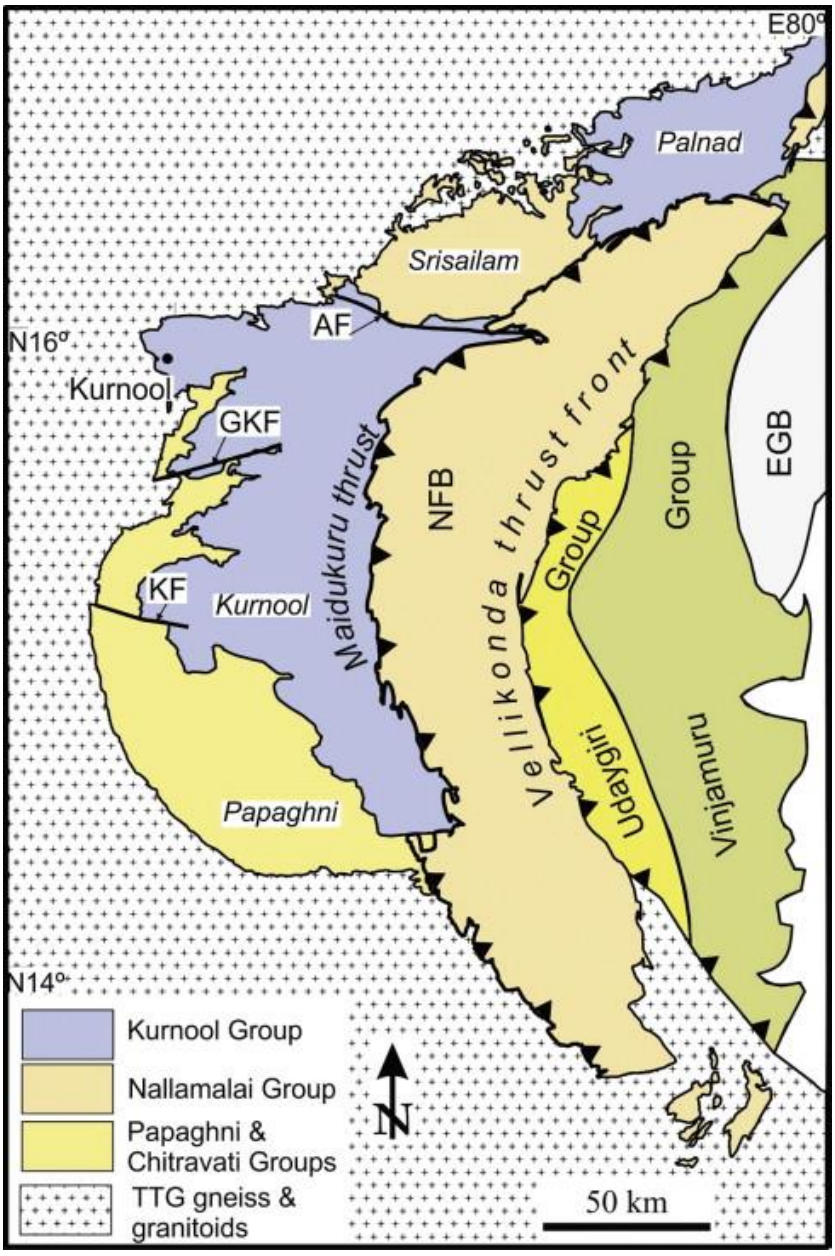

Fig. 1.8 Simplified geological map of the Cuddapah Basin (modified after **Saha and Tripathy, 2012**). Western margin of the basin is convex and developed over the Eastern Dharwar; whereas the eastern margin is concave and has a contact with Nellore schist belt and Eastern Ghat Belt

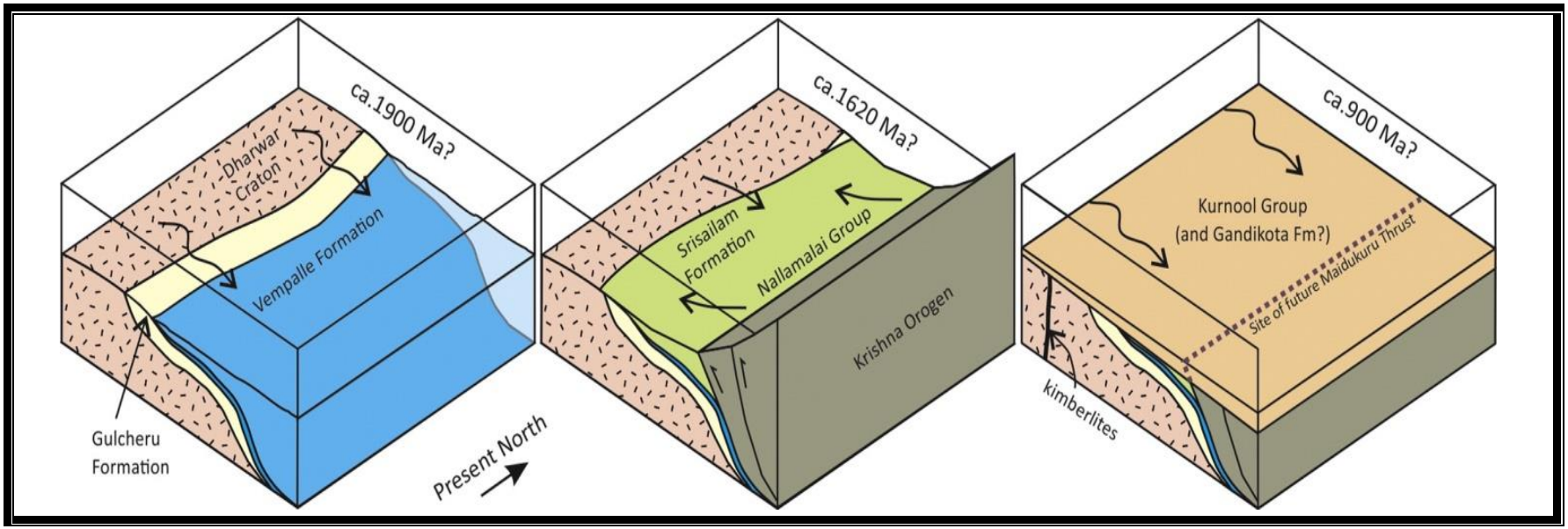

Fig. 1.9 Palaeogeographical cartoons interpreting the tectonic situation of the three main stages of basin formation. Initially, the Cuddapah Basin formed as a Paleoproterozoic rift-passive margin on the edge of the Eastern Dharwar Craton (**Collins et al., 2015**). By the end of the Paleoproterozoic, the Ongole Domain (and Enderby Land in Antarctica) collided with the passive margin, whence it evolved into a foreland basin in front of the resulting Krishna Orogen. After a period of erosion, the latest Mesoproterozoic to Neoproterozoic Kurnool Group reflects small-scale tectonic movements craton ward of the Tonian Eastern Ghats Orogen and erosion of the Eastern Dharwar Craton.

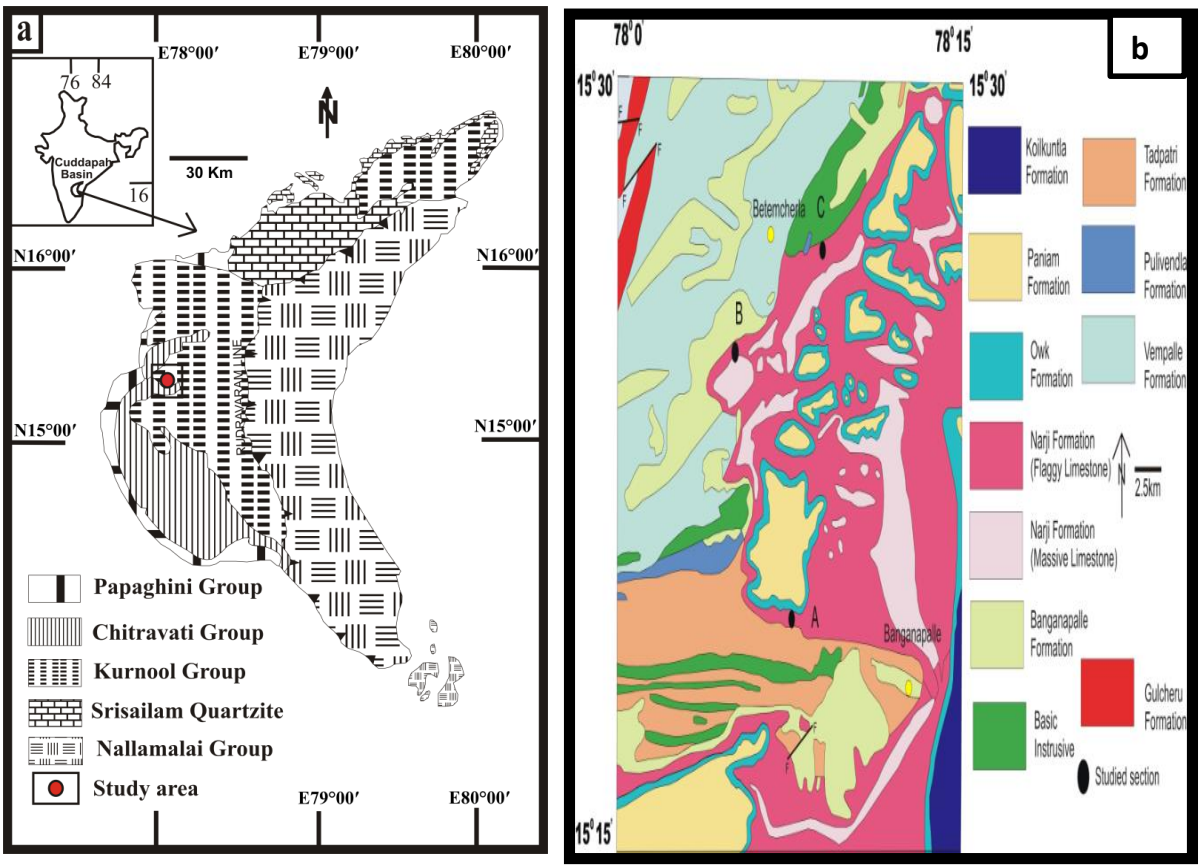

Fig. 1.10 Geological maps of the study area (a) Generalized geological map of the Cuddapah Basin (modified after Geological survey of India 1:2 million scale map, 1998); (b) Detail of the north-western Cuddapah Basin showing locations of the measured sections investigated in this study (modified after Survey of India Quadrangle map number 57E, 1:250000 scale.

Table 1.1 Detailed stratigraphy of the Cuddapah Basin (modified after **Saha and Patranabis-Deb, 2014**)

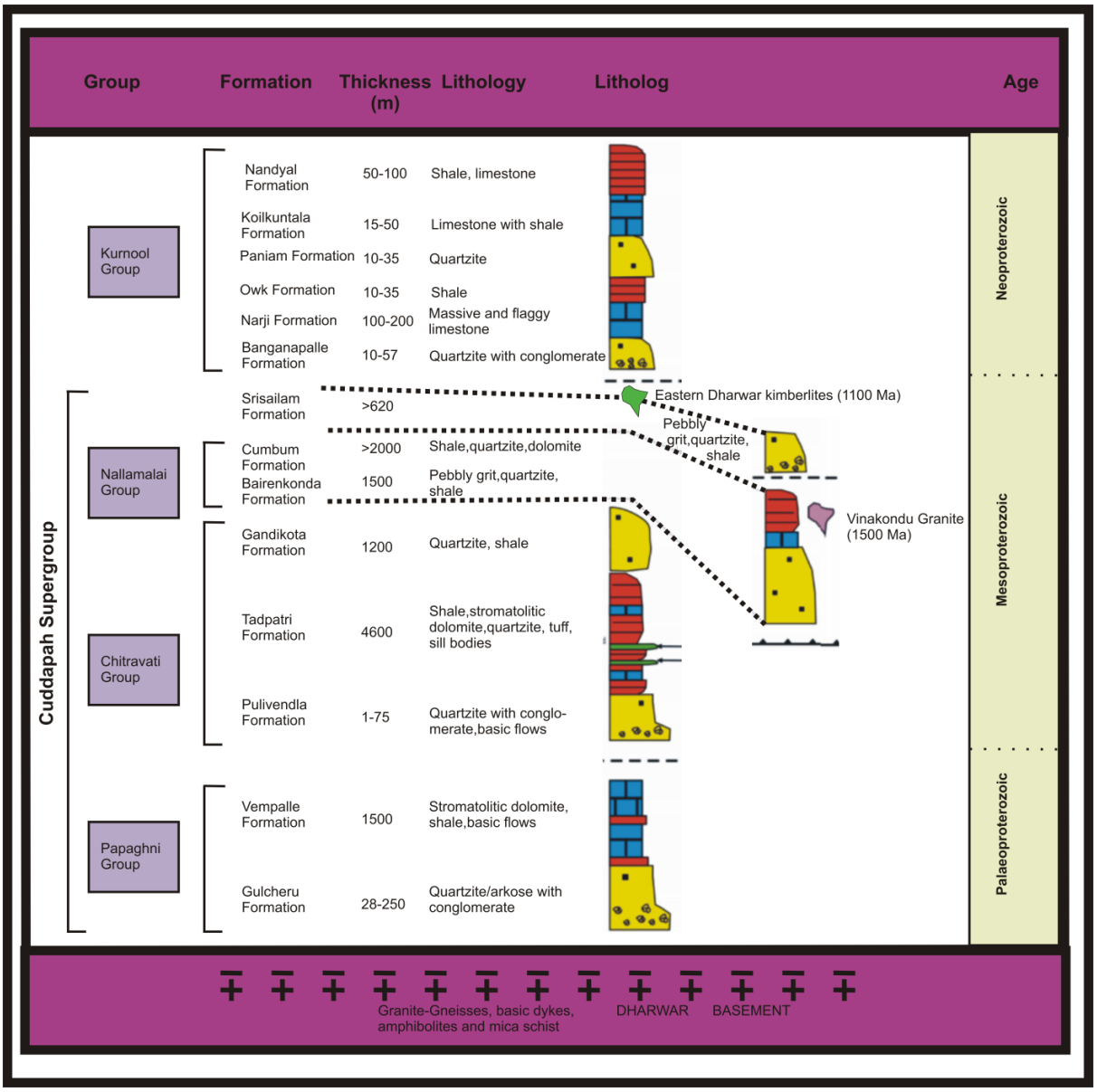

Table 1.2 A brief summary on the ages of different Formations from Kurnool Group

Sl. No.	Related work with references	Proposed age of Kurnool Group
1	Carbonate xenolith (from Bhima or Kurnool?) in the kimberlite of 1090 Ma from Siddanapalli **(Dongre et al., 2008)**	Mesoproterozoic or older than 1090 Ma.
2	1.3-1.4 Ga lamproite (detrital zircon age) within the Tadpatri shale **(Joy et al., 2012).** Suggest these lamproites as source of diamond for Banganapalle Quartzite. Cf**., (Kumar et al, 2021).**	Mesoproterozoic (1.3-1.4 Ma) or later
3	Carbonaceous remains from the Owk Shales in Kurnool basin **(Sharma and Shukla, 1999)**	Neoproterozoic
4	Single near-concordant age of 913±11 Ma **(Collins et al., 2015)** for detrital zircon from Paniam Quartzite	Neoproterozoic
5	Discussion on the age of Kurnool Group in the volume Geology of India **(Ramakrishnan and Vaidyanathan, 2008)**	Neoproterozoic
6	Diamonds in Banganapalle Quartzite suggested to have derived from ~1090 Ma **(Kumar et al., 1993)** old kimberlite pipes west of the basin margin **(Tripathy and Saha, 2013).**	Neoproterozoic i.e., maximum age younger than ~1090 Ma
7	980±110 Ma (Rb–Sr age, **Crawford and Compston, 1973)** of dolerite sills intruded within basement granitoid and overlain by the Kurnool Group	Neoproterozoic (at least after 980 Ma)

8	Palaeomagnetic studies **(Goutham et al., 2006)**	Riphean-Vendian boundary (~700Ma)
9	Helically-coiled microfossils (Obruchevella sp.) and Organic walled microfossils from Owk Shale **(Sharma and Shukla, 2012; Shukla et al., 2020)**	Ediacaran age (Late Neoproterozoic; 635 Ma to 541 Ma)
10	Occurrence of worm burrows in the Narji carbonate sequence **(Vijayam, 1967)**	Ediacaran age
11	Bioturbation structures from the Narji **Formation (Arya and Rao, 1979)**	Late Proterozoic age
12	Palaeontological studies **(Gururaja et al., 2000)**	Precambrian-Cambrian boundary age
13	Early Palaeozoic microplankton in the Kurnool basin **(Salujha et al., 1972)**	Early Palaeozoic age

CHAPTER-2

GEOLOGICAL SETTINGS AND STRATIGRAPHY

2.1 REGIONAL GEOLOGY AND STRATIGRAPHY

King (1872) has first given the four-fold classification **(Table 2.1)** which described the lithostratigraphy of the Cuddapah Basin. Later on, no detailed work has been carried out for the last 60 years. Thereafter (**Pascoe, 1950)** proposed a four-fold classification. Later (**Narayanaswami, 1966)** represented the tectonic framework and the revised it with fivefold classification. Cheyair Group with Nagari Quartzite and Pullampet Formation conformably overlies above the Chitravati Group and separated from the overlying Bairenkonda Quartzite with an unconformity. The volcanic activity in the Cuddapah Basin has given specific position in the stratigraphic column spatially and temporally. Several volcanic activities are also recorded in the Vemaplle –Vemula sector. **(Geological Survey of India, 1981) and also (Rao et al., 1987) (Table 2.2)** further reviewed and represented a fourfold division keeping stratigraphic code in mind. In this thesis grossly, the above-mentioned scheme is followed.

The Cuddapah Supergroup of rocks starts with the deposition of siliciclastic sediments constituting the Papaghni Group. The Papaghni Group consists of basal Gulcheru Quartzite which is siliciclastic dominant and the upper Vempalle Formation bearing siliciclastic-carbonate.

The basal Gulcheru Quartzite overlies the Archean unconformity is siliciclastic dominant and is composed of polymictic conglomerate. It is interbedded with gritty trough cross bedded sandstone grading into thin shale unit. The initiation of Gulcheru Quartzite is marked by conglomerate in the northern and central part of the western periphery of the basin. This conglomerate unit grades into sandy unit which further grades into shale unit in this part of the Gulcheru exposures. At Parnapalle- Dadithota region, the conglomerate attains maximum thickness of about 7m. Beyond Parnapalle

a thinning trend has been observed in the conglomerate unit. Whereas in other places Gulcheru formation starts with sandstone but without conglomerate. The sandstone unit gradually starts becoming thicker beyond Palkonda village and attains maximum thickness in the Guvvalacheruvu locality, which is the type area of Gulcheru Quartzite. Aeolian sediments within the Gulcheru Formation may be considered to be amongst the oldest Paleoproterozoic Aeolian sediments of the world **(Basu et al., 2014).** The Gulcheru Quartzite also contains of trace fossils **(Saha, 2006),** and organic-mat-induced sedimentary structures **(Chakraborti and Shome, 2010).** It represents the interaction between microbial communities and siliciclastic sediments in one of the oldest Paleoproterozoic intracratonic basins in India.

The transition zone in between **Gulcheru and Vempalle formation** is well marked in Kummarampalle area. It is marked by the presence of interbedding of terrigenous siltstone, cherty mudstone, calc-arenite and dolomitic siltstone. It is lying on the trough cross bedded gritty quartzite followed by the deposition of red shale. The thickness of carbonate gradually increases towards the top.

The thickness of Vempalle is about 1900 m overlying Gulcheru Quartzite (**Roy, 1947)**. The Vempalle sedimentation starts with occurrence of laminites over siliciclastic mudstone of Gulcheru Quartzite. The formation grades into alternate lime-mud layer towards thick siliciclastic mudstone layer. Thick stromatolite layer is present over the limestone horizon. It is then capped by oolite and intraformational conglomerate. At Nandemandalam area the lower part of the Vempalle formation is not exposed well due to the village but the upper part is well exposed. The upper part is sometimes disturbed by the presence of sill and dykes and volcanic intrusions. The steatite and asbestos deposits in the upper part of this formation, grades into alternate layers of small stromatolitic dolomites and mud deposition. An ideal succession which

includes dolomite, shale, mudstone, intraformational conglomerate, chert, sills of basic rocks and huge stromatolitic dolomite is thickest in this region. Dolomites in the region contain various types of stromatolites. At some places stromatolitic dolomites are present above and below the current-bedded calcareous and siliceous oolitic beds containing microfossils (**Schopf and Prasad, 1978).**

The Chitravati formation overlies the Papaghni Group. It consists of basal Pulivendla Quartzite; the Tadpatri Formation; and the Gandikota Quartzite. The Papaghni-Chitravati transition is affected by sporadic episode of mafic flows associated with sills and dykes in the underlying Vempalle Formation.

Pulivendla Quartzite unconformable overlies Vempalle Formation with paraconformity marking between them. This transition is well defined by the medium- to thick bedded well-sorted quartz arenite with thin pebble beds in the basal part which grades upwards into a coarser sandstone with trough cross bed. Their thickness is much less varying from (10-50m) but is marked by non-interrupted phase of sedimentation (**Meijerink, 1984**).

Tadpatri formation have thickness of about 4600m.It overlies Pulivendla Quartzite (Formation). It contains a continuous brown, earthy shales with intercalated limestone with chert and jasper bands. There are few dykes and sills within the Tadpatri formation having similar properties Vempalle intrusive. (**Crawford and Compston, 1973)** noted amygdaloidal basalts, ash beds, sills and intrusions consisting of gabbro and dolerite.

Tadpatri Formation is overlain by the Gandikota Quartzite**.** The contact between them is gradational from thinly bedded sand shale intercalated layer to amalgamated quartzite layer. It is mainly exposed in the east-central part of the Papaghni sub-basin as inliers. Gandikota Quartzite mainly composed of well-rounded well-sorted

medium- to coarse grained quartz arenite with large (up to 0.7m) planar tabular to large trough cross stratification and shale.

The Nallamalai Fold Belt (NFB) located in the eastern part of the Cuddapah Basin. It consists of folded and faulted metasedimentary rocks resting over the Chitravati Group. There is discordant relationship between Chitravati Group and the Nallamalai Group. It is due to thrust contact hence, the Nallamalai Group may be allochthonous in origin **(Saha and Tripathy, 2012b).** The Nallamalai Group consists of the lower sandstone-dominated Bairenkonda Quartzite is highly folded in the Nallamalai hills and the upper Cumbum Formation, consisting mainly of shales with sandstone and dolomite intercalations.

Nagari Quartzite is age equivalent to Bairenkonda Formation. In the southern part of it rests over Papaghni group and it is marked by angular unconformity between them whereas further south it is exposed over granitic basement. It mainly composed of basal oligomictic conglomerate with pebbles of quartzite dominating over chert, jasper and vein quartz set in a siliceous and ferruginous matrix.

The succeeding to **Cumbum Formation** is preserved within the synclinal and anticlinal troughs of the Nallamalai hill. This is basically an argillaceous unit with intercalations of quartzite and dolomite at various levels. Carbonate rocks occurring at various levels within this Formation are the host rocks for base metal mineralization. The Cumbum shales are mostly carbonaceous in nature with the carbon (C) varies between 0.5 to 3 wt.%. The Pullampet Formation which is equivalent to **Cumbum Formation** is more calcareous and contains beds of barite and black shales **(Mathur, 1996).** The overlying arenaceous Srisailam Quartzite is a glauconite-bearing ferruginous quartzite occurring in the form of a plateau.

The Kurnool Group (500m thick) is unconformably overlies Cuddapah Supergroup (**Fig 2.1a and 2.1b)** with a basal oligomictic conglomerate made up of subrounded pebbles of chert, jasper, quartzite, barites, black shales and ferruginous shales in the Kurnool and Palnad subbasin. The Kurnool subbasin is in the west-central part of the Cuddapah basin and lies between the northern Srisailam subbasin and the southern Papaghni subbasin. The Palnad subbasin forms the north-eastern part of the crescent shaped Cuddapah basin.

The name Kurnool Group was first coined by **(King, 1872)** after the town Kurnool. He classified the Kurnool Group into four formations as Banganapalle, Jammalanduga, Paniam and Khandair, of which Banganapalle is the oldest and the Kundair is the youngest.

Later (**Dutta, 1962)** classified the Kurnool Group into lower and upper Kurnool which further recognised a disconformity between lower Kurnool Owk shales and Upper Kurnool Panium Quartzite. He computed the total thickness of Kurnool Group as 615 m, of which lower Kurnool consisting of quartzites, limestones, shales account for about 221m and the upper Kurnool consisting of Quartzite, limestone and shale account for 394m. Subsequently 6 divisions- BQ, NL, OS, PQ, KL and NS were made.

Later, (**Meijerink et al., 1983)** divided the Kurnool Group into 3 formations, as B, P and Kundain Formation and has observed a Paracoformity between B and P Formation. He computed the total thickness of the Kurnool Group to be about 600m.

Banganapalle Quartzite is the lowermost member of the Kurnool Group. It has the basal unit of lower conglomerate bed followed successively by grit, quartzite and shale (**King, 1872**). The sequence of Banganapalle Quartzite in the type area is as follows Quartzite, Conglomerate, Shale then again followed by Conglomerate. This unit overlaps several units of Cuddapah Supergroup. Conglomerate is oligomictic,

consisting of sub-rounded pebbles of chert, jasper and quartzite. Barytes is also noticed as pebbles in the conglomerate **(Rao et al., 1987).** It is dark red, grey or brown coloured.

Narji Limestone rests conformably over the Banaganapalle Quartzite. The contact between them is sharp. The limestone is mainly massive and laminated type. The colour of the limestone varies from grey, dark grey, pinkish grey, buff, brown and green. The total thickness of Narji Limestone ranges from 120 to 180m and accounts for one-third of the total thickness of the Kurnool Group ((**Rao et al., 1987**). Structurally the Narji Limestones are very little disturbed, almost horizontal and the inclination of the strata rarely exceeds 10°. It breaks with conchoidal fracture **(Rao et al., 1987).** This limestone is of cement grade and used in industry. It is presumed that during this period the basin attained its maximum extent and depth.

The Owk shales are mostly yellow, grey, pale pink, brown and dull green coloured and are finely laminated, generally silty in nature. Owk shales are often ochreous in nature. This is very well laminated thin bedded unit consisting of silty claystone within thin beds of fine-grained quartzite (**Richards et al., 1968**). The average thickness is about 20m. The general strike is conformable with the underlying Narji limestone.

Paniam Quartzite forms the Upper Kurnool arenite member. It is divided into plateau and pinnacle quartzite. The study area is mainly plateau quartzite but typical pinnacle nature which distinguishes the Paniam quartzite from rest of the quartzite of the Kurnool Group and Cuddapah Supergroup. These quartzites rest unconformably over the Owk shales. The Quartzite is massive and compact quartzites which are mainly Orthoquartzites. Quartzites are medium to fine grained with a thickness of about 25m.

Koilkuntla Limestone, overlying the Paniam Quartzite is the carbonates of upper Kurnool. The Koilkuntla Limestone has an average thickness of about 30m and it is

dark grey coloured, flaggy in nature with pyrite crystals. This member is divided into lower siliceous limestone, middle cement grade calcareous limestone and the upper siliceous limestone **(Rao et al., 1987)**. In some places the basal limestone shows irregular dips from 40° - 50°. The basal limestone is wavy in nature with rugged surface on account of differential weathering. The high dip angles and crushing in this area are probably due to post Kurnool Thrust in the area. Highly calcareous middle strata are well bedded and yield good slabs. Towards the top, the colour of the limestone changes from grey to purple and the composition from more calcareous to more argillaceous as they are succeeded by Nandyal shales.

The Upper Kurnool argillaceous facies is represented by **Nandyal shale.** The Nandyal shale is composed of a lower shaly flag bed and an upper shaly limestone bed (**Bathurst, 1987; Rao et al., 1987**). Shales are purple, mauve, dark grey to greenish grey coloured and breaks into sharp edges (**King, 1872**). They are calcareous in nature. Nandyal shales generally show parallel lamination and devoid of current and wave formed structures. It is deposited in low energy environment. Bedding in shales varies from paper thin to relatively massive form. This can be related to the quietness of the sea bottom during or immediately after the deposition of the shales. The thickness of the Nandyal Shale varies from 100 to 300m.

2.2 BASEMENT ROCKS

Basement rocks are recorded in the SW part of Palnad Sub basin. Hornblende schist forms the oldest rock and are overlain by banded ferruginous quartzites (BFQ). This BFQ are overlain by a basal conglomerate which separates meta sediments of Archean from unmetamorphosed younger Kurnool rocks.

2.3 LITHOLOGICAL DESCRIPTION

The chief lithological units in the Kurnool Group are Conglomerate, Sandstone, Quartzite, Shale, Limestones and Dolomites. The limestones are of great economic importance in which it is utilized for the manufacture of cement and as building and road material. The lithological sequence of Kurnool Group is of Orthoquartzite-Limestone-Shale association with two cycles of sedimentation, containing two shale formations (Owk and Nandyal), two limestone formations (Narji and Koilkuntla) and two Quartzite formations (Banganapalle and Paniam). An orderly repetition of a sequence of beds or laminae occurs, suggesting a cycle or repeated recurrence of certain conditions during the deposition, such as might be related to weather, season, climate etc., such a sequence which may be repeated again and again is called a "Cyclothem". Thus, two cycles of sedimentation which commences with pebble bed/conglomerate through sandstone, quartzite, limestone and ends with shale sequence. Again, starts with pebble bed and ends with shale.

2.3.1 ARENITES

The arenites of Kurnool Group are noticed in two formations, one in Banganapalle and the other in Paniam. Banganapalle Formation which forms the basal units rests unconformably over the denuded edges of Cuddapahs, consisting of conglomerate bed followed successively by sandstone and quartzite. This formation is seen in the western margin of the basin and it does not continue southwards along the western margin nor is it exposed along eastern margin anywhere. This conglomerate is oligomictic consisting of rounded to subrounded pebbles of chert, jasper, quartz, quartzite and shale. The sandstones are generally medium grained and

ferruginous in nature, whereas fine grained white coloured sandstones are seen at several places. The quartzites of this group is of dark grey, red and brown. Paniam Quartzite forms the Upper Kurnool arenite member. The member is divided into plateau and pinnacle quartzite.

2.3.2 ARGILLITES

The argillite facies are noticed both in the lower as well as upper Kurnool, represented by Owk, and Nandyal shales respectively. The Owk shales which are younger to the Narji limestone form a continuous strip of outcrop. The Owk shales are mostly yellow, grey, pale pink, brown and dull green coloured and are finely laminated, generally silty in nature. Nandhyal shale is composed of a lower shaly flag bed and an upper shaly limestone bed. Shales are purple, calcareous in nature. Nandyal shales generally exhibit parallel lamination and absence of current and wave formed structures is observed.

2.3.3 CARBONATES

Carbonates are the major lithological unit in Kurnool Group. In the lower Kurnool's, Narji limestone represents the carbonate facies and the Koilkuntala represents the upper Kurnool. Narji limestone is divisible into lower flaggy, middle massive and upper flaggy units. The limestone is grey, dark grey, buff, brown and green in colour. The most persistent beds of the Narji limestones are the grey massive limestone and Narji calcareous flags. The carbonates of upper Kurnool are noticed in the Palnad sub basin and are termed as Koilkuntala limestone. The limestone has an average thickness of about 30m and are dark grey coloured, flaggy in nature with pyrite crystals here and there.

2.4 GEOLOGY AND STRATIGRAPHIC SEQUENCE OF THE STUDY AREA

The sediments of Kurnool Group are deposited in two isolated sub basins within Cuddapah basin with reference to their geographical position (**Rao et al., 1987**). The first one is Kurnool sub basin, located at the west-central part and the second one is termed as Palnad sub basin located in north-eastern part of Cuddapah. The two sub basins are 75 km apart, with the Srisailam Quartzite covering the gap.

Our study area of Narji Formation is part of Kurnool sub basin having thickness of about 150m.Three sections are chosen for investigation within the Narji Formation. The first section is along the road cut section (15°18’45.00’’N, 78°07’35.76’’E) of Patapadu-Yaganti hills, located around 11Km from the town of Banaganapalle in Kurnool District. The second section is around Betamcherla hills (15°25'18.49" N, 78°05'6.20" E) and the third section is the Kottala hills (15°27'36.68" N, 78°08'34.30" E). Both the second and third section is located about 20km from the town Banaganapalle in Kurnool District, Andhra Pradesh. The first section Yagantipalle lie unconformable over Tadpatri Formation, the second section Betamcherla lies over Bagannapali Formation whereas the third section of Kottala lies nonconformable over igneous dyke.

The Narji Limestone within the Kurnool Sub-basin is deposited conformably over the clastic rocks of the Bagannapali Formation. The lower portion of the Narji Formation mainly consists of massive grey limestone with occasional development of siliceous rich layers which is followed by siliceous pink and purple laminated limestone with thin lenticular lenses of gritty ferruginous sandstone (**Patranabis Deb et al., 2012**). The occurrence of pyrite and chert bearing bluish-grey to dark grey high graded mas-

sive limestone along with alternating laminated siliceous limestone layer is also very common within the Narji Formation. The development of thin and discrete beds of intraformational conglomerate is also recorded within the Narji limestone (**Patranabis Deb et al., 2012**). The massive and the laminated units show symmetrical distribution throughout the sections till it show a gradational contact with the yellowish Owk shale towards the top. The layers are mostly separated by paleokarstic surfaces.

2.5 MAFIC IGNEOUS ACTIVITY AFFECTING THE CUDDAPAH

Numerous Precambrian mafic dykes cross cut the Dharwar craton. The major igneous suites associated with the Vempalle and Tadpatri Formation is dolerite, picrite and gabbro sills, basaltic flows, ignimbrites and ash-fall tuffs in the western part of the basin. Dolerite sills are found in the Nagari quartzite, Pullampet and Cumbum Formations. Also, kimberlite dikes and syenite stocks are present in some part of Cumbum. Large exposure of granite/gneiss within domal structures of the Cumbum Formation occurs as intrusive into the sedimentary pile or as reactivated portions of the basement. The volcanogenic bedded barite deposits associated with barium-rich acid volcanics in the Pullampet Formation is most significant and economically important volcanic episode in this basin.

The Vempalle and Tadpatri Formations are marked by basic flows and sills which may represents as cone sheet with a centre within the basin while their counterparts represented by radial dykes outside the basin. The igneous intrusion shows flow banding and comprises of plagioclase, clinopyroxene and olivine. Chemically these sills and basic flows are similar to the primary picritic magma having a mantle source.

The picrite-gabbro sill of Pulivendla is found to be distinctly unique in being a prototype.

The first phase of igneous activity in this basin is represented by the basic volcanic activity in the Vempalle period (**Fig. 2.2**). The basic and acid volcanic activity along with sedimentation in the Tadpatri Formation represents the second phase. The extensive igneous activity in the form of intrusion of dolerite, gabbro and picrite sills in the Vempalle and Tadpatri Formation represent the third phase of igneous activity of the basin. The Barium and iron oxide rich phase in the Cumbum Formation represents the fourth phase of igneous activity in the Cuddapah basin. The basic igneous activity in the Nagari Quartzite, Pullumpet and Cumbum Formation suggests the fifth phase of igneous activity while the intrusion of granite into the Cumbum Formation North eastern part of the basin represents the sixth and final phase of igneous activity.

Vempalle Formation is the only stratigraphic unit that contains a sequence of lava flows (**Anand et al., 2003**). The upper surfaces of flows show amygdales showing sub aerial exposures filled with epidote, calcite and zeolite. The thickest lava flows are recorded in the southern part of the basin at Pulivendla, Vempalle and Animala (up to 50m). At Pulivendla, a basic lava flow conformably overlies the Vempalle Formation dolomites and marks the highest stratigraphic unit of the Papaghni Group. At Malkapuram, ~15 km east of Dhone, lava flows are recorded in the northern part of the basin. Here, hydrothermally altered basaltic lavas form ~50m high ridge overlying stromatolitic dolomites and appear to have pillow shapes with chert infillings. Bethamcherla and Gattimanikonda (**Fig. 2.2**) are the northernmost exposures of lavas in the Cuddapah Basin having similar in appearance and

composition to the Animala lava flows and reach a total outcrop thickness of ~50-100 m (**Anand et al., 2003**).

SW part of the Proterozoic Cuddapah basin of Eastern Dharwar craton has thrown light into two significant phases of pyroclastic volcanic activity associated with the Vempalle Formation in Papaghni subbasin. Occurrence of a significant pyroclastic agglomerate at the contact zone of Vempalle dolomite of Papaghni Group and Pulivendla quartzite of Chitravati Group represents a significant event of the mafic phase of pyroclastic volcanic activity, while the finely laminated felsic tuff within the intercalated reddish siltstone, chert and dolomite sequence in the lower part of Vempalle Formation represents the felsic phase of pyroclastic activity (**Sesha Sai., 2014**). The pyroclastic agglomerate zone indicates pyroclastic volcanism wherein the highly vesicular rock with rounded basalt clasts often show embayed contact of welded nature with the matrix, represents a significant tectono-magmatic event of explosive volcanic activity that is contemporaneous with the culmination of the carbonate precipitation of Vempalle dolomite and marks the termination of sedimentation in Papaghni Group in southwestern part of Cuddapah basin during Paleoproterozoic times.

Tadpatri Formation has numerous mafic-ultramafic sills exposed at different stratigraphic levels having the highest thickness of about 200m. It is highly differentiated, extends along the western margin of the Cuddapah Basin and intrudes stromatolitic dolomites and shales of the lower Tadpatri Formation. Relatively thin (~20m), single gabbroic and basaltic-doleritic sills occur higher up in the sequence (**Anand et al., 2003**).

The Cumbum Formation intruded by two small (25-30m in diameter) syenite plugs, at Racherla and Giddalur, in the central part of the Cuddapah Basin (**Fig. 2.2**). These

plugs are highly resistant to erosion compared to the surrounding shales. The syenite mainly composed of pink phenocrysts (5-10mm) acting as phenocryst with groundmass of K-feldspar. They have also undergone extensive hydrothermal alteration. At Chelima and Zangamarajupalle, the Cumbum Formation is intruded by Lamproite dykes (**Fig. 2.2**). Most probable they are contemporaneous with kimberlites that outcrop in the Dharwar Craton (**Chalapathi Rao et al., 1996**) and Cuddapah Basin syenite intrusions.

The Kurnool basin also experienced fewer igneous activities. The first report on tuff beds is taken from the Owk Shale in the Proterozoic Kurnool subbasin in southern India is presented by **(Saha and Tripathy, 2012a).** The rhyolitic to rhodacitic tuffs, overlying shelfal limestones formed at depths below storm wave base, have rheomorphic features indicating viscoelastic flow, and showing geochemical signatures of rhyolitic to rhyodacitic unwelded to welded tuffs, which is having similar features from other Proterozoic intracratonic basins like Vindhyan and Chhattisgarh basins in India.

Major igneous suites associated with Vempalle and Tadpatri Formations in the western part of the basin are dolerite, picrite, sills, basaltic flows, ashfall tuffs **(King, 1872; Rao et al., 1987)** and in the eastern part of the basin dolerite sills, kimberlitic dykes and syenite stocks are found **(Rao et al., 1987)**

The igneous activity associated with Cuddapah Basin can be sub-divided into six stages. The stages are described below:

Stage A: Sub-aerial eruption of basic lava flows after the deposition of Vempalle Formation;

Stage B: The volcanic activity represented by fine-grained basic rocks and tuffs within Tadpatri Formation;

Stage C: Intrusion of sills of picritic and doleritic composition into the Vempalle and Tadpatri succession marks;

Stage D: The barium and iron-oxide rich volcanic activity which was contemporaneous with the Pullampet/Cumbum Formation;

Stage E: The intrusion of basic dykes and alkaline rocks into the rocks of Nallamalai Fold Belt;

Stage F: Intrusion of granitic rocks into the Nallamalai Basin.

2.6 MAFIC DYKE SWARMS

Three different sets of dyke swarms transect the Dharwar craton having different trends, frequencies and episodes during Paleoproterozoic. They are emplaced before or during the formation of the Cuddapah basin (**Murthy et al., 1987; Mohanty, 2011**; **Fig. 2.3 and 2.4).** One set is almost parallel to the regional schistosity and gneissosity (NNW-SSE). The second set perpendicularly cut the first set. The third set cut across the second set at an angle of 45º. Although several such dyke swarms are found, three most prominent one occurs: (i) those to the southeast of the Cuddapah basin, (ii) dyke swarms around Bangalore in the EDC and (iii) those around Tiptur in WDC. Nature of these dykes are segmented echelon and occasionally arcuate. The dyke swarms present around the margin of the basin are dolerite-gabbro, although amphibolite, peridotite and syenite dykes are also present. Eastern margin of the basin is mostly devoid of dykes except few dolerite and lamprophyre dykes in the east-central and northern parts of the basin. At least five sequences of dyke emplacement have been distinguished during a time span of ~ 2100 to 600 Ma within 20 to 50 km around the margin of the Cuddapah basin. The oldest dyke groups, oriented in N-S, E-W, and WNW to NW directions are tholeiitic, and are older than 1700 Ma. Other

dyke groups, oriented WNW to NW, NNE to ENE, and N-S, are partly tholeiitic and partly alkaline, and could fall within the time range of 1700 (+) to 600 Ma. Paleo-Mesoproterozoic intracratonic Cuddapah Basin consist of dyke swarms are considered to be the result of thermal events responsible for its initiation and development (**Rao, 2005**).

Recently, **(Belica et al., 2014)** reported new paleomagnetic and geochronologic results from the Dharwar craton (south India) from 2.37 to 1.88 Ga. The presence of a ~85,000 km radiating dyke swarm with a fanning angle of 65° is confirmed within Peninsular India at 1.88 Ga. North of the Cuddapah basin the dykes are oriented NW-SE and progress to an E-W orientation further south, converging at a focal point southeast of the basin.

2.7 STRUCTURAL SETTING

The rocks of Cuddaph and Kurnool group gently dip easterly. **(Narayanaswami, 1966)** was the first to tell first-order folding involving the whole Cuddapah Basin, to form an 'asymmetrical synclinorium', with a gently dipping western limb and intensely folded eastern limb.

The NNE-SSW strike in the northern parts of the basin swings through an N-S trend in the central parts, to NNW-SSE orientation in the south. The Rudravaram line divides the Cuddapah basin into two broad structural sectors **(Meijerink et al., 1984 and Fig 2.5).** The western part of this line is gently deformed, except in the vicinity of cross-faults, and exposes the 'stratotypes' of the various stratigraphic units. Eastern part of this up to the eastern thrust margin of the Cuddapah basin, the sediments are intensely deformed, and this arcuate belt is recognized as the Nallamalai Fold Belt (NFB) **(Fig. 2.6).** The intensity of deformation increases progressively eastwards, and

four, sub-parallel zones having typical structural characters have been recognized by **(Meijerink et al., 1984)**. They are divided into (a) monoclinal structures, (b) low-amplitude, harmonic folds, (c) disharmonic folds and (d) tight, isoclinal folds, successively from west to east in the NFB.

The sedimentary units of the Cuddapah and Kurnool Formation show gentle dip (5º-15º) easterly. **(Narayanaswami, 1966**) presented the tectonic framework of the basin. He was the first to mention the first-order folding which involve the whole Cuddapah Basin, to form an 'asymmetrical synclinorium', with a gently dipping western limb and intensely folded eastern limb.

The strike of the basin gradually changes from NNE-SSW strike in the north to -S trend in the central parts, to NNW-SSE orientation in the south. The Rudravaram line divides the Cuddapah basin into two broad structural sectors. The western part of this line is slightly deformed except in the vicinity of cross-faults, and exposes the 'stratotypes' of the various stratigraphic units. In the eastern part of this line till the eastern thrust margin of the Cuddapah basin the sediments are severely deformed, and this arcuate belt is recognized as the Nallamalai Fold Belt (NFB) **(Fig. 2.6).** The intensity of deformation gradually increases eastwards. Four, sub-parallel zones having typical structural characters have been recognized by **(Meijerink et al., 1984).** These zones are (a) monoclinal structures, (b) low-amplitude, harmonic folds, (c) disharmonic folds and (d) tight, isoclinal folds, successively from west to east in the NFB.

The Nallamalai Fold Belt (NFB) is situated in proximity and west of the southern part of the Eastern Ghats belt (Krishna province), can be comparable to external part of an orogen. A number of faults like Gani-Kalva and Kona faults in the western part of the basin are identified cutting across undeformed Papaghni sub-basin (**Narayanaswami,**

1966; Tripathy and Saha, 2015). A strike-slip to extensional tectonic regime is indicated through fault-slip analysis from lower Cuddapah group of rocks in around of these faults (**Tripathy and Saha, 2015**). This further suggests that the initiation of Kurnool sub-basin is fault controlled (**Tripathy and Saha, 2013, 2015**).

The Cuddapah Basin composed of North plunging asymmetrical synclinorium. The western limb of this synclinorium is essentially gently dipped and non-folded whereas the eastern limb is characteristically highly folded, overturned and thrusted (**Narayanaswami, 1966**). Tectonic impression in the form of domal up-warps within the middle part of the Cuddapah Basin formed during the waning stage of the Cuddapah and Kurnool deposition or during subsequent orogeny due to vertical tectonism, resulted from the reactivation of deep-seated faults (**Kaila et al., 1979**).

The intra cratonic set-up and contraction deformation of the Neoproterozoic successions in the Palnad sub-basin which is situated in the north-eastern part of Cuddapah basin and similar crustal shortening in contemporaneous succession lying west of the Eastern Ghat Granulite Belt (EGGB) and Nellore Schist Belt (NSB) arc considered to be in relation to the proposed geodynamic evolution of the Rodinia and Gondwana supercontinents (**Saha and Chakraborty, 2003**). Tectonic shortening in the Palnad sub-basin (northeast Cuddapah), partitioned into top-to-west northwest thrust shear, flexural folds and cleavage development under overall E-W contraction, suggests foreland style continental shortening within intracratonic set-up. A thrust sheet containing the Nallamalai rocks and overlying the Kurnool rocks in the northeastern part of Palnad sub-basin exhibits tight to isoclinals folds and slaty (phyllitic) cleavage, which can be correlated with early Mesoproterozoic deformation structures in the northern Nallamalai Fold Belt (NFB). NNE-SSW trending folds and cleavage affect the Kurnool Group and overprint earlier structures in the thrust sheet.

Thrusting of the Nallamalai rocks and the later structures may have been related to convergence of the Eastern Ghats and the East-Dharvar-Bastar craton during Early Neoproterozoic (Greenvillian) and/or later rejuvenation related to Pan-African amalgamation of East and West Gondwana.

2.8 GEOCHRONOLOGICAL CONSTRAINTS ON STRATIGRAPHIC DEVELOPMENT

Geochronological studies have been countered on the mafic dyke swarms, kimberlite and lamproites in and around the Cuddapah basin **(Crawford and Compston, 1973; Murthy et al., 1987; Kumar et al., 1993; Rao et al., 1996). Murthy et al., (1987)** have established K-Ar ages of a mafic lava flow in the Vempalle Formation to be 1841±71Ma, and tuffs in the Tadpatri Formation to be 1371± 45Ma. Sills recorded in the Tadpatri Formation are 958±35Ma and 309±29Ma old **(Murthy et al., 1987).** The Rb-Sr age determination on some of these mafic lava flows in the Vempalle Formation has yielded 1583±147Ma (**Crawford and Compston, 1973).** A lamproite dyke near Chelima in the Nallamalai Group gave an Rb-Sr age 1225±140Ma (on whole rock and Phlogopite) and the Pullivendla sills in the lower Cuddapah Supergroup gave an age of 908±110Ma **(Crawford and Compston, 1973).** The latter dates may be too young because further dating by whole rock analysis of the same sill by the Rb/Sr method has yielded an age of 1704±112Ma **(Bhaskar Rao et al., 1993).** Biotite and clinopyroxene analysed from two samples of the same sill yield an age of 1811 and 1831Ma age which may be an absolute upper age limit for sedimentation of the Papaghani and the Chitravati groups into which it intrudes **(Murthy et al., 1987). Zachariah et al., (1999)** determined the Pb, Sr, Nd, isotopic compositions on uranium mineralized and barren stromatolitic dolomite samples from

the Vempalle and Tadpatri Formations of Cuddapah Supergroup. Their analysis yielded Pb–Pb age of 1756±29Ma that is interpreted as the time of U mineralization and as a minimum age for carbonate sedimentation and dolomitization within the rocks. The folded Nallamalai Group is intruded along its eastern margin by 1573-Ma-old granite **(Crawford and Compston, 1973)** and Chelima lamproite dated around 1400Ma **(Chalapathi Rao et al., 1996).** This analysis fixes the upper age limit of the Cuddapah Supergroup. On the basis of this data set it is clear that the Papaghani Group (comprising the Gulcheru Formation and the Vempalle Formation) is Palaeoproterozoic in age. The initiation of sedimentation starts around 1800Ma and ends around 1400Ma.A brief summary on dating has been given in **Table 2.3**.

The Kurnool Group is thought to be Neoproterozoic in age. It is considered to be younger than 1140 Ma. The minimum and the maximum age of the Kurnool shales are considered to be 500 Ma(K/Ar) (Pb/Sr) respectively. The age of limestone xenolith found is considered to be late Mesoproterozoic (>1090 Ma). The upper age limit is considered to be >1.1 Ga (**Rao et al., 2010**). Previously the only age constrains available have been from fossil **(Gupta, 1998; Sharma and Shukla, 1999; Chaudhuri, 2002)** and age constrains from Cuddapah supergroup **(Rao et al., 1994; Chakraborty et al., 1999; Makintosh, 2010). Ediacaran disc has been reported from the Paniam Quartzite.** Sediments from Banaganapalle Formation, Paniam Formation and Narji Limestone have been dated detrital zircon U-Pb ages, and O and C stable isotopes. The diamond bearing Banganpalle Quartzite of Kurnool are believed to be sourced from Vajrakarur Kimberlite which has been dated as 1140 Ma **(Crawford and Compston, 1973; Sharma and Shukla, 2012).** The maximum age of the Kurnool Group is 980 Ma (Rb/Sr) and minimum age of 500 Ma(K/Ar)

(P.K,Raman., 1997; Sharma and Shukla, 2012). **Dongre et al., (2008); Bertram, (2010)** studied the minerology, major and trace element geochemistry, stable isotope studies of a limestone xenoliths which is found to be intruded in the Siddanpalli Kimberlite. It suggested Late Mesoproterozoic age (older than 1090 Ma) to the Kurnool basin. The Bhima and the Kurnool basins were the closest sedimentary rocks inferred to be inter-connected at the time of kimberlite intrusion. Helically coiled fossils from the Narji limestone and Owk Shale of the Kurnool district (**Sharma and Shukla, 2012)** assigned to late Neoproterozoic to Early Cambrian sediments.

FIGURES AND TABLES

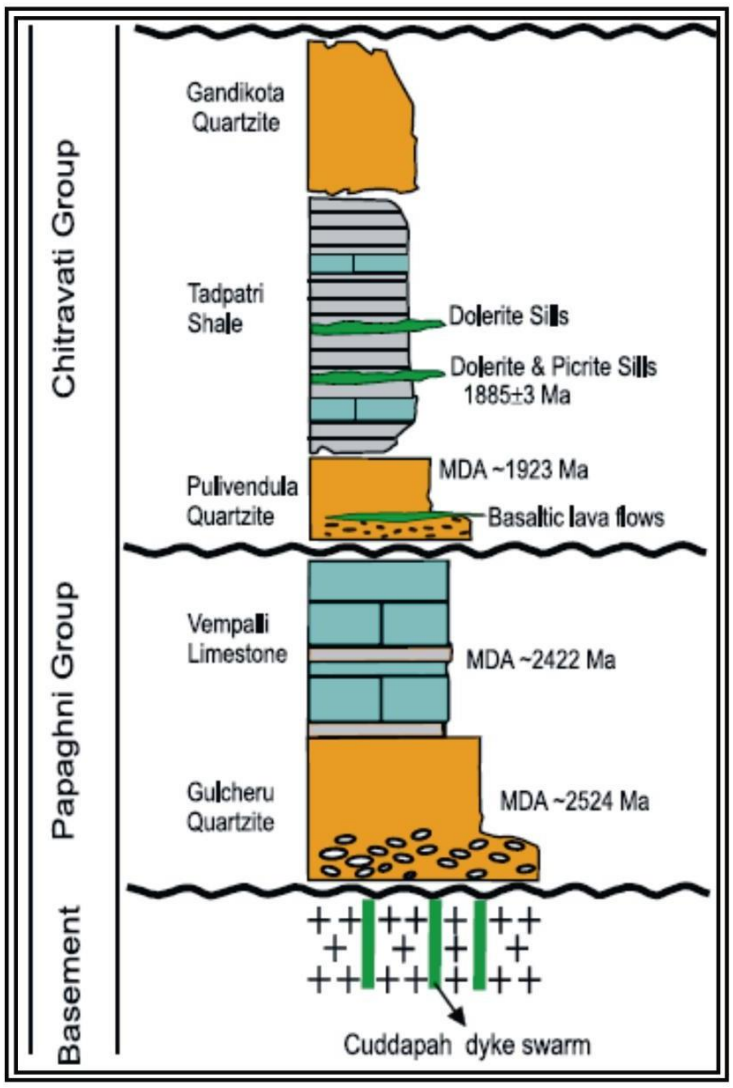

Fig. 2.1a Lithostratigraphy of the Papaghni and Chitravati groups, Cuddapah Basin, India. (After **Kumar et al., 2015**). MDA- maximum depositional age

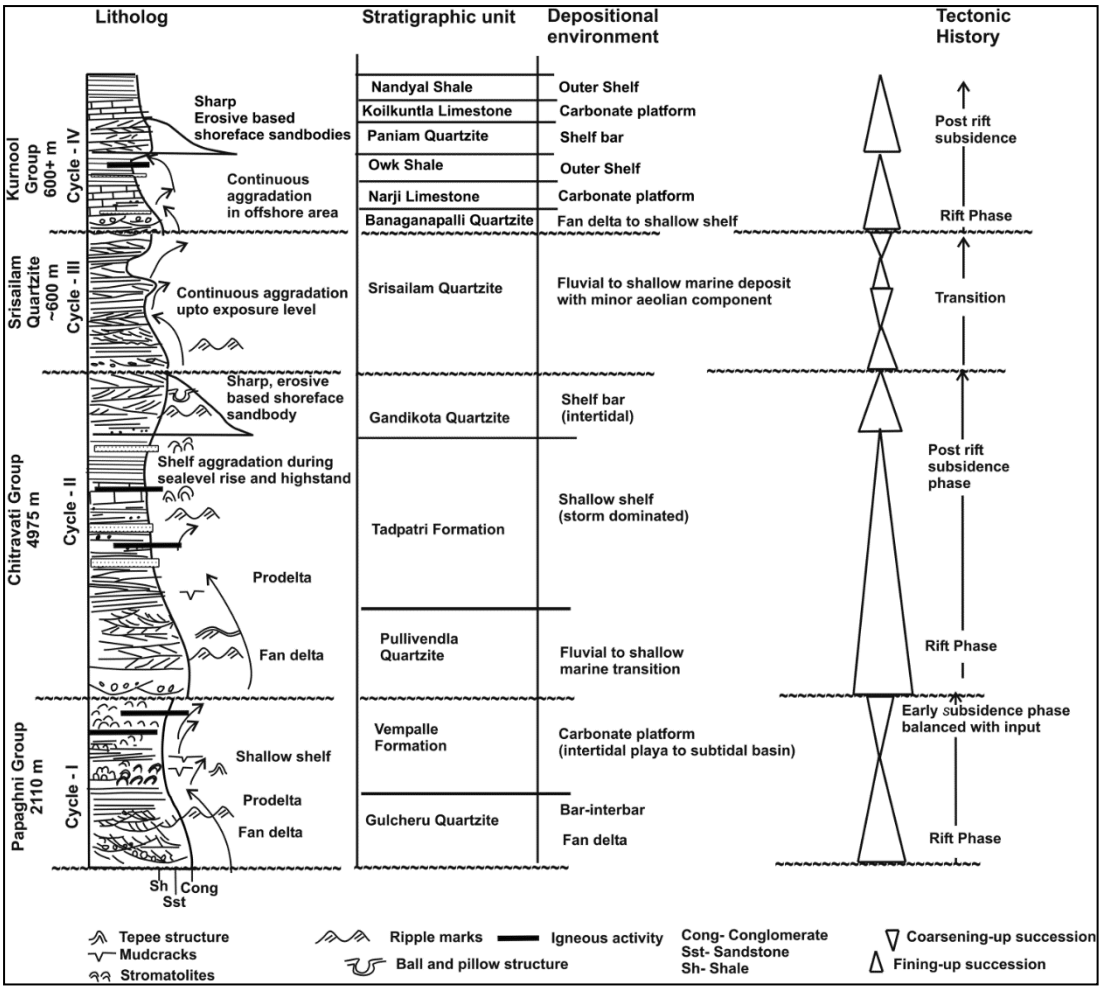

Fig. 2.1b Lithostratigraphy of the Srisailam and Kurnool groups, Cuddapah Basin. (**After S. Patranabis-deb et al., 2012).** MDA- maximum depositional age

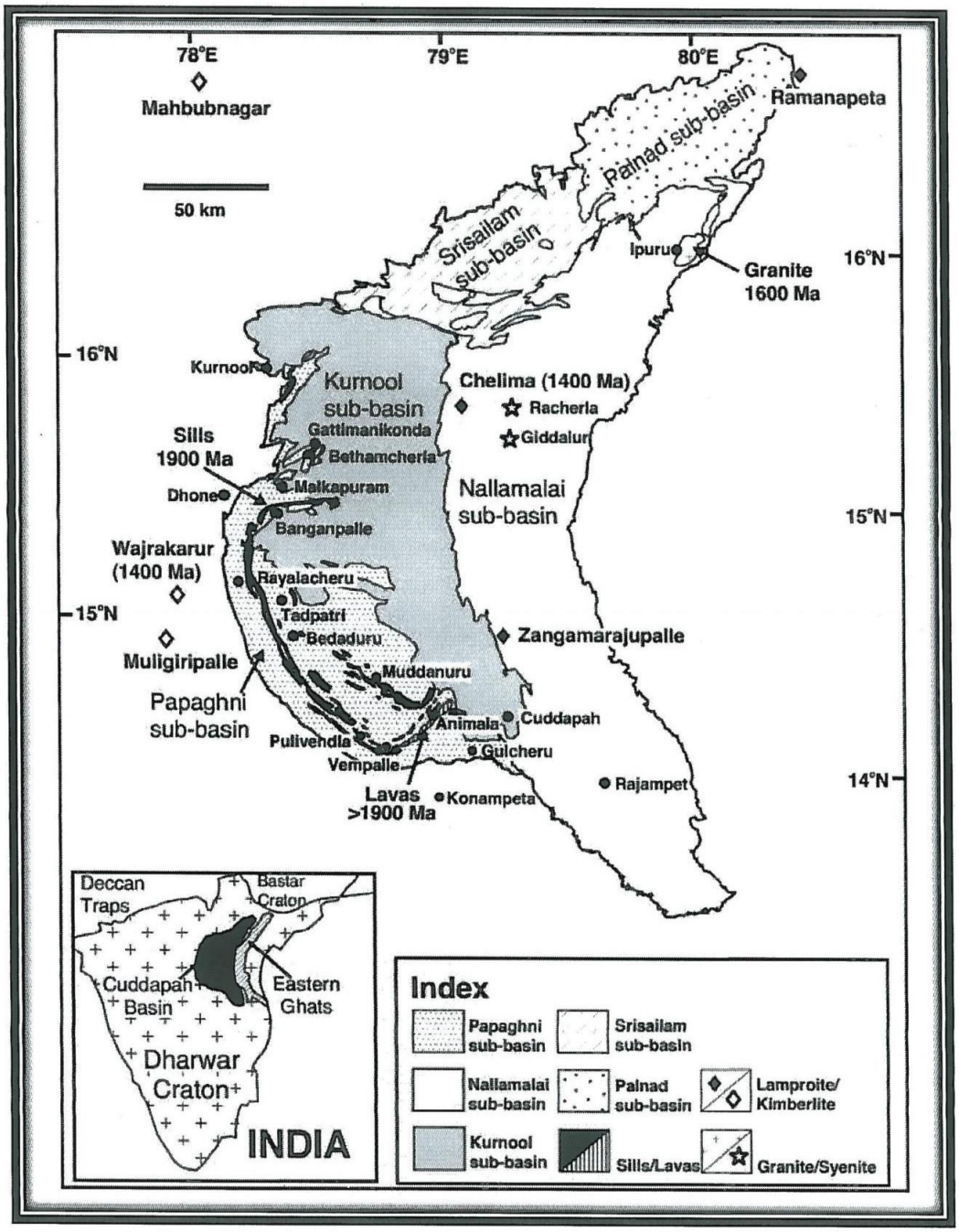

Fig. 2.2 Geological map of the Cuddapah Basin (modified after **Nagaraja Rao and Ramalingaswamy, 1976**)

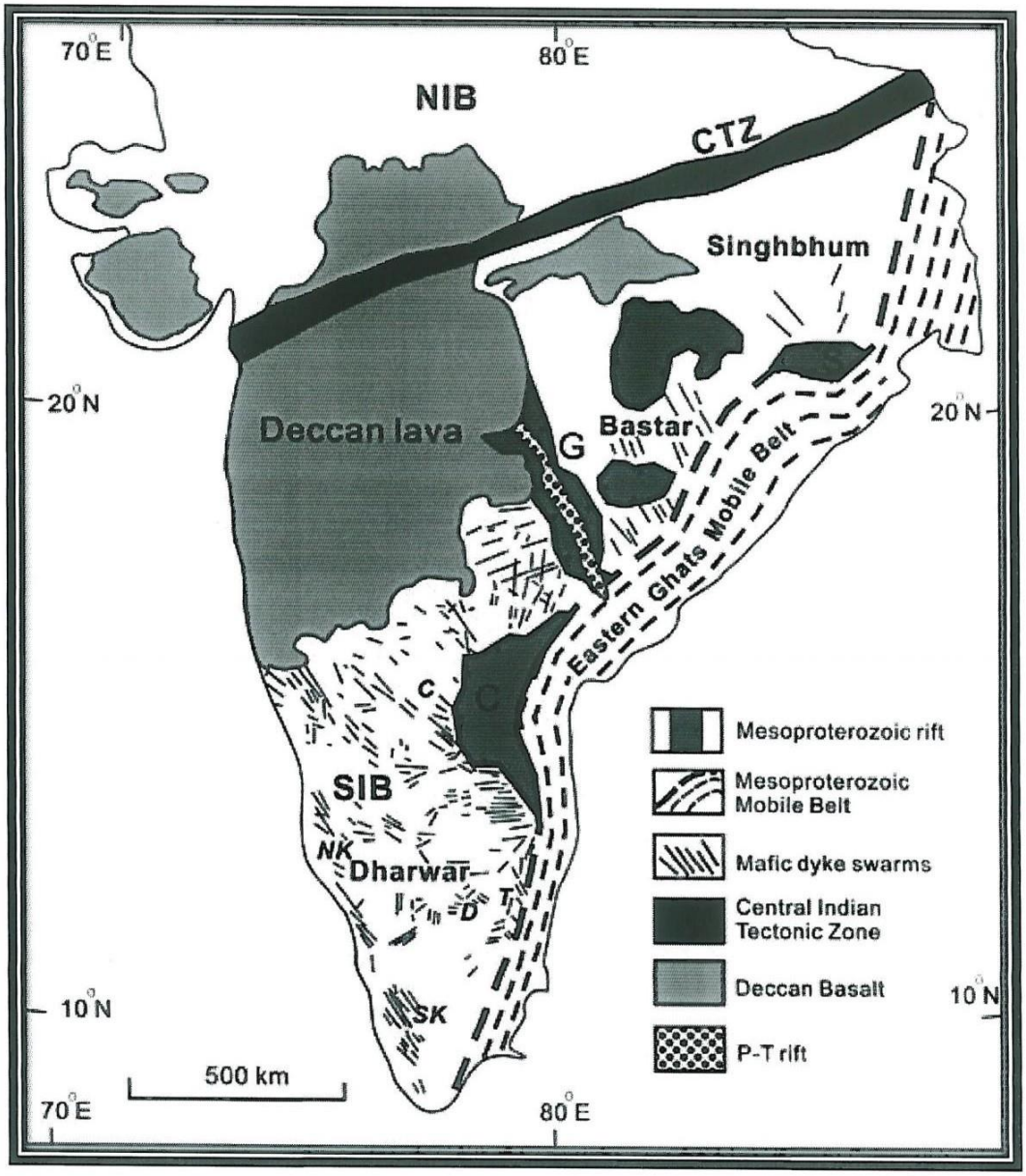

Fig. 2.3 The Paleo-Mesoproterozoic dyke swarms and rifts within the Indian Craton. NIB-North Indian Block, SIB- south Indian Block, CTZ- Central tectonic zone, C- Cuddapah Basin, G- Godavari Basin, S- Singhbhum Basin, c- Dykes around Cuddapah Basin, D- Dharmapuri dykes, T- Tiruvannamalai dykes, NK- North Kerala dykes, SK- South Kerala dykes (after **Hou et al., 2008**)

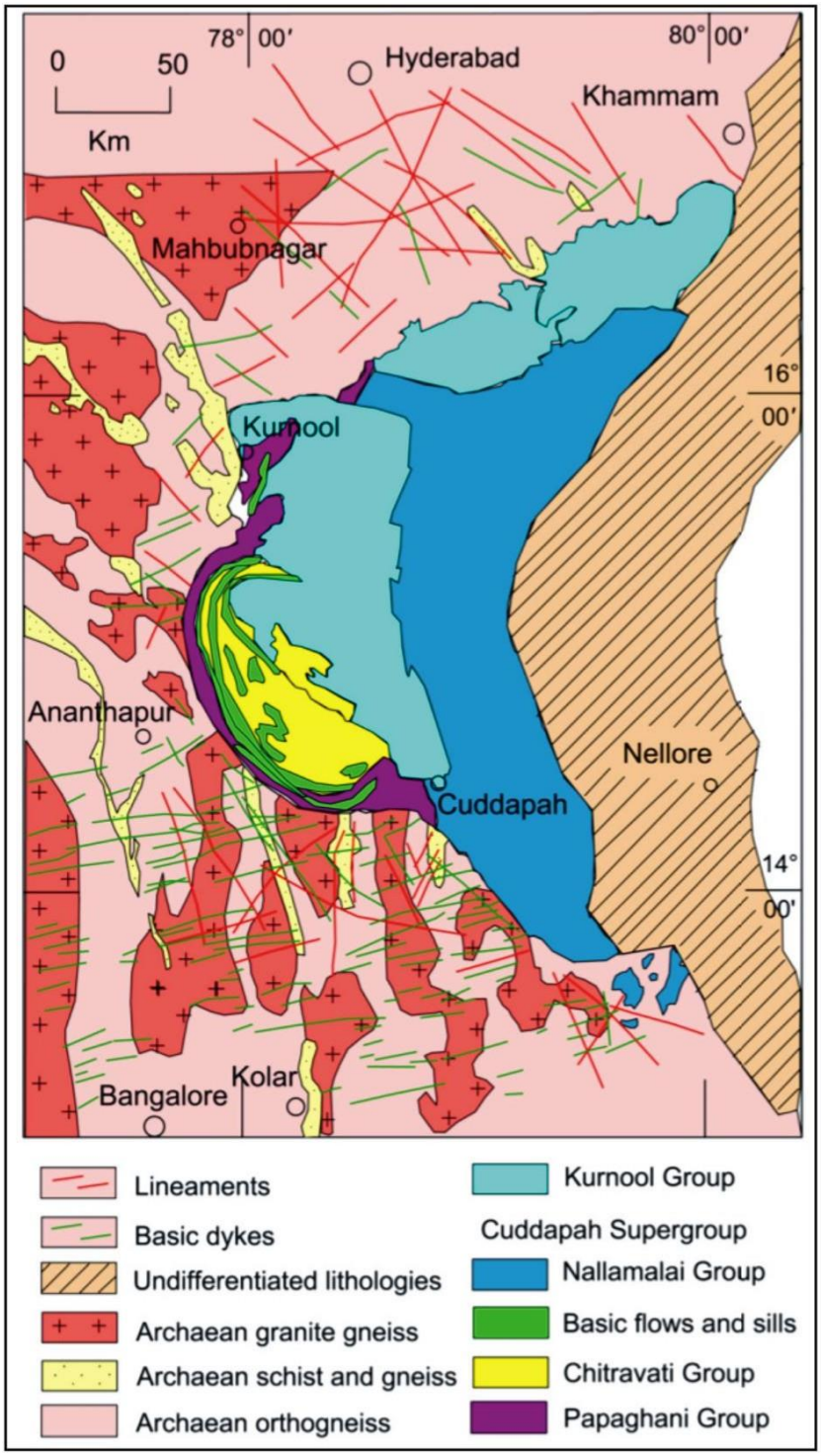

Fig. 2.4 Detailed geology of the Dharwar craton and the Cuddapah basin, showing truncation of mafic dykes and lineaments along the boundary of the Dharwar craton and the Cuddapah basin (after **Mohanty, 2011**)

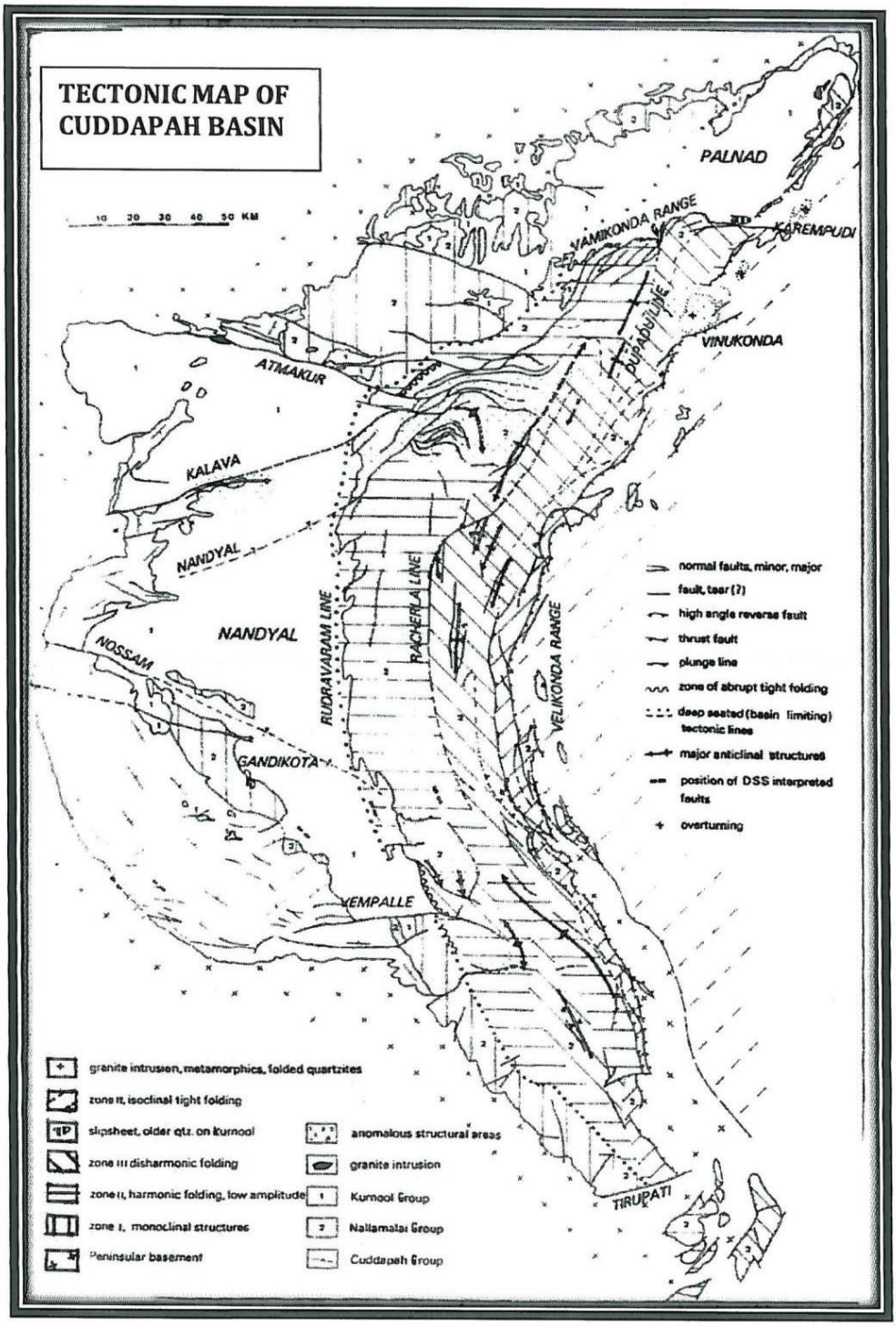

Fig. 2.5 Tectonic map of Cuddapah Basin showing overall structural pattern on either side of Rudravaram line (after **Meijerink et al., 1984**)

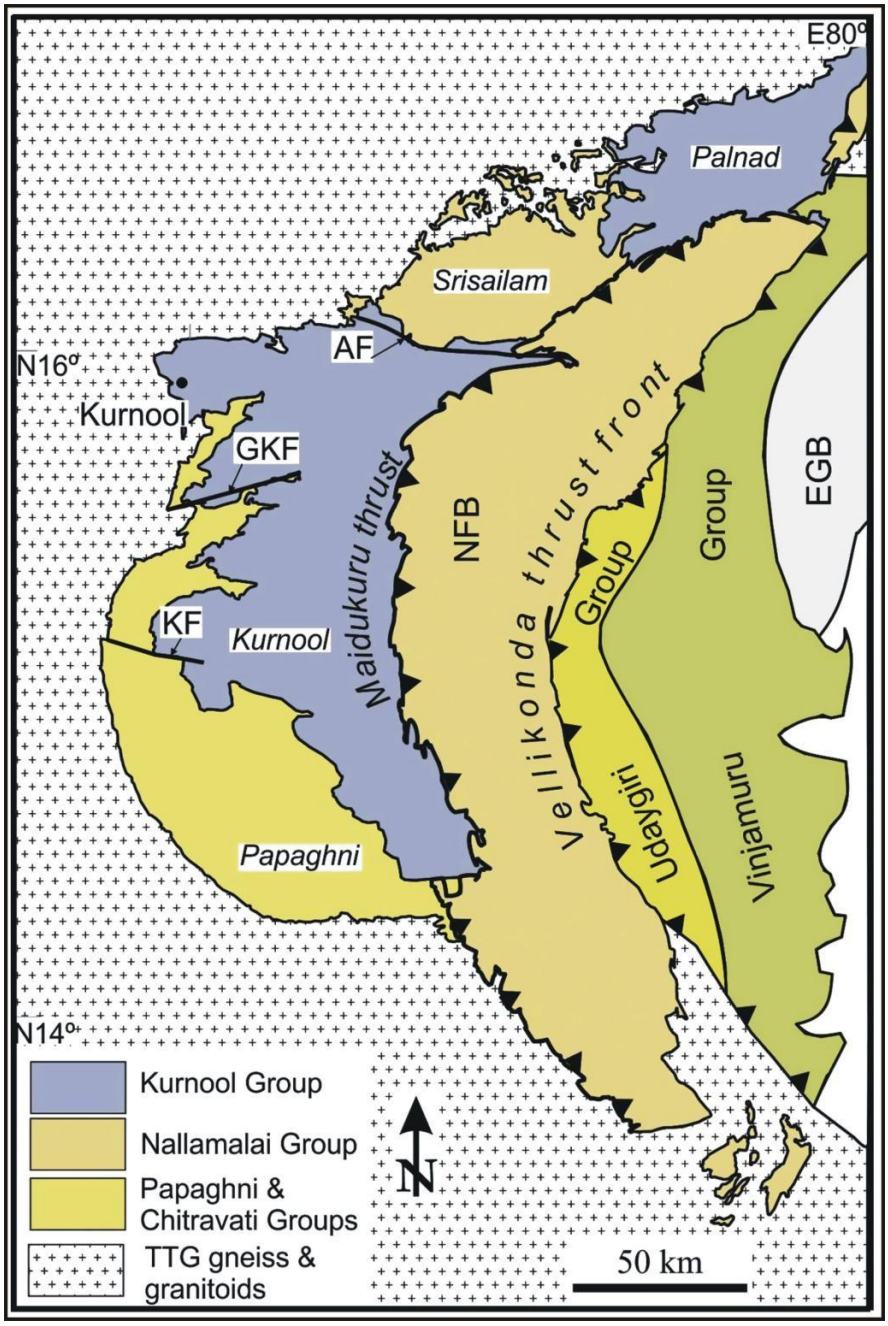

Fig. 2.6 Geological map of the Cudddaph Basin showing the sub-basins, boundary thrusts of the Nallamalai Fold Belt (NFB) and Nellore Schist Belt (NSB). The Udaygiri and Vinjamuru groups represent two distinct domains within the NSB. In the western part of the basin the lower Cuddapah rock groups (Papaghni and Chitravati Groups), the younger Kurnool Group, and the Srisailam Formation are outcropped. The Palnad subbasin is in the northeastern part. Gani–Kalva Fault (GKF), Atmakur Fault (AF) and Kona Fault (KF) are the main transverse faults within Cuddapah Basins (after **Saha and Patranabish-Deb, 2014**)

Table 2.1 Lithostratigraphic classification of Kadapah Formation (Cuddapah Supergroup) (Proposed by **King, 1872**)

Formation	Bed	Units
Kadapah	Kistnah	Sreeshalum Quartzite Kolamnala Slates Iralakonda Quartzite
	----------Unconformity----------	
	Nullamullay	Cumbum SlatesByrenconda Quartzite
	Chey-air	Tadapurtee (Poolumpett) slates with limestones Poolavaindla or Naggery Quartzites
	Paupugnee	Vaimpully Slates and Limestones Goolcheroo Quartzites

Table 2.2 Stratigraphy of the Cuddapah Basin (Proposed by **Rao et al., 1987**)

GROUP		FORMATION	LITHOLOGY	AGE
KURNOOL		Nandyal (50-100 m)	Shale/ Limestone	Neoproterozoic
		Koilkuntala (15-50 m)	Limestone with shale	
		Paniam(10-35 m)	Quartzite	
		Owk (10-15 m)	Shale	
		Narji(100-200 m)	Massive Limestone, Flaggy Limestone	
		Banganapalli (10-15 m)	Quartzite with conglomerate	
------Unconformity------				
CUDDAPAH SUPERGROUP		Srisailam (300 m)	Pebbly grit, Quartzite, Heterolithic Shales and stone	Mesoproterozoic
	------Unconformity------			
	NALLAMALAI	Cumbum (~ Pullampet Shale) (2000 m)	Shale, Dolomitic limestone, Quartzite	
		Bairenkonda (~ Nagari Quartzite) (5500 m)	Pebbly grit, Quartzite, Heterolithic Shales and stone	
	------Unconformity------			
	CHITRAVATI	Gandikota (300 m)	Quartzite, Pebble beds	Mesoproterozoic
		Tadpatri (4600 m)	Shale, Quartzite, Stromatolitic dolomite with mafic flows, Sills and Dykes	
		Pulivendla (1-75 m)	Conglomerate, Quartzite	
	------Unconformity------			
	PAPAGHNI	Vempalle (1900m)	Stromatolitic dolomite, Shale, Basic flows and intrusive	Paleoproterozoic
		Gulcheru (30-210 m)	Conglomerate, Feldspathic sandstone and quartzite	
------Unconformity------				
DHARWAR CRATON				Archean

CHAPTER-3

FACIES ANALYSIS

3.1 INTRODUCTION

Sum of the characteristics of a sedimentary unit can be mentioned as sedimentary facies in which the characteristics include the dimensions, sedimentary structures, grain sizes, types, colour and biogenic content of that particular sedimentary rock (**Middleton, 1973; Nichols, 2009**). When the description of a sedimentary unit is particularly confined to the physical and chemical properties of the rock, the sedimentary unit is referred to as lithofacies. In that case, the characteristics of lithofacies are determined by the physical and chemical processes of transport, and deposition of the sediments. Further, by interpreting the sediment in terms of the physical and chemical conditions at the time of deposition, the paleoenvironment can be reconstructed. Hence, three sections from the eastern part of Cuddapah Basin are chosen **to study the detailed constituent facies as well as depositional environment of the Narji strata, in order to better understand the development of a carbonate deposits in a Neoproterozoic marine system.** The detailed locations of the studied sections are already discussed in Chapter 1**.**

3.2 FACIES ANALYSIS

The sedimentological analyses performed on the Narji rocks reveal the presence of six lithofacies, vis, quartzite bearing massive purple limestone facies, laminated limestone facies, calcareous shale facies, heterolithic facies, massive whitish grey limestone facies and intra-formational conglomerate facies (**Table 3.1; Fig 3.1**). The detailed descriptions of these facies with their indicative depositional environment are described below:

1. Quartzite-bearing massive purple limestone facies (N-1)

This is the lowermost facies resting over different underlying lithology at different places within the study area. At Betamcherla, it overlies the Banganapalli Quartzite with gradational contact. But in the Yaganti-Patapadu area these facies (**Fig 3.2**) rests unconformably on the Tadpatri Shales. Similarly, in the Kottala area, non-conformable contact with igneous dyke is observed. These coarse-grained facies are featured by bifurcating symmetrical ripple (R.I. = 5–8) (**Fig 3.3**) and syneresis cracks. The lower 3–4 m of the succession is quartzite dominated, intercalated with limestones. Gradually the siliceous layers are decreased and increasing in massive beds towards the top is recorded. The rocks are well jointed also.

Interpretation: The overall presence of coarse-grained detrital material within this facies indicates deposition in moderate-to-high energy environment. Bifurcating ripple marks are generated by to and fro action of the water agitated by tides and waves, probably in shallow-marine condition (**Chakrabarti and Shome, 2007; Panja et al., 2017**). The syneresis cracks frequently associated with calcareous sediment indicate a swelling in the soft substrate which is a result of salinity changes in the marine environment (**Chakrabarti and Shome, 2007**). The development of this crack system may be due to shrinkage under sub aerial condition upon the loss of water in the subtidal zone (**Chakrabarti and Shome, 2007**). Clastic lamination within the carbonates indicates deposition in low-to-moderate energy subtidal marine environment (**Flugel, 2010; Ali et al., 2013; Hashmie et al., 2016**).

2. Laminated limestone facies (N-2)

It is grey to dark grey-coloured laminated limestone with thickness ranging from 1 to 7 m (**Fig 3.4**) having undulatory contact with underlying and overlying lithology.

The laminations are horizontal to slightly wavy (**Fig 3.5),** mostly lined with ferruginous and clayey material. They are less than 1 cm thick and are mostly parallel to sub-parallel. These laminations have distinct colour and composition, therefore can be easily distinguished from each other. The iron leaching is commonly observed on the surface. Planar, trough, hummocky cross-bedding and pinch and swell structure are also observed. The height and length of individual trough ranges are between 20 and 30 cm and 2 and 2.5 m, respectively. Occurrence of glauconite is also recorded within these studied facies.

Interpretation: High amount of suspension fall out along with carbonate precipitation indicate low-energy quiet environment. The trough cross-bedding indicates migrations of mega ripples/sand waves. The troughs and hummocky were probably formed by oscillatory motion of storm waves affecting the bottom (**Hamblin and Walker, 1979; Ahmad et al., 2017**). Pinch and swell structure is formed in layered, ductile rocks due to layer-parallel extension in which thickening takes place due to lateral contraction and thinning due to stretching (**Knaust, 2002**). The thick units of limestone represent time of increased carbonate precipitation while clay indicates terrigenous influx (**Chakrabarti et al., 2014; Hersi et al., 2016**). The lamination may have been deposited from suspension by clay or colloidal particles or under the influence of tidal currents (**Komatsu et al., 2014**). Occurrence of glauconite indicates shallow marine depositional environment (**Naik et al., 2016**). This interlaminated clay within limestone may be formed by tidal processes, possibly due to seasonally controlled fluctuations of sediment supply (**Ahmad et al., 2015**). Hence, these facies are probably deposited by suspension activity in shallow, quiet water with the periodic influx of the tidal currents and waves, in an intertidal environment (**Patranabis Deb, 2005**).

3. Calcareous shale facies (N-3)

The calcareous shale facies are reddish-brown in colour, almost 3 m in thickness, brittle and micaceous in nature. It is positioned in the lowermost part of the studied sections having well defined fissility plane (**Fig 3.6**). This facies are dominated mostly of calcareous clay with crudely laminated carbonate mud and some detrital quartz.

Interpretation: Mud and clay indicate deposition in low-energy anoxic environment through suspension and deposition (**Srivastava and Gawande, 2006; Srivastava and Singh, 2017**). This facies seems to be mainly deposited in calm and low-energy shallow subtidal environment (**Al-Juboury et al., 2015**).

4. Heterolithic facies (N-4)

This facies (**Fig 3.7**) is laterally continuous, highly weathered, carbonate dominated and found in association with mud and clay intermixed with each other without any distinct lamination as well as in grain size (**Fig 3.8**). Diagenetic concretion is present. A huge amount of detrital material of sand-sized particle is also observed which is also found in association with glauconite and ferruginous quartz veins. Slump and load structures are also observed in this layer. Load structure is slight bulges and knobby bodies showing contorted laminations. Small scale effect of slumping is observed within the layer like minor slippage along of sub-vertical beddings along sub horizontal planes.

Interpretation: Dominance of carbonate along with detrital elements indicate comparably high-energy environment. According to **(Dapples, 1967)**, clay minerals with quartz and K-felspar give rise to glauconite indicating reducing environment in which small amount of iron oxide may be present. Glauconite is deposited where rate

of sedimentation is slow in partially restricted, reducing marine environment **(Galliher, 1935; Naik et al., 2016**). Intermixing of layers of shale with clay pockets with little matrix indicate shallow marine set-up with storm erosion (**Bertram, 2012**). Gravity, rapid deposition, difference in compaction, and density contrast between the layers play an important role for the formation of the slump and load structures (**Collinson et al., 2006**). Small-scale effect of slumping is caused by the down slope movement of sediment under gravity due to increase in pore pressure (**Auchter et al., 2016; Panja et al., 2017**). The heterolithic unit can be assumed to be deposited in intertidal set-up near to the shore (**Grime and Cuthbert, 1945; Bekker and Erickson, 2003; Panja et al., 2019**).

5. Massive whitish grey limestone facies (N-5)

This is the dominant among all facies having sharp contact with underlying and overlying unit. They have variable thickness of few metres to several metres (**Fig 3.9**). They are fine-grained, highly compact and very hard. Wavy, nodular, and lenticular chert unit (**Fig 3.10**) are commonly present within the limestone. This facies are also associated with tepee structures, which are later filled by cement and sediments.

Interpretation: Massive natured with the absence of any detrital input within these facies indicate deposition in low-energy environment. Presence of chert nodules and concretions are probably formed during diagenesis **(GL Lo Forte and Palma, 2002)**. Decrease in the pH condition within the seawater led to the precipitation of chert nodules (**Hesse, 1988, 1989; Mathur et al., 2014**). Presence of tepee structures points their formation in shallow carbonate saturated water where fractured and bedded marine limestone is bounded by micritic cements and undergoing diagenesis (**Kendell and Warren, 1987; GL Lo Forte and Palma, 2002)**. The deposition takes place through

suspension and precipitation in restricted isolated basin mostly free from terrigenous influx depending on climate, sea level and tectonics (**Srivastava and Gawande, 2006; Srivastava and Singh, 2017**). Therefore, it can be predicted that massive whitish grey limestone facies is mainly deposited in a low energy shallow subtidal environment (**LaMaskin and Elrick, 1997**).

6. Intra-formational conglomerate facies (N-6)

This facies of Neoproterozoic Narji Limestone is narrow, laterally discontinuous facies, erratically distributed throughout the region but most commonly found in Yaganipalle area; rarely exceed 1 m lying over massive purple limestone. The facies, consisting of limestone clasts, are mostly tabular in nature (**Fig 3.11**) (long axes range from 12 to 30 cm), whereas few are sub-rounded to rounded pebbles/cobbles (long axes ranging from 5 to 15 cm). These lime clasts are poorly sorted with in micritic and coarse-grained siliceous matrix. This facies is devoid of any sedimentary structure except crude alignment of tabular clasts. The lower and upper boundary is marked by undulatory surface and truncated abruptly by massive whitish grey limestone facies.

Interpretation: Presence of bimodal clasts within comparatively fine-grained matrix indicates that deposition is taken place in moderate to high-energy environment. The wavy bounding surface may indicate deposition from fluid-gravity flows in a standing mass of water where abrupt change in flow velocity has resulted in the deposition of conglomerate (**Nemec and Steel, 1984 a, b; Chakrabarti and Shome, 2007**). This conglomerate seems to be the product of reworked sediments derived by subaqueous non-cohesive deep sub-tidal debris flow (**Dasgupta et al., 2005; Chakrabarti et al., 2014**) that have originated from a well-cemented platform rim by the storm currents or mild local seismic activity from the early lithified beds (**Patranabis Deb et al., 2012**).

The bimodal size distribution indicates co-sedimentation of bedload and suspended load in fluctuating energy regime.

3.3 KARST FEATURES IN THE NARJI LIMESTONE

The massive limestone is well karstified, present along the hill cut section of Narji. Karst features have developed under more humid condition through dissolution processes, which were equally active due to location of carbonate aquifers in similar contexts than the Narji limestone aquifer. They have developed in a confined limestone aquifer setting where diffuse infiltration took place across quartzite and shale layers. Later, surface runoff and progressive erosion of the quartzite and shale resulted in the exposure of Narji limestone at the earth surface. It is fed by sinking streams issued from quartzite hills that diffuse infiltration through the limestone plateau. Also, because of high-intensity flashy rainfall resulted in runoff and karst formation (**Dar et al., 2011**).

3.4 DEPOSITIONAL ENVIRONMENTS AND PLATFORM DEVELOPMENT

Field observation including vertical facies variation, lateral facies transition, contacts of beds and various sedimentary structures with rest of the lithological data of the studied sections assist to depict the depositional environment of Narji Formation. A total number of six facies has been identified within the studied sections those are mainly deposited in a fluctuating condition of intertidal and subtidal environment. Broadly Narji deposits represent a transgressive phase where Narji carbonate platform is deposited on top of fan complex after attesting subsidence and then further transforming the basin into a large epicontinental sea (c.f. **Patranabis Deb et al., 2012**). Identified six facies within the studied sections not only indicates hybrid depositional conditions but also signature with the features of periodic sub aerial exposure through

paleokarstic layer, interpreting that deposition took place in intertidal—subtidal paleoenvironment.

The array of facies of Narji Formation may be grouped into two facies associations (FA-1) intertidal, and (FA-2) subtidal. Within the recorded facies, the laminated limestone and heterolithic facies are deposited in intertidal zone (below mean low-tide level but above fair-weather wave base), the other facies which include quartzite-bearing massive purple limestone, calcareous shale, massive whitish grey limestone and intra-formational conglomerate facies are deposited in extended shallow subtidal environment (below the fair-weather wave base but above the storm wave base). The Narji formation starts with deposition in moderate to high energy shallow subtidal environment. A list of studied facies associated with the intertidal and subtidal environment along with the probable interpretation has been listed in **Table 3.2**. A schematic profile of carbonate facies with minor clastic intercalation of Narji Formation with their depositional environment is shown in **Fig 3.12**.

The initiation of Narji Formation begins with the deposition of quartzite bearing massive limestone probably deposited in a shallow subtidal environment over Banganapalli Formation that seems to be deposited in a fan-delta set-up (**Patranabis Deb et al., 2012**). These quartzites are the detrital materials derived from the underlying Banganapalli Quartzite formation. The grains are rounded to sub-rounded indicating a distal mode of transportation. The ripple marks indicate an oscillatory wave action and synaeresis cracks on the surface of the limestone indicate sub-areal exposure in near-shore to the beach setting. Presence of detrital material in the basal limestone indicates a link between the land and the carbonate platform. The heterolithic facies is deposited in intertidal tidal flat during the slack water phase of tide and/or after storm events (**Panja et al., 2017**). The occurrence of glauconite indicate slow rate of sedimentation

during recession stage in shallow marine condition (**Chattoraj et al., 2009; Srivastava and Singh, 2017**). The massive micrite dominated limestone seems to be deposited principally in subtidal regime within the framework of restricted carbonate platform (**Patranabis Deb et al., 2012**). Both tidal and storm influenced deposition of laminated limestone facies consisting of clay laminae of variable thickness. The irregular channels and fractures are formed in this limestone during early diagenesis and subaerial exposure **(GL Lo Forte and RM Palma , 2002; Srivastava and Singh, 2017**). Towards the end of deposition, the semi-consolidated lime mud is probably disturbed due to mild-tectonic activity resulting in intraformational conglomerate. Hummocks indicates sporadic storm event affecting the sea bed.

The horizontal distribution of these facies association, based on the distribution and genetic interpretation of facies helps to reconstruct an intertidal–subtidal depositional model (**Fig 3.12**). This carbonate platform seems to have a low-gradient slope (**Patranabis Deb et al., 2012**). The shallowest of these facies in this carbonate platform is the laminated limestone and heterolithic facies of intertidal environment. The abrupt lithological transition from basal siliciclastic dominated strata to carbonate strata suggest sea-level rise or relation with regional denudation of the siliclastic source region. Overall, the Narji formation shows an aggregational pattern where majority of the intertidal facies are deposited in the lower part of the section, while majority of the subtidal facies are deposited in the upper part of the studied section with continued rise in sea level with moderate sedimentary influx and carbonate deposition that keeps pace with increased accommodation.

The Narji Formation is mainly dominated by limestone compared to the underlying Banaganaplle Quartzite and overlying Shales of Kurnool Basin. This thick deposition

of limestone is mainly due to chemical precipitation of carbonate into an intertidal–subtidal platformal depositional environment.

Formation of the supercontinent Rodinia took place at the end of Mesoproterozoic and beginning of the Neoproterozoic (**Rogers and Santosh, 2009**). According to some authors Columbia may have converted to Rodinia without true dispersal (**Piper, 2013**) and configuration of pre-Gondwana continents. It is more correlated with the upper Riphaean (1000–650 M.A) of Lakhanda and Uy Group, and the Vendian Yocloma Group (**Khudoley et al., 2001**) occurring at the eastern margin of Siberian platform. Kurnool Formation lithology is deposited along with other coeval basin-fills around the globe during the formation of Rodinia. Hence, it is very interesting if we compare the Narji Formation lithology with other coeval successions during the critical time of formation of Rodinia.

The Jagdalpur Formation of Indravati Group, India, can be compared with Narji Formation as the depositional age of this formation is almost 700–1100 Ma (**Mukherjee et al., 2012**) which is very much similar with the depositional age of the Narji Formation. The Jagdalpur Formation is dominated by limestone with lesser amount of shale and this is very much similar with the Narji Formation. Development of stromatolites is well recorded in the upper part of the Jagdalpur Formation. However, occurrence of stromatolites is not reported in Narji Formation. This may be due to the anoxic environment prevailing during the deposition of the Narji Formation lithology (**Roy et al., 2018**).

Similarly, the Shahabad and Katamdevarahalli Formation of Bhima basin, India, are age equivalent with the Narji Formation. Shahabad and Katamdevarahalli Formation are dominated with massive, flaggy limestones with minor clastic inputs, pyrite and chert nodules. The succession is very much similar with the Narji Formation rocks and

is inferred to be deposited in a shallow marine carbonate platform. **Roy et al., (2018)** have already performed a geochemical comparison between Bhima limestones and Narji limestones, which showed similar depositional conditions for both the formations. Hence, it may be concluded that depositional set-up of the limestone dominated formations during this particular time period is almost identical with some local variation in oxic/anoxic condition which further leads/perturbs the development of algal bodies like stromatolites.

Globally, there are some reports of coeval successions of Narji Formation. Within these, the early Neoproterozoic Beck Spring Dolomite of California, USA (**Tucker, 1982**) is very much identical with the Narji Formation. Both the formations deposited in a carbonate platform with similar type of marine diagenetic history. Beck Spring Dolomite is dominantly consisting of carbonate which is precipitated from anoxic, ferruginous seawater. Therefore, the depositional environment is also similar for both the formations. Facies analysis with recorded sedimentary structures depict that the Beck Spring Dolomite is deposited in a shallow subtidal to upper intertidal marine environments (**Shafer, 1983; Tucker, 1983; Marian and Osborne, 1992; Harwood and Sumner, 2012**) similar to the Narji Formation.

The Weiji Formation of the Huaibei Group that was deposited along the southern margin of the North China Craton is also believed to be coeval successions of Narji Formation of early Tonian age. The age of the Weiji Formation is constrained between 913 ± 10 and 1069 ± 27 Ma by LA-ICP-MS U-Pb dates of diabase sills and detrital zircons (**Yang et al., 2012; Zhu et al., 2019**). There is a similarity between the deposition of both the formation. The Huaibei Group is also dominant of The Huaibei Group (Fig. 1c) consists of siliciclastic rocks in the lower part (Lanling, Xinxing, and Jushan formations) and carbonate rocks (Jiayuan, Zhaowei, Niyuan, Jiudingshan,

Zhangqu, Weiji, Shijia, Wangshan, Jinshanzhai, and Gouhou formations) in the middle and upper parts, indicating continuous extension and a transition from rift to drift basin (Zhao et al., 2018). The taxa of stromatolites such as Baicalia baicalica, Colonnella moniasa, Conophyton cylindricus, Conophyton ocularoides, and Jacutophyton ramosum have been reported in the middle of the Weiji Formation, indicating suboxic subtidal environments similar to the Narji Formation.

Comparing with these all formations, it can be attributed that they are the ancient analogues of Narji Formations. Hence, we can conclude that all the coeval successions of Narji Formation rocks throughout the globe indicate a similar type of depositional pattern during this time interval (early Neoproterozoic) especially during the breaking and amalgamation of Rodinia.

FIGURES AND TABLES

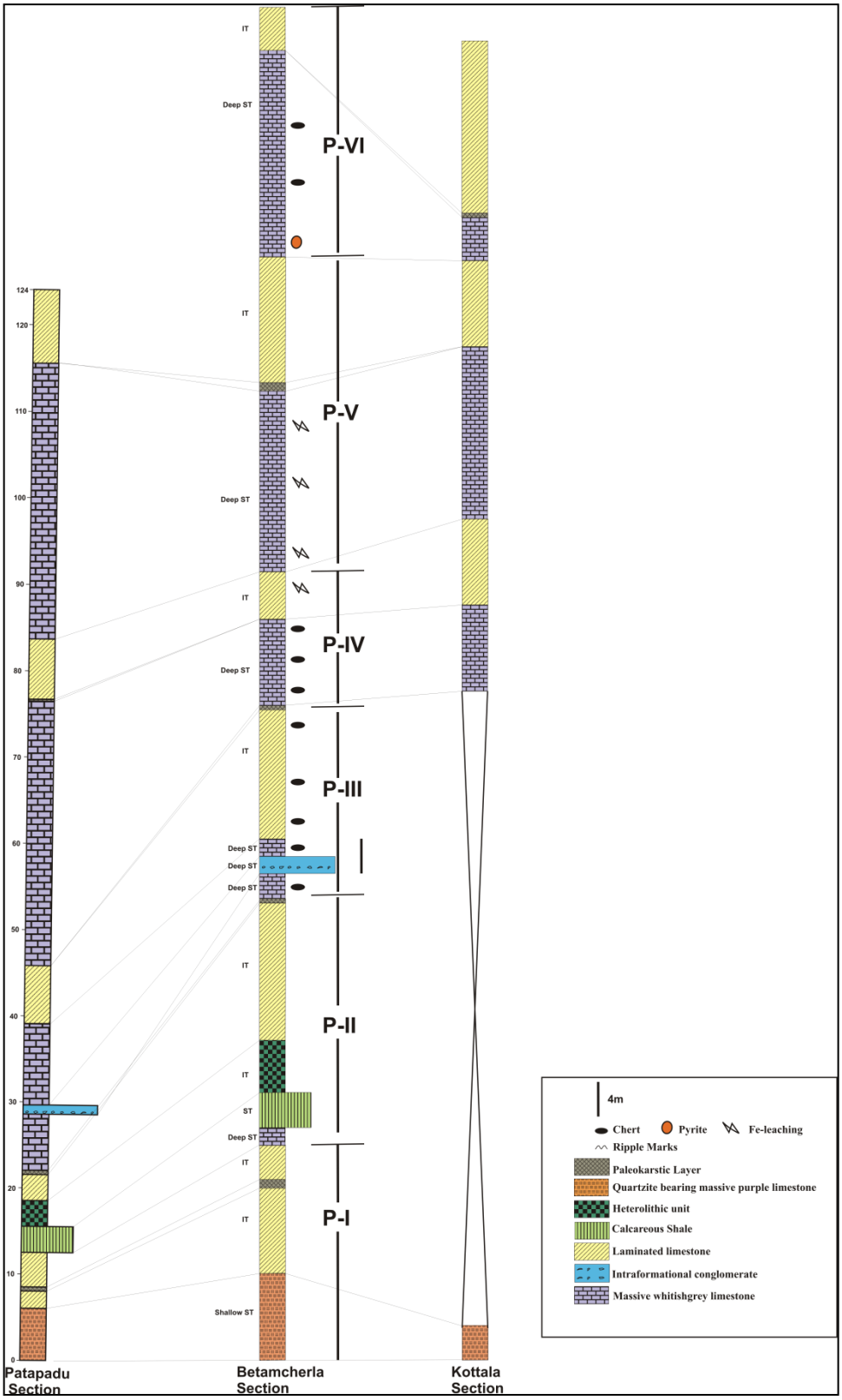

Fig. 3.1 Litholog of the studied sections from Narji Formation, Cuddapah Basin, Cuddapah Supergroup, India

Fig. 3.2 Field photograph of comparatively coarse-grained Quartzite-bearing massive purple limestone (N1) (15°18’45.00’’N, 78°07’35.76’’E), recorded from the Patapadu section Cuddapah Basin, India. Scale: Diameter of the coin- 2.40 cm

Fig. 3.3 Field photograph of coarse-grained Quartzite-bearing massive purple limestone facies (N1) (15°18’45.00’’N, 78°07’35.76’’E), with bifurcating Symmetrical ripple mark (R.I. = 5–8) in plan view and recorded from Kottala section, Cuddapah Basin, India. Length of the diagonal scale- 15.20 cm

Fig. 3.4 Field photograph of straight to wavy laminated limestone facies (N2) characterized by irregularly undulated layers, recorded from Betamcherla section, Cuddapah Basin, India. Scale: Diameter of the coin- 2.70 cm.

Fig. 3.5 Field photograph of lamination of dark grey and light streaks of clay within laminated limestone facies (N2) (15°18’45.00’’N, 78°07’35.76’’E). Note the elephant skin weathering structure, recorded at the top surface in the Betamcherla section, Cuddapah Basin, India. Scale: Length of the hammer- 31.80 cm

Fig. 3.6 Field photograph of calcareous shale facies (N3) with well-defined fissility plane, recorded within the lowermost part of Patapadu Section, Narji Formation Patapadu section, Cuddapah Basin, India. Scale: Length of the hammer- 31.80 cm

Fig. 3.7 Field photograph of clay and mud layer within heterolithic facies (N4), recorded in the Patapadu Section Cuddapah Basin, India. Note the discontinuous value of lamination and also intermixing of clay and mud with distortion. Scale: Length of the hammer- 31.80 cm

Fig. 3.8 Field photograph of top surface of the heterolithic facies(N4) from Patapadu section, Cuddapah Basin, India. Note the intermixing of clay and mud. Scale: Length of the hammer- 31.80 cm

Fig. 3.9 Field photograph of Massive white grey limestone(N5) (15°18’45.00’’N, 78°07’35.76’’E) showing macro stylolite and iron leaching from Patapadu section, Cuddapah Basin, India. Scale: Length of the hammer- 31.80 cm

Fig. 3.10 Field photograph of occurrence of lenticular type chert nodules and bands of chert within massive limestone facies(N5), recorded from Betamcherla Section, Cuddapah Basin, India. Scale: Diameter of the coin- 2.70 cm

Fig. 3.11 Field photograph of Intraformational conglomerate facies(N6). Note the tabular and sub rounded micritic clasts within poorly sorted siliceous matrix, recorded from Patapadu Section, Cuddapah Basin, India. Length of the diagonal scale- 15.20 cm

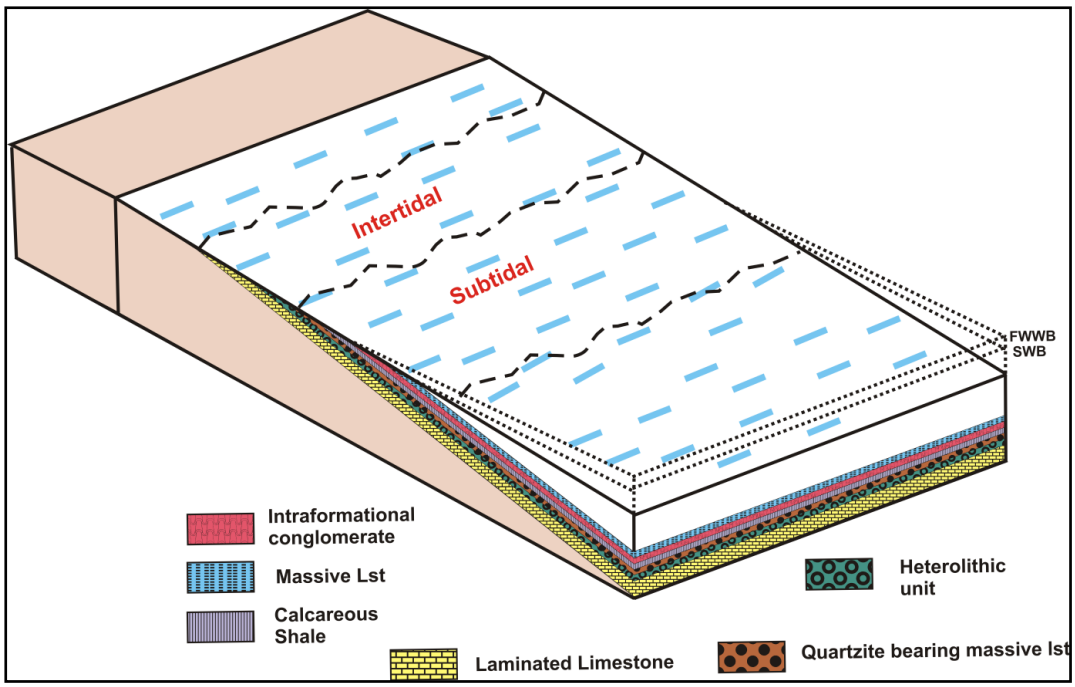

Fig. 3.12 Paleoenvironmental reconstruction of the Neoproterozoic Narji Formation carbonate platform showing the distribution of facies

Table 3.1 Summarized table of the facies recognized in the studied sections of the Narji Formation, Kurnool Basin, India

Facies Code	Facies Name	Lithology	Sedimentary structures	Trends
N-1	Quartzite bearing massive purple limestone	Massive Limestone with pockets of sandstone	Stylolite, ripples, synaeresis cracks	Laterally continuous
N-2	Laminated limestone	Limestone with lamination of fine-grained terrigenous silt	Lamination, Planar and trough cross bed	Laterally continuous
N-3	Calcareous Shale	Clay with crudely laminated carbonate mud and some detrital quartz and sparite.	Micro stylolite	Laterally continuous
N-4	Heterolithic Facies	Mud and clay intermixed layer with detrital materials and associated with ferruginous and quartz vein	Veins, load and slump structure	Laterally continuous
N-5	Massive whitish grey limestone	Massive limestone	Chert nodules, concretion	Laterally continuous
N-6	Intra-formational conglomerate facies	Clasts of micrite within sandstone	Crude alignment of tabular clasts	Laterally discontinuous

Table 3.2 Summarized table of the facies associations with their constituent facies and depositional environment, recognized in the studied sections of the Narji Formation, Kurnool Basin**,** India

Facies associations	Constituent facies code	Depositional Environment
FA-1	Laminated limestone (N-2) and Heterolithic facies (N-4)	Intertidal
FA -2	Quartzite bearing massive purple limestone (N-1), Calcareous shale facies (N-3) Massive whitish grey limestone (N-5) and Intra-formational conglomerate (N-6)	Subtidal

CHAPTER-4

PRESSURE SOLUTION STRUCTURE-STYLOLITE

4.1 INTRODUCTION

In structural geology and diagenesis, pressure solution or pressure dissolution is a deformation mechanism that involves the dissolution of minerals at grain-to-grain contacts into an aqueous pore fluid in areas of relatively high stress and either deposition in regions of relatively low stress within the same rock or their complete removal from the rock within the fluid. It is an example of diffusive mass transfer.

Stylolite have been derived from Greek word means stylos or pillar; and lithos means stone. These are zigzag surfaces within a rock mass at which mineral material within the rock has been removed by pressure dissolution due to diagenesis and/or tectonic features **Kerrich, (1978 a,b); (Robin, 1978).** They are produced by differential vertical movement under pressure accompanied by solution. This results in a process that decreases the total volume of rock. They are recognized from there irregular planes of discontinuity between two rock units in the shape of columns and pyramids. The two rock units appear to be interlocked or mutually interpenetrating. Well-developed macro and micro stylolite are seen within in the carbonate rocks of Kurnool group, Andhra Pradesh. Earlier **(Vijayam and Reddy, 1973); (Malur and Nagendra, 1988)** and **(Madesh et al., 2012)** reported micro stylolites from Precambrian carbonate rocks. The occurrence of macro and micro stylolite in Kurnool group was reported first by **(Vijayam and Reddy, 1973)**. Stylolite study from Narji Limestone was carried by **Natarajan, (1976)** and **Harish, (1995)**. Our present work mainly focuses on the classification and origin of micro stylolite within the Narji Limestone reflecting the probable effect on sedimentological, diagenetic process and tectonic influence or disturbance in the area.

4.2 ORIGIN OF MICROSTYLOLITES

The three different theories based on the origin and formation of stylolite has been proposed. **Wagner, (1913)** and **Stockdale, (1922)** proposed theory is based on solution pressure, whereas **Rothpletz, (1900)** proposed theory is based on contraction pressure and finally **Rothpletz, (1900); Shaub, (1939); Marsh, (1968),** and **Prokopovich's, (1952)** suggest subaqueous solution theory on the origin and formation of stylolite.

Based on thin section studies, the majority of stylolite are the product of diagenesis and pre-lithification which is supported by **Sorby, (1908)** and **Amstutz and Park, (1967)**. The pre-lithification origin of the stylolite, takes place through the pressure solution during compaction. It is well supported by the presence of residual seam, and other insoluble material along the stylolite surface. This process starts during early diagenesis and act as one of the important factors in promoting induration by supplying cement (Particularly with carbonate rocks). The process of stylolitization or pressure solution phenomenon proceeded first by dissolving the carbonate material at one point, then at another and thus the process continued. The stylolites are not always continuous but occur as discontinuous patches in some areas. The horizontal stylolites are due to lithification of the sediments, when the layers have undergone a strong dynamic pressure effect. Sometimes it is caused due to pressure generated by the overburden rock mass or probable due to tectonic influence. Stylolite structures mostly concentrate around where the dissolution occur, where easily soluble material will be pressed out of the rock and insoluble substances at the contact remain intact as relicts relatively enriched. The different types and nature of micro stylolites are dependent upon the depth of burial, grain fabric relations, composition of the host rock, the Eh, pH and temperature conditions. The study of stylolite in the carbonate rocks of Narji Formation

of Kurnool group helps us to understand the diagenetic processes and tectonic disturbance in the area apparently bears evidence for tectonic disturbance during the diagenetic processes.

It is observed that some microstylolites are initially inclined which branches later (**Fig 4.1**). It is caused by action of two successive differential pressure phenomena. It may be due to disturbance acting in different direction forming microstylolite of low amplitude. Some of the thin section's studies indicate diagenesis like presence of dolomite grains (**Fig 4.2**) while other indicates micro faulting. These micro faults lack significant continuity within the host rocks (**Fig 4.3**). Along stylolite, symbol of pre-lithification, pressure solution during compaction is identified. All these are well supported by the presence of residual seam having insoluble residual material along stylolite surface. Initially there is deposition of sediment which may be associated with water. The fine-grained carbonate sediment mostly occurs with pyrite and clay. Pressure solution leads to chemical compaction which results in stylolite and solution seams formed under burial conditions. Due to dynamic pressure effect during lithification the stylolite layers becomes mostly parallel or horizontal with respect to bedding plane. The pressure is generated by overlying rocks or due to tectonic influence during compaction and dewatering of sediments (**Madesh et al., 2012; Roy et al.,2018**).

During this process there is volume contraction and differential pressure due to loss of water and porosity. It is caused by occlusion of pores by late diagenetic subsurface cements (**Wong and Oldershaw, 1981**). Stylolitization changes original depositional textures and produces new diagenetic fabrics. The soluble materials are pressed out of the rocks and the insoluble materials at the contacts remain intact as relicts forming stylolite seams.

4.3 OCCURRENCE OF STYLOLITE

Stylolite are regarded as the thin contacts of discontinuity. In cross section they have undulating to zig-zag surface but in plan they resemble like conical or columnar projections with intervening depressions such that the opposing sides fit together in a complementary manner.

Stylolite most commonly present in homogeneous rocks, like carbonates, cherts, sandstones and more rarely in certain igneous rocks (**Park and Schot, 1968**). Studying the development of stylolite is important for understanding the sedimentological, diagenetic and stratigraphic aspects.

The development of pressure solution structures both macro and micro grades are geometrically of different types and are seen associated with Narji limestone belonging to lower Kurnool. They are recorded near Betamcherla to Banganapalle region. The development of stylolite is prominent in the Narji Limestone which is based on the variation in their physical characters in the following facies:

1. quartzite bearing massive purple limestone,
2. laminated limestone,
3. calcareous shale,
4. heterolithic,
5. massive whitish grey limestone
6. intra-formational conglomerate

The association of stylolite structures in these rocks can be briefly summed up as follows.

1. The stylolite is mostly prominent in Quartzite bearing massive purple limestone.

2. Variation in stylolite patterns has been much confined to the fine grained and compact rock.
3. The stylolite structures are characteristics property of Narji carbonates and further can be used as one of the most important tools to decipher the intensity and severity of local disturbances or probable tectonic influence over the studied area.
4. Stylolite are also used as a guide to recognize the nature of bedding and in estimating the thickness of limestone.

4.4 CLASSIFICATION OF MACROSTYLOLITE

The stylolite patterns are classified based on their geometric and genetic aspects. **Park and Schot, (1968)** defined two types of stylolites-

i) Aggregate stylolite with amplitudes greater than the grain diameter of the rock and

ii) Intergranular stylolite with amplitudes smaller than the grain size of the host rock.

Horizontal, inclined, vertical and cross cutting types of stylolites are found in the limestones. The classification of stylolite was suggested by **Park and Schot, (1968)**. These structures are of both macroscopic and microscopic. The stylolite surface is marked by interlocking or mutual interpenetration of two sides. This type of mutual interpenetration is observed in many places of the basin. The surface is variable in nature. Based on the geometrical features **Park and Schot, (1968)** have proposed the following six patterns of stylolites;

1. Simple or primitive wave like type
2. Suture type

3. Up-peak (rectangular) type
4. Down peak (rectangular) type
5. Sharp-peak type
6. Seismogram type

In the present work on Narji Stylolite, these structures are associated with the carbonates. They are classified based on the geometric aspects and orientation with respect to the bedding planes and are correlated with the patterns of **Park and Schot, (1968)**. The detailed study of stylolite in carbonates of Kurnool Group (**Table 1**) has revealed the occurrence of some new stylolite patterns not reported so far. The patterns are as follows:

a) Geometric classification

i. Simple wavy type
ii. Suture type
iii. Undulatory type
iv. Seismogram type
v. Sharp peak type
vi. Suture ridge type

i. Simple wavy type: In this type of stylolite, the crest and trough regions are smooth, gentle and show wave like appearance, which are aligned parallel to bedding (**Fig 4.4**) and is slightly different from the signature classification of **Park and Schot, (1968)**.

ii. Suture type: In this type of stylolite, the suture resembles like ammoniod suture pattern. The crest and trough of the stylolite structure are interlocked and joined into each other. They occur like small anticline and syncline which is symmetrically distributed (**Fig 4.5**) through the unit.

iii. Undulatory type: In this, the stylolite shows undulation of greater amplitude like similar folds. (**Fig 4.6**).

iv. Seismogram type: This type of stylolite exhibits seismic wave like pattern, where the crest and trough portions are sharp.

v. Sharp peak type: Stylolite of this type exhibits crests and troughs with sharp long projections.

vi. Suture ridge type: This type of stylolite is almost similar to that of the suture type, but project a constant ridge at certain parts towards the crest of the stylolite, thus making the suture ridge like pattern.

b) **Classifications of stylolite in relation to the bedding plane:** Under this type of classification stylolite are classified based on their orientation with respect to the bedding plane. There are three types of such stylolite, namely:

i. Suture vertical type

ii. Inclined-horizontal cross cutting type

iii. Vertical-horizontal cross cutting type

i. Suture vertical type: Such types of stylolites are interlocking in nature and are perpendicular to the bedding plane. They are observed in both tectonically and non-tectonically areas and are formed by pressure acting at right angles to the bedding.

ii. Inclined-horizontal cross cutting type: In this type of stylolite the horizontal stylolite is displaced by inclined stylolite and could therefore be called inclined – horizontal cross cutting type. The inclined stylolite usually represents the major form of stylolite seams and have greater amplitude than the inclined stylolite. This combination was result of two successive pressure systems.

iii. Vertical-horizontal cross cutting type: In this type, the horizontal stylolite is displaced by vertical stylolite and hence it is called as vertical horizontal cross cutting type. Such a combination was apparently due to the action of two successive differential pressure phenomenon.

4.5 CLASSIFICATION OF MICROSTYLOLITES

Micro stylolites occurring in the Narji Limestone (**Table 2**) are mostly parallel, inclined and vertical with respect to the bedding plane and are identified by their irregular nature. Their penetrative columns contain insoluble residue within them. These residues sometimes vary within their individual crest and trough regions. These structures have varied in amplitude; wavelength and shape result in different geometric pattern. The classification of micro stylolite is based on

(a) Geometrical parameters and

(b) Attitude with respect to bedding.

(a) Geometrical classification:

Earlier geometric classification was given by **Park and Schot, (1968)** into six different types. **Malur et al. (1988 and 1992)** classified micro stylolite from Bhima Basin based on the pure geometry and bedding orientation. Based on the geometric aspects, the micro stylolite of Narji is classified into two groups which are described below:

Simple wavy type

i) Simple wavy parallel type

ii) Simple wavy non-parallel type

Suture type

i) Suture non parallel type

ii) Suture ridge type

iii) Simple suture type

iv) Suture branching type

v) Suture interconnecting branching type

vi) Seismogram type

i) Simple wavy parallel type: Wavy micro stylolite has small and gentle undulation with small amplitude (**Malur and Nagendra, 1988; Madesh et al., 2012**). Their crest and trough are mostly smooth, gentle and wavy (**Fig 4.7-4.11**). They run parallel to the bedding surface. Some bedding parallel stylolite also show irregular anastomosing micro stylolite sets in limestone.

ii) Simple wavy non-parallel type: The non-parallel types are mostly interconnecting and branching types. Mostly found in layered sedimentary rocks, like carbonates. The residual clay materials are irregularly distributed within the stylolite (**Fig 4.7-4.10**). The simple suture type resembles like ammonoid suture pattern (**Fig 4.11**). Their anticline and synclinal patter of suture are symmetrically distributed. They are mostly non-parallel and asymmetrically distributed. Also, some of them show low amplitude and sharp peaked which running parallel or separating laminated micrite and micro spar. They also have interlocking project ions in either side. They are formed due to differential pressure solution phenomena forming suture of various amplitude (**Fig 4.11**). They mostly occur in quartz bearing limestone.

(b) Attitude with respect to bedding:

With respect to the bedding plane, they are generally horizontal, inclined and vertical in attitude. Horizontal micro stylolite (**Fig 4.12**) is developed parallel to bedding plane and it is common in almost all carbonate rocks.

Horizontal type: Horizontal micro stylolite is commonly associated with all types of carbonates always developed parallel to the bedding.

Vertical type: Vertical micro stylolite is always developed perpendicular to the bedding and is mostly found along the fracture planes (**Fig 4.13**). They are formed when the pressure act at right angle to the bedding.

Inclined or oblique type: These stylolites are inclined to the bedding and they are of variable inclination. During our petrographic studies we have observed five different types of micro stylolite structures. They are as follows:

a) **Inclined type:** These stylolites are asymmetrical in nature developed small anticlines and synclines. Crests and troughs are gentle and smooth. They are inclined with respect to the bedding plane **(Fig 4.14).** This type of stylolite may be found in rocks both affected and unaffected by structural activity.

b) **Inclined - Branching type:** They are mostly inclined but branches off later where the branching is variable in nature. Initially they have high amplitude but later the amplitude becomes during branching. Since the micro stylolite structure is inclined to the bedding, it is recognized as inclined-branching type (**Fig 4.15**)**.**

c) **Vertical - Horizontal cross cutting type**: In this type the horizontal micro stylolite is displaced by the vertical one, which is perpendicular to the bedding (**Fig 4.16**). The development of vertical structures was prior to the development of horizontal microstylolites. The cross-cutting relationship may be due to the action of two successive differential pressure phenomenon during the early diagenetic processes. This type of microstylolites is developed in very fine-grained limestones and dolomites.

d) **Interconnecting network type:** This type of micro stylolite is developed due to the combination of horizontal, inclined and vertical micro stylolite having relatively of

higher amplitude. They are either horizontal or inclined to the bedding. The suture shows network feature. This type of stylolite (**Fig 4.17**) might have formed due to the disturbances acting in different directions.

4.6 MICROSTYLOLITE AND HOST ROCK RELATIONSHIP

The Narji limestone of upper Kurnool are mostly fine grained contains both micro and macro stylolite. The limestones are mostly massive and compact, fine-grained with grey, dark grey, green, brown and buff colours. Other accessory minerals are quartz and pyrite. The quartz grains are mostly subhedral and euhedral. They have their distinct geometric forms and structure. Insoluble minerals, like clays, pyrite and calcite, occur within the stylolite and are fairly visible in some samples. The stylolite seams can be easily distinguishable from the material and the composition of the host rock which it contains. Due to cryptocrystalline nature of the carbonate rocks the identification of individual minerals under the petrological microscope is very difficult. They are mostly devoid of clay materials but some show irregular, discontinuous confined to crest and trough regions. The stylolite gives evidence of probable disturbance in the area.

The association of the stylolite structures in these rocks can be briefly summed up as follows:

1. Most of the stylolite are devoid of clay matters.
2. The fined grained limestone show more variety in stylolite.
3. Effect of mild tectonic disturbances probably occurred in these regions.

FIGURES AND TABLES

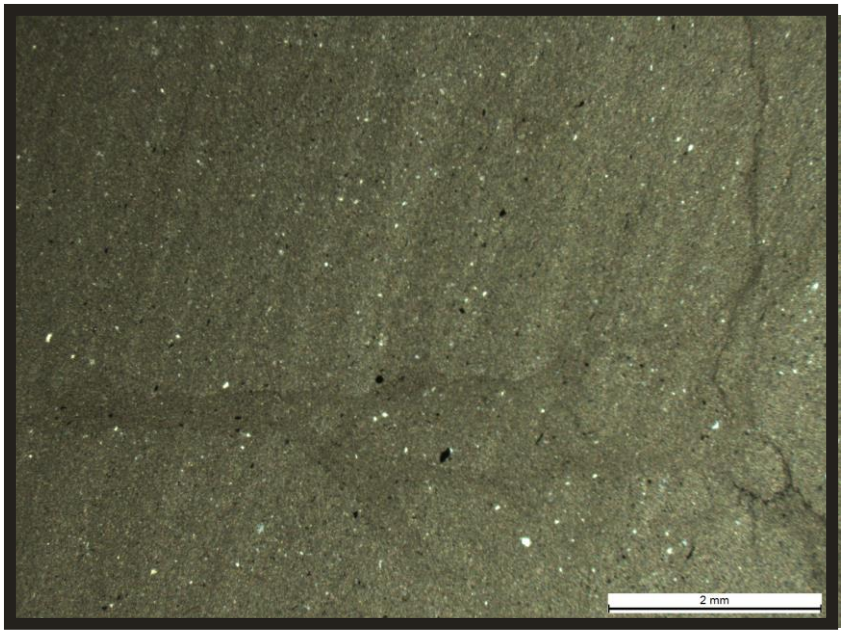

Fig 4.1 Photomicrograph showing inclined microstylolite of massive limestone facies of Patapadu Section, Cuddapah Basin, India. Note also branching of microstylolite.

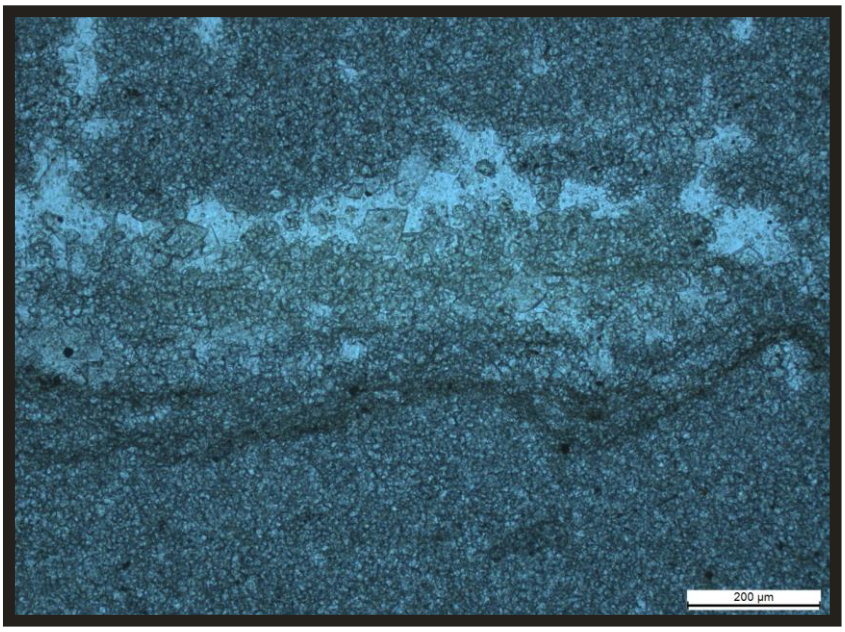

Fig 4.2 Photomicrograph showing dolomite grains along stylolite, recorded from Patapadu Section, Cuddapah Basin, India.

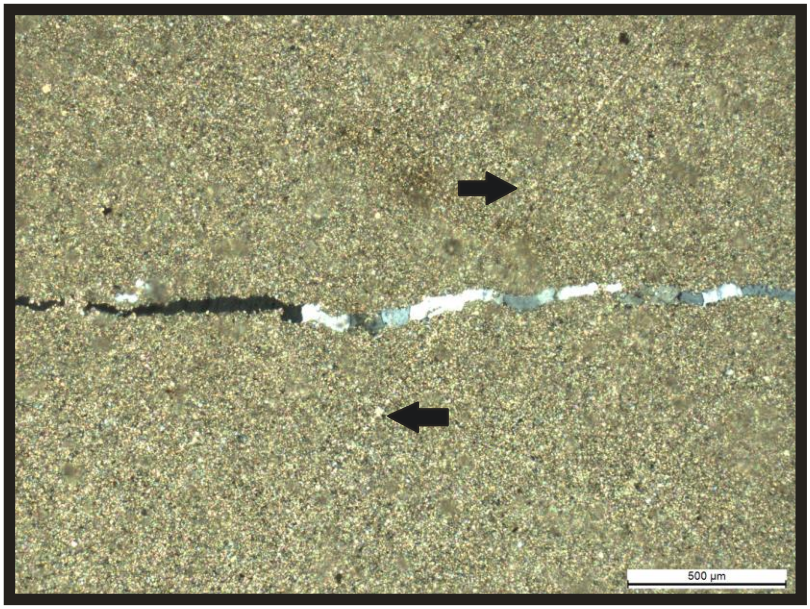

Fig 4.3 Photomicrograph showing micro fault cross cutting the stylolite, from Patapadu Section, Cuddapah Basin, India.

Fig 4.4 Macro stylolite– (Simple wavy type) noticed in Narji Limestone recorded from from Patapadu Section, Cuddapah Basin, India. Length of the hammer- 31.80 cm

Fig 4.5 Macro stylolite – Suture type stylolite structure noticed in Narji Limestone from Patapadu Section, Cuddapah Basin. Scale: Length of the diagonal scale- 15.20 cm

Fig 4.6 Macro stylolite– Undulatory type stylolite structure noticed in Narji Limestone from Patapadu Section, Cuddapah Basin. Scale: Length of the hammer- 31.80 cm

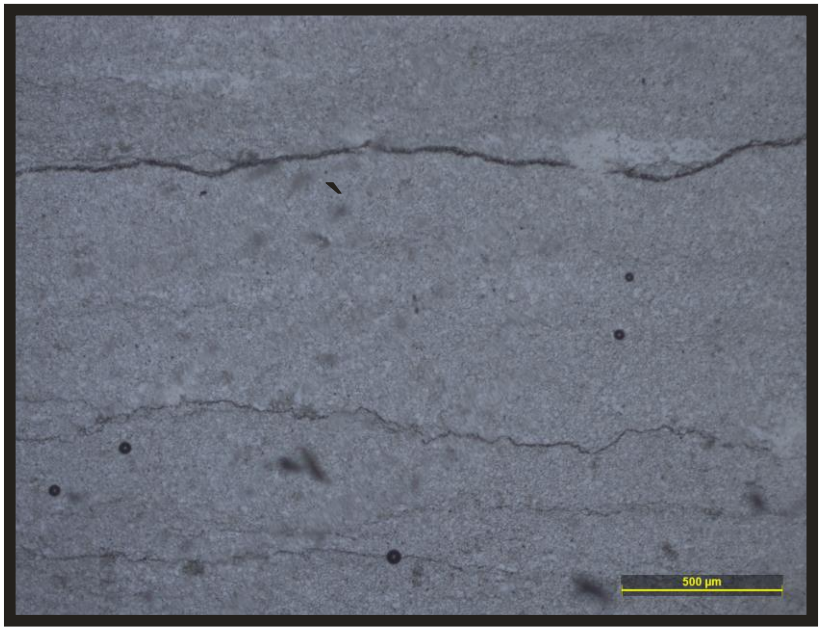

Fig 4.7 Photomicrograph showing small and gentle undulatory type micro stylolite from Patapadu Section, Cuddapah Basin.

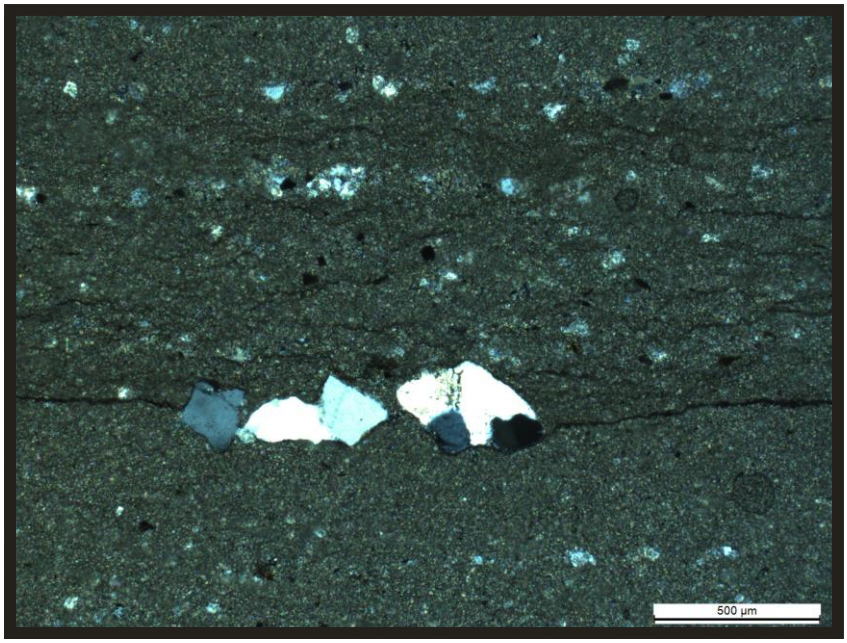

Fig 4.8 Photomicrograph showing simple isolated micro stylolite with large sparite grains from Patapadu Section, Cuddapah Basin.

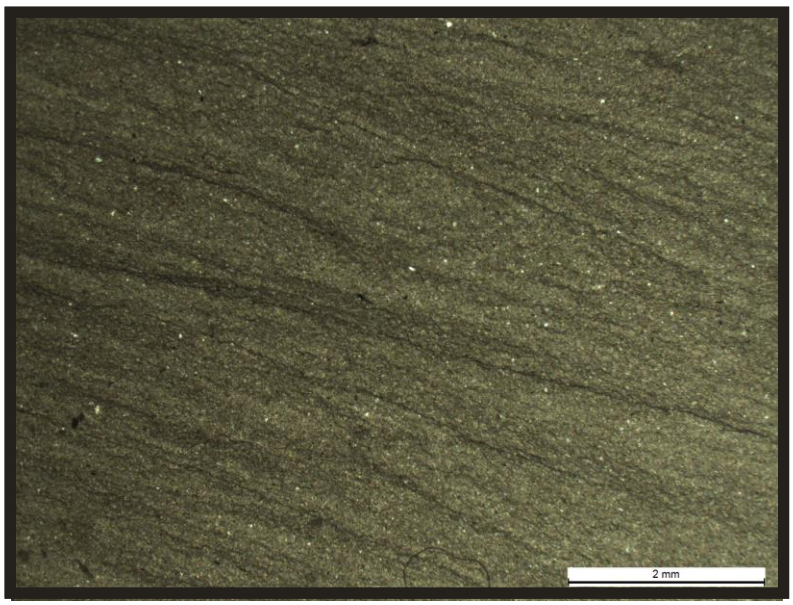

Fig 4.9 Photomicrograph showing smooth crest and trough micro stylolite from from Betamcherla Section, Cuddapah Basin.

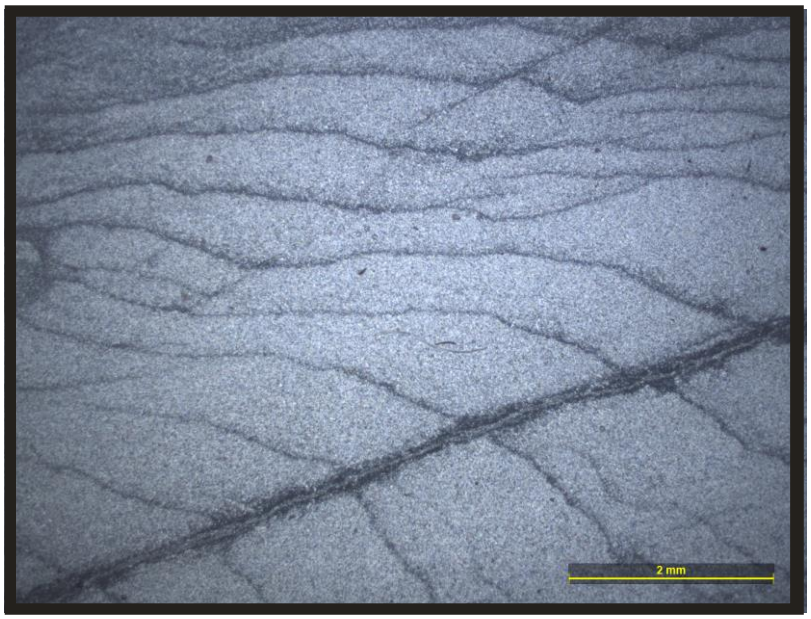

Fig 4.10 Photomicrograph showing stylolite running bedding parallel, irregular and anastomosing across the laminated limestone unit near Betamcherla area, Narji Formation, Cuddapah Basin, Andhra Pradesh from Betamcherla Section, Cuddapah Basin.

.

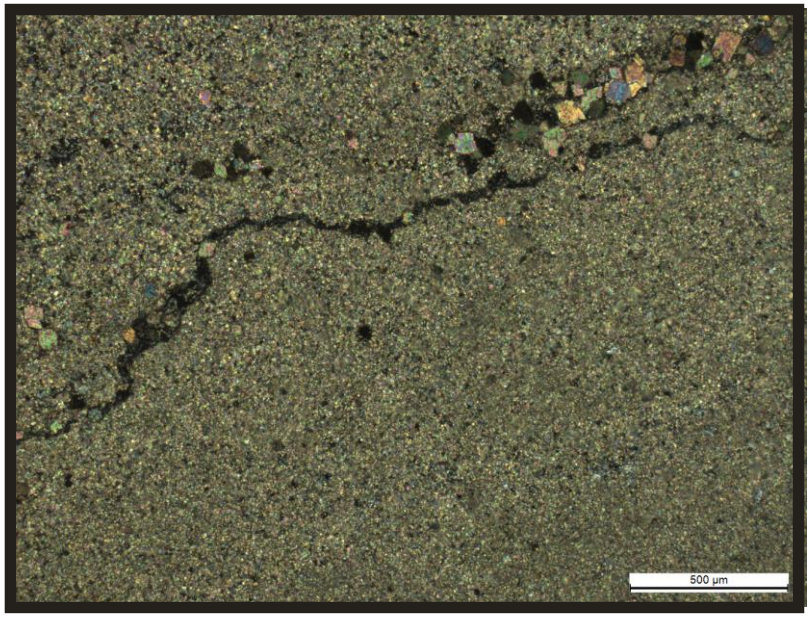

Fig 4.11 Photomicrograph showing simple suture type resembling like ammonoid suture pattern from Patapadu Section, Cuddapah Basin.

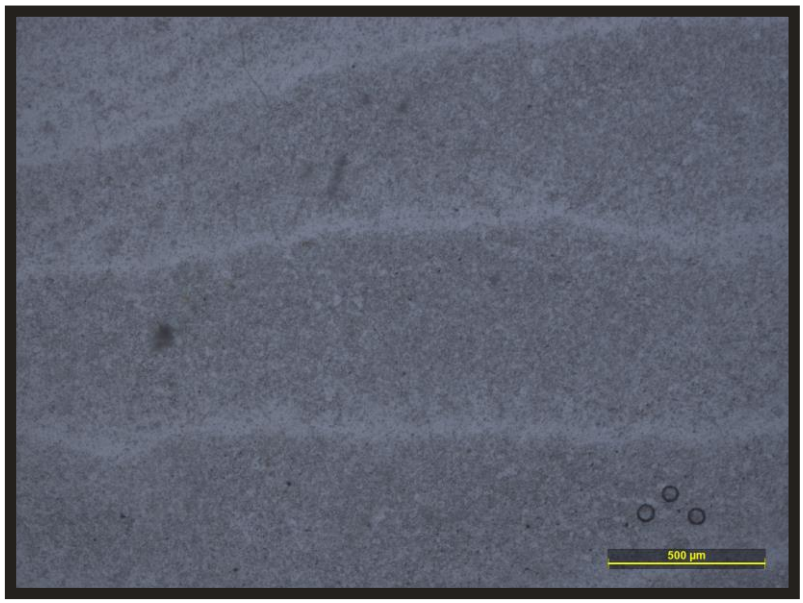

Fig 4.12 Photomicrograph showing horizontal micro stylolite developed parallel to bedding plane from Patapadu Section, Cuddapah Basin.

.

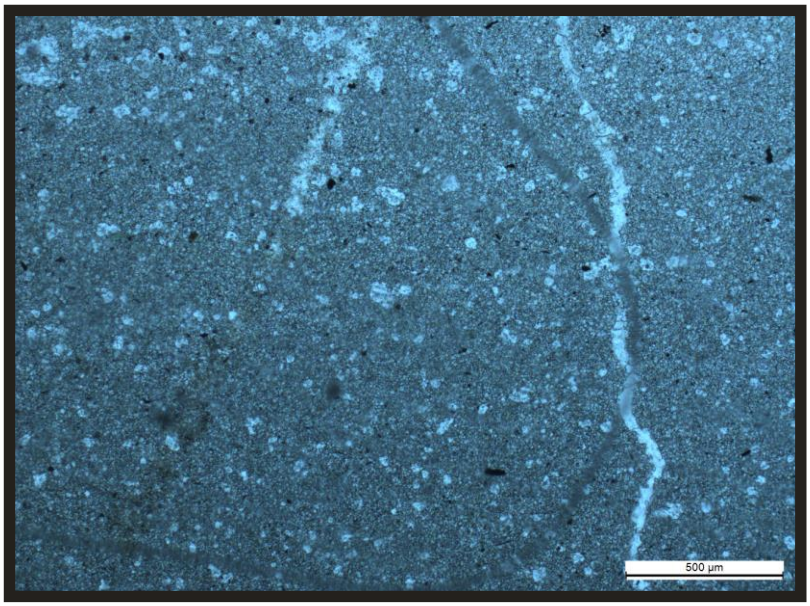

Fig 4.13 Photomicrograph showing microstylolite formed perpendicular to the bedding from Patapadu Section, Cuddapah Basin.

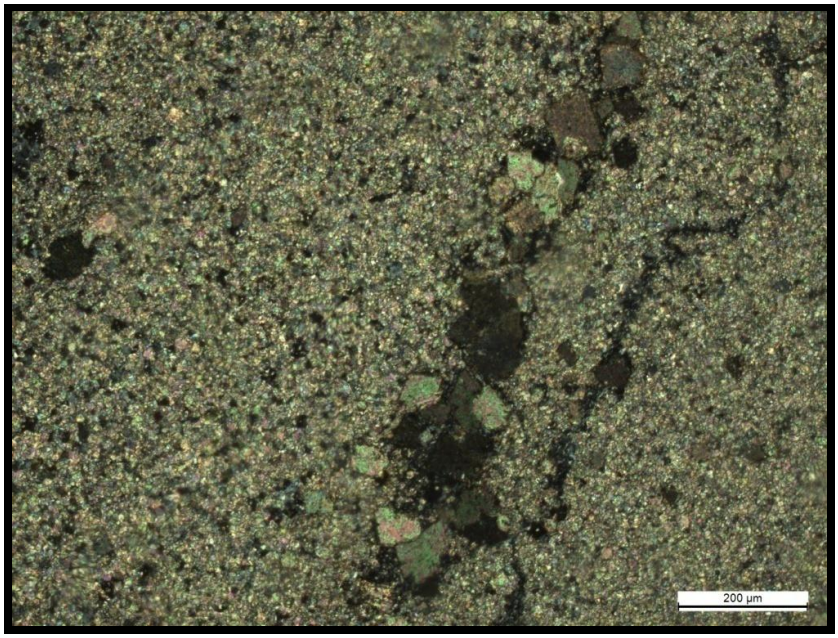

Fig 4.14 Photomicrograph of inclined microstylolite within a micrite dominant matrix from Patapadu Section, Cuddapah Basin.

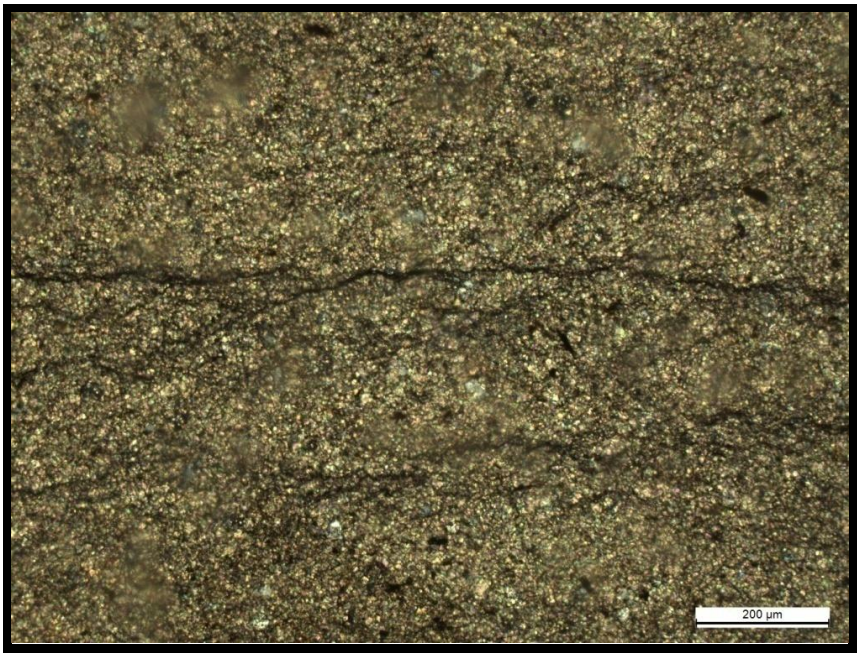

Fig. 4.15 Photomicrograph of micro stylolite with inclined branching from Patapadu Section, Cuddapah Basin.

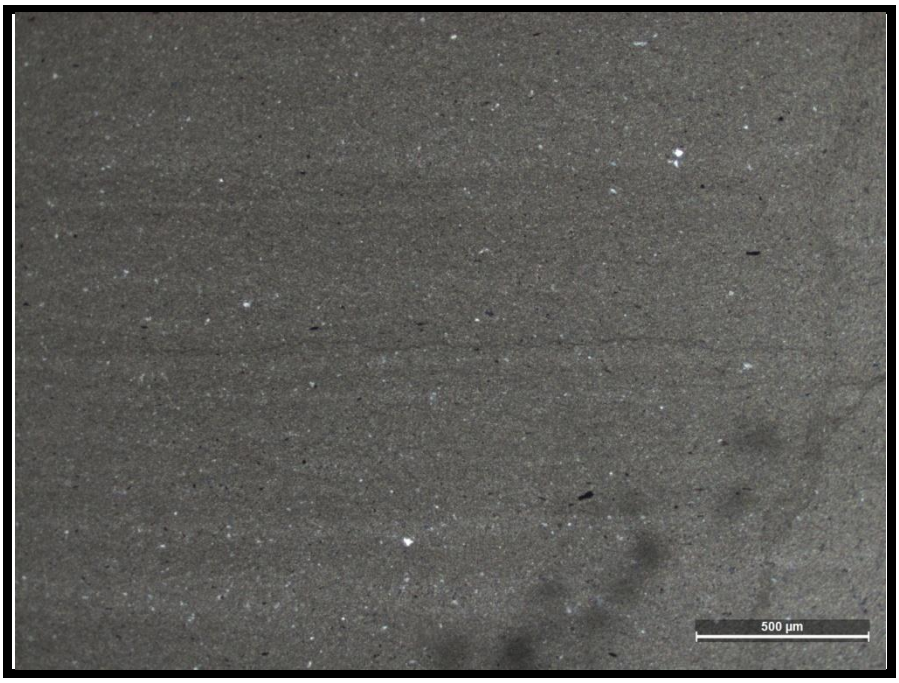

Fig 4.16 Photomicrograph of Vertical-Horizontal cross cutting type micro stylolite from Patapadu Section, Cuddapah Basin.

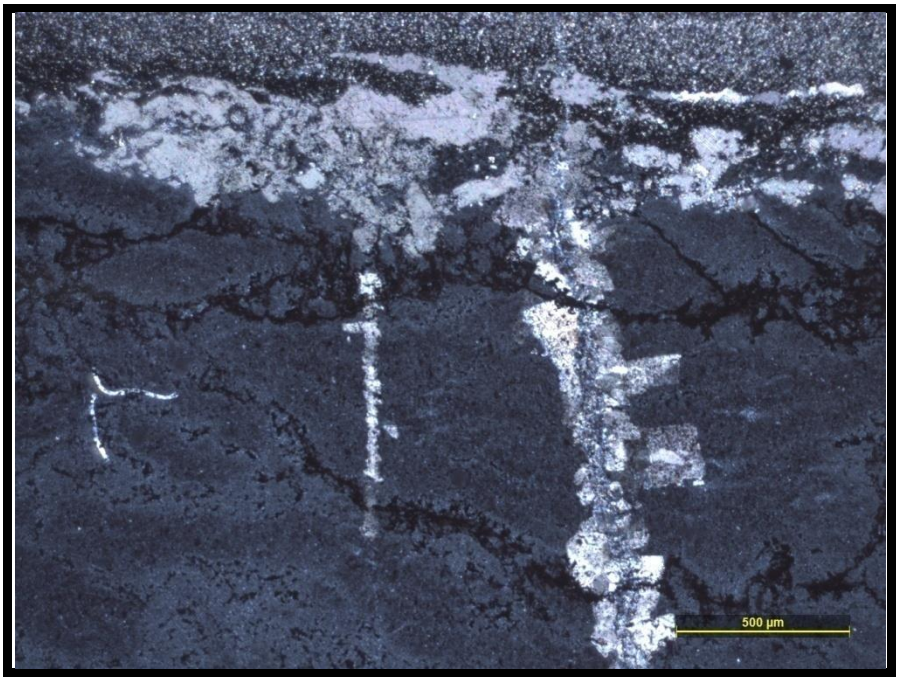

Fig 4.17 Photomicrograph of interconnecting network type stylolite from Kottala Section, Cuddapah Basin.

Table 4.1 Classification of macrostylolite recorded in Narji Formation

Basis of Classification	Classification types	Comments
Geometric	Simple wavy type	The crest and trough regions are smooth, gentle and shows wave like appearance
	Suture type	The crest and trough of the stylolite structure are interlocked and joined into each other
	Undulatory type	Stylolite shows undulation of greater amplitude like similar folds
	Seismogram type	Stylolite exhibits seismic wave like pattern, where the crest and trough portions are sharp
	Sharp peak type	Stylolite exhibits crests and troughs with sharp long projections.
	Suture ridge type	Suture with ridge like pattern towards the crest
Bedding plane	Suture vertical type	Stylolite are interlocking in nature and are perpendicular to the bedding plane
	Inclined-horizontal cross cutting type	In this type of stylolite, the horizontal stylolite is displaced by inclined stylolite
	Vertical-horizontal cross cutting type	In this type, the horizontal stylolite is displaced by vertical stylolite

Table 4.2 Classification of microstylolite recorded in Narji Formation

Basis of Classification	Classification types	Comments
Geometric	Simple wavy type	(a) Simple wavy parallel type (b) Simple wavy non-parallel type
	Suture type	(a) Suture non-parallel type (b) Suture ridge type (c) Simple suture type (d) Suture branching type (e) Suture interconnecting branching type (f) Seismogram type
Bedding plane	Horizontal type	Horizontal and parallel to the bedding plane
	Vertical type	Perpendicular to the bedding plane
	Inclined or oblique type	(a) Inclined type (b) Inclined branching type (c) Vertical-horizontal cross cutting type (d) Interconnecting network type

CHAPTER-5

GEOCHEMISTRY OF CARBONATES

5.1 INTRODUCTION

The petrography studies followed by geochemistry of carbonate rocks are frequently used to depict the controlling factors those are responsible for the carbonate sedimentation during and after the deposition. It basically assists to depict the nature of the provenance, weathering history of source area, and the paleo oxidation conditions during deposition of sediment, which are further used to elucidate the evolution of the ancient depositional basin. **Armstrong-Altrin et al., (2003, 2011); Nagarajan et al., (2011); Hua et al., (2013); Khelen et al., (2017); Hernandez-Hinojosa., (2018); Tobia (2018); Taylor and McLennan, (1985)** have suggested that Rb and Cs among LILE (Rb, Cs, Sr, Ba) of trace elements, which is present in marine carbonate rocks are highly depleted compared to the PAAS and REE when significantly suffered by clastic contaminations. For this reason, these elements are frequently applied in provenance studies **(Condie, 1995; Armstrong-Altrin et al., 2009, 2013; Nagarajan et al., 2011; Lokesh Bharani, 2015; Singh et al., 2016).** Not only that, siliciclastic input as well as paleo redox condition can be clearly identified through the geochemical study of carbonates **(Armstrong-Altrin et al., 2003; Fu et al., 2011; Hua et al., 2013).** Hence, **detailed elemental geochemistry (major, trace, and REE) of the Narji Limestone is performed to elucidate the provenance, paleo weathering, and paleoenvironmental set up of the Narji Formation during the Neoproterozoic time period.**

5.2 PETROGRAPHY OF THE NARJI LIMESTONE

The Narji carbonate rocks reveal the presence of three types of limestone lithofacies, namely, quartzite bearing massive purple limestone, massive whitish grey limestone, and laminated limestone facies as discussed in the chapter.

Quartzite bearing massive purple limestone facies:

Within the studied area, this limestone facies unconformably lie over the Tadpatri formation with a thickness of 6.5 m. The thin lenses and pockets of quartzite have been encountered within the limestones which may have been derived from underlying clastic rocks of Tadpatri Formation. Sedimentary features like ripple marks **(Fig 5.1)** and syneresis cracks are also frequently observed. Microscopic studies reveal that the facies is micrite dominated with scattered distributions of quartz grains **(Fig 5.2).** A gradual decrease in siliceous material with a gradual increase in carbonate content from base to top within this facies is also recorded. Microscopic analysis reveals that calcite acts as a cementing material among the quartz grains, **(Fig 5.3)** indicating diagenetic processes.

Massive whitish grey limestone facies:

This massive limestone facies is mostly micrite dominated and occurs at several stratigraphic levels of the studied section with a thickness variation from 6.5 to 32.0 m. They are fine-grained, highly compact, and very hard **(Fig 5.4).** Wavy, nodular, and lenticular chert are present within this facies. It is also associated with numerous stylolite structures both macroscopic and microscopic levels **(Fig 5.5)**. This facies is also found in association with rounded to sub-rounded pyrite grains, especially at the uppermost part of the succession. It appears opaque in transmitted light. There is an evidence of iron leaching and partial replacement to sparite along the boundary of the pyrite grains **(Fig 5.6).**

Laminated limestone facies:

This grey to dark grey coloured laminated limestone facies is observed throughout the studied section with a thickness variation from 2.0 to 8.5 m **(Fig 5.7)**.

The laminations are mostly less than 1 cm, parallel to sub-parallel in nature and commonly composed of clayey material. The evidence of iron-leaching is also observed on the surface. Microscopic studies of this facies indicate the dominance of clay and micrite with coarse micro sparitic mosaic of equant crystal in some samples **(Fig 5.8).** The lamination also contains minor amount of fine-grained terrigenous silt with glauconite **(Fig 5.9)** in the lowermost part of the unit. Veins of sparite within the micrite are also observed under microscope, and occasionally, this fine-grained micrite is replaced by coarse sprite grains. The patchy distribution of neomorphic cement indicates late-stage diagenetic processes **(Folk, 1964; Sherman et al., 1999; Ramkumar, 2004).**

5.3 GEOCHEMISTRY OF THE NARJI LIMESTONE

For geochemical analysis ten number of fresh, un-weathered samples are collected from all the carbonate facies. Facies wise sample id is listed in **Table 5.1.**

5.3.1 Results

5.3.1.1 Major oxides

Table 5.2 represents the analytical result of the major oxide along with loss of ignition (LOI) of the Narji limestones. A wide range of CaO wt.% (31.45 to 72.03) is recorded with an average value of 47.87% **(Table 5.2)**. Also, SiO_2wt% reflects a wide variation (14.27 to 45.92 wt.%) with an average 25.97**(Table 5.2).** Negative correlation ($r = -0.62$) between Ca and Si is found from the bivariate plot of Cao and SiO_2. Hence, we may infer different source of origin of Ca and Si of the studied samples **(c.f. Nagarajan et al., 2011).** Bivariate plot of SiO_2 vs.TiO_2 ($r = 0.81$, $n = 10$; **Fig 5.10**) and SiO_2 vs. Al_2O_3 ($r = 0.89$,$n = 10$; **Fig 5.10**) is showing positive correlation whereas the bivariate plot of CaO vs. TiO_2 ($r = -0.28$, $n = 10$; **Fig 5.10**) and CaO vs. Al_2O_3 ($r = -$

0.48, n = 10; **Fig 5.10**) showing negative correlation and these suggest that the source of TiO_2 and Al_2O_3 is similar with the source of SiO_2 and also indicate that there is a terrigenous input within the Narji limestones **(Lokesh Bharani, 2015; Sen and Mishra, 2015; Madhavaraju et al., 2016)**. Clastic contaminations within the studied limestones are also observed from the average ratio of Al_2O_3/TiO_2(16.67) and K_2O/Al_2O_3 (0.21) **(Sen and Mishra, 2015)**. The average concentration of MgO within the samples is 0.53 wt.% and the SiO_2 vs. MgO bivariate diagram exhibits significant positive correlation (r = 0.57, n = 10; **Fig 5.10**), indicating silicification processes during early diagenetic stage **(Kang et al., 2022).** Bivariate diagram of Fe_2O_3 vs. SiO_2 also reflects positive correlation in-between Si and Fe (r = 0.79, n = 10; **Fig 5.10**), and this further indicates that the Fe concentration within the limestones is related with the detrital input. The very low Na_2O content **(Table 5.2)** in the Narji limestones suggests that either the limestones were formed initially from a low Na_2O concentrated solution or inferred recrystallization of the limestone **(Madhavaraju and Lee, 2009; Lokesh Bharani, 2015).**

5.3.1.2 Trace Elements

Table 5.3 lists the analytical result of the trace element concentrations of the studied samples (n = 10). PAAS normalized trace elements of these limestones are plotted in (**Fig 5.11)**. Within the LILE (Rb, Cs, Sr, Ba), Rb and Cs are highly depleted compared to the PAAS **(Fig 5.11).** Sr concentration within these limestones is near to the PAAS value (200 ppm; **Taylor and McLennan, 1985**) **(Table 5.3; Fig 5.11).** In case of Ba concentration, some limestone samples (N2, N3, N6, N7, and N8) are showing slightly to moderate depletion and the rest of the samples (N1, N4, N5, N9, and N10) showing slightly to moderate enrichment compared to PAAS. The high Ba content in few limestone samples may be due to K-feldspar breakdown from granitic

source **(Condie et al., 1995; Armstrong-Altrin et al., 2013; Lokesh Bharani, 2015).** The PAAS normalized ferromagnesian trace elements (Co, Ni, Cr, and V) are showing depletion in **(Fig 5.11).** Within all of the HFSE (Zr, Y, Nb, Hf, Th, and U), Zr is highly depleted and the rest of the HFSEs are moderately to slightly depleted (except Nb concentration inN3 sample; **Fig 5.11**).

5.3.1.3 Rare Earth Elements

Table 5.4 lists the analytical result of the rare earth element concentrations (REE) of the Narji limestones (n = 10). The REE concentrations within the studied limestones show wide range of variation from 16.93 to 53.27 ppm with an average of 35.31 ppm **(Table 5.4)**. PAAS normalized REE + Y pattern of these limestones is plotted in **(Fig 5.12)** and a clear Sm anomaly is observed. Within the limestone samples, Sm has a positive correlation with SiO_2 (r = 0.70, n = 10), TiO_2 (r = 0.70, n =10), and Al_2O_3 (r = 0.71, n = 10) and has a negative correlation with CaO (r = − 0.65, n = 10). This indicates that the source of Sm is similar with the source of SiO_2, TiO_2, andAl_2O_3, and its enrichment is probably due to the clastic contamination within the samples. Analytical result of $(La/Yb)_{SN}$ ratio (0.39 to 1.21, with an average 0.59; **Table 5.5**) of the samples is relatively lower than the terrigenous materials **(Sholkovitz, 1990; Condie, 1991)** which suggests that the REE is influenced by LREE depleted carbonate particles **(Armstrong-Altrin et al., 2009; Nagarajan et al., 2011)**. This $(La/Yb)_{SN}$ ratio of Narji limestones is very much similar with the $(La/Yb)_{SN}$ ratio of Neoproterozoic Bhima limestones as well as with late Neoproterozoic shallow marine platform carbonate **(Table 5.6).** $(Dy/Yb)_{SN}$ ratios (1.00 to 1.54, average 1.39; **Table 5.5**) of the studied limestones are relatively higher than the $(Dy/Yb)_{SN}$ ratio of modern seawater which is 0.8–1.1**(Singh et al., 2016).** The high $(Dy/Yb)_{SN}$ ratios of the

limestones exhibit HREE enrichment rather than LREE **(Nagarajan et al., 2011; Singh et al., 2016).** The Narji limestones are showing seawater like REE + Y pattern (LREE depleted, HREE enriched to flat) with negative Eu (average Eu/Eu* = 0.27, **Table 5.5**) and positive Ce anomaly (average Ce/Ce* = 2.33, **Table 5.5**).

5.4 Discussion

5.4.1 Source of REE

The REE pattern in sedimentary rock is often used to characterize source rock **(Armstrong-Altrin et al., 2015 a, b; Khelen et al., 2017; Tobia, 2018; Mitra et al., 2018)**. PAAS normalized REE values of the analysed samples are mostly depleted and this indicates the terrigenous input within the Narji limestones **(Akhdar, 2015**; **Devi and Duarah, 2015; Sen and Mishra, 2015)**. The studied limestones are reflecting a wide range of variation in ΣREE concentration (16.93 to 53.27, average 35.31; **Table 5.4**), and this is more or less comparable with typical marine carbonate value, which is 28 ppm **(Chen et al., 2014)**. These wide ranges of variation in ΣREE concentration are also as a result of variation in terrigenous materials within the limestone samples. The $(Nd/Yb)_{SN}$ ratios of the samples vary from 0.40 to 0.53 (except sample N-3, **Table 5.5)** and this is similar with the other $(Nd/Yb)_{SN}$ ratios of the Proterozoic carbonate rocks that have seawater-like REE patterns **(Table 5.6).** This clearly indicates that the Narji limestone samples retained the original marine water characteristics. Er/Nd ratio can be used as a proxy to represent the effect of LREE/HREE fractionation in modern and ancient marine system **(German and Elderfield, 1989).** In marine condition, the Er/Nd ratio is near 0.27 (**De Baar et al., 1988; Abedini and Calagari, 2015).** Therefore, limestones with higher Er/Nd ratio explain the seawater condition, preserved by the marine carbonate. Er/Nd ratio less than 0.1 indicate addition of detrital material as well as diagenetic process within the carbonates **(De Baar et al., 1988; Abedini and**

Calagari, 2015; Tobia, 2018). The Er/Nd ratios of the studied samples are within 0.06 to 0.22 with an average of 0.17 **(Table 5.5, Fig 5.13)** which is relatively low compared to the normal marine water. These points to an influence of terrigenous input compared to the chemical precipitation during deposition and activation of diagenetic process rather than activation of normal seawater during sedimentation. Out of 10 analysed samples, the N3 sample shows the Er/Nd value less than 0.1 **(Table 5.5, Fig 5.13)** and this suggests maximum influence of detrital material within N3 sample.

Most of the Narji limestones are showing very much similar sea-water like REE + Y pattern. But during carbonate precipitation from seawater, variable degree of contamination of detrital material suppressed the seawater signatures. The limestone samples are showing recognizable positive correlation of ΣREE with SiO_2 (r = 0.57; n = 10), TiO_2 (r = 0.58; n = 10), Al_2O_3 (r = 0.66; n = 10), and Fe_2O_3(r = 0.62; n = 10) and negative correlation with CaO (r = − 0.71; n = 10) (**Fig 5.14)** This indicates the presence of terrigenous fraction and this is the most probable source of REE within the Narji samples. The terrigenous source of REE is more proved by the strong positive correlation of ΣREE with Th, Cr, Sc, and Y elements (**Fig 5.14; Sen and Mishra, 2015; Shaltami, 2015; Ramos-Vázquez et al., 2017; Anaya-Gregorio et al., 2018; Hernández-Hinojosa et al., 2018).**

5.4.2 Behaviour of europium

The Eu/Eu* ratios of the Narji samples are within 0.13 to 0.29 (except N3, Eu/Eu* 1.02; **Table 5.5)**. Except N3, all the analysed samples show negative Eu anomaly in the Narji limestones. Positive Eu anomaly in PAAS-normalized REE pattern may be due to hydrothermal solution which originates in a deep-sea environment **(Worash and Valera, 2002; Armstrong-Altrin et al., 2003)** or due to

diagenetic change **(Tobia, 2018; Abedini and Calagari, 2015).** The Narji limestones are deposited in a shallow marine carbonate platform; therefore, local enrichment of feldspar as well as diagenetic changes may lead to positive Eu anomaly for N3 sample. Negative Eu anomaly also indicates retention of the original marine water characteristics within the limestone samples. Without Eu anomalies, these carbonates were possibly precipitated from "low" temperature (<200°C) hydrothermal fluids or burial diagenetic fluids **(Zhang et al., 2014).**

5.4.3 Y/Ho ratio and seawater chemistry

Fig 5.13 shows the variation of Y/Ho ratio within the samples which can be further treated as a proxy of marine environment **(Bau, 1996; Allwood et al., 2010; Tobia and Aqrawi, 2016).** In modern marine environment, Y/Ho ratio varies in between 40 and90 **(Bau, 1996)** whereas volcanic ash has chondritic Y/Ho ratio in between 26 and 28 **(Kamber and Webb, 2001).** The Y/Ho ratios of the Narji limestones vary in between 30.05 and 45.45 **(Table 5.5; Fig 5.13)** with an average value of 35.68. This suggests that the limestones were deposited in a marine environment, but due to the terrigenous input or due to diagenesis process, the average Y/Ho ratio of the limestones is decreased **(Abedini and Calagari, 2015; Tobia, 2018).** This Y/Ho ratio is also very much similar like other Neoproterozoic shallow marine platform carbonates, Bhima limestones, and Rhotas limestones **(Table 5.6).**

5.4.4 Ce anomaly–reflection on paleo redox condition

Real and apparent Ce anomalies can be differentiated among each other by using Pr/Pr* which can be formulated as $[Pr/ (0.5\ Ce + 0.5\ Nd)]_{SN}$ **(Khelen et al., 2017).** If Pr/Pr* = 1, it indicates apparent Ce anomalies due to the overabundance of La. The Ce anomalies are indicated when Pr/Pr* ratio is > 1 or < 1. When Pr/Pr* are> 1, then the

Ce anomalies are taken as negative whereas it becomes positive when Pr/Pr* < 1 **(Bau and Dulski, 1996).** In this present study except N3, all the studied samples have Pr/Pr* < 1 **(Table 5.5).**

Several studies have been performed on the utilization of Ce anomaly in the marine phase for assuming the palae-oceanographic situations **(Nath et al., 1997; Hua et al., 2013; Khelen et al., 2017).** To resolve the depositional redox condition, Ce anomalies are frequently applied because Ce valency and solubility vary based on redox condition. Under oxidized condition, Ce^{3+}oxidizes into Ce^{4+} and this result in Ce dissociate from the rest of the REEs. This leads to negative Ce anomaly **(Bau and Dulski, 1996; Hua et al., 2013)**. The positive Ce anomaly indicates that calcite and dolomite formed in anoxic settings and further supports a shallow iron reduction zone. In our study, most of the Narji limestones (except N3) are showing positive Ce anomaly (Ce/Ce* > 1, **Table 5.5**) which indicates their deposition was in an anoxic condition.

5.4.5 Elemental ratios in Narji limestones–reflection on pale redox condition

Trace element concentration as well as elemental ratio is frequently used to identify the redox condition of carbonate deposits **(Wright et al., 1984; Jones and Manning, 1994; Armstrong-Altrin et al., 2015a).** U/Th ratio is higher than 1.25 indicates suboxic to anoxic depositional environment **(Armstrong-Altrin et al., 2003).** In this context, the U/Th ratios of the Narji limestones vary in between 1.73 and 4.19 **(Table 5.5, Fig 5.13)** with an average of 2.60 and this clearly indicates their deposition in suboxic to anoxic environment. V/ (V + Ni) ratio has been also frequently applied by several workers to identify the paleo redox condition of carbonates **(Rimmer, 2004; Ramos-Vázquez et al., 2017).** Carbonate samples whose V/ (V + Ni) ratio is greater than 0.5 imply that their deposition is in suboxic/anoxic condition. In this study, the

Narji limestones show higher V/ (V + Ni) ratio (0.92 to 0.96, **Table 5.5**) and therefore clearly indicates that deposition was in anoxic condition.

5.5 CONCLUSION

- The Narji carbonate rocks reveal the presence of three types of limestone lithofacies, namely, quartzite bearing massive purple limestone, massive whitish grey limestone, and laminated limestone facies.
- The geochemical signatures of the carbonate rocks from Neoproterozoic Narji Formation elucidate significant knowledge regarding the depositional environment.
- Within the major oxides, a wide range of CaO (31.45 to 72.03 wt.%) and SiO_2(14.27 to 45.92 wt.%) is recorded and the correlation between CaO and SiO_2 reflects negative correlation ($r = -0.62$) in between Ca and Si which clearly indicates that Ca and Si are from different modes of origin. Relatively higher concentration of SiO_2 within these limestones suggests clastic input within the limestones.
- PAAS normalized REE + Y pattern shows seawater like REE + Y pattern (depleted LREE and enriched to flat HREE) with negative Eu anomaly.
- The Er/Nd ratio varies from 0.06 to 0.22 with an average 0.17 and this point towards terrigenous input within the limestones.
- The Y/Ho ratios vary in between 30.05 and 45.45, and this also suggests that the limestones were deposited in a marine environment but due to the terrigenous input or contamination, the Y/Ho ratio is slightly decreased.
- Positive Ce anomaly, high U/Th (> 1.25), and V/ (V + Ni) (>0.5) ratios of Narji limestones clearly indicate that their deposition was in a suboxic to anoxic condition.

.

FIGURES AND TABLES

Fig. 5.1 Field photograph of sinuous crested ripple resembling like tuning fork within quartzite bearing massive limestone (15°18’45.00’’N, 78°07’35.76’’E) from Cuddapah Basin. (Length of diagonal scale- 15.20 cm)

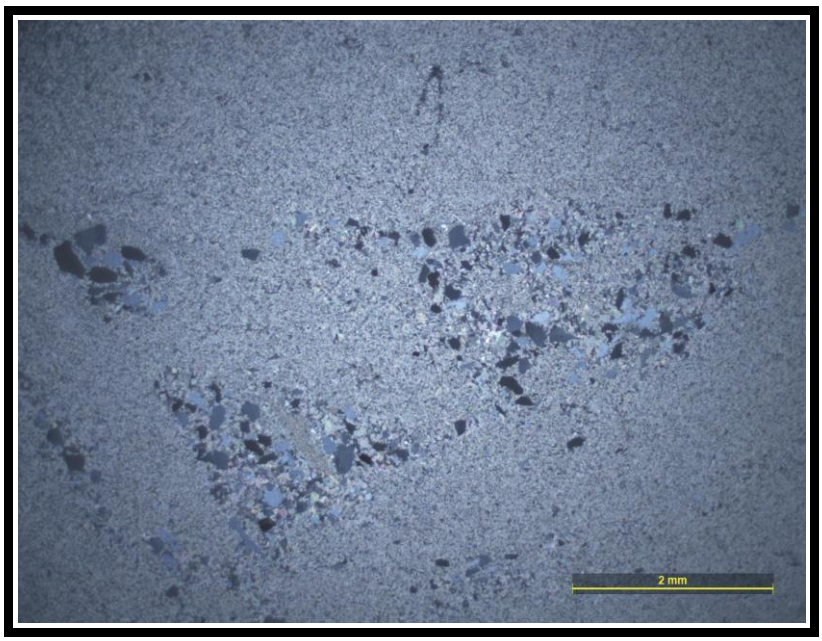

Fig. 5.2 Photomicrograph of patchy distribution of quartzite within micrite dominated limestone in quartzite bearing massive limestone facies (15°18’45.00’’N, 78°07’35.76’’E) from Cuddapah Basin, India.

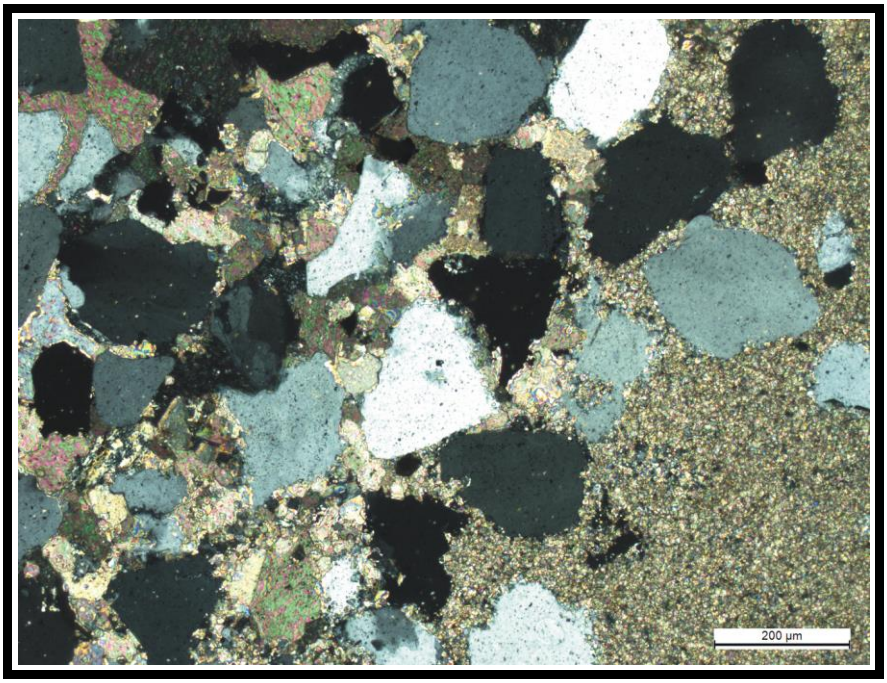

Fig. 5.3 Photomicrograph of calcite cementation in the pore spaces in between the quartz grains (15°18’45.00’’N, 78°07’35.76’’E) from Cuddapah Basin

Fig. 5.4 Photograph of massive whitish limestone of Narji Formation. (Length of the hammer- 31.80 cm) (15°18’45.00’’N, 78°07’35.76’’E) from Cuddapah Basin

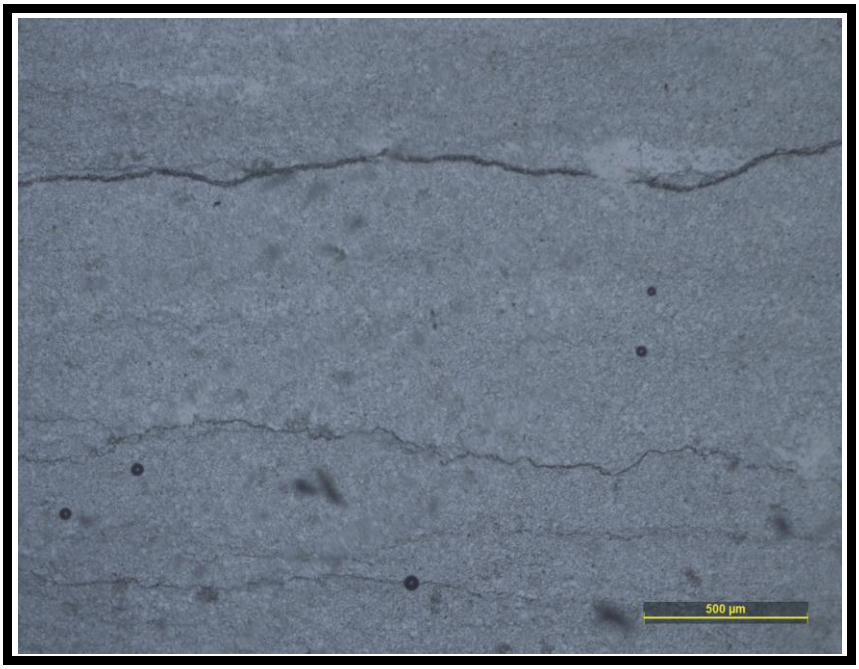

Fig. 5.5 Photomicrograph of different types of stylolites within massive whitish limestone (15°18’45.00’’N, 78°07’35.76’’E) from Cuddapah Basin

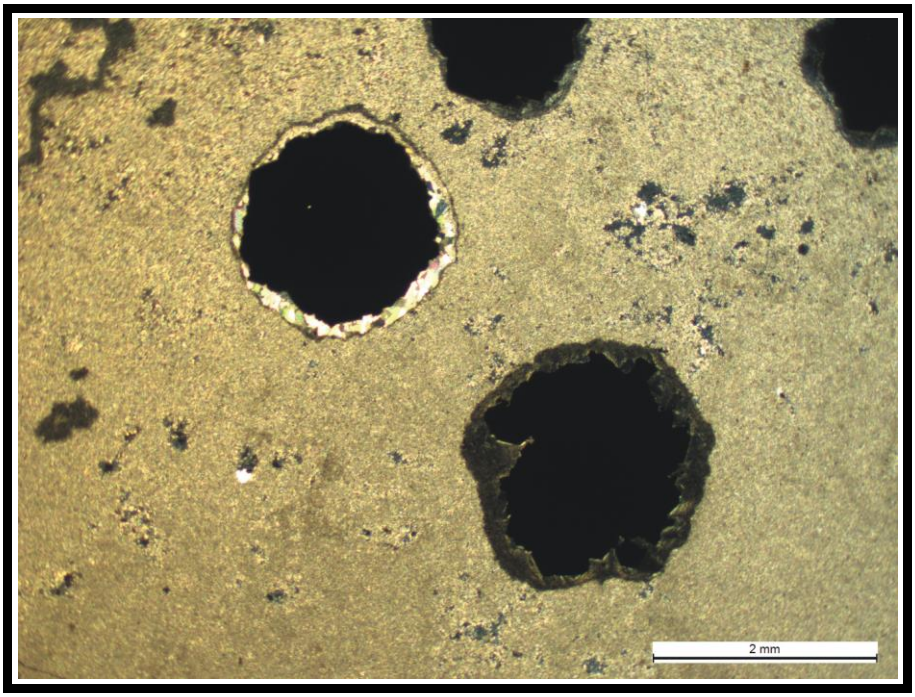

Fig. 5.6 Photomicrograph of scattered crystals of pyrite within limestone, the margins of the pyrite are surrounded by sparite that probably formed as a residue after the replacement of pyrite by calcite, (15°18’45.00’’N, 78°07’35.76’’E) from Cuddapah Basin

Fig. 5.7 Photograph of straight and wavy laminated limestone characterized by irregular undulated layers (15°18’45.00’’N, 78°07’35.76’’E) from Cuddapah Basin**. (**Length of the hammer- 31.80 cm)

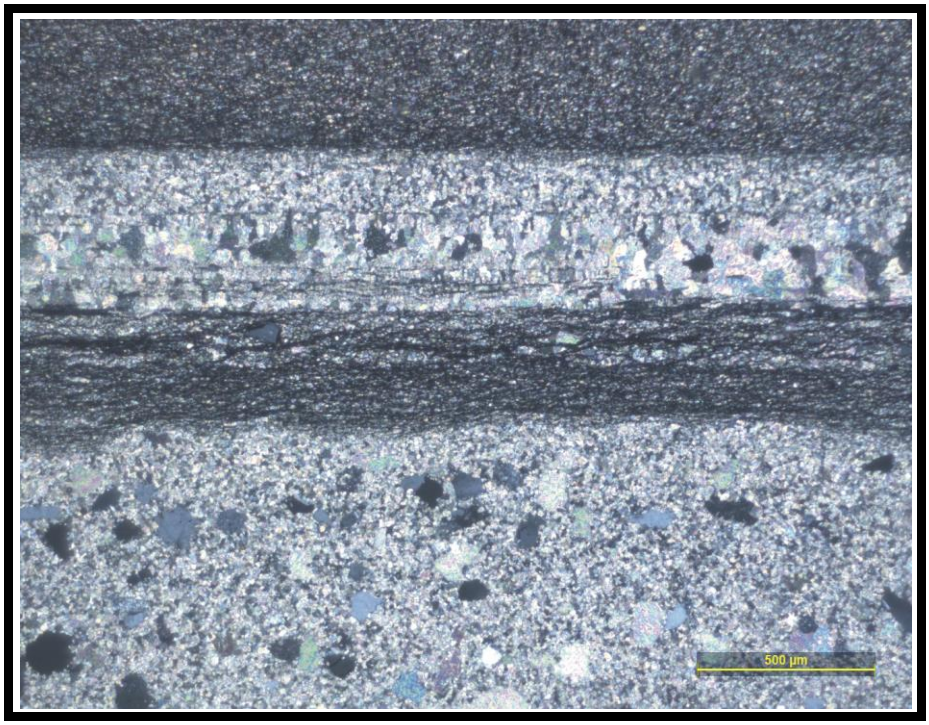

Fig.5.8 Photomicrograph of dark streaks of clay within limestone interlaminated with light coloured coarse sparite crystal (15°18’45.00’’N, 78°07’35.76’’E) from Cuddapah Basin

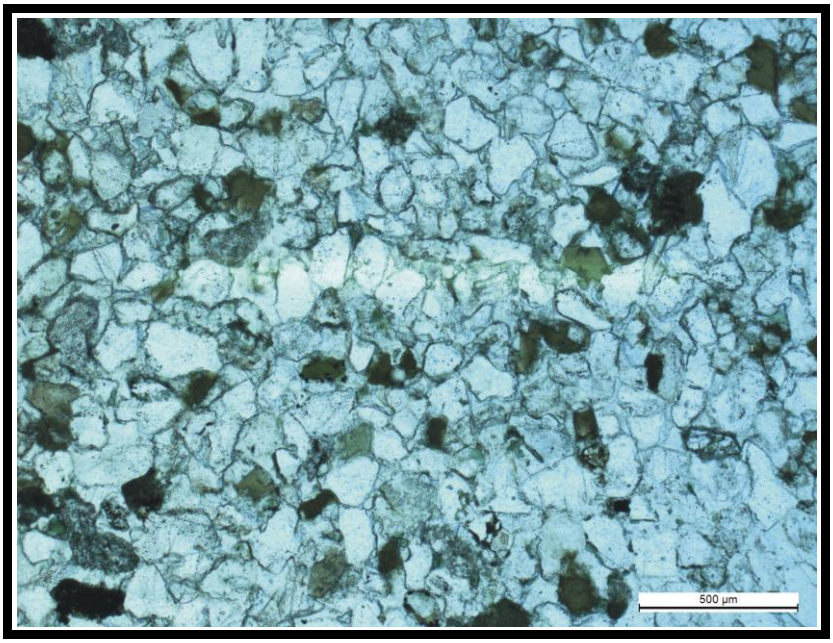

Fig. 5.9 Photomicrograph of lowermost part of the calcareous shale facies (15°18’45.00’’N, 78°07’35.76’’E) from Cuddapah Basin. Note green colour glauconite sand. Most glauconite grains within the micritic matrix are replaced by Fe-calcite.

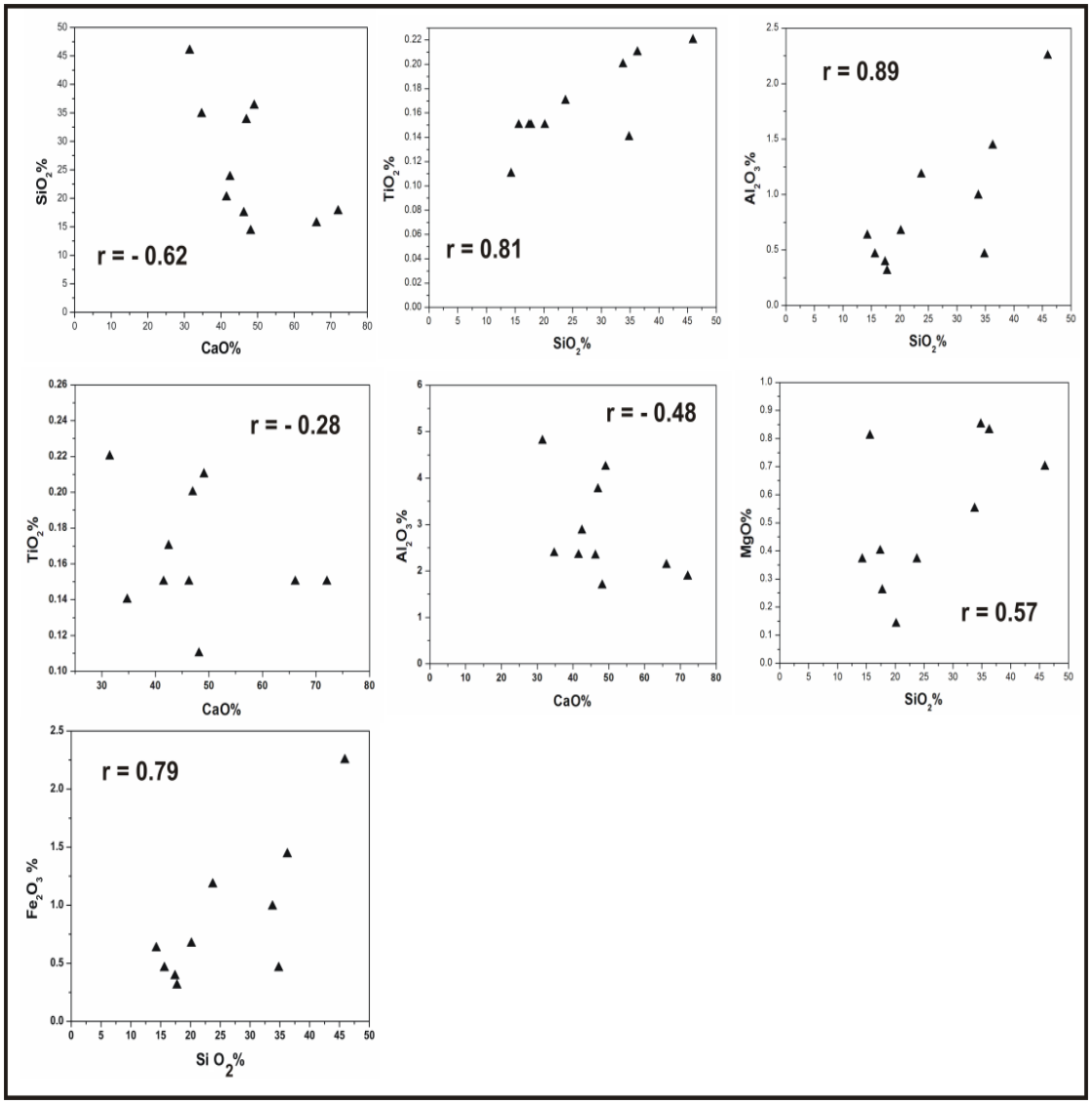

Fig. 5.10 Bivariate plots of SiO_2, TiO_2, Al_2O_3, against CaO, and TiO_2, Al_2O_3, MgO, Fe_2O_3, against SiO_2 in Narji limestones

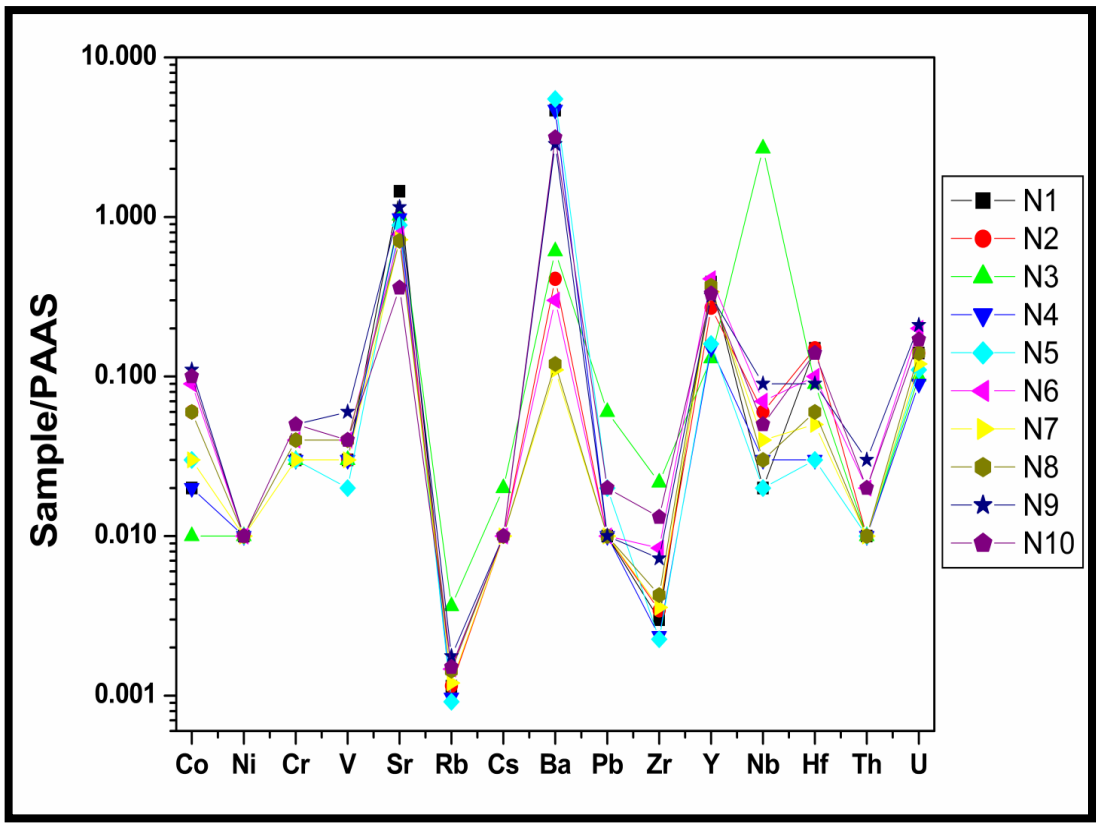

Fig. 5.11 Distribution of PAAS normalized trace elements of Narji limestones. PAAS value is defined from **Taylor and McLennan, (1985)**

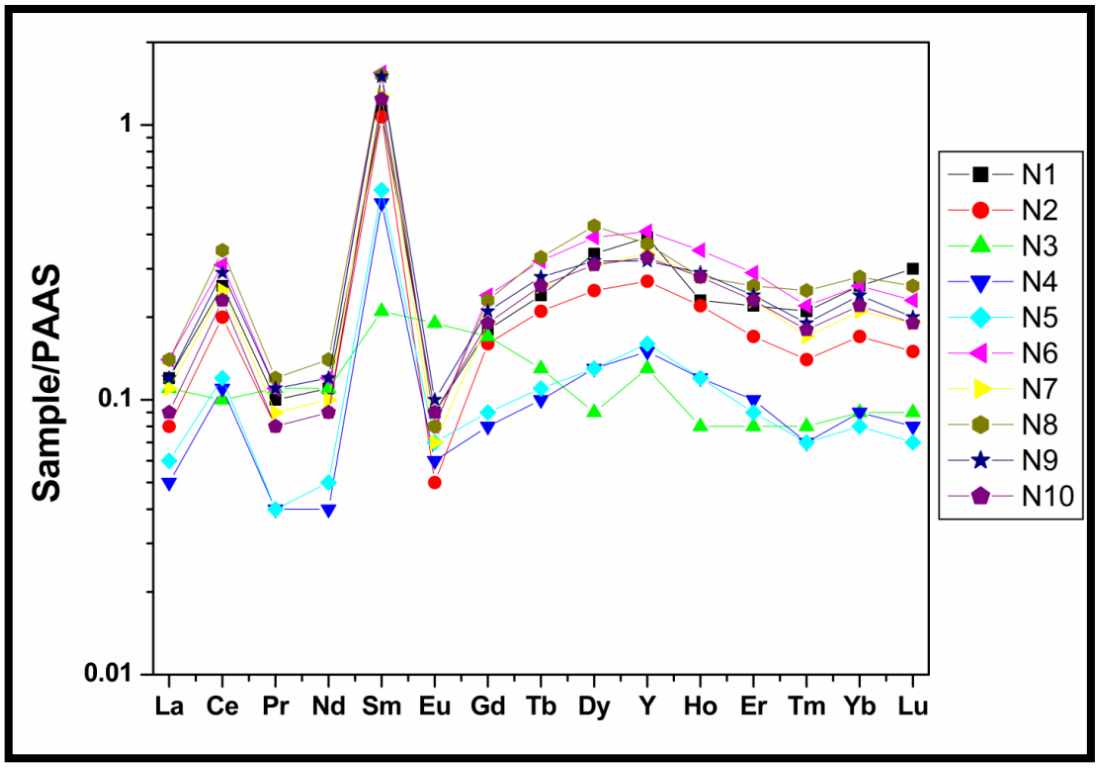

Fig. 5.12 Distribution of PAAS normalized REE+Y patterns of Narji limestones. PAAS value is defined from **Taylor and McLennan, (1985)**

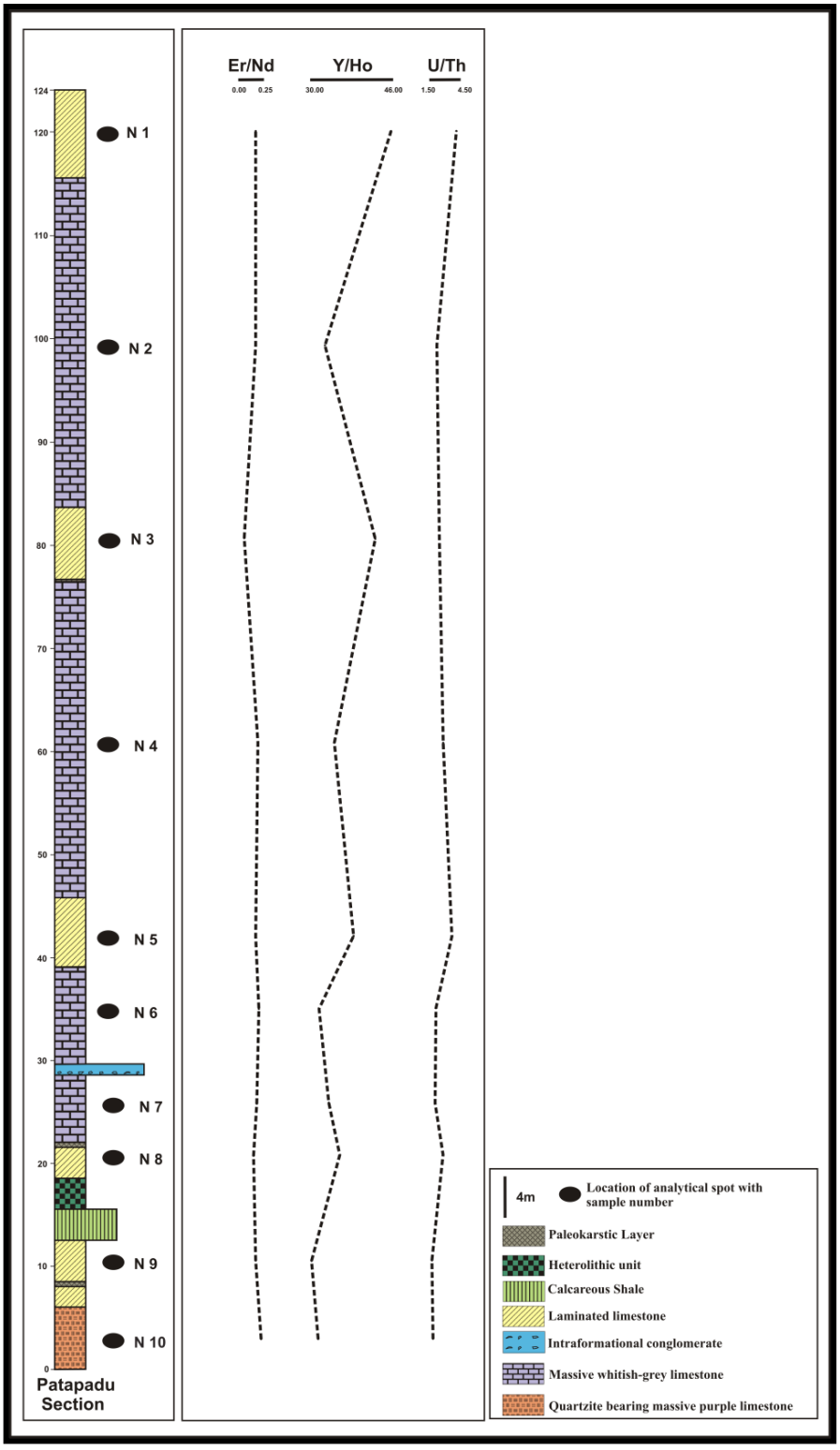

Fig. 5.13 Litholog of the measured stratigraphic section with the positions of the limestone samples collection. Er/Nd, Y/Ho and U/Th ratios of the Narji limestones are also plotted, showing their vertical variations within the studied section.

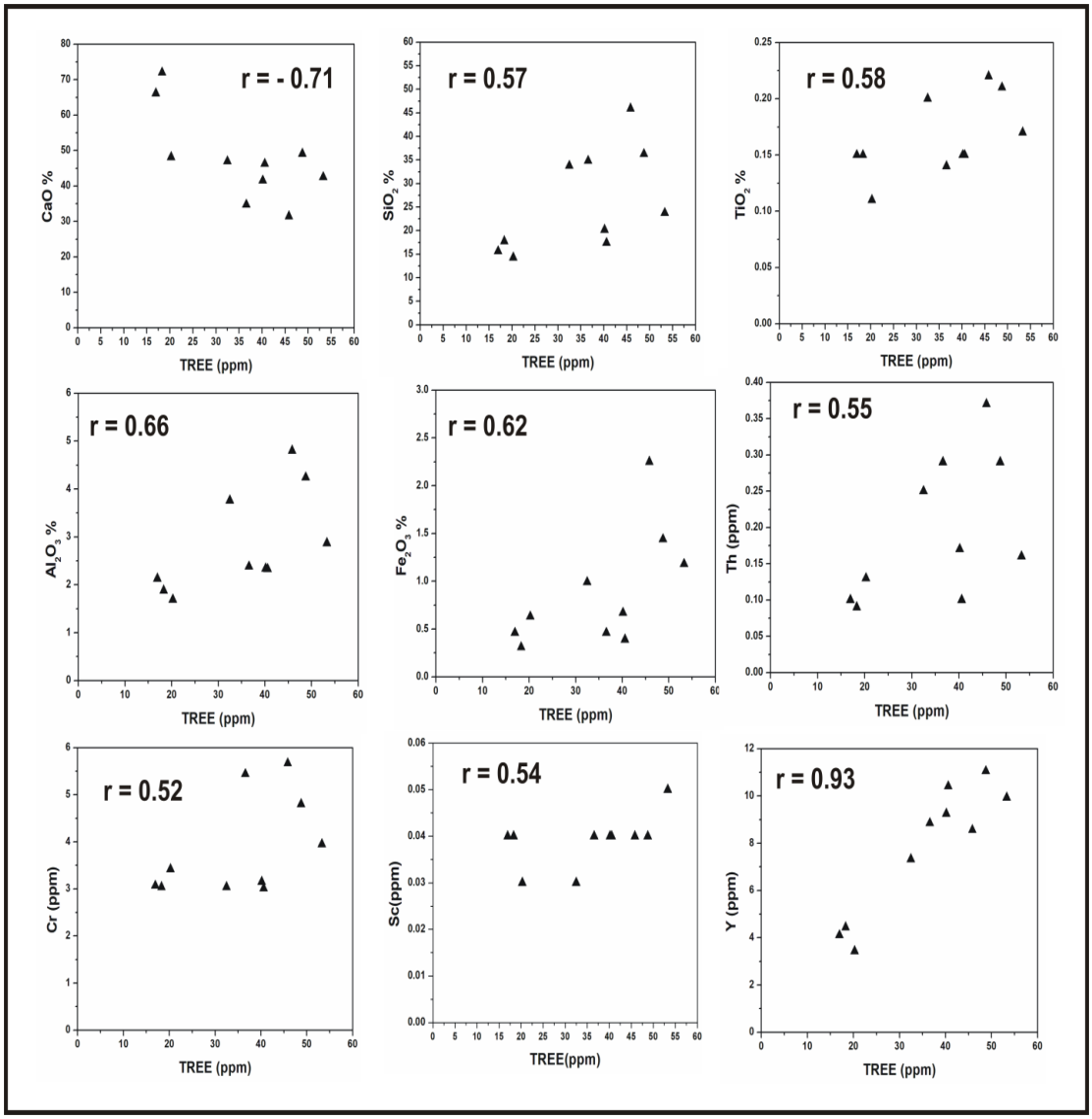

Fig. 5.14 Bivariate plots of major oxide (%) and trace elements (in ppm) of Narji limestones against ∑REE

Table 5.1 Lithology of the geochemically analyzed Narji Limestone samples

Sample number	Lithology
N1	Laminated limestones
N2	Massive whitish grey limestone
N3	Laminated limestones
N4	Massive whitish grey limestone
N5	Laminated limestones
N6	Massive whitish grey limestone
N7	Massive whitish grey limestone
N8	Laminated limestones
N9	Laminated limestones
N10	Quartzite bearing massive purple limestone

Table 5.2. Major oxides (wt.%) content in the Narji limestones, Kurnool Basin with the average value of PAAS **(Taylor and McLennan, 1985)**

Sample no.	SiO_2	TiO_2	Al_2O_3	MnO	Fe_2O_3	CaO	MgO	Na_2O	K_2O	P_2O_5	LOI	TOTAL	K_2O/Al_2O_3	Al_2O_3/TiO_2
N-1	17.40	0.15	2.33	-	0.39	46.26	0.40	-	0.30	0.80	31.46	99.49	0.13	15.53
N-2	33.76	0.20	3.76	0.01	0.99	46.95	0.55	-	0.87	0.97	11.36	99.42	0.23	18.80
N-3	14.27	0.11	1.69	0.03	0.63	48.14	0.37	0.02	0.35	0.09	33.94	99.64	0.21	15.36
N-4	15.63	0.15	2.13	-	0.46	66.11	0.81	-	0.30	0.18	13.98	99.75	0.14	14.20
N-5	17.74	0.15	1.88	0.02	0.31	72.03	0.26	-	0.25	0.96	6.00	99.60	0.13	12.53
N-6	36.26	0.21	4.24	0.02	1.44	49.08	0.83	0.01	0.97	0.64	5.65	99.35	0.23	20.19
N-7	20.16	0.15	2.34	-	0.67	41.52	0.14	-	0.57	0.59	33.37	99.51	0.24	15.60
N-8	23.74	0.17	2.87	-	1.18	42.48	0.37	-	0.73	0.61	27.54	99.69	0.25	16.88
N-9	45.92	0.22	4.80	0.03	2.25	31.45	0.70	-	1.15	0.27	12.90	99.69	0.24	21.82
N-10	34.81	0.14	2.38	0.01	0.46	34.72	0.85	0.03	0.58	0.31	25.27	99.56	0.24	17.00
Average	25.97	0.17	2.84	0.01	0.88	47.87	0.53	0.01	0.61	0.54	20.15	99.57	0.21	16.71
PAAS	62.80	0.99	18.90	7.22	0.11	2.20	1.30	1.20	3.70	0.16	6.00	104.58	0.20	19.09

Table 5.3. Trace elements (in ppm) concentrations in the Narji limestones, Kurnool Basin with the average value of PAAS **(Taylor and McLennan, 1985)** and obtained values for the standard, JLS-1.

Sample no.	**N-1**	**N-2**	**N-3**	**N-4**	**N-5**	**N-6**	**N-7**	**N-8**	**N-9**	**N-10**	**Average of Narji samples**	**PAAS**	**JLS-1**
Trace elements													
V	4.53	4.79	4.03	4	3.61	6.14	4.67	6.25	9.2	6.59	5.38	150	3.769
Cr	3.01	3.04	3.42	3.07	3.04	4.8	3.15	3.95	5.67	5.44	3.86	110	3.194
Co	0.44	1.48	0.13	0.56	0.79	2.01	0.76	1.33	2.57	2.35	1.24	23	0.067
Ni	0.3	0.33	0.32	0.31	0.31	0.34	0.3	0.31	0.41	0.33	0.33	55	0.287
Sc	0.04	0.03	0.03	0.04	0.04	0.04	0.04	0.05	0.04	0.04	0.04	16	0.022
Cu	0.31	0.25	0.32	0.25	0.33	0.28	0.24	0.28	0.26	0.26	0.28	50	0.226
Zn	6.38	4.01	3.99	5.06	5	3.7	3.06	4.8	6.07	3.54	4.56	85	2.363
Ga	B.D.	B.D.	0.62	B.D.	B.D.	B.D.	B.D.	B.D.	B.D.	B.D.	0.62	17.5	0.097
Rb	0.18	0.18	0.58	0.16	0.15	0.23	0.19	0.23	0.28	0.24	0.24	160	0.189
Sr	289.65	199.78	203.59	196.26	178.07	156.43	143.91	141.53	230.11	72.27	181.16	200	279.232
Y	10.41	7.32	3.43	4.11	4.44	11.05	9.25	9.93	8.56	8.85	7.74	27	0.188
Zr	0.63	0.72	4.55	0.5	0.47	1.77	0.75	0.9	1.52	2.76	1.46	210	3.879
Nb	0.04	0.11	5.1	0.05	0.04	0.13	0.08	0.06	0.17	0.1	0.59	1.9	1.221
Cs	0.05	0.1	0.32	0.04	0.04	0.11	0.1	0.1	0.16	0.2	0.12	15	0.064
Ba	3036.45	263.84	398.02	3045.97	3570	196	74.47	80.6	1857	2043	1456.65	650	427.865
Hf	0.74	0.21	0.09	0.16	0.15	0.51	0.25	0.31	0.45	0.72	0.36	5	0.088
Ta	0.01	0.02	0.03	0.01	0.01	0.02	0.01	0.01	0.02	0.01	0.02	-	0.014
Pb	0.26	0.3	1.15	0.25	0.42	0.3	0.26	0.28	0.28	0.34	0.38	20	1.075
Th	0.1	0.25	0.13	0.1	0.09	0.29	0.17	0.16	0.37	0.29	0.2	14.6	0.026
U	0.43	0.57	0.32	0.28	0.33	0.63	0.36	0.44	0.65	0.52	0.45	3.1	1.573

Table 5.4. REE concentration (in ppm) in the studied Narji limestones, Kurnool Basin with the average value of PAAS **(Taylor and McLennan, 1985)** and obtained values for the standard, JLS-1.

Sample no.	N-1	N-2	N-3	N-4	N-5	N-6	N-7	N-8	N-9	N-10	Average of Narji Samples	PAAS	JLS-1
La	4.76	3.21	4.19	1.97	2.11	5.26	4.31	5.48	4.75	3.3	3.94	38.2	0.109
Ce	20.39	16.26	7.95	8.42	9.26	24.35	20.09	27.95	23.18	18.32	17.62	79.6	0.725
Pr	0.86	0.69	0.98	0.36	0.37	1.01	0.83	1.08	0.97	0.72	0.79	8.83	0.033
Nd	3.8	2.96	3.85	1.48	1.53	4.18	3.51	4.86	3.99	3.02	3.32	33.9	0.12
Sm	6.26	5.92	1.15	2.87	3.19	8.58	7.1	8.43	8.33	6.87	5.87	5.55	0.093
Eu	0.09	0.06	0.2	0.06	0.07	0.09	0.08	0.08	0.1	0.09	0.09	1.08	0.006
Gd	0.83	0.75	0.78	0.38	0.41	1.12	0.9	1.06	1	0.89	0.81	4.66	0.052
Tb	0.19	0.16	0.1	0.08	0.08	0.24	0.2	0.25	0.21	0.2	0.17	0.77	0.003
Dy	1.57	1.16	0.42	0.59	0.6	1.8	1.47	2.04	1.51	1.44	1.26	4.68	0.025
Ho	0.23	0.22	0.08	0.12	0.12	0.35	0.28	0.28	0.28	0.28	0.22	0.99	0.003
Er	0.64	0.5	0.23	0.28	0.26	0.82	0.64	0.75	0.67	0.66	0.54	2.85	0.011
Tm	0.09	0.06	0.03	0.03	0.03	0.09	0.07	0.1	0.08	0.07	0.06	0.41	0.002
Yb	0.74	0.48	0.25	0.26	0.24	0.74	0.59	0.8	0.67	0.63	0.54	2.82	0.01
Lu	0.13	0.06	0.04	0.03	0.03	0.1	0.08	0.11	0.09	0.08	0.08	0.43	0.028
∑LREE/∑ HREE	8.18	8.58	9.49	8.56	9.34	8.26	8.49	8.88	9.16	7.6	8.6	9.49	-
∑REE	40.58	32.49	20.25	16.93	18.3	48.73	40.15	53.27	45.83	36.57	35.31	184.77	-

Table 5.5. Elemental ratios and anomalies of the studied Narji limestones. Ce/Ce* = $Ce_{SN}/ (La_{SN} \times Pr_{SN})^{0.5}$; Eu/Eu* = $Eu_{SN}/ (Sm_{SN} \times Gd_{SN})^{0.5}$; Pr/Pr*= $[Pr/ (0.5Ce+ 0.5Nd)]_{SN}$

Sample no.	Eu/Eu*	Ce/Ce*	Pr/Pr*	$(Nd/Yb)_{SN}$	$(La/Yb)_{SN}$	$(Dy/Yb)_{SN}$	Y/Ho	Er/Nd	V/(V+Ni)	U/Th
N-1	0.19	2.33	0.53	0.43	0.47	1.27	45.45	0.17	0.94	4.19
N-2	0.13	2.52	0.54	0.51	0.49	1.46	32.91	0.17	0.94	2.26
N-3	1.02	0.91	1.04	1.26	1.21	1.00	42.56	0.06	0.93	2.48
N-4	0.29	2.32	0.54	0.48	0.57	1.39	34.79	0.19	0.93	2.87
N-5	0.29	2.43	0.51	0.53	0.65	1.50	38.43	0.17	0.92	3.68
N-6	0.14	2.43	0.53	0.47	0.52	1.47	31.83	0.2	0.95	2.15
N-7	0.14	2.45	0.53	0.49	0.54	1.49	33.38	0.18	0.94	2.06
N-8	0.13	2.65	0.50	0.51	0.51	1.54	35.87	0.15	0.95	2.78
N-9	0.17	2.49	0.54	0.50	0.52	1.36	30.05	0.17	0.96	1.73
N-10	0.18	2.75	0.51	0.40	0.39	1.38	31.55	0.22	0.95	1.79
Average	0.27	2.33	0.58	0.56	0.59	1.39	35.68	0.17	0.94	2.60

Table 5.6. Average geochemical values of the Narji Limestones compared to the other Proterozoic carbonate rocks of India showing seawater like REE patterns

Element's ratio	Narji Limestone[a]	Shallow marine platform carbonate[b]	Bhima Limestone[c]	Rohtas Limestone
TREE (ppm)	32.81±13.03	3.36±2.55	32.2±13.3	68.87±9.25
Y/Ho	35.38±5.03	35.90±13.25	38.13±21.35	33.30±6.77
Er/Nd	0.16±0.04	0.25±0.17	0.15±0.03	0.08±0.02
Eu/Eu*	0.21±0.27	-	1.51±0.64	0.62±0.05
Ce/Ce*	2.25±0.52	-	0.57±0.08	0.92±0.04
$(La/Yb)_{SN}$	0.56±0.23	0.68±0.47	0.732±0.12	1.31±0.58
$(Nd/Yb)_{SN}$	0.53±0.25	0.65±0.39	0.64±0.08	1.08±0.35
$(Dy/Yb)_{SN}$	1.38±0.16	1.10±0.25	1.20±0.13	1.19±0.14

[a] Present study, n=10; [b] Mazumdar et al. (2003), n=15; [c] Nagarajan et al. (2011), n=18;

[d] Sen and Mishra. (2015), n=7

CHAPTER-6
INTERGRATION

6.1 INTRODUCTION

Integration of data represented so far is very much important for depicting the evolution of Kurnool sub-basin of the Cuddapah Basin during the deposition of carbonate dominated Narji formation. Before synthesizing the generalized data of the study, a cursory look on the several clues related to these aspects as emerged from the earlier chapters is discussed here.

6.2 CLUES FROM FACIES ANALYSIS

The facies documented in the Narji Formation are mainly deposited in a carbonate dominated platform, over the Banganapalle Quartzite. The Neoproterozoic Narji Formation of Cuddapah Basin in an around along the road cut section of Patapadu-Yaganti hills, Betamcherla hills and Kottala hills areas consists essentially of three facies associations representing (a)intertidal, and (b) subtidal environments. Intertidal facies association is considered as the shallowest facies association and the facies includes laminated limestone and heterolithic facies. Laminated limestone facies mainly deposited by suspension activity in shallow, quiet water with the periodic influx of the tidal currents and waves, in an intertidal environment. Within laminated limestone high amount of suspension fall out along with carbonate precipitation indicate low-energy quiet environment. Presence of comparatively coarser material along with finer carbonates within heterolithic facies indicates a comparably high-energy environment. The heterolithic unit mainly deposited in intertidal set-up near to the shore (**Grime and Cuthbert, 1945; Bekker and Errickson, 2003; Panja et al., 2019**). The facies which developed within the subtidal facies' association are Quartzite-bearing massive purple limestone facies, Calcareous shale facies, Massive whitish grey limestone facies, and Intra-formational conglomerate facies. The overall

presence of coarse-grained detrital material within Quartzite-bearing massive purple limestone facies indicates deposition in moderate-to-high energy environment. The syneresis cracks frequently associated with calcareous sediment indicate a swelling in the soft substrate which is a result of salinity changes in the sub-tidal marine environment. Overall finer grain size within calcareous shale facies indicates deposition of this facies in comparatively low energy environment. This facies seems to be mainly deposited in calm and low-energy environment of shallow subtidal environment (**Al-Juboury et al., 2015**). Presence of high amount of micrite and absence of any detrital input within massive whitish grey limestone facies indicate deposition in low-energy environment. Presence of pyrite in the facies indicates euxinic and reducing condition. The deposition takes place through suspension and precipitation in restricted isolated basin in a low energy shallow subtidal environment. Presence of bimodal clasts within comparatively fine-grained matrix indicates that deposition of intra-formational conglomerate facies is taken place in moderate to high-energy environment of subtidal regime. This conglomerate seems to be the product of reworked sediments derived by subaqueous non-cohesive deep sub-tidal debris flow (**Dasgupta et al., 2005; Chakrabarti et al., 2014**) that have been originated from a well-cemented platform rim by the storm currents or mild local seismic activity from the early lithified beds (**Patranabis Deb et al., 2012**). The bimodal size distribution indicates co-sedimentation of bedload and suspended load in fluctuating energy regime.

6.3 CLUES FROM STYLOLITE

The stylolite is mostly formed perpendicular to the compressive stress that may come from overburden pressure or tectonic event. Concerning stylolitization due to overburden pressure, the formation is parallel to the bedding, this is only sustained if the compression direction is constant and does not change. In the case of tectonic event,

stylolite tends to be transverse to the bedding plane and therefore generates a good indication of the compression history of the zone (**Rigby, 1953**). Again, stylolitization occurs due to tectonic stresses or increase of overburden pressure rock. stylolitization causes decreases in the porosity, permeability and reduction of bed thickness of the host limestone.

The microstylolites within Narji limestones help to depict the sedimentary, diagenetic process and tectonic disturbance within the study area.

The wavy and simple suture types reveal many features which can be explained by the pressure solution theories. Presence of dolomite grains along the micro stylolite indicates diagenesis. The pre lithification process was identified by the presence of residual seam, insoluble material, micro faults and suture type stylolite. The presence of residual clay capping in the stylolite indicates the solution pressure theory or origin. The horizontal, vertical and inclined stylolite evidence from the successive pressure system indicates local disturbance and tectonic activity in this area with varied direction of action of these forces.

6.4 CLUES FROM PETROGRAPHIC ANALYSIS

Petrographic analysis of quartzite bearing massive limestone facies indicates presence of detrital sandstones and stings of clastic lamination within the micrite indicates deposition in low-to-moderate energy shallow intertidal to subtidal environment (**Flugel, 2010; Ali et al., 2013; Hashmie et al., 2016**). Within laminated limestone facies the lamination may have been deposited from suspension by clay or colloidal particles or under the influence of tidal currents (**Komatsu et al., 2014**). Occurrence of glauconite indicates shallow marine depositional environment (**Naik et al., 2016**). Overall finer grain size of the calcareous shale facies indicates deposition of

this lithology in comparatively low energy environment. Further mud and clay indicate deposition in low-energy anoxic environment through suspension and deposition (**Srivastava and Singh, 2017**).

Presence of pyrite within the massive whitish grey limestone facies indicates euxinic and reducing condition during the deposition. Presence of high amount of micrite in this limestone facies demonstrates a low energy environment of deposition (**Adachi et al., 2004**).

6.5 CLUES FROM GEOCHEMICAL ANALYSIS

The geochemical signatures of the carbonate rocks from Neoproterozoic Narji Formation elucidate significant knowledge regarding the depositional environment. Within the major oxides, a wide range of CaO (31.45 to 72.03 wt.%) andSiO_2(14.27 to 45.92 wt.%) is recorded and the correlation between CaO and SiO_2 reflects negative correlation ($r = -0.62$) in-between Ca and Si which clearly indicates that Ca and Si are from different modes of origin. Relatively higher concentration of SiO_2 within these limestones suggests clastic input within them limestones. PAAS normalized REE + Y pattern shows seawater like REE + Y pattern (depleted LREE and enriched to flat HREE) with negative Eu anomaly. The Er/Nd ratio varies from0.06 to 0.22 with an average 0.17 and this points terrigenous input within the limestones. The Y/Ho ratio varies in between30.05 and 45.45, and this also suggests that the limestones were deposited in a marine environment but due to the terrigenous input or contamination, the Y/Ho ratio is slightly decreased. Positive Ce anomaly, high U/Th (> 1.25), and V/(V + Ni) (>0.5) ratios of Narji limestones clearly indicate that their deposition was in a suboxic to anoxic condition.

6.6 DISCUSSION

6.6.1 EVOLUTION OF KURNOOL SUB-BASIN DURING THE DEPOSITION OF THE NARJI FORMATION LITHOLOGY

The initiation of deposition of Narji Formation begins with the deposition of quartzite bearing massive limestone probably deposited in a shallow subtidal environment over the Banganapalli Formation that seems to be deposited in a fan-delta set-up (**Patranabis Deb et al., 2012**). These quartzites are the detrital materials derived from the underlying Banganapalli Quartzite Formation. The grains are rounded to sub-rounded indicating a distal mode of transportation. The ripple marks indicate an oscillatory wave action and synaeresis cracks on the surface of the limestone indicate sub-areal exposure in near-shore to the beach setting. Presence of detrital material in the basal limestone indicates a link between the land and the carbonate platform. The heterolithic facies is deposited in intertidal tidal flat during the slack water phase of tide and/or after storm events (**Panja et al., 2017**). The occurrence of glauconite indicate slow rate of sedimentation during recession stage in shallow marine condition (**Chattoraj et al., 2009; Srivastava and Singh, 2017**). The massive micrite dominated limestone seems to be deposited principally in subtidal regime within the framework of restricted carbonate platform (**Patranabis Deb et al., 2012**). Both tidal and storm influenced deposition of laminated limestone facies consisting of clay laminae of variable thickness. The irregular channels and fractures are formed in this limestone during early diagenesis and subaerial exposure (**Srivastava and Gawande, 2006**; **Srivastava and Singh, 2017**). Towards the end of deposition, the semi-consolidated lime mud is probably disturbed due to mild-tectonic activity resulting in intraformational conglomerate. Hummocks indicates sporadic storm event affecting the sea bed.

The Narji Formation is mainly dominated by limestone compared to the underlying Banaganaplle Quartzite and overlying Owk Shales of Kurnool Basin. This thick deposition of limestone is mainly due to chemical precipitation of carbonate into an intertidal–subtidal platformal depositional environment. The horizontal, vertical and inclined stylolite indicates local disturbance and tectonic activity in this area with varied direction of action of these forces which are very common in extensional set-up (**Madesh et al., 2012**).

6.6.2 COMPARISON OF NARJI FORMATION WITH OTHER COEVAL SUCCESSIONS

Formation of the supercontinent Rodinia took place at the end of Mesoproterozoic and beginning of the Neoproterozoic (**Rogers and Santosh, 2009**). According to some authors Columbia may have converted to Rodinia without true dispersal (**Piper, 2013**) and configuration of pre-Gondwana continents. It is more correlated with the upper Riphaean age (1000–650 M.A) of Lakhanda and Uy Group, and the VendianYocloma Group (**Khudoley et al., 2001**) occurring at the eastern margin of Siberian platform. Kurnool Group lithology is deposited along with other coeval basin-fills around the globe during the formation of Rodinia. Hence, it is very interesting if we compare the Narji Formation lithology with other coeval successions during the critical time of formation of Rodinia.

The Jagdalpur Formation of Indravati Group, India, can be compared with Narji Formation as the depositional age of this formation is almost 700–1100 Ma (**Mukherjee et al., 2012**) which is very much similar with the depositional age of the Narji Formation. The Jagdalpur Formation is dominated by limestone with lesser amount of shale and this is very much similar with the Narji Formation. Development

of stromatolites is well recorded in the upper part of the Jagdalpur Formation. However, occurrence of stromatolites is not reported in Narji Formation. This may be due to the anoxic environment prevailing during the deposition of the Narji Formation lithology (**Roy et al., 2018**).

Similarly, the Shahabad and Katamdevarahalli Formation of Bhima basin, India, are age equivalent with the Narji Formation. Shahabad and Katamdevarahalli Formation are dominated with massive, flaggy limestones with minor clastic inputs, pyrite and chert nodules. The succession is very much similar with the Narji Formation rocks and is inferred to be deposited in a shallow marine carbonate platform. **Roy et al., (2018)** have already performed a geochemical comparison between Bhima limestones and Narji limestones, which showed similar depositional conditions for both the formations. Hence, it may be concluded that depositional set-up of the limestone dominated formations during this particular time period is almost identical with some local variation in oxic/anoxic condition which further leads/perturbs the development of algal bodies like stromatolites.

Globally, there are some reports of coeval successions of Narji Formation. Within these, the early Neoproterozoic Beck Spring Dolomite of California, USA (**Tucker, 1982**) is very much identical with the Narji Formation. Both the formations deposited in a carbonate platform with similar type of marine diagenetic history. Beck Spring Dolomite is dominantly consisting of carbonate which is precipitated from anoxic, ferruginous seawater. Therefore, the depositional environment is also similar for both the formations. Facies analysis with recorded sedimentary structures depict that the Beck Spring Dolomite is deposited in a shallow subtidal to upper intertidal marine environments (**Shafer, 1983; Tucker, 1983; Marian and Osborne, 1992; Harwood and Sumner, 2012**) similar to the Narji Formation.

The Weiji Formation of the Huaibei Group that was deposited along the southern margin of the North China Craton is also believed to be coeval successions of Narji Formation of early Tonian age. There is remarkably similarity in deposition between both the litho-successions. Presence of certain kind of stromatolite taxa reported in the middle of the Weiji Formation, indicates suboxic subtidal environments (**Qian et al., 2001**). Hence the overall environment of deposition is presumed to be similar to the Narji Formation.

Comparing with these all formations, it can be attributed that they are the ancient analogues of Narji Formation. Hence, we can conclude that most of the coeval successions of Narji Formation rocks throughout the globe indicate a similar type of depositional pattern during this time interval (early Neoproterozoic) especially during the fragmentation and amalgamation of Rodinia.

6.7 CONCLUSION

- The array of facies of Narji Formation may be grouped into two facies associations (FA-1) intertidal, and (FA-2) subtidal.
- Within the recorded facies, the laminated limestone facies and heterolithic facies are deposited in intertidal zone (below mean low-tide level but above fair-weather wave base), the other facies which include quartzite-bearing massive purple limestone facies, calcareous shale facies, massive whitish grey limestone facies and intra-formational conglomerate facies are deposited in extended shallow subtidal environment (below the fair-weather wave base but above the storm wave base).
- The Narji formation starts with deposition in moderate to high energy shallow subtidal environment.

- The horizontal, vertical and inclined stylolite evidence from the successive pressure system indicates local disturbance and tectonic activity in this area with varied direction of action of these forces
- Analysed Er/Nd, Y/Ho ratios clearly indicates the terrigenous input within the Narji limestones. Positive Ce anomaly, high U/Th (> 1.25), and V/ (V + Ni) (>0.5) ratios of Narji limestones clearly indicate that their deposition was in a suboxic to anoxic condition.
- **Hence the sedimentological and geochemical studies on Neoproterozoic Narji limestones of Cuddapah Basin reveals the deposition of sediments under suboxic to anoxic condition in a subtidal-intertidal carbonate dominated platform experiencing local tectonic disturbances in the extensional Kurnool sub-basin of Proterozoic Cuddapah Basin.**

BIBLIOGRAPHY

1. A.K., Saha, D., Deb, G.K., Deb, S.P., Mukherjee, M.K. and Ghosh, G., 2002. The Purana basins of southern cratonic province of India-a case for Mesoproterozoic fossil rifts. Gondwana Research, 5(1), pp.23-33.

2. Abedini, A. and Calagari, A.A., 2015. Rare earth element geochemistry of the Upper Permian limestone: the Kanigorgeh mining district, NW Iran. Turkish Journal of Earth Sciences, 24(4), pp.365-382.

3. Absar, N., Nizamudheen, B.M., Augustine, S., Managave, S. and Balakrishnan, S., 2016. C, O, Sr and Nd isotope systematics of carbonates of Papaghni sub-basin, Andhra Pradesh, India: Implications for genesis of carbonate-hosted stratiform uranium mineralisation and geodynamic evolution of the Cuddapah basin. Lithos, 263, pp.88-100.

4. Adachi, N., Ezaki, Y. and Liu, J., 2004. The fabrics and origins of peloids immediately after the end-Permian extinction, Guizhou Province, South China. Sedimentary Geology, 164(1-2), pp.161-178.

5. AHMAD, A., IRSHAD, R. and Ghulam, B.H.A.T., 2015. Facies and diagenetic evolution of the Bathonian-Oxfordian mixed siliciclastic-carbonate sediments of the Habo Dome, Kachchh Basin, India. Volumina Jurassica, 13(1), pp.83-104.

6. Ahmad, F., Quasim, M.A., Ghaznavi, A.A., Khan, Z. and Ahmad, A.H.M., 2017. Depositional environment of the Fort Member of the Jurassic Jaisalmer Formation (western Rajasthan, India), as revealed from lithofacies and grain-size analysis. Geologica Acta, 15(3), pp.153-167.

7. Akhdar, N.E., 2015. Geochemistry of the Shahat Marl Member, Wadi Az Zad, Al Jabal Al. Arabian Journal of Earth Sciences, 2(3).

8. Ali, C.A. and Mohamed, K.R., 2013. Microfacies and diagenesis in the Setul Limestone in Langkawi and Perlis. Bulletin of the Geological Society of Malaysia, 59, pp. 59-66.

9. Al-Juboury, A.I., Al-Haj, M.A. and Jabbar, W.J., 2015. Facies analysis and depositional environment of the geli khana formation (Middle Triassic), Northern Iraq. Arabian Journal of Geosciences, 8(7), pp.4765-4777.

10. Allwood, A.C., Kamber, B.S., Walter, M.R., Burch, I.W. and Kanik, I., 2010. Trace elements record depositional history of an Early Archean stromatolitic carbonate platform. Chemical Geology, 270(1-4), pp.148-163.

11. Amstutz, G.C. and Park, W.C., 1967. Stylolites of diagenetic age and their role in the interpretation of the southern Illinois fluorspar deposits. Mineralium Deposita, 2(1), pp.44-53.

12. Anand, M., Gibson, S.A., Subbarao, K.V., Kelley, S.P. and Dickin, A.P., 2003. Early Proterozoic melt generation processes beneath the intra-cratonic Cuddapah Basin, southern India. Journal of Petrology, 44(12), pp.2139-2171.

13. Anaya-Gregorio, A., Armstrong-Altrin, J.S., Machain-Castillo, M.L., Montiel-García, P.C. and Ramos-Vázquez, M.A., 2018. Textural and geochemical characteristics of late Pleistocene to Holocene fine-grained deep-sea sediment cores (GM6 and GM7), recovered from southwestern Gulf of Mexico. Journal of Paleogeography, 7(1), pp.1-19.

14. Armstrong-Altrin, J.S., Lee, Y.I., Verma, S.P. and Worden, R.H., 2009. Carbon, oxygen, and strontium isotope geochemistry of carbonate rocks of the upper Miocene Kudankulam Formation, southern India: Implications for paleoenvironment and diagenesis. Geochemistry, 69(1), pp.45-60.

15. Armstrong-Altrin, J.S., Machain-Castillo, M.L., Rosales-Hoz, L., Carranza-Edwards, A., Sanchez-Cabeza, J.A. and Ruíz-Fernández, A.C., 2015. Provenance and depositional history of continental slope sediments in the Southwestern Gulf of Mexico unraveled by geochemical analysis. Continental Shelf Research, 95, pp.15-26.

16. Armstrong-Altrin, J.S., Madhavaraju, J., Sial, A.N., Kasper-Zubillaga, J.J., Nagarajan, R., Flores-Castro, K. and Rodríguez, J.L., 2011. Petrography and stable isotope geochemistry of the cretaceous El Abra Limestones (Actopan), Mexico: Implication on diagenesis. Journal of the Geological Society of India, 77(4), pp.349-359.

17. Armstrong-Altrin, J.S., Nagarajan, R., Balaram, V. and Natalhy-Pineda, O., 2015. Petrography and geochemistry of sands from the Chachalacas and Veracruz beach areas, western Gulf of Mexico, Mexico: constraints on provenance and tectonic setting. Journal of South American Earth Sciences, 64, pp.199-216.

18. Armstrong-Altrin, J.S., Nagarajan, R., Madhavaraju, J., Rosalez-Hoz, L., Lee, Y.I., Balaram, V., Cruz-Martínez, A. and Avila-Ramírez, G., 2013. Geochemistry of the Jurassic and Upper Cretaceous shales from the Molango Region, Hidalgo, eastern Mexico: Implications for source-area weathering, provenance, and tectonic setting. Comptes Rendus Geoscience, 345(4), pp.185-202.

19. Armstrong-Altrin, J.S., Verma, S.P., Madhavaraju, J., Lee, Y.I. and Ramasamy, S., 2003. Geochemistry of upper Miocene Kudankulam limestones, southern India. International Geology Review, 45(1), pp.16-26.

20. Arya, B.C. and Rao, C.N., 1979. Bioturbation structures from the middle Proterozoic Narji Formation, Kurnool Group, Andhra Pradesh, India. Sedimentary Geology, 22(3-4), pp.127-134.

21. Auchter, N.C., Romans, B.W. and Hubbard, S.M., 2016. Influence of deposit architecture on intrastratal deformation, slope deposits of the Tres Pasos Formation, Chile. Sedimentary Geology, 341, pp.13-26.

22. Banerjee, R., Bahukhandi, N.K., Rahman, M., Achar, K.K., Ramesh Babu, P.V., Umamaheswar, K. and Parihar, P.S., 2012. Lithostratigraphic and radiometric appraisal of deeper parts of Srisailam and Palnad sub-basins in Kottapullareddipuram-Achchammagunta- Rachchamallepadu area, Guntur district, Andhra Pradesh. Expl. Res. Atm. Miner, 22, pp.55-69.

23. Barkat, R., Chakraborty, P.P., Saha, S. and Das, K., 2020. Alluvial architecture, paleohydrology and provenance tracking from the Neoproterozoic Banganapalle formation, Kurnool Group, India: An example of continental sedimentation before land plants. Precambrian Research, 350, p.105930.

24. Basu, A. and Bickford, M.E., 2015. An alternate perspective on the opening and closing of the intracratonic Purana basins in peninsular India. Journal of the Geological Society of India, 85(1), pp.5-25.

25. Basu, H., Sastry, R.S., Achar, K.K., Umamaheswar, K. and Parihar, P.S., 2014. Paleoproterozoic fluvio-aeolian deposits from the lower Gulcheru Formation, Cuddapah Basin, India. Precambrian Research, 246, pp.321-333.

26. Bathurst, R.G., 1987. Diagenetically enhanced bedding in argillaceous platform limestones: stratified cementation and selective compaction. Sedimentology, 34(5), pp.749-778.

27. Bau, M. and Dulski, P., 1996. Distribution of yttrium and rare-earth elements in the Penge and Kuruman iron-formations, Transvaal Supergroup, South Africa. Precambrian Research, 79(1-2), pp.37-55.

28. Bau, M., 1996. Controls on the fractionation of isovalent trace elements in magmatic and aqueous systems: evidence from Y/Ho, Zr/Hf, and lanthanide tetrad effect. Contributions to Mineralogy and Petrology, 123(3), pp.323-333.

29. Bekker, A. and Eriksson, K.A., 2003. A Paleoproterozoic drowned carbonate platform on the southeastern margin of the Wyoming Craton: a record of the Kenorland breakup. Precambrian Research, 120(3-4), pp.327-364.

30. Belica, M.E., Piispa, E.J., Meert, J.G., Pesonen, L.J., Plado, J., Pandit, M.K., Kamenov, G.D. and Celestino, M., 2014. Paleoproterozoic mafic dyke swarms from the Dharwar craton; paleomagnetic poles for India from 2.37 to 1.88 Ga and rethinking the Columbia supercontinent. Precambrian Research, 244, pp.100-122.

31. Bertram, C.N., 2010. Sedimentology, age and stable isotope evolution of the Kurnool Group, Cuddapah basin (Doctoral dissertation).

32. Bertram, G.T., 2012. Seismic and sequence stratigraphic analysis. Regional geology and tectonics: Principles of geologic analysis, 1, p.864.

33. Beukes, N.J., 1987. Facies relations, depositional environments and diagenesis in a major early Proterozoic stromatolitic carbonate platform to basinal sequence, Campbellrand Subgroup, Transvaal Supergroup, Southern Africa. Sedimentary Geology, 54(1-2), pp.1-46.

34. Bharani, P.L., Shwetha, S., Madesh, P. and Shivakumar, D., 2015. X-ray diffraction studies of carbonate rocks around western part of palnad sub basin, Guntur district, Andhra Pradesh. International Journal of Advanced Research in IT and Engineering, 4(7), pp.1-7.

35. Bhaskar Rao, Y.J., Pantulu, G.V.C., Damodara Reddy, V. and Gopalan, K., 1994. Time of early sedimentation and volcanism in the Proterozoic Cuddapah basin,

south India: evidence from the Rb-Sr age of Pulivendla mafic sill. MEMOIRS-GEOLOGICAL SOCIETY OF INDIA, pp.329-338.

36. Bhaskar Rao, Y.J., Pantulu, G.V.C., Reddy, V.D. and Gopalan, K., 1993. Rb–Sr evidence India. In Sixth National Symposium on Mass Spectrometry, Preprint volume, Dehradun, pp. 445-447.

37. Bhattacharji, S., 1981. Evolution of an intracratonic basin. Evolution of an Intracratonic Cuddapah Basin. Inst. Ind. Penns. Geol. Pub]., Hyderabad, AP. Monogr, 1, pp.7-28.

38. Bhattacharji, S., 1986. Astenospheric upwelling, lineament activation, magmatic episodes and ore mineral localization in Proterozoic basin evolution on the Archaean Indian shield, Int. Basement Tect. Assoc., Publ. S, pp.187-200.

39. Bhattacharji, S., 1987. Lineaments and igneous episodes in the evolution of intracratonic Proterozoic basins on the Indian shield. In Geological evolution of Peninsular India. Petrological and structural aspects, pp. 1-15.

40. Bhattacharji, S., Singh, R.N., 1984. Thermomechanical structure of the southern part of the Indian Shield and its relevance to Precambrian basin evolution. Tectonophysics 105, pp.103–120.

41. Bickford, M.E., Saha, D., Schieber, J., Kamenov, G., Russell, A. and Basu, A., 2013. New U-Pb ages of zircons in the Owk Shale (Kurnool Group) with reflections on Proterozoic porcellanites in India. Journal of the Geological Society of India, 82(3), pp.207-216.

42. Bradley, D.C., 2011. Secular trends in the geologic record and the supercontinent cycle. Earth-Science Reviews, 108(1-2), pp.16-33.

43. Butchi Babu B *, Pradeep Kumar V and Rama Rao Ch, (2008). Estimation of Thickness of Limestone Formation in Part of Kurnool Sub Basin from Aeromagnetic anomalies, 7th International conference & exposition on petroleum Geophysics: http:// www.spgindia.org/2008/422.pdf)

44. Cawood, P.A. and Hawkesworth, C.J., 2014. Earth's middle age. Geology, 42(6), pp.503-506.

45. Chakrabarti G, Shome D, Kumar S, Stephens GM III, Kah LC (2014) Carbonate platform development in a Paleoproterozoic extensional basin, Vempalle formation, Cuddapah basin, India. J Asian Earth Sci 91, pp.263–279.

46. Chakrabarti, G. and Shome, D., 2007. Reworked diamictite accumulation as debris flow in aqueous medium-an example from late Paleoproterozoic basal Gulcheru formation, Cuddapah Basin, India. Himalayan Geology, 28(1), pp.87-98.

47. Chakrabarti, G. and Shome, D., 2010. Interaction of microbial communities with clastic sedimentation during Paleoproterozoic time—An example from basal Gulcheru Formation, Cuddapah basin, India. Sedimentary Geology, 226(1-4), pp.22-28.

48. Chakrabarti, G., Shome, D., Kumar, S., Stephens III, G.M. and Kah, L.C., 2014. Carbonate platform development in a Paleoproterozoic extensional basin, Vempalle formation, Cuddapah basin, India. Journal of Asian Earth Sciences, 91, pp.263-279.

49. Chakrabarti, Gopal, and Debashish Shome. (2010): "Interaction of microbial communities with clastic sedimentation during Paleoproterozoic time—An example from basal Gulcheru Formation, Cuddapah basin, India." Sedimentary Geology 226, no. 1-4, pp. 22-28.

50. Chakraborty, B.K., 2000. Precambrian geology of India—a synoptic view. Geol Surv India Spec Publ, 55, pp.1-12.

51. Chakraborty, P.P., 1999. Facies pattern and depositional motif in an immature trench-slope basin, Eocene Mithakhari Group, Middle Andaman, India. Journal of the Geological Society of India, 53, pp.271-284.

52. Chakraborty, P.P., Dey, S. and Mohanty, S.P., 2010. Proterozoic platform sequences of Peninsular India: implications towards basin evolution and supercontinent assembly. Journal of Asian Earth Sciences, 39(6), pp.589-607.

53. Chakraborty,P.P., Pal, T., Gupta,T., 1999.Geological Society of India.

54. Chalapathi Rao, N.V., Anand, M., Dongre, A. and Osborne, I., 2010. Carbonate xenoliths hosted by the Mesoproterozoic Siddanpalli Kimberlite Cluster (Eastern Dharwar craton): implications for the geodynamic evolution of southern India and its diamond and uranium metallogenesis. International Journal of Earth Sciences, 99(8), pp.1791-1804.

55. Chalapathi Rao, N.V., Anand, M., Dongre, A. and Osborne, I., 2010. Carbonate xenoliths hosted by the Mesoproterozoic Siddanpalli Kimberlite Cluster (Eastern Dharwar craton): implications for the geodynamic evolution of southern India and its diamond and uranium metallogenesis. International Journal of Earth Sciences, 99(8), pp.1791-1804.

56. Chalapathi Rao, N.V., Miller, J.A., Pyle, D.M., Madhavan, V.,1996. New Proterozoic K, Ar ages for some kimberlite and lamproites from Cuddapah Basin and Dharwar craton, South India: evidence for non-contemporaneous emplacement. Precambrian Research,79(4), pp.363-369.

57. Chatterjee, N. and Bhattacharji, S., 2001. Petrology, geochemistry and tectonic settings of the mafic dikes and sills associated with the evolution of the Proterozoic Cuddapah Basin of south India. Journal of Earth System Science, 110(4), pp.433-453.

58. Chattoraj, S., Banerjee, S. and Saraswati, P.K., 2009. Petrographic study on modes of occurrence of glauconitic pellets from Late Paleocene to Early Eocene Naredi Formation, Western Kutch, Gujarat. Jour. Geol. Soc. India, 73, pp.567-574.

59. Chaudhuri, A.K., Saha, D., Deb, G.K., Deb, S.P., Mukherjee, M.K. and Ghosh, G., 2002. The Purana basins of southern cratonic province of India-a case for Mesoproterozoic fossil rifts. Gondwana Research, 5(1), pp.23-33.

60. Chen, Y.J. and Santosh, M., 2014. Triassic tectonics and mineral systems in the Qinling Orogen, central China. *Geological Journal*, *49*(4-5), pp.338-358.

61. Chetty, T.R.K., 2011. Tectonics of Proterozoic Cuddapah basin, Southern India: a conceptual model. Journal of the Geological Society of India, 78(5), pp.446-456.

62. Collins, A.S., Patranabis-Deb, S., Alexander, E., Bertram, C.N., Falster, G.M., Gore, R.J., Mackintosh, J., Dhang, P.C., Saha, D., Payne, J.L. and Jourdan, F., 2015. Detrital mineral age, radiogenic isotopic stratigraphy and tectonic significance of the Cuddapah Basin, India. Gondwana Research, 28(4), pp.1294-1309.

63. Collinson, J.W., Hammer, W.R., Askin, R.A. and Elliot, D.H., 2006. Permian-Triassic boundary in the central transantarctic Mountains, Antarctica. Geological Society of America Bulletin, 118(5-6), pp.747-763.

64. Condie, K.C., Dengate, J. and Cullers, R.L., 1995. Behavior of rare earth elements in a paleo weathering profile on granodiorite in the Front Range, Colorado, USA. Geochimica et Cosmochimica Acta, 59(2), pp.279-294.

65. Conrad, J.E., Hein, J.R., Chaudhuri, A.K., Patranabis-Deb, S., Mukhopadhyay, J., Deb, G.K. and Beukes, N.J., 2011. Constraints on the development of Proterozoic basins in central India from 40Ar/39Ar analysis of authigenic glauconitic minerals. Bulletin, 123(1-2), pp.158-167.

66. Craig, H., 1957. Isotopic standards for carbon and oxygen and correction factors for mass-spectrometric analysis of carbon dioxide. Geochimica et cosmochimica acta, 12(1-2), pp.133-149.

67. Crawford, A.R. and Compston, W., 1973. The age of the Cuddapah and Kurnool systems, southern India. Journal of the Geological Society of Australia, 19(4), pp.453-464.

68. Dapples, E.C., 1967. Silica as an agent in diagenesis. In Developments in sedimentology (Vol. 8, pp. 323-342). Elsevier.

69. Dar, F.A., Perrin, J., Riotte, J., Gebauer, H.D., NARAyANA, A.C. and Shakeel, A., 2011. Karstification in the Cuddapah Sedimentary Basin, southern India: implications for groundwater resources. Acta Carsologica, 40(3).

70. Das, K., Yokoyama, K., Chakraborty, PP and Sarkar, A., 2009. Basal tuffs and contemporaneity of the Chattisgarh and Khariar basins based on new dates and geochemistry. The Journal of Geology, 117 (1), pp.88-102.

71. Dasari, M.R., 1989. Isotopic variations in limestones from Kurnool sediments in Cuddapah basin, India. Geological Society of India, 33(5), pp.447-449.

72. Dasgupta, P.K. and Biswas, A., 2006. Rhythms in Proterozoic sedimentation: an example from Peninsular India. Satish Serial Publishing House.

73. Dasgupta, P.K., Biswas, A. and Mukherjee, R., 2005. 11. Cyclicity in Paleoproterozoic to Neoproterozoic Cuddapah supergroup and its significance in basinal evolution. In Developments in Sedimentology (Vol. 57, pp. 313-354). Elsevier.

74. De Baar, H.J., German, C.R., Elderfield, H. and Van Gaans, P., 1988. Rare earth element distributions in anoxic waters of the Cariaco Trench. Geochimica et Cosmochimica Acta, 52(5), pp.1203-1219.

75. Deb, S.P., 2005. Tidal shelf sedimentation in the Neoproterozoic Chattisgarh succession of central India. Journal of earth system science, 114(3), pp.211-226.

76. Devi, K.R. and Duarah, B.P., 2015. Geochemistry of Ukhrul limestone of Assam-Arakan subduction basin, Manipur, Northeast India. Journal of the Geological Society of India, 85(3), pp.367-376.

77. Dobmeier, C.J. and Raith, M.M., 2003. Crustal architecture and evolution of the Eastern Ghats Belt and adjacent regions of India. Geological Society, London, Special Publications, 206(1), pp.145-168.

78. Dongre, A., Chalapathi Rao, N.V. and Kamde, G., 2008. Limestone xenolith in Siddanpalli Kimberlite, Gadwal granite-greenstone terrain, eastern Dharwar craton, Southern India: remnant of Proterozoic platformal cover sequence of Bhima/Kurnool Age?. The Journal of Geology, 116(2), pp.184-191.

79. Drury, S.A., Harris, N.B.W., Holt, R.W., Reeves-Smith, G.J. and Wightman, R.T., 1984. Precambrian tectonics and crustal evolution in South India. The Journal of Geology, 92(1), pp.3-20.

80. Dutt, N.V.B.S., 1962. Geology of the Kurnool System of rocks in Cuddapah and the southern part of Kurnool district. Rec. Geol. Surv. India, 87(3), pp.549-604.

81. Dutt, N.V.B.S., 1975. Geology and mineral resources of Andhra Pradesh. Andhra Pradesh Academy of Sciences.

82. Ernst, R.E., Bleeker, W., Söderlund, U. and Kerr, A.C., 2013. Large Igneous Provinces and supercontinents: Toward completing the plate tectonic revolution. Lithos, 174, pp.1-14.

83. Flügel, E. and Munnecke, A., 2010. Microfacies of carbonate rocks: analysis, interpretation and application (Vol. 976, p. 2004). Berlin: springer.

84. Folk, R.L., 1964. Some aspects of recrystallization of ancient limestones. AAPG Bulletin, 48(4), pp.525-525.

85. Frank, T.D., Kah, L.C. and Lyons, T.W., 2003. Changes in organic matter production and accumulation as a mechanism for isotopic evolution in the Mesoproterozoic Ocean. Geological Magazine, 140(4), pp.397-420.

86. French, J.E., Heaman, L.M., Chacko, T. and Srivastava, R.K., 2008. 1891–1883 Ma Southern Bastar–Cuddapah mafic igneous events, India: A newly recognized large igneous province. Precambrian research, 160(3-4), pp.308-322.

87. Fu, X., Wang, J., Zeng, Y., Tan, F. and He, J., 2011. Geochemistry and origin of rare earth elements (REEs) in the Shengli River oil shale, northern Tibet, China. Geochemistry, 71(1), pp.21-30.

88. Galliher, E.W., 1935. Geology of glauconite. AAPG Bulletin, 19(11), pp.1569-1601.

89. German, C.R. and Elderfield, H., 1989. Rare earth elements in Saanich Inlet, British Columbia, a seasonally anoxic basin. Geochimica et Cosmochimica Acta, 53(10), pp.2561-2571.

90. Gopakumar, B. and Waghmare, M., 2016. Nature of occurrence of phosphatic bands in Owk Formation, Neoproterozoic Kurnool basin, Andhra Pradesh. Journal of the Geological Society of India, 88(2), pp.213-221.

91. Goswami, S., Dey, S., Zakaulla, S. and Verma, M.B., 2020. Active rifting and bimodal volcanism in Proterozoic Papaghni sub-basin, Cuddapah basin (Andhra Pradesh), India. Journal of Earth System Science, 129(1), pp.1-31.

92. Goutham, M.R., Subbarao, K.V., Prasad, C.V.R.K., Piper, J.D.A. and Miggins, D.P., Margin of Cuddapah Basin, India: Part 2 Palaeomagnetism and Ar/Ar Geochronology. Dyke Swarms: Keys for Geodynamic Interpretation, pp. 73-93.

93. Grim, R.E. and Cuthbert, F.L., 1945. Some Clay-Water Properties of Certain Clay Minerals. Journal of the American Ceramic Society, 28(3), pp.90-95.

94. Gupta, A., 1998. Primordial storms: an overview of depositional environments in Mid-Late Proterozoic platforms of India. Gondwana Research, 1(2), pp.291-298.

95. Gupta, S., Vimal, R., Banerjee, R., Ramesh Babu, P.V. and Maithani, P.B., 2010. Sedimentation pattern and depositional environment of Banganapalle Formation in southwestern part of Palnad subbasin, Guntur District, Andhra Pradesh. Gond. Geol. Magz., spl, 12, pp.59-70.

96. Gururaja, M.N., Ashok Kumar, P., Rao, C.V. and Chauhan, R.H., 2000. Precambrian-Cambrian boundary strata in Cuddapah basin, Andhra Pradesh. Geol. Surv. India Spec. Publ, 55, pp.155-162.

97. Hamblin, A.P. and Walker, R.G., 1979. Storm-dominated shallow marine deposits: the Fernie–Kootenay (Jurassic) transition, southern Rocky Mountains. Canadian Journal of Earth Sciences, 16(9), pp.1673-1690.

98. Harish, V. and Basavarajappa, H., 2000. Petrography and Geochemistry of Late Proterozoic Siliciclastics from Kurnool group, Kurnool sub basin, Andhra Pradesh. Jour. Indian Associations of Sedimentologists. 19, pp. 93-105.

99. Harish, V., K. N. P. Narasimha, and H. T. Basavarajappa, 2003. Petrography and fluid inclusion studies on late Proterozoic Palnad siliciclastics, Kurnool Group, Andhra Pradesh. Journal of the Geological Society of India. 61 (5), pp 612-618.

100. Harish, V.,1995. Unpublished Ph.D. thesis, Univ.of Mysore.

101. Harwood, C.L. and Sumner, D.Y., 2012. Origins of microbial microstructures in the Neoproterozoic Beck Spring Dolomite: variations in microbial community and timing of lithification. Journal of Sedimentary Research, 82(9), pp.709-722.

102. Hashmie, Afshin, Ali Rostamnejad, Fariba Nikbakht, Mansour Ghorbanie, Peyman Rezaie, and Hossien Gholamalian. "Depositional environments and sequence stratigraphy of the Bahram Formation (middle–late Devonian) in north of Kerman, south-central Iran." Geoscience Frontiers 7, no. 5 (2016): 821-834.

103. Henderson, B., Collins, A.S., Payne, J., Forbes, C. and Saha, D., 2014. Geologically constraining India in Columbia: the age, isotopic provenance and geochemistry of the protoliths of the Ongole Domain, Southern Eastern Ghats, India. Gondwana Research, 26(3-4), pp.888-906.

104. Hernandez-Hinojosa, Violeta, Patricia C. Montiel-Garcia, John S. Armstrong-Altrin, Ramasamy Nagarajan, and Juan J. Kasper-Zubillaga., 2018. "Textural and geochemical characteristics of beach sands along the western Gulf of Mexico, Mexico." Carpathian Journal of Earth and Environmental Sciences, 13 (1), pp. 161-174.

105. Hersi, O. Salad, I. A. Abbasi, and A. Al-Harthy, 2016. "Sedimentology, rhythmicity and basin-fill architecture of a carbonate ramp depositional system with intermittent terrigenous influx: The Albian Kharfot Formation of the Jeza-Qamar Basin, Dhofar, Southern Oman." Sedimentary Geology, 331, pp.114-131.

106. Hesse, R., 1988. Diagenesis# 13. Origin of chert: Diagenesis of biogenic siliceous sediments. Geoscience Canada, 15(3), pp.171-192.

107. Hesse, R., 1989. " Drainage systems" associated with mid-ocean channels and submarine yazoos: Alternative to submarine fan depositional systems. Geology, 17(12), pp.1148-1151.

108. Heyne, B., 1814. Tracts, Historical And Statistical, On India: With Journals Of Several Tours Through Various Parts Of The Peninsula: Also, An Account Of Sumatra, In A Series Of Letters; Illustrated By Maps And Other Plates. Baldwin.

109. Hoffman, P.F., Tirrul, R., King, J.E., St-Onge, M.R. and Lucas, S.B., 1988. Axial projections and modes of crustal thickening, eastern Wopmay orogen, northwest Canadian shield. DOI- 10.1130/SPE218-p1

110. Hou, G., Santosh, M., Qian, X., Lister, G.S. and Li, J., 2008. Configuration of the Late Paleoproterozoic supercontinent Columbia: insights from radiating mafic dyke swarms. Gondwana Research, 14(3), pp.395-409.

111. Hua, G., Yuansheng, D., Lian, Z., Jianghai, Y., Hu, H., Min, L. and Yuan, W., 2013. Trace and rare earth elemental geochemistry of carbonate succession in the Middle Gaoyuzhuang Formation, Pingquan Section: Implications for Early Mesoproterozoic Ocean redox conditions. Journal of Paleogeography, 2(2), pp.209-221.

112. Jones, B. and Manning, D.A., 1994. Comparison of geochemical indices used for the interpretation of palaeoredox conditions in ancient mudstones. Chemical geology, 111(1-4), pp.111-129.

113. Joy, S., Jelsma, H., Tappe, S. and Armstrong, R., 2015. SHRIMP U–Pb zircon provenance of the Sullavai Group of Pranhita–Godavari Basin and Bairenkonda Quartzite of Cuddapah Basin, with implications for the Southern Indian Proterozoic tectonic architecture. Journal of Asian Earth Sciences, 111, pp.827-839.

114. Joy, S., Jelsma, H.A., Preston, R.F. and Kota, S., 2012. Geology and diamond provenance of the Proterozoic Banganapalle conglomerates, Kurnool Group, India. Geological Society, London, Special Publications, 365(1), pp.197-218.

115. Kaila, K.L., Reddy, P.R., Krishna, V.G., Roy Chowdhury, K., Tewari, H.C., Murty, P.R.K. and Tripathi, K.M., 1979. Crustal investigations in India from deep seismic soundings. Geophys. Res. Bull, 17, pp.273-292.

116. Kale, V.S. and Phansalkar, V.G., 1991. Purana basins of peninsular India: a review. Basin Research, 3(1), pp.1-36.

117. Kale, V.S., 1991. Constraints on the evolution of the Purana basins of peninsular India. J. Geol. Soc. India, 38(3), pp.231-252.

118. Kale, V.S., 2016. Proterozoic basins of Peninsular India: status within the global Proterozoic systems. Proceedings of the Indian National Science Academy, 82(3), pp.461-477.

119. Kale, V.S., Saha, D., Patrabnis-Deb, S., Sesha Sai, V.V., Tripathy, V. and Patil-Pillai, S., 2020. Cuddapah Basin, India: A Collage of proterozoic subbasins and terranes. Proceedings of the Indian National Science Academy, 86(1), p.137.

120. Kamal, M. and BE, V., 1982. Intraformational conglomerate of the Banganapalle Formation, Kurnool Group. Current Science, 51, pp. 196.

121. Kamber, B.S. and Webb, G.E., 2001. The geochemistry of late Archaean microbial carbonate: implications for ocean chemistry and continental erosion history. Geochimica et Cosmochimica Acta, 65(15), pp.2509-2525.

122. Kang, J., LI, C., Dong, L. and Xiao, S., 2022. Early Diagenetic Dolomite as a Potential Archive of Paleo-redox Fluctuations in an Early Tonian Marine Basin. Acta Geologica Sinica-English Edition.

123. Kendall, C.G.S.C. and Warren, J., 1987. A review of the origin and setting of tepees and their associated fabrics. Sedimentology, 34(6), pp.1007-1027.

124. Kerrich, R. and Allison, I., 1978. Flow mechanisms in rocks: microscopic and mesoscopic structures, and their relation to physical conditions of deformation in the crust. Geoscience Canada, 5 (3).

125. Kerrich, R., 1978. An historical review and synthesis of research on pressure solution.

126. Khelen, A.C., Manikyamba, C., Ganguly, S., Singh, T.D., Subramanyam, K.S.V., Ahmad, S.M. and Reddy, M.R., 2017. Geochemical and stable isotope signatures of Proterozoic stromatolitic carbonates from the Vempalle and Tadpatri Formations, Cuddapah Supergroup, India: Implications on paleoenvironment and depositional conditions. Precambrian Research, 298, pp.365-384.

127. Khelen, A.C., Manikyamba, C., Tang, L., Santosh, M., Subramanyam, K.S.V. and Singh, T.D., 2020. Detrital zircon U-Pb geochronology of stromatolitic carbonates from the greenstone belts of Dharwar Craton and Cuddapah basin of Peninsular India. Geoscience Frontiers, 11(1), pp.229-242.

128. Khudoley, A.K., Rainbird, R.H., Stern, R.A., Kropachev, A.P., Heaman, L.M., Zanin, A.M., Podkovyrov, V.N., Belova, V.N. and Sukhorukov, V.I., 2001. Sedimentary evolution of the Riphean–Vendian basin of southeastern Siberia. Precambrian Research, 111(1-4), pp.129-163.

129. King, W., 1872. The Cuddapah and Kurnool formations in Madras Presidency. Memoir. Geological Survey of India, 8(1), pp.1-346.

130. Kinsman, D.J., 1969. Modes of formation, sedimentary associations, and diagnostic features of shallow-water and supratidal evaporites. AAPG Bulletin, 53(4), pp.830-840.

131. Knaust, D., 2002. Pinch-and-swell structures at the Middle/Upper Muschelkalk boundary (Triassic): evidence of earthquake effects (seismites) in the Germanic Basin. International Journal of Earth Sciences, 91(2), pp.291-303.

132. Komatsu, T., Naruse, H., Shigeta, Y., Takashima, R., Maekawa, T., Dang, H.T., Dinh, T.C., Nguyen, P.D., Nguyen, H.H., Tanaka, G. and Sone, M., 2014. Lower Triassic mixed carbonate and siliciclastic setting with Smithian–Spathian anoxic to dysoxic facies, An Chau basin, northeastern Vietnam. Sedimentary Geology, 300, pp.28-48.

133. Krishnaswamy, V.S., 1981. Geological Survey of India. Calcutta, 3, pp.169-188.

134. Kumar, A., Padma Kumari, V.M., Dayal, A.M., Murthy, D.S.N., Gopalan, K.1993.Rb Sr ages of Proterozoic Kimerlite of India: evidence for contemporaneous emplacement. Precambrian Research,62(3), pp.227-237.

135. Kumar, A., Parashuramulu, V. and Nagaraju, E., 2015. A 2082 Ma radiating dyke swarm in the Eastern Dharwar Craton, southern India and its implications to Cuddapah basin formation. Precambrian Research, 266, pp.490-505.

136. Kumar, A., Talukdar, D., Rao, N.C., Burgess, R. and Lehmann, B., 2022. Mesoproterozoic 40Ar–39Ar ages of some lamproites from the Cuddapah Basin and Eastern Dharwar Craton, southern India: implications for diamond provenance of the Banganapalle Conglomerates, age of the Kurnool Group and Columbia tectonics. Geological Society, London, Special Publications, 513(1), pp.157-178.

137. Kumar, B., Das Sharma, S., Shukla, M., 1999. Chronostratigraphic implication of carbon and oxygen isotopic compositions of the Proterozoic Bhima carbonates, southern India. Journal of the Geological Society of India, 53, pp. 593- 600.

138. Kumar, S.P., Shaikh, A.M., Patel, S.C., Sheikh, J.M., Behera, D., Pruseth, K.L., Ravi, S. and Tappe, S., 2021. Multi-stage magmatic history of olivine–leucite lamproite dykes from Banganapalle, Dharwar craton, India: evidence from compositional zoning of spinel. *Mineralogy and Petrology*, *115*(1), pp.87-112.

139. Kumar, Y., Sharma, M., Goswami., 2022.Possible Ediacaran disc from the Paniam Quartzite, Kurnool Group, South India.122(8), pp.885-887.

140. La Maskin, T.A. and Elrick, M., 1997. Sequence stratigraphy of the Middle to Upper Devonian Guilmette. Paleozoic sequence stratigraphy, biostratigraphy, and biogeography, 321, p.89.

141. Lakshminarayana, G., Bhattacharjee, S. and Kumar, A., 1999. Palaeocurrents and depositional setting in the Banganapalle Formation, Kurnool sub-basin, Cuddapah basin, Andhra Pradesh. Journal of Geological Society of India, 53, pp.255-260.

142. Lo Forte, G.L. and Palma, R.M., 2002. Facies, microfacies, and diagenesis of late Callovian-early Oxfordian carbonates (La Manga Formation) in the west central Argentinean high Andes. Carbonates and Evaporites, 17(1), pp.1-16.

143. Lokesh Bharani, P., 2015. Sedimentology provenance and depositional environments of Kurnool group palnad sub basin Andhra Pradesh South India.

144. Madesh, P., Lokesh Bharani, P. and Baby Shwetha, S., 2012. Study of microstylolite from carbonate rocks of Kurnool group, Andhra Pradesh, South India. Indian Journal of applied Research, 1(2).

145. Madhavaraju, J. and Lee, Y.I., 2009. Geochemistry of the Dalmiapuram Formation of the Uttatur Group (Early Cretaceous), Cauvery basin, southeastern India: Implications on provenance and paleo-redox conditions. Revista mexicana de ciencias geológicas, 26(2), pp.380-394.

146. Madhavaraju, J., Löser, H., Lee, Y.I., Santacruz, R.L. and Pi-Puig, T., 2016. Geochemistry of Lower Cretaceous limestones of the Alisitos Formation, Baja California, Mexico: Implications for REE source and paleo-redox conditions. Journal of South American Earth Sciences, 66, pp.149-165.

147. Makintosh, J.N., 2010. Age and Basin Evolution of Cuddapah Supergroup India. Ph.D. dissertation, The University of Adelaide, Australia

148. Malcolmson, J.G., 1840. XXXVIII.—On the Fossils of the Eastern Portion of the Great Basaltic District of India. Transactions of the Geological Society of London, 2(3), pp.537-575.

149. Malone, S.J., Meert, J.G., Banerjee, D.M., Pandit, M.K., Tamrat, E., Kamenov, G.D., Pradhan, V.R. and Sohl, L.E., 2008. Paleomagnetism and detrital zircon geochronology of the Upper Vindhyan Sequence, Son Valley and Rajasthan, India: A ca. 1000 Ma closure age for the Purana Basins? Precambrian Research, 164(3-4), pp.137-159.

150. Malur, M., Rudraiah, M. and Nagendra, R., 1992. Microstylolites from Kurkunta Formation, Bhima Group. Journal of the Mysore University: Science (including medicine and engineering). Section B, 32, p.186.

151. Malur, M.N. and Nagendra, R., 1988. Microstylolites in late precambrian carbonate rocks, Karnataka, South India. Journal of the Geological Society of India, 32(5), pp.430-432.

152. Marian, ML and Osborne, RH, 1992. Petrology, petrochemistry, and stromatolites of the middle to late Proterozoic Beck Spring Dolomite, eastern Mojave Desert, California. Canadian Journal of Earth Sciences, 29 (12), pp.2595-2609.

153. Marsh, O.C., 1868. On the origin of the so called lignites or epsomite. Amer. Assoc. Adv. Sci., Proc., 16, pp.135-143.

154. Mathur, R., Raj, B.U. and Balaram, V., 2014. Petrographic characteristics of the Proterozoic Vempalle carbonates, Cuddapah Basin, India and their implications. Journal of the Geological Society of India, 84(3), pp.267-280.

155. Mathur, R.K., 1996.Setting and situ characterization methodologies for deep geological repository in India. Proceedings of the 1996 international conference on deep geological disposal of radioactive waste.

156. Mazumdar, A., Tanaka, K., Takahashi, T. and Kawabe, I., 2003. Characteristics of rare earth element abundances in shallow marine continental platform carbonates of Late Neoproterozoic successions from India. Geochemical Journal, 37(2), pp.277-289.

157. Meert, J.G. and Pandit, M.K., 2015. The Archaean and Proterozoic history of Peninsular India: tectonic framework for Precambrian sedimentary basins in India. Geological Society, London, Memoirs, 43(1), pp.29-54.

158. Meert, J.G., Pandit, M.K., Pradhan, V.R. and Kamenov, G., 2011. Preliminary report on the paleomagnetism of 1.88 Ga dykes from the Bastar and Dharwar cratons, Peninsular India. Gondwana Research, 20(2-3), pp.335-343.

159. Meert, J.G., Pandit, M.K., Pradhan, V.R., Banks, J., Sirianni, R., Stroud, M., Newstead, B. and Gifford, J., 2010. Precambrian crustal evolution of Peninsular India: a 3.0-billion-year odyssey. Journal of Asian Earth Sciences, 39(6), pp.483-515.

160. Meijerink, A.M.J., Rao, D.P. and Rupke, J., 1984. Stratigraphic and structural development of the Precambrian Cuddapah Basin, SE India. Precambrian Research, 26(1), pp.57-104.

161. Middleton, G.V., 1973. Johannes Walther's law of the correlation of facies. Geological Society of America Bulletin, 84(3), pp.979-988.

162. Mishra, D.C., 2011. Long hiatus in Proterozoic sedimentation in India: Vindhyan, Cuddapah and Pakhal Basins—A plate tectonic model. Journal of the Geological Society of India, 77(1), pp.17-25.

163. Mitra, R., Chakrabarti, G. and Shome, D., 2018. Geochemistry of the Palaeo–Mesoproterozoic Tadpatri shales, Cuddapah Basin, India: Implications on provenance, paleo weathering and paleo redox conditions. Acta Geochimica, 37(5), pp.715-733.

164. Mohanty, S., 2011. Paleoproterozoic assembly of the Napier Complex, Southern India and Western Australia: implications for the evolution of the Cuddapah basin. Gondwana Research, 20(2-3), pp.344-361.

165. Mukherjee, A., Bickford, M.E., Hietpas, J., Schieber, J. and Basu, A., 2012. Implications of a newly dated ca. 1000-Ma rhyolitic tuff in the Indravati Basin, Bastar Craton, India. The Journal of Geology, 120(4), pp.477-485.

166. Mukherjee, S., Goswami, S. and Mukherjee, A., 2019. Structures and their tectonic implications of the southern part of Cuddapah Basin, Andhra Pradesh, India. Iranian Journal of Science and Technology, Transactions A: Science, 43(2), pp.489-505.

167. Murthy, Y.G.K., 1981. The Cuddapah basin: A review of Basin development and basement framework relations. In Fourth Workshop on 'Status, Problems, and Programmes in Cuddapah Basin', Institute of India Peninsular Geology, Hyderabad (pp. 51-72).

168. Murthy, Y.G.K., Babu Rao, V., Guptasarma, D., Rao, J.M., Rao, M.N. and Bhattacharji, S., 1987. Tectonic, petrochemical and geophysical studies of mafic dyke swarms around the Proterozoic Cuddapah basin, South India. Mafic dyke swarms, 34, pp.303-316.

169. Naganjaneyulu, K. and Harinarayana, T., 2004. Deep crustal electrical signatures of eastern Dharwar craton, India. Gondwana Research, 7(4), pp.951-960.

170. Nagaraja Rao, B.K. and Ramalingaswamy, G., 1976. Some new thoughts on the stratigraphy of Cuddapah Supergroup. In Seminar on Kaladgi---Badami, Bhima and Cuddapah Supergroup. Mysore, India.

171. Nagaraja Rao, B.K., Rajurkar, S.T., Ramalingaswamy, G. and Ravindra Babu, B., 1987. Stratigraphy, structure and evolution of the Cuddapah basin. Mem. Geol. Soc. India, 6, pp.33-86.

172. Nagarajan, R., Madhavaraju, J., Armstrong-Altrin, J.S. and Nagendra, R., 2011. Geochemistry of Neoproterozoic limestones of the Shahabad formation, Bhima basin, Karnataka, southern India. Geosciences Journal, 15(1), pp.9-25.

173. Naik, S.S., Khadge, N.H., Valsangkar, A.B., Das, A., Fernandes, C.E. and Loka Bharathi, P.A., 2016. Relationship of sediment-biochemistry, bacterial morphology, and activity to geotechnical properties in the Central Indian Basin. Marine Georesources & Geotechnology, 34(1), pp.21-32.

174. Nance, W.B. and Taylor, S.R., 1976. Rare earth element patterns and crustal evolution—I. Australian post-Archean sedimentary rocks. Geochimica et Cosmochimica Acta, 40(12), pp.1539-1551.

175. Narayanaswami, S., 1966. Tectonics of the Cuddapah basin. Geological Society of India, 7, pp.33-50.

176. Natarajan, V. and Nair, S.R., 1977. Post-Kurnool thrust and other structural features in the northeast part of the Palnad basin, Krishna district, Andhra Pradesh. Geological Society of India, 18(3), pp.111-116.

177. Natarajan, V., 1976. Stylolites in the Narji Limestones From Jaggay Yapeta Area, Krishna District, Andhra Pradesh.

178. Nath, B.N., Bau, M., Rao, B.R. and Rao, C.M., 1997. Trace and rare earth elemental variation in Arabian Sea sediments through a transect across the oxygen minimum zone. Geochimica et Cosmochimica Acta, 61(12), pp.2375-2388.

179. Nemec, W. and Steel, R.J., 1984. Alluvial and coastal conglomerates: their significant features and some comments on gravelly mass-flow deposits.

180. Newbold, C., 1846. Art. XI. —Summary of the Geology of Southern India. Journal of the Royal Asiatic Society, 8(15), pp.213-270.

181. Nichols, G., 2009. Sedimentology and stratigraphy. John Wiley & Sons.

182. Panja, M., Chakrabarti, G. and Shome, D., 2017. Depositional system of an open coast tidalflat-an example from Paleoproterozoic Vempalle Formation, Cuddapah Basin, India. Carpathian Journal of Earth and Environmental Sciences, 12(1), pp.269-282.

183. Panja, M., Chakrabarti, G. and Shome, D., 2019. Earthquake induced soft sediment deformation structures in the Paleoproterozoic Vempalle Formation (Cuddapah basin, India). Carbonates and Evaporites, 34(3), pp.491-505.

184. Park, W.C. and Schot, E.H., 1968. Stylolites; their nature and origin. Journal of Sedimentary Research, 38(1), pp.175-191.

185. Pascoe, E.H., 1950. A manual of the geology of India and Burma Pt I. Geol. Surv. India Publ., Calcutta, 483p.

186. Patil, D.J., Sharma, D., Kumar, B., Dayal, A.M. and Shukla, M., 2002. Carbon, oxygen and strontium isotope geochemistry of carbonate rocks from Kurnool Group, southern India. Geological Society of India, 60(6), pp.615-622.

187. Patranabis-Deb, S., Bickford, M.E., Hill, B., Chaudhuri, A.K. and Basu, A., 2007. SHRIMP ages of zircon in the uppermost tuff in Chattisgarh basin in central India

require~ 500-Ma adjustment in Indian Proterozoic stratigraphy. the Journal of Geology, 115(4), pp.407-415.

188. Patranabis-Deb, S., Saha, D. and Tripathy, V., 2012. Basin stratigraphy, sea-level fluctuations and their global tectonic connections—evidence from the Proterozoic Cuddapah Basin. Geological Journal, 47(2-3), pp.263-283.

189. Paul, A.K., Rajagopalan, V., Shivakumar, K. and Verma, M.B., 2013. Mineral chemistry of radioactive and associated phases from neoproterozoic unconformity-Related proximal uranium deposit at Koppunuru, Palnad sub-basin, Guntur District, Andhra Pradesh, India. Journal of Applied Geochemistry, 15(2), p.135.

190. Perrin, J., Ahmed, S. and Hunkeler, D., 2011. The effects of geological heterogeneities and piezometric fluctuations on groundwater flow and chemistry in a hard-rock aquifer, southern India. Hydrogeology Journal, 19(6), pp.1189-1201.

191. Piper, J.D., 2013. A planetary perspective on Earth evolution: lid tectonics before plate tectonics. Tectonophysics, 589, pp.44-56.

192. Prokopovich, N., 1952. The origin of stylolites. Journal of Sedimentary Research, 22(4), pp.212-220.

193. Qian, Q., Chung, S.L., Lee, T.Y. and Wen, D.J., 2003. Mesozoic high-Ba–Sr granitoids from North China: geochemical characteristics and geological implications. Terra Nova, 15(4), pp.272-278.

194. Rajurkar, S.T., 1963. Discoidal impressions akin to Fermoria from the Owk Shales of Kurnool district, Andhra Pradesh. Indian Minerals, 17(3), pp.306-307.

195. Rajurkar, S.T., 1977. Structure and correlation of the Upper Cuddapah strata in the northern part of the Cuddapah basin, Andhra Pradesh. Unpubl, PhD thesis. Nagpur University, 1-12.

196. Ramakrishnan, M. and Vaidyanadhan, R., 2008. Geology of India, vols. 1 and 2. Geological Society of India. Text Book Series.

197. Ramam, P.K., 1997. Geology of Andhra Pradesh. Geological Society of India.

198. Ramkumar, M., 2004. Lithology, petrography, microfacies, environmental history and hydrocarbon prospects of the Kallankurichchi Formation, Ariyalur Group, south India. Palaeontology, Stratigraphy, Facies.

199. Ramos-Vázquez, M.A., Armstrong-Altrin, J.S., Rosales-Hoz, L., Machain-Castillo, M.L. and Carranza-Edwards, A., 2017. Geochemistry of deep-sea sediments in two cores retrieved at the mouth of the Coatzacoalcos River delta, western Gulf of Mexico, Mexico. Arabian Journal of Geosciences, 10(6), pp.1-19.

200. Ramos-Vázquez, M.A., Armstrong-Altrin, J.S., Rosales-Hoz, L., Machain-Castillo, M.L. and Carranza-Edwards, A., 2017. Geochemistry of deep-sea sediments in two cores retrieved at the mouth of the Coatzacoalcos River delta, western Gulf of Mexico, Mexico. Arabian Journal of Geosciences, 10(6), pp.1-19.

201. Rao, D.M. and Gokhale, K.V.G.K., 1973. Ripple marks in quartzites from Kurnool Supergroup, Cuddapah Basin, India. Journal of Sedimentary Research, 43(4).

202. Rao, G.P., 2005. Orthogonal dykes around the Cuddapah basin—a paleomagnetic study. J. Indian Geophys. Union, 9, pp.1-11.

203. Rao, N.C., Miller, J.A., Pyle, D.M. and Madhavan, V., 1996. New Proterozoic K□ Ar ages for some kimberlites and lamproites from the Cuddapah Basin and Dharwar Craton, South India: evidence for non-contemporaneous emplacement. Precambrian Research, 79(3-4), pp.363-369.

204. Rao, T., 1995. A New Occurrence of Kimberlite Near Kotakonda, Mahboobnagar District, Andhra-Pradesh-Reply. Journal Of the Geological Society of India, 45(5), Pp.606-607.

205. Rasmussen, B., Bose, P.K., Sarkar, S., Banerjee, S., Fletcher, I.R. and McNaughton, N.J., 2002. 1.6 Ga U-Pb zircon age for the Chorhat Sandstone, lower Vindhyan, India: Possible implications for early evolution of animals. Geology, 30(2), pp.103-106.

206. Ravikant, V., 2010. Palaeoproterozoic (~ 1.9 Ga) extension and breakup along the eastern margin of the Eastern Dharwar Craton, SE India: New Sm–Nd isochron age constraints from anorogenic mafic magmatism in the Neoarchean Nellore greenstone belt. Journal of Asian Earth Sciences, 37(1), pp.67-81.

207. Ray, J.S., Martin, M.W., Veizer, J. and Bowring, S.A., 2002. U-Pb zircon dating and Sr isotope systematics of the Vindhyan Supergroup, India. Geology, 30(2), pp.131-134.

208. Ray, J.S., Veizer, J. and Davis, W.J., 2003. C, O, Sr and Pb isotope systematics of carbonate sequences of the Vindhyan Supergroup, India: age, diagenesis, correlations and implications for global events. Precambrian Research, 121(1-2), pp.103-140.

209. Richards, P.W., Jhanwar, M.L., Rajurkar, S.T. and Phadttare, P.N., 1968. Stratigraphy of the lower part of the Kurnool Group in west central Cuddapah Basin, Andhra Pradesh. Geol. Surv. India, Open File Rep, (2).

210. Rigby, J.K., 1953. Some transverse styolites [New Mexico-Texas]. Journal of Sedimentary Research, 23(4), pp.265-271.

211. Rimmer, S.M., 2004. Geochemical paleoredox indicators in Devonian–Mississippian black shales, central Appalachian Basin (USA). Chemical Geology, 206(3-4), pp.373-391.

212. Robin, P.Y.F., 1978. Pressure solution at grain-to-grain contacts. Geochimica et Cosmochimica Acta, 42(9), pp.1383-1389.

213. Rogers, J.J. and Santosh, M., 2009. Tectonics and surface effects of the supercontinent Columbia. Gondwana Research, 15(3-4), pp.373-380.

214. Rothpletz, A., 1900. Über eigenthümliche Deformationen jurassischer Ammoniten durch Drucksuturen und deren Beziehungen zu den Stylolithen. Munich Kön.-bayer. Akad. d. Wissensch.

215. Roy, A., Chakrabarti, G. and Shome, D., 2018. Geochemistry of the Neoproterozoic Narji limestone, Cuddapah Basin, Andhra Pradesh, India: implication on palaeoenvironment. Arabian Journal of Geosciences, 11(24), pp.1-13.

216. Roy, A., Chakrabarti, G. and Shome, D., 2020. Neoproterozoic sedimentation and depositional environment: an example from Narji Formation, Cuddapah Basin, India. Journal of Sedimentary Environments, 5(4), pp.559-574.

217. Roy, A.K., 1947.Geology of the Dhone Taluk and neighboring parts, Kurnool district, Unpublished article, (1945-1946),. Geological Survey of India Progress Report.

218. Roy, A., Chakrabarti, G., and Shome, D., 2018. Study of Micro-Stylolite based on Geometry and Bedding Relationship Pattern in Neoproterozoic Narji Limestone from Betamcherla–Banganapalle Area of Kurnool Sub-Basin, Andhra Pradesh, South India. IJAR, 5(3), pp. 454-458.

219. Saha, D. and Chakraborty, S., 2003. Deformation pattern in the Kurnool and Nallarnalai Groups in the northeastern part (Palnad area) of the Cuddapah Basin, South

India and its implication on Rodinia/Gondwana tectonics. Gondwana Research, 6(4), pp.573-583.

220. Saha, D. and Mazumder, R., 2012. An overview of the Palaeoproterozoic geology of Peninsular India, and key stratigraphic and tectonic issues. Geological Society, London, Special Publications, 365(1), pp.5-29.

221. Saha, D. and Patranabis-Deb, S., 2014. Proterozoic evolution of Eastern Dharwar and Bastar cratons, India–an overview of the intracratonic basins, craton margins and mobile belts. Journal of Asian Earth Sciences, 91, pp.230-251.

222. Saha, D. and Tripathy, V., 2012. Palaeoproterozoic sedimentation in the Cuddapah Basin, south India and regional tectonics: a review. Geological Society, London, Special Publications, 365(1), pp.161-184.

223. Saha, D., Ghosh, G., Chakraborty, A.K. and Chakraborti, S., 2006. Comparable Neoproterozoic sedimentary sequences in Palnad and Kurnool subbasins and their paleogeographic and tectonic implications. Indian Journal of Geology, 78(1-4), pp.175-192.

224. Sai, V.S., Tripathy, V., Bhattacharjee, S. and Khanna, T.C., 2017. Paleoproterozoic magmatism in the Cuddapah basin, India. J. Ind. Geophys. Union (November 2017), 21(6), pp.516-525.

225. Sai, V.S., Tripathy, V., Bhattacharjee, S. and Khanna, T.C., 2017. Paleoproterozoic magmatism in the Cuddapah basin, India. J. Ind. Geophys. Union (November 2017), 21(6), pp.516-525.

226. Saluja, S. K., Rehman, K. and Arora, C. M. 1971. Plant microfossils from the Vindhyans of Son Vallay, India. J. geol. Soc. India, 12, pp. 24-33.

227. Salujha, S.K., Rehman, K. and Arora, C.M., 1971. Plant microfossils from the Vindhyans of Son valley, India. Geological Society of India, 12(1), pp.24-33.

228. Schopf, J.W. and Prasad, K.N., 1978. Microfossils in Collenia-like stromatolites from the Proterozoic Vempalle Formation of the Cuddapah basin, India. Precambrian Research, 6(3-4), pp.347-366.

229. Seilacher, A., 1967. Bathymetry of trace fossils. Marine geology, 5(5-6), pp.413-428.

230. Sen, S.N. and Narasimha Rao, C., 1968, January. Igneous activity in Cuddapah Basin and adjacent areas and suggestions on the paleogeography of the Basin. In Proceedings of symposium on Upper Mantle Project. NGRI, Hyderabad, pp. 261-284.

231. Sen, Shinjana and Meenal Mishra (2015) Geochemistry of Rohtas Limestone from Vindhyan Supergroup, Central India: Evidences of detrital input from Bundelkhand Craton. Geochemistry International, Vol. 53, No. 12, pp.1107–1122.

232. Sesha Sai, V.V., 2014. Pyroclastic volcanism in Papaghni sub-basin, Andhra Pradesh: Significant Paleoproterozoic tectonomagmatic event in SW part of the Cuddapah basin, Eastern Dharwar craton. Journal of the Geological Society of India, 83(4), pp.355-362.

233. Shafer, D.C., 1983. Petrology and depositional environments of the Beck Spring Dolomite, southern Death Valley region. California [MS thesis]: Davis, University of California, 195.

234. Sharma, M. and Shukla, M., 1999. Carbonaceous mega remains from the Neoproterozoic Owk Shales Formation of the Kurnool Group, Andhra Pradesh, India. Current Science, pp.1247-1251.

235. Sharma, M. and Shukla, Y., 2012. Occurrence of helically coiled microfossil Obruchevella in the Owk Shale of the Kurnool Group and its significance. Journal of earth system science, 121(3), pp.755-768.

236. Sharma, M. and Shukla, Y.O.G.M.A.Y.A., 2016. The Palaeobiological remains of the Owk Shale, Kurnool Basin: A discussion on the age of the basin. Journal of the Palaeontological Society of India, 61(2), pp.175-187.

237. Shaub, B.M., 1939. The origin of stylolites. Journal of Sedimentary Research, 9(2), pp.47-61.

238. Sheppard, S., Rasmussen, B., Zi, J.W., Somasekhar, V., Sarma, D.S., Mohan, M.R., Krapež, B., Wilde, S.A. and McNaughton, N.J., 2017. Sedimentation and magmatism in the Paleoproterozoic Cuddapah Basin, India: Consequences of lithospheric extension. Gondwana Research, 48, pp.153-163.

239. Sherman, C.E., Fletcher, C.H. and Rubin, K.H., 1999. Marine and meteoric diagenesis of Pleistocene carbonates from a nearshore submarine terrace, Oahu, Hawaii. Journal of Sedimentary Research, 69(5), pp.1083-1097.

240. Sholkovitz, E.R., 1990. Rare-earth elements in marine sediments and geochemical standards. Chemical geology, 88(3-4), pp.333-347.

241. Shukla, Y., Sharma, M. and Sergeev, V.N., 2020. Organic walled microfossils from the Neoproterozoic Owk Shale, Kurnool Group, South India. Palaeoworld, 29(3), pp.490-511.

242. Singh, A.K., Tewari, V.C., Sial, A.N., Khanna, P.P. and Singh, N.I., 2016. Rare earth elements and stable isotope geochemistry of carbonates from the mélange zone of Manipur ophiolitic Complex, Indo-Myanmar Orogenic Belt, Northeast India. Carbonates and evaporites, 31(2), pp.139-151.

243. Singh, A.P. and Mishra, D.C., 2002. Tectonosedimentary evolution of Cuddapah basin and Eastern Ghats mobile belt (India) as Proterozoic collision: gravity, seismic and geodynamic constraints. Journal of Geodynamics, 33(3), pp.249-267.

244. Sorby, H.C., 1908. On the application of quantitative methods to the study of the structure and history of rocks. Quarterly Journal of the Geological Society, 64(1-4), pp.171-233.

245. Srivastava, A.K. and Gawande, R.R., 2006.Petrography of upper Gondwana sediments (Early Cretaceous) of Bairam-Belkher area, Amravati District, Maharashtra and Betul District, Madhya Pradesh.Gondwana Geological Magazine 21(1): 1-12.

246. Srivastava, V.K. and Singh, B.P., 2017. Facies analysis and depositional environments of the early Eocene Naredi Formation (Nareda locality), Kutch, Western India. Carbonates and Evaporites, 32(3), pp.279-293.

247. Stockdale, P.B., 1922. Stylolites; the nature and origin, Indiana Univ. Studies, 11, pp.1-97.

248. Taylor, P.N., Chadwick, B., Moorbath, S., Ramakrishnan, M. and Viswanatha, M.N., 1984. Petrography, chemistry and isotopic ages of Peninsular Gneiss, Dharwar acid volcanic rocks and the Chitradurga Granite with special reference to the late Archean evolution of the Karnataka Craton, southern India. Precambrian Research, 23(3-4), pp.349-375.

249. Taylor, S.R. and McLennan, S.M., 1985. The continental crust: its composition and evolution.

250. Tobia, F.H. and Aqrawi, A.M., 2016. Geochemistry of rare earth elements in carbonate rocks of the Mirga Mir Formation (Lower Triassic), Kurdistan Region, Iraq. Arabian Journal of Geosciences, 9(4), pp.1-13.

251. Tobia, F.H., 2018. Stable isotope and rare earth element geochemistry of the Baluti carbonates (Upper Triassic), Northern Iraq. Geosciences Journal, 22(6), pp.975-987.

252. Tripathy, V. and Saha, D., 2013. Plate margin paleostress variations and intracontinental deformations in the evolution of the Cuddapah basin through Proterozoic. Precambrian Research, 235, pp.107-130.

253. Tripathy, V. and Saha, D., 2015. Inversion of calcite twin data, paleo stress reconstruction and multiphase weak deformation in cratonic interior–Evidence from the Proterozoic Cuddapah basin, India. Journal of Structural Geology, 77, pp.62-81.

254. Tucker, M.E., 1982. Precambrian dolomites: petrographic and isotopic evidence that they differ from Phanerozoic dolomites. Geology, 10(1), pp.7-12.

255. Tucker, M.E., 1983. Diagenesis, geochemistry, and origin of a Precambrian dolomite; the Beck Spring Dolomite of eastern California. Journal of Sedimentary Research, 53(4), pp.1097-1119.

256. Venkatachalapathy, V. and Man, R., 1992. Precambrian-Cambrian boundary in the Kurnool basin of southern Indian Peninsula. In 29th international geological congress (Kyoto, 24 August-3 September 1992).

257. Vijayam, B.E. and Reddy, G.V., 1973. Microstylolites in Narji Limestones from Kurnool district, Andhra Pradesh. Jour. Ind. Acad. Geosc, 16(2).

258. Vijayam, B.E., BE, V. and PH, R., 1976. Tectonic framework of sedimentation in the western part of Palnad Basin, Andhra Pradesh.

259. Wagner, G. and Noetling, F., 1913. Stylolithen und drucksuturen. G. Fischer.

260. Wan, B., Xiao, W., Han, C., Windley, B.F., Zhang, L., Qu, W. and Du, A., 2014. Re–Os molybdenite age of the Cu–Mo skarn ore deposit at Suoerkuduke in East Junggar, NW China and its geological significance. Ore Geology Reviews, 56, pp.541-548.

261. Wong, P.K. and Oldershaw, A., 1981. Burial cementation in the Devonian, Kaybob reef complex, Alberta, Canada. Journal of Sedimentary Research, 51(2), pp.507-520.

262. Worash, G. and Valera, R., 2002. Rare earth element geochemistry of the Antalo Super sequence in the Mekele Outlier (Tigray region, northern Ethiopia). Chemical Geology, 182(2-4), pp.395-407.

263. Wright, J., Seymour, R.S. and Shaw, H.F., 1984. REE and Nd isotopes in conodont apatite: variations with geological age and depositional environment. Conodont biofacies and provincialism, 196, pp.325-340.

264. Yang, C., Yang, C., LI, G., Liao, J. and Gong, J., 2012. Mesozoic tectonic evolution and prototype basin characters in the southern East China Sea Shelf Basin. Marine Geology & Quaternary Geology, 32(3), pp.105-111.

265. Zachariah, J.K., Rao, Y.B., Srinivasan, R. and Gopalan, K., 1999. Pb, Sr and Nd isotope systematics of uranium mineralised stromatolitic dolomites from the Proterozoic Cuddapah Supergroup, south India: constraints on age and provenance. Chemical Geology, 162(1), pp.49-64.

266. Zhang, H.F., Zhai, M.G., Santosh, M., Wang, H.Z., Zhao, L. and Ni, Z.Y., 2014. Paleoproterozoic granulites from the Xinghe graphite mine, North China Craton: Geology, zircon U–Pb geochronology and implications for the timing of deformation, mineralization and metamorphism. Ore Geology Reviews, 63, pp.478-497.

267. Zhao, J.H., Zhang, S.B. and Wang, X.L., 2018. Neoproterozoic geology and reconstruction of South China. Precambrian Research, 309, pp.1-5.

268. Zhu, R., Cui, J., Deng, S., Luo, Z., Lu, Y. and Qiu, Z., 2019. High-precision Dating and Geological Significance of Chang 7 Tuff Zircon of the Triassic Yanchang

Formation, Ordos Basin in Central China. Acta Geologica Sinica-English Edition, 93(6), pp.1823-1834.

SUPPLEMENTARY MATERIALS

Supplementary Material: 1

Supercontinent assembly and break-up related to Kurnool Basin

The late Mesoproterozoic and early Neoproterozoic time-period is one of the most remarkable time intervals in Earth's history. During this time, we can see the assembly and break-up of the supercontinent Rodinia that was related to the supercontinent Gondwanaland by global superplume events and rapid true polar wander event(s), repeated low-latitude glaciations, and finally the explosion of multicellular life (**McMenamin and McMenamin, 1990**). Rodinia and Pangaea are the two supercontinents includes almost all the continents on Earth. Despite the secular nature of Earth's evolution (and thus its tectonic processes), there are remarkable similarities between them: (1) They both had a lifespan of ca. 150 Ma: ca. 900 Ma to ≥750 Ma for Rodinia (this work), and ca. 320 Ma to 180–160 Ma for Pangaea **(e.g., Li and Powell, 2001; Veevers, 2004**); (2) The break-up of both supercontinents started with broad mantle upwellings (or superplumes) beneath them, resulting in widespread bimodal magmatism (including plume magmatism) and continental rifting. The formation and break-up of Pangea also coincided with the occurrence of geomagnetic superchrons (**Larson, 1991b; Eide and Torsvik, 1996**), but there are still inadequate data for assessing the presence of similar events during the history of Rodinia.

The basin in western Australia is age equivalent to Cuddapah and Kurnool formations which is containing similar rock formations. The formation of red beds both in India and Australia contemporaneously at near equatorial latitudes. Thus, the Proterozoic palaeomagnetism and palaeoclimatic information from India and Australia seems similar. Based on palaeomagnetic poles, palaeolatitudes, palaeoclimatic and structural evidence it is suggested that India and Australia collided possibly during Neoproterozoic times in an attempt to form larger Gondwana (**Gournl Mt et al., 2006).**

Supplementary Material: 2

Raw data used for geochemical classification of **Narji Limestone**. The data has been plotted in **Fig. 5.13** in Chapter-5.

Samples	**Er/Nd**	**Y/Ho**	**U/Th**
S-1	0.17	45.45	4.19
S-2	0.17	32.91	2.26
S-3	0.06	42.56	2.48
S-4	0.19	34.79	2.87
S-5	0.17	38.43	3.68
S-6	0.20	31.83	2.15
S-7	0.18	33.38	2.06
S-8	0.15	35.87	2.78
S-9	0.17	30.05	1.73
S-10	0.22	31.55	1.79

Supplementary Material: 3

Clastic contaminations ratio within the studied limestones of **Narji Limestone** in Chapter-5

NUMBER	LITHOLOGY	**K_2O/Al_2O_3**	**Al_2O_3/TiO_2**
N-1	Laminated limestone facies	0.13	15.53
N-2	Massive whitish grey limestone facies	0.23	18.80
N-3	Laminated limestone facies	0.21	15.36
N-4	Massive whitish grey limestone facies	0.14	14.20
N-5	Laminated limestone facies	0.13	12.53
N-6	Massive whitish grey limestone facies	0.23	20.19
N-7	Massive whitish grey limestone facies	0.24	15.60
N-8	Laminated limestone facies	0.25	16.88
N-9	Laminated limestone facies	0.24	21.82
N-10	Quartzite bearing massive purple limestone facies:	0.24	17.00

PHOTO GALLERY

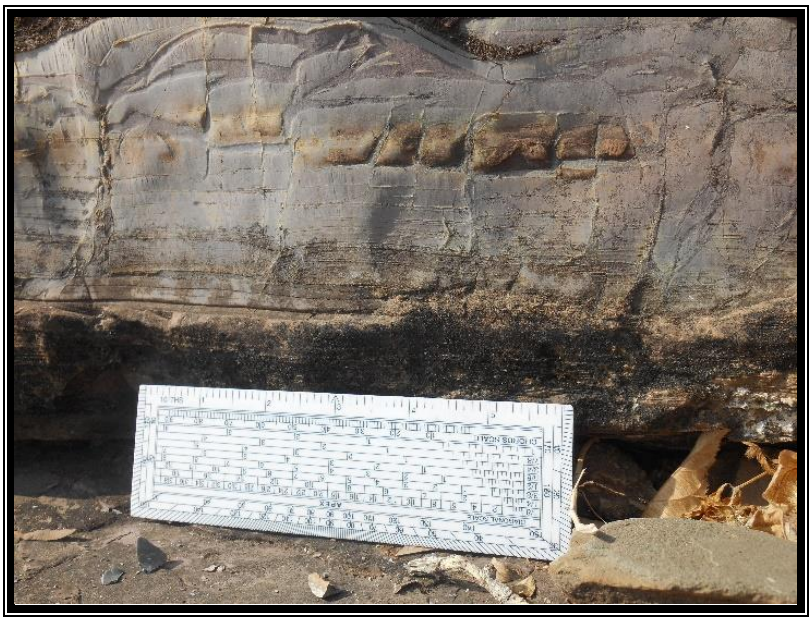

Fig 1. Deformed limestone bed with pinch and swell structure recorded in Patapadu section from Narji Formation which suggests tectonically induced sedimentation during Neoproterozoic time period. Length of the diagonal scale- 15.20 cm

Fig 2. Occurrence of Flaggy quartzite is observed in Patapadu Yantipalli section from Narji Formation. The limestones at base are thick bedded slaby and splintary. They are overlain by the calcareous flags. Diameter of the coin - 2.70 cm

Fig 3. Occurrence of Competent and incompetent bedding of limestone and shale in Patapadu Yantipalli section from Narji Formation. The length of the marker 13.90 cm

Fig 4. Pits in massive limestone observed in Patapadu Yantipalli section from Narji Formation which indicates the chemical weathering in limestone. Diameter of the coin - 2.40 cm

Fig 5. Water marks observed in Patapadu Yantipalli section from Narji Formation with plumose fractures (or feather-like fractures) (Bankwitz 1965). Plumose structures are thought to develop in response to local variations of the stress field (Syme-Gash 1971) and result from an advancing fracture front in closely spaced planes of weakness in an anisotropic material (Ernstson and Schinker 1986). Length of the marker pen 13.90 cm

Fig 6. Iron nodules observed in limestones which depict precipitation of iron oxide from iron-rich solutions in Patapadu Yantipalli section of Narji Formation. The length of the marker pen 13.90 cm

Fig 7. Occurrence of the iron nodules with comparatively larger in size within the Narji limestone, recorded from the Patapadu Yantipalli section.

Fig 8. Elephant skin weathering feature observed in Patapadu Yantipalli section from Narji Formation due to exposure of rock surface to rain. Length of the marker pen 13.90 cm

Fig 9. Paleokarstic layer observed in Patapadu Yantipalli section from Narji Formation. The paleokarst profile is interpreted as having developed mainly in the vadose zone on limestones that were partly cemented but had high intergranular porosity and permeability. The length of the hammer - 31.80 cm

Fig 10. Boundary between Narji limestone and overlying owk shales recorded from Patapadu Yantipalli section

Fig 11. Brown Paleokarstic layer observed in Patapadu section which develops over the limestone facies. Length of the hammer - 31.80 cm

Fig 12. Intrusion of quartz vein within calcareous shale observed in Patapadu section. The length of the scale - 15.20 cm

Fig 13. Quartz vein within calcareous shale, recorded from Patapadu Yantipalli section. The length of the hammer - 31.80 cm

Fig 14. Rain imprints on Narji limestone observed in Patapadu Yantipalli section. Length of the hammer - 31.80 cm

Fig 15. Intercalation of shale and limestone facies from Narji Formation which recorded from the Betamcherla area. Length of the hammer is - 31.80 cm

Fig 16. Small scale folding within the limestone facies is observed in Betamcherla area. Length of the scale - 15.20 cm

Fig 17. Iron concretion within limestone facies, recorded from Betamcherla area which are mainly formed from oxidation of pyrite. Dimension of the coin - 2.70 cm

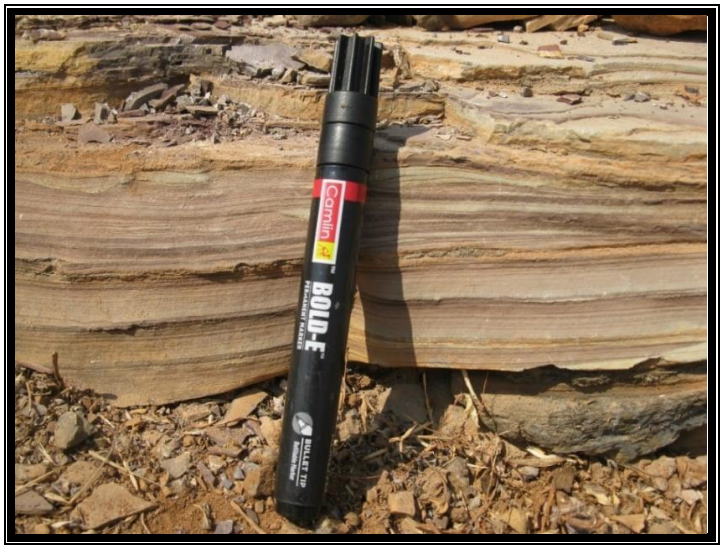

Fig 18. Occurrence of Rhymitites within the Betamcherla limestone of Narji Formation.

Fine laminations are made up clay and carbonates. Length of the marker pen 13.90 cm

Fig 19. Mudcracks observed in Narji limestone in Betamcherla area. Mudcracks are diagnostic sedimentary structures indicating subaerial exposure of sediment surfaces, with alternating wet and dry conditions. Diameter of the coin 2.70 cm.

PUBLICATIONS

Original Paper | Published: 18 December 2018

Geochemistry of the Neoproterozoic Narji limestone, Cuddapah Basin, Andhra Pradesh, India: implication on palaeoenvironment

Adrika Roy ✉, Gopal Chakrabarti & Debasish Shome

Arabian Journal of Geosciences **11**, Article number: 784 (2018) | Cite this article

274 Accesses | **9** Citations | Metrics

Abstract

The Neoproterozoic Narji Formation of Cuddapah Basin, Southern India is mainly composed of limestones with minor amount of clastic rocks. Limestones are massive as well as laminated and occasionally chert bearing. Geochemistry (major, trace, and REE) of limestones is studied to strengthen the knowledge on depositional environment of Narji Formation in the direction to better figure out the development of Cuddapah Basin during Neoproterozoic era. Average SiO_2 (25.97), Al_2O_3/TiO_2 (16.67), and K_2O/Al_2O_3 (0.21) ratios suggest clastic contamination in the Narji limestones. PAAS (Post Archean Australian Shale) normalized REE + Y pattern of Narji limestones are showing seawater like REE + Y pattern. The Er/Nd and Y/Ho ratios (average 0.17 and 35.68, respectively) of Narji limestones indicate the retention of normal seawater character with the signatures of terrigenous input and diagenesis process. Positive Ce anomaly, high U/Th (> 1.25), and V/(V + Ni) (> 0.5) ratios of Narji limestones clearly indicate their deposition in dyoxic to anoxic condition.

Arabian Journal of Geosciences (2018) 11:784
https://doi.org/10.1007/s12517-018-4135-9

ORIGINAL PAPER

Geochemistry of the Neoproterozoic Narji limestone, Cuddapah Basin, Andhra Pradesh, India: implication on palaeoenvironment

Adrika Roy[1] · Gopal Chakrabarti[2] · Debasish Shome[1]

Received: 25 June 2018 / Accepted: 30 November 2018

Abstract

The Neoproterozoic Narji Formation of Cuddapah Basin, Southern India is mainly composed of limestones with minor amount of clastic rocks. Limestones are massive as well as laminated and occasionally chert bearing. Geochemistry (major, trace, and REE) of limestones is studied to strengthen the knowledge on depositional environment of Narji Formation in the direction to better figure out the development of Cuddapah Basin during Neoproterozoic era. Average SiO_2 (25.97), Al_2O_3/TiO_2 (16.67), and K_2O/Al_2O_3 (0.21) ratios suggest clastic contamination in the Narji limestones. PAAS (Post Archean Australian Shale) normalized REE + Y pattern of Narji limestones are showing seawater like REE + Y pattern. The Er/Nd and Y/Ho ratios (average 0.17 and 35.68, respectively) of Narji limestones indicate the retention of normal seawater character with the signatures of terrigenous input and diagenesis process. Positive Ce anomaly, high U/Th (> 1.25), and V/(V + Ni) (> 0.5) ratios of Narji limestones clearly indicate their deposition in dyoxic to anoxic condition.

Keywords Geochemistry · Trace elements · REE · Paleooxidation · Neoproterozoic · Narji · Cuddapah

Introduction

Cuddapah Basin is known as the second largest in size among the Purana basins of Peninsular Indian shild which records widespread development of sandstone, shale and carbonate deposits of Palaeoproterozoic to Neoproterozoic age (Kale 2016). Based on the sedimentological aspects, Patranabis-Deb et al. (2012) described the depositional history of Cuddapah Basin into four different cycles, namely, Papaghni, Chitravati, Srisailam, and Kurnool cycle. Sedimentation within this Cuddapah Basin during Neoproterozoic time period is mainly represented by the Kurnool cycle. The sediments of Kurnool Group are deposited in two isolated sub basin within Cuddapah basin with reference to their geographical position (Nagarajan Rao et al. 1987). The first one is Kurnool sub basin, located at the west-central part and the second one is named the Palnad sub basin located in north-eastern part of Cuddapah. The two sub basins are 75 km apart, with the Srisailam Quarzite covering the gap. The formations that belong to this Kurnool group are Banganapalli, Narji, Owk, Paniam, Koilkuntla, and Nandyal. Within these formations, Narji Formation is mainly composed of limestone with minor amount of shale and sandstone units. The Narji Limestone is of extensive economic importance as the carbonate is of cement grade (Mouli Chandra et al. 2012).

Geochemistry of carbonate rocks is frequently used to depict the controlling factors that are responsible for the carbonate sediment characterization during and after the deposition (Armstrong-Altrin et al. 2003, 2011; Nagarajan et al. 2011; Hua et al. 2013; Khelen et al. 2017; Tobia 2018). Not only that, siliciclastic input as well as paleoredox condition can be clearly indentified through the geochemical study of carbonates (Armstrong-Altrin et al. 2003; Fu et al. 2011; Hua et al. 2013). Previous works within the Neoproterozoic Narji Formation are mainly based on the sedimentological aspects and suggest their deposition in a carbonate platform (Patranabis-Deb et al. 2012). There is a report of limited work on geochemistry of the Narji Formation from Palnad sub-basin (Lokesh Bharani 2015). Therefore, a systematic, detailed work focused on geochemical aspects of Narji limestone is much more required to strengthen the knowledge not only

✉ Adrika Roy
adrika.geology@gmail.com

[1] Department of Geological Sciences, Jadavpur University, Kolkata 700032, India

[2] Education Directorate, Government of West Bengal, Kolkata 700091, India

Published online: 18 December 2018

on depositional environment within the Kurnool sub-basin but also for deciphering paleoredox condition, siliciclastic input, and seawater chemistry during deposition Narji Limestone. Therefore, the present work is taken with the aim to better understand the geochemical characteristics of Narji limestones with an objective to highlight the palaeoenvironment of Narji Formation during the Neoproterozoic time period.

Geological setting

The intracratonic Cuddapah Basin of Peninsular Indian Shield is developed over the Eastern Dharwar Craton with an area coverage of 45,000 km^2 (Chakrabarti et al. 2014). Stratigraphically, Cuddapah Basin is sub-divided into Cuddapah Supergroup and Kurnool Group which preserves 12-km thickened sedimentary and volcanic strata (Nagaraja Rao et al. 1987; Table 1; Fig. 1a). Cuddapah Supergroup is consisting of Papaghni, Chitravati, Nallamalai Groups, and Srisailam Formation from base to top and the Kurnool Group is consisting of Banganapalli, Narji, Owk, Paniam, Koilkuntla, and Nandyal Formation from base to top (Table 1; Nagaraja Rao et al. 1987). Each group is interrupted by basin-wide unconformities and composed of clastic as well as carbonate group of rocks and reflects a grossly fitted fining upward succession (Nagaraja Rao et al. 1987; Patranabis-Deb et al. 2012). Within the Kurnool Group, Narji Formation is sandwiched in between clastic rocks of Banganapalli and Owk Formation with a thickness variation in between 100 and 200 m (Nagaraja Rao et al. 1987). Lithologically, Narji Formation is dominated by massive as well as laminated limestone with minor amount of shale and sandstone (Madesh et al. 2012). Occurrence of chert as nodules and thin layers is also observed within the limestone beds.

Numerous studies (Zachariah et al. 1999; Anand et al. 2003; French et al. 2008) have shown that the sedimentation within Cuddapah Supergroup represents the Palaeo to Mesoproterozoic time period. Crawford and Compston (1973) and Chakrabarti et al. (2014) further suggest that the base rocks of Kurnool group is not older than 1090 Ma and may be younger than 870 Ma (Neoproterozoic) and also predict its age equivalent to the Neoproterozoic rocks of upper Vindhyan Basin. Bertram (2012) also shows that the sedimentation within the Kurnool Group in between late

Table 1 Stratigraphy of the Cuddapah Basin (after Nagaraja Rao et al. 1987)

Group		Formation	Lithology	Age
KURNOOL		Nandyal (50–100 m)	Shale/Limestone	Neoproterozoic
		Koilkuntala (15–50 m)	Limestone with shale	
		Paniam (10–35 m)	Quartzite	
		Owk (10–15 m)	Shale	
		Narji (100–200 m)	Massive limestone, Flaggy limestone	
		Banganapalli (10–15 m)	Quartzite with conglomerate	
------Unconformity------				
CUDDAPAH SUPERGROUP		Srisailam (300 m)	Pebbly grit, Quartzite, Heterolithic shales and sandstone	Mesoproterozoic
	------Unconformity------			
	NALLAMALAI	Cumbum (~ Pullampet Shale) (2000 m)	Shale, Dolomitic limestone, Quartzite	
		Bairenkonda (~ Nagari Quartzite) (5500 m)	Pebbly grit, Quartzite, Heterolithic Shales and sandstone	
	------Unconformity------			
	CHITRAVATI	Gandikota (300 m)	Quartzite, Pebble beds	Mesoproterozoic
		Tadpatri (4600 m)	Shale, Quartzite, Stromatolitic dolomite with mafic flows, Sills and dykes	
		Pulivendla (1–75 m)	Conglomerate, Quartzite	
	------Unconformity------			
	PAPAGHNI	Vempalle (1900 m)	Stromatolitic dolomite, Shale, Basic flows and intrusive	Palaeoproterozoic
		Gulcheru (30–210 m)	Conglomerate, Feldspathic sandstone and quartzite	
------Unconformity------				
DHARWAR CRATON				Archean

Mesoproterozoic to Neoproterozoic. Therefore, based on these previous works, it can be assumed that the Narji limestones mainly represent the Neoproterozoic era.

Materials and methods

Ten (N1–N10) unweathered limestone samples were collected from the outcrop of the Narji Formation. The samples N1, N3, N5, N8, and N9 are laminated limestones and N2, N4, N6, N7 are massive whitish gray limestones and N10 is quartzite bearing massive purple limestone. The area is located in and around Patapadu-Yaganti hills (Fig. 1b) (15°18′45.00″ N, 78°07′35.76″ E), west-central part of the Cuddapah Basin and the thickness of the studied section is 124 m. Figure 2 shows the stratigraphic position of the sample collection from the studied section. To wash out the contamination, all the limestone samples were first cleaned thoroughly in distilled water. These all cleaned samples were further air dried which was followed by powdering in an agate mortar and finally sieved through a 200 ASTM mesh. For petrographic study, rock samples were sliced into small pieces, and section perpendicular to the bedding plane was chosen for grounding and polishing to make a thickness of 0.03 mm. Further, a cover slip is placed over the thin section to avoid contamination and oxidation.

The major element concentrations were obtained from a Bruker model S4 Pioneer sequential wavelength—dispersive X-ray fluorescence (XRF) spectrometer, whereas the trace and rare earth elements were analyzed through high resolution inductively which is coupled by plasma mass spectrometer (HR-ICPMS) in which JLS-1 was used as the standard. The values obtained for the standard; JLS-1 is provided in Tables 3 and 4. Initially, 50 mg of each sample was taken in Savillex vessels, and then, 10 mL of 7:3 HF–HNO_3 acid mixtures was added to that sample. The vessels were then tightened and they are placed on the hot plate at a temperature about 150 °C for 50 h. Later on, the vessels were opened and a single drop of $HClO_4$ was added to the mixtures. These mixtures were further evaporated to near dryness at 160 °C. The remaining residues of each vessel were dissolved by adding 20 mL of 1:1 HNO_3–Milli-Q water, and they are placed on the hot plate for 30–45 min at 100 °C to dissolve all suspended particles in it. Afterwards, Rhodium solution (in an amount 5 mL) was added as an internal standard to each vessel, and the volume was raised to 250 mL by adding Milli-Q water (Milli-Q is a trademark which describes 'ultrapure' water of "Type-1"). The high density polyethylene (HDPE) bottles are used to store this solution. Around 5 mL of this solution was again mixed with 50 mL Milli-Q water (1:10 ratio). It is then stored in Eppendorf tubes for analysis. The analytical precision of the geochemical data is better than 5% RSD.

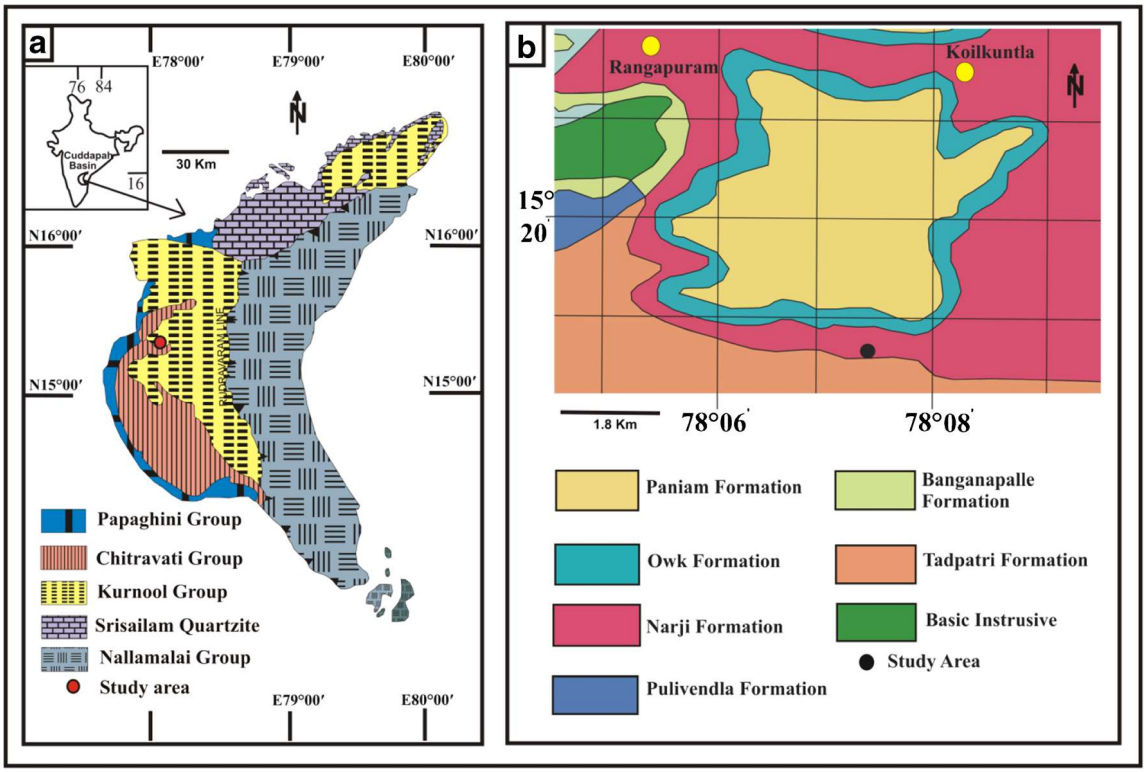

Fig. 1 Geological maps of the study area. **a** Generalized geological map of the Cuddapah basin (modified after Geological survey of India 1:2000000 map, 1998); **b** West-central part of Cuddapah basin showing location of the measured section investigated in this study (modified after Survey of India Quadrangle map number 57I, 1981; 1:250000)

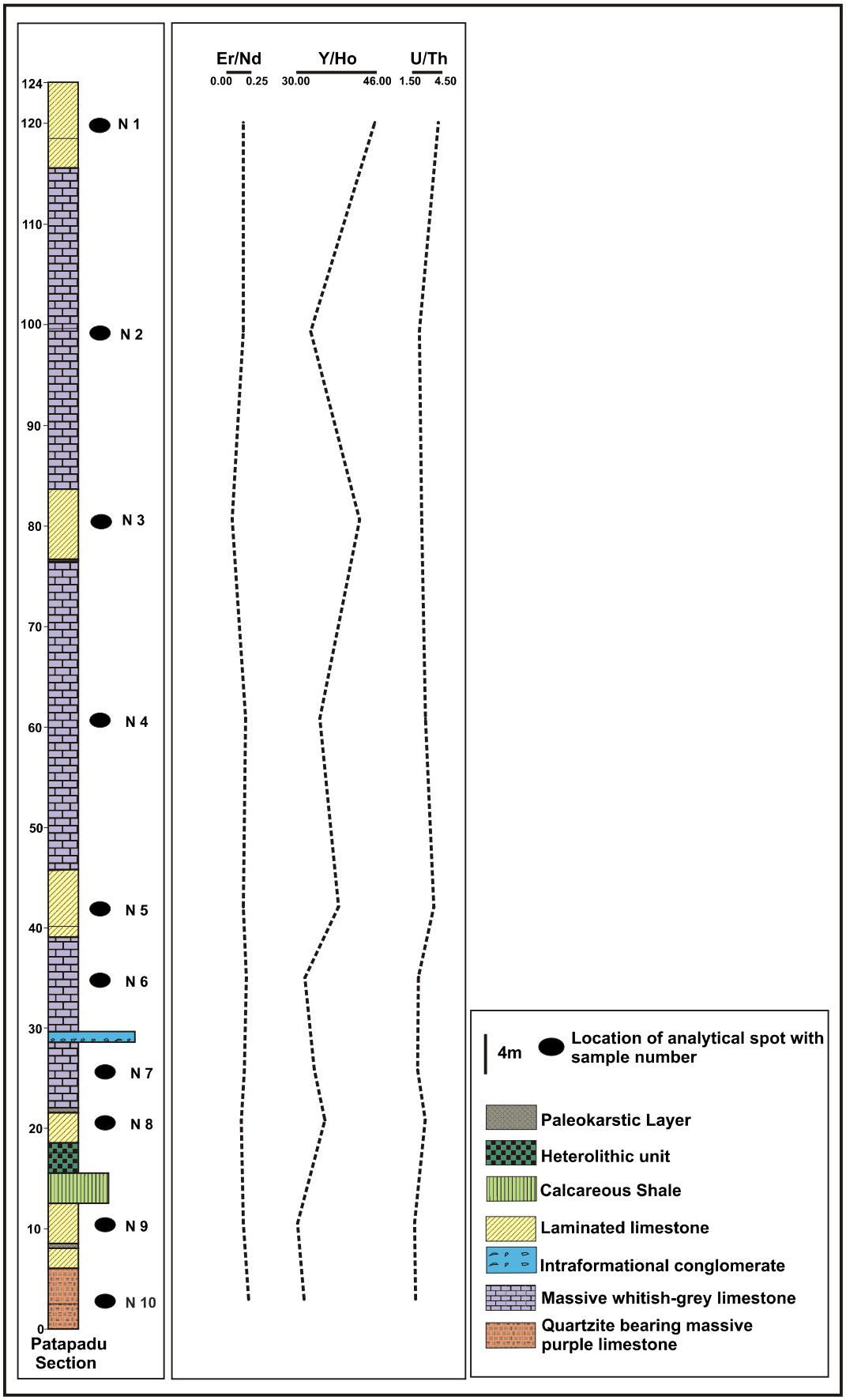
Er/Nd
0.00 0.25
Y/Ho
30.00 46.00
U/Th
1.50 4.50
124
120
110
100
90
80
70
60
50
40
30
20
10
0
N 1
N 2
N 3
N 4
N 5
N 6
N 7
N 8
N 9
N 10
Patapadu Section
4m
Location of analytical spot with sample number
Paleokarstic Layer
Heterolithic unit
Calcareous Shale
Laminated limestone
Intraformational conglomerate
Massive whitish-grey limestone
Quartzite bearing massive purple limestone

◀ **Fig. 2** Lithology of the measured stratigraphic section with the positions of the limestone sample collection. Er/Nd, Y/Ho, and U/Th ratios of the Narji limestones are also plotted, showing their vertical variations within the studied section

Results

Petrography

The Narji rocks reveal the presence of three types of limestone lithofacies, namely, quartzite bearing massive purple limestone, massive whitish splintery limestone, and laminated limestone facies.

Quartzite bearing massive purple limestone

Within the studied area, this limestone facies is unconformably lying over the Tadpatri formation with a thickness of 6.5 m. Thin lenses and pockets of quartzite have been encountered within the limestones which may have been derived from underlying clastic rocks of Tadpatri Formation. Sedimentary features like ripple marks (Fig. 3a) and syneresis cracks are also frequently observed. Microscopic studies reveal that the facies is micrite dominated with scattered distributions of quartz grains (Fig. 3b). A gradual decrease in siliceous material with a gradual increase in carbonate content from base to top within this facies is also recorded. Under microscope, calcite acts as a cementing material among the quartz grains (Fig. 3c) indicating diagenetic processes.

Massive whitish gray limestone

This massive limestone facies is mostly micrite dominated and occurs at different stratigraphic levels of the studied section with a thickness variation from 6.5 to 32.0 m. They are fine grained, highly compact, and very hard (Fig. 3d). Wavy, nodular, and lenticular chert are present within this facies. It is also associated with numerous stylolitic structures both macroscopic and microscopic levels (Fig. 3e). This facies is also

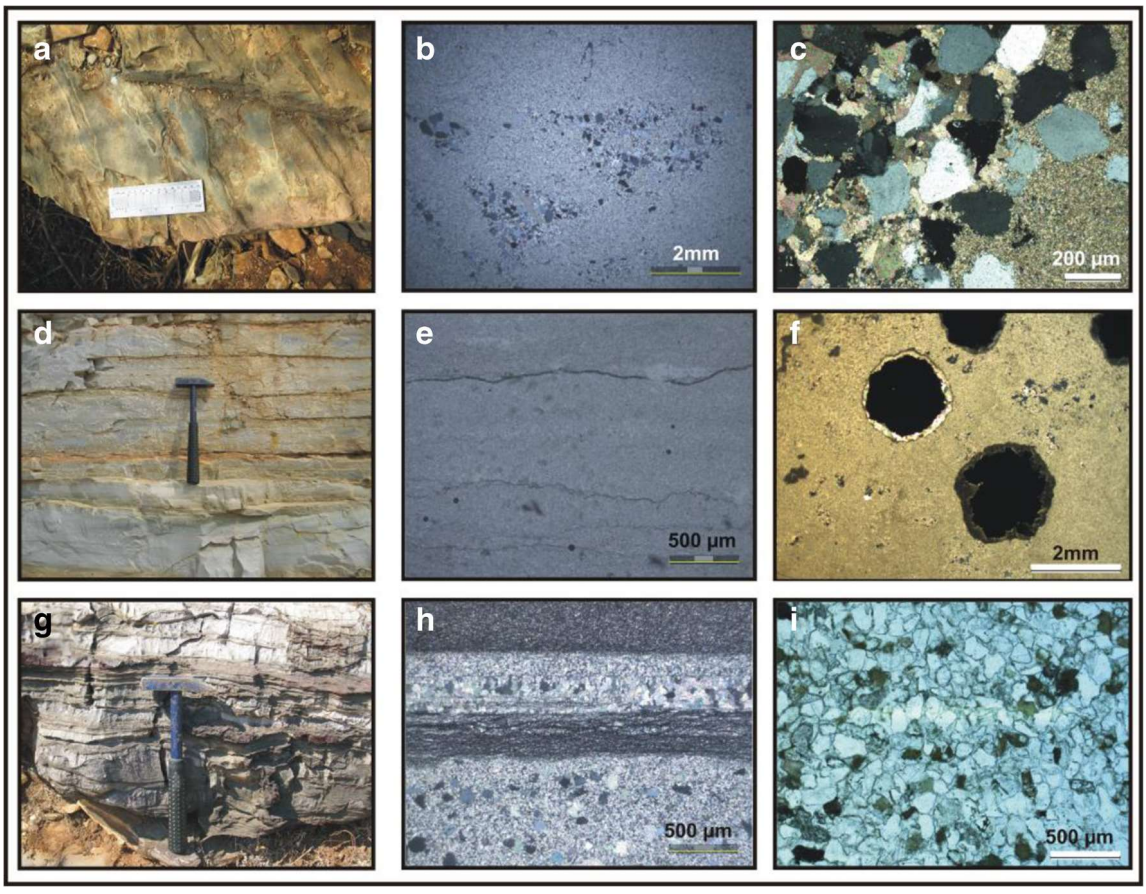

Fig. 3 Narji limestones from the studied area. **a** Sinius crested ripple resembling like tuning fork within Quarzite bearing massive limestone, **b** patchy distribution of quarzite within micrite dominated limestone, **c** calcite cementation in the remaining pore spaces in between the quartz grains, **d** massive whitish limestone of Narji Formation, **e** different types of stylolite within massive whitish limestone, **f** scattered crystals of pyrite within limestone, the margins of the pyrite are surrounded by sparite that probably formed as a residue after the replacement of pyrite by calcite, **g** straight and wavy laminated limestone characterized by irregular undulated layers, **h** dark streaks of clay within limestone interlaminated with light colored coarse sparite crystal, **i** green sand; composed mainly of glauconite in the lowermost part of the unit. Most glauconite grains within the micritic matrix are replaced by Fe-calcite

found in association with rounded to sub-rounded pyrite grains, especially at the uppermost part of the succession. It appears opaque in transmitted light. There is an evidence of iron leaching and partial replacement to sparite along the boundary of the pyrite grains (Fig. 3f).

Laminated limestone facies

This gray to dark gray colored laminated limestone facies is observed throughout the studied section with a thickness variation from 2.0 to 8.5 m (Fig. 3g). The laminations are mostly less than 1 cm, parallel to sub-parallel in nature and commonly composed of clayey material. The evidence of iron-leaching is also observed on the surface. Microscopic studies of this facies indicate the dominance of clay and micrite with coarse microsparitic mosaic of equant crystal in some samples (Fig. 3h). The lamination also contains minor amount of fine grained terrigenous silt with glauconite (Fig. 3i) in the lower most part of the unit. Veins of sparite within the micrite are also observed under microscope, and occasionally, this fine grained micrite is replaced by coarse sparite grains. The patchy distribution of neomorphic cement indicates late stage diagenetic processes (Folk 1965; Sherman et al. 1999; Ramkumar 2004).

Major element concentrations

Table 2 represents the analytical result of the major oxide along with loss of ignition (LOI) of the Narji limestones. A wide range of CaO wt% (31.45 to 72.03) is recorded with an average value of 47.87% (Table 2). Also, SiO_2 wt% reflects a wide variation (14.27 to 45.92 wt%) with an average 25.97 (Table 2). Negative correlation ($r = -0.62$) between Ca and Si is found from the bivariate plot of Cao and SiO_2. Hence, we may infer different source of origin of Ca and Si of the studied samples (c.f. Nagarajan et al. 2011). Bivariate plot of SiO_2 vs. TiO_2 ($r = 0.81$, $n = 10$; Fig. 4) and SiO_2 vs. Al_2O_3 ($r = 0.89$, $n = 10$; Fig. 4) is showing positive correlation whereas the bivariate plot of CaO vs. TiO_2 ($r = -0.28$, $n = 10$; Fig.4) and CaO vs. Al_2O_3 ($r = -0.48$, $n = 10$; Fig. 4) showing negative correlation and these suggest that the source of TiO_2 and Al_2O_3 is similar with the source of SiO_2 and also indicate that there is a terrigeneous input within the Narji limestones (Lokesh Bharani 2015; Sen and Mishra 2015; Madhavaraju et al. 2016). Clastic contaminations within the studied limestones are also observed from the average ratio of Al_2O_3/TiO_2 (16.67) and K_2O/Al_2O_3 (0.21) (Sen and Mishra 2015). The average concentration of MgO within the samples is 0.53 wt% and the SiO_2 vs. MgO bivariate diagram exhibits significant positive correlation ($r = 0.57$, $n = 10$; Fig. 4) indicating silicification processes during early diagenetic stage. Bivariate diagram of Fe_2O_3 vs. SiO_2 also reflects positive correlation in between Si and Fe ($r = 0.79$, $n = 10$; Fig. 4), and this further indicates that the Fe concentration within the limestones is related with the detrital input. The very low Na_2O content (Table 2) in the Narji limestones suggests that either the limestones were formed initially from a low Na_2O concentrated solution or inferred recrystallization of the limestone (Madhavaraju and Lee 2009; Lokesh Bharani 2015).

Trace element concentrations

Table 3 lists the analytical result of the trace element concentrations of the studied samples ($n = 10$). PAAS normalized trace elements of these limestones are plotted in Fig. 5. Within the LILE (Rb, Cs, Sr, Ba), Rb and Cs are highly depleted compared to the PAAS (Fig. 5). Sr concentration within these limestones is near to the PAAS value (200 ppm; Taylor

Table 2 Major oxides (wt%) content in the Narji limestones, Cuddapah Basin with the average value of PAAS (Taylor and McLennan 1985)

Sample no.	SiO_2	TiO_2	Al_2O_3	MnO	Fe_2O_3	CaO	MgO	Na_2O	K_2O	P_2O_5	LOI	TOTAL	K_2O/Al_2O_3	Al_2O_3/TiO_2
N-1	17.40	0.15	2.33	B.D.	0.39	46.26	0.40	B.D.	0.30	0.80	31.46	99.49	0.13	15.53
N-2	33.76	0.20	3.76	0.01	0.99	46.95	0.55	B.D.	0.87	0.97	11.36	99.42	0.23	18.80
N-3	14.27	0.11	1.69	0.03	0.63	48.14	0.37	0.02	0.35	0.09	33.94	99.64	0.21	15.36
N-4	15.63	0.15	2.13	B.D.	0.46	66.11	0.81	B.D.	0.30	0.18	13.98	99.75	0.14	14.20
N-5	17.74	0.15	1.88	0.02	0.31	72.03	0.26	B.D.	0.25	0.96	6.00	99.60	0.13	12.53
N-6	36.26	0.21	4.24	0.02	1.44	49.08	0.83	0.01	0.97	0.64	5.65	99.35	0.23	20.19
N-7	20.16	0.15	2.34	B.D.	0.67	41.52	0.14	B.D.	0.57	0.59	33.37	99.51	0.24	15.60
N-8	23.74	0.17	2.87	B.D.	1.18	42.48	0.37	B.D.	0.73	0.61	27.54	99.69	0.25	16.88
N-9	45.92	0.22	4.80	0.03	2.25	31.45	0.70	B.D.	1.15	0.27	12.90	99.69	0.24	21.82
N-10	34.81	0.14	2.38	0.01	0.46	34.72	0.85	0.03	0.58	0.31	25.27	99.56	0.24	17.00
Average	25.97	0.17	2.84	0.01	0.88	47.87	0.53	0.01	0.61	0.54	20.15	99.57	0.21	16.71
PAAS	62.80	0.99	18.90	7.22	0.11	2.20	1.30	1.20	3.70	0.16	–	98.58	0.20	19.09

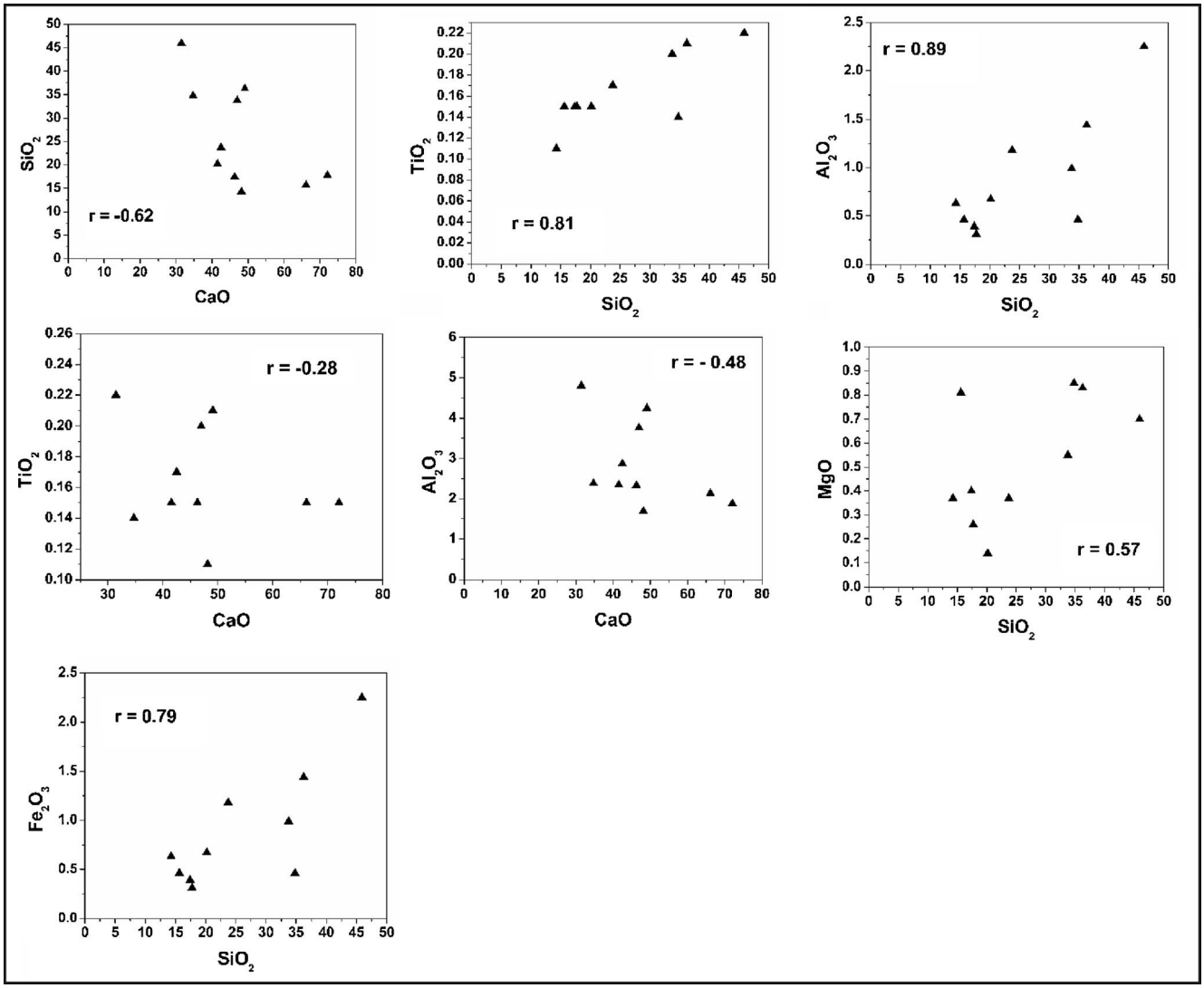

Fig. 4 Bivariate plots of the major oxides (in wt%) of Narji limestones

and McLennan 1985) (Table 3; Fig. 5). In case of Ba concentration, some limestone samples (N2, N3, N6, N7, and N8) are showing slightly to moderate depletion and the rest of the samples (N1, N4, N5, N9, and N10) showing slightly to moderate enrichment compared to PAAS. The high Ba content in few limestone samples may be due to K-feldspar breakdown from granitic source (Condie et al. 1995; Armstrong-Altrin et al. 2013; Lokesh Bharani 2015). The PAAS normalized ferromagnesian trace elements (Co, Ni, Cr, and V) are showing depletion in Fig. 5. Within all of the HFSE (Zr, Y, Nb, Hf, Th, and U), Zr is highly depleted and the rest of the HFSEs are moderately to slightly depleted (except Nb concentration in N3 sample; Fig. 5).

Rare earth element concentrations

Table 4 lists the analytical result of the rare earth element concentrations (REE) of the Narji limestones ($n = 10$). The REE concentrations within the studied limestones show wide range of variation from 16.93 to 53.27 ppm with an average of 35.31 ppm (Table 4). PAAS normalized REE + Y pattern of these limestones is plotted in Fig. 6 and a clear Sm anomaly is observed. Within the limestone samples, Sm has a positive correlation with SiO_2 ($r = 0.70$, $n = 10$), TiO_2 ($r = 0.70$, $n = 10$), and Al_2O_3 ($r = 0.71$, $n = 10$) and has a negative correlation with Cao ($r = -0.65$, $n = 10$). This indicates that the source of Sm is similar with the source of SiO_2, TiO_2, and Al_2O_3, and its enrichment is probably due to the clastic contamination within the samples. $(La/Yb)_{SN}$ ratio (0.39 to 1.21, with an average 0.59; Table 5) of the samples is relatively lower than the terrigenous materials (1.3 Sholkovitz 1990 and 1 Condie 1991) which suggests that the REE is influenced by LREE depleted carbonate particles (Armstrong-Altrin et al. 2009; Nagarajan et al. 2011). This $(La/Yb)_{SN}$ ratio of Narji limestones is very much similar with the $(La/Yb)_{SN}$ ratio of Neoproterozoic Bhima limestones as well as with late

Table 3 Trace elements (in ppm) concentrations within the Narji limestones, Cuddapah Basin with the average value of PAAS (Taylor and McLennan 1985) and obtained values for the standard, JLS-1

Sample no.	V	Cr	Co	Ni	Sc	Cu	Zn	Ga	Rb	Sr	Y	Zr	Nb	Cs	Ba	Hf	Ta	Pb	Th	U
N-1	4.53	3.01	0.44	0.30	0.04	0.31	6.38	B.D.	0.18	289.65	10.41	0.63	0.04	0.05	3036	0.74	0.01	0.26	0.10	0.43
N-2	4.79	3.04	1.48	0.33	0.03	0.25	4.01	B.D.	0.18	199.78	7.32	0.72	0.11	0.10	264	0.21	0.02	0.30	0.25	0.57
N-3	4.03	3.42	0.13	0.32	0.03	0.32	3.99	0.62	0.58	203.59	3.43	4.55	5.10	0.32	398	0.09	0.03	1.15	0.13	0.32
N-4	4.00	3.07	0.56	0.31	0.04	0.25	5.06	B.D.	0.16	196.26	4.11	0.50	0.05	0.04	3046	0.16	0.01	0.25	0.10	0.28
N-5	3.61	3.04	0.79	0.31	0.04	0.33	5.00	B.D.	0.15	178.07	4.44	0.47	0.04	0.04	3570	0.15	0.01	0.42	0.09	0.33
N-6	6.14	4.80	2.01	0.34	0.04	0.28	3.70	B.D.	0.23	156.43	11.05	1.77	0.13	0.11	197	0.51	0.02	0.30	0.29	0.63
N-7	4.67	3.15	0.76	0.30	0.04	0.24	3.06	B.D.	0.19	143.91	9.25	0.75	0.08	0.10	74	0.25	0.01	0.26	0.17	0.36
N-8	6.25	3.95	1.33	0.31	0.05	0.28	4.80	B.D.	0.23	141.53	9.93	0.90	0.06	0.10	80	0.31	0.01	0.28	0.16	0.44
N-9	9.20	5.67	2.57	0.41	0.04	0.26	6.07	B.D.	0.28	230.11	8.56	1.52	0.17	0.16	1858	0.45	0.02	0.28	0.37	0.65
N-10	6.59	5.44	2.35	0.33	0.04	0.26	3.54	B.D.	0.24	72.27	8.85	2.76	0.10	0.20	2043	0.72	0.01	0.34	0.29	0.52
Average	5.38	3.86	1.24	0.33	0.04	0.28	4.56	0.62	0.24	181.16	7.74	1.46	0.59	0.12	1457	0.36	0.02	0.38	0.20	0.45
PAAS	150.00	110.00	23.00	55.00	16.00	50.00	85.00	17.50	160.00	200.00	27.00	210.00	1.90	15.00	650	5.00	–	20.00	14.60	3.10
JLS-1	3.769	3.194	0.067	0.287	0.022	0.226	2.363	0.097	0.189	279.232	0.188	3.879	1.221	0.064	428	0.088	0.014	1.075	0.026	1.573

Neoproterozoic shallow marine platform carbonate (Table 6). $(Dy/Yb)_{SN}$ ratios (1.00 to 1.54, average 1.39; Table 5) of the studied limestones is relatively higher than the $(Dy/Yb)_{SN}$ ratio of modern seawater which is 0.8–1.1(Singh et al. 2016). The high $(Dy/Yb)_{SN}$ ratios of the limestones exhibit HREE enrichment rather than LREE (Nagarajan et al. 2011; Singh et al. 2016). The Narji limestones are showing seawater like REE + Y pattern (LREE depleted, HREE enriched to flat) with negative Eu (average Eu/Eu* = 0.27, Table 5) and positive Ce anomaly (average Ce/Ce* = 2.33, Table 5).

Discussions

Source of REE

The REE pattern in sedimentary rock is often used to characterize source rock (Armstrong-Altrin et al. 2015a, b; Khelen et al. 2017; Tobia 2018; Mitra et al. 2018). PAAS normalized REE values of the analyzed samples are mostly depleted and this indicates the terrigenous input within the Narji limestones (Devi and Duarah 2015; Sen and Mishra 2015). The studied limestones are reflecting a wide range of variation in ∑REE concentration (16.93 to 53.27, average 35.31; Table 4), and this is more or less comparable with typical marine carbonate value, which is 28 ppm (Chen et al. 2014). These wide ranges of variation in ∑REE concentration are also as a result of variation in terrigenous materials within the limestone samples. The $(Nd/Yb)_{SN}$ ratios of the samples vary from 0.40 to 0.53 (except sample N-3, Table 5) and this is similar with the other $(Nd/Yb)_{SN}$ ratios of the Proterozoic carbonate rocks that have seawater-like REE patterns (Table 6). This clearly indicates that the Narji limestone samples retained the original marine water characteristics. Er/Nd ratio can be used as a proxy to represent the effect of LREE/HREE fractionation in modern and ancient marine system (German and Elderfield 1989). In marine condition, the Er/Nd ratio value is near 0.27 (De Baar et al. 1988; Abiding and Calagari 2015). Therefore, limestones with higher Er/Nd ratio explain the seawater condition, preserved by the marine carbonate. Er/Nd ratio less than 0.1 indicates addition of detrital material as well as diagenetic process within the carbonates (De Baar et al. 1988; Abiding and Calagari 2015; Tobia 2018). The Er/Nd ratios of the studied samples are within 0.06 to 0.22 with an average of 0.17 (Table 5) which is relatively low compared to the normal marine water. This points to an influence of terrigenous input compared to the chemical precipitation during deposition and activation of diagenetic process rather than activation of normal seawater during sedimentation. The N3 sample shows the Er/Nd value less than 0.1 (Table 5, Fig. 2) and this suggests maximum influence of detrital material within N3 sample.

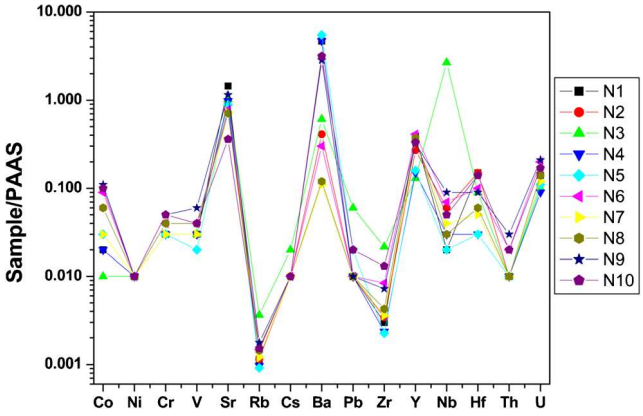

Fig. 5 Distribution of PAAS normalized trace elements of Narji limestones. PAAS value is defined from Taylor and McLennan (1985)

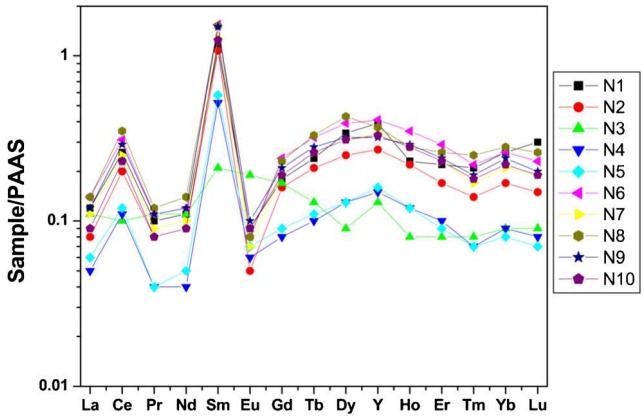

Fig. 6 Distribution of PAAS normalized REE + Y patterns of Narji limestones. PAAS value is defined from Taylor and McLennan (1985)

Most of the Narji limestones are showing very much similar sea-water like REE + Y pattern. But during carbonate precipitation from seawater, variable degree of contamination of detrital material suppressed the seawater signatures. The limestone samples are showing recognizable positive correlation of ΣREE with SiO_2 ($r = 0.57$; $n = 10$), TiO_2 ($r = 0.58$; $n = 10$), Al_2O_3 ($r = 0.66$; $n = 10$), and Fe_2O_3 ($r = 0.62$; $n = 10$) and negative correlation with CaO ($r = -0.71$; $n = 10$) (Fig. 7). This indicates the presence of terrigenous fraction and this is the most probable source of REE within the Narji samples. The terrigenous source of REE is more proved by the strong positive correlation of ΣREE with Th, Cr, Sc, and Y elements (Fig. 7; Sen and Mishra 2015; Shaltami 2015; Ramos-Vázquez et al. 2017; Anaya-Gregorio et al. 2018; Hernández-Hinojosa et al. 2018).

Behavior of europium

The Eu/Eu* ratios of the Narji samples are within 0.13 to 0.29 (except N3, Eu/Eu* 1.02; Table 5). Except N3, all the analyzed samples show negative Eu anomaly in the Narji limestones. Positive Eu anomaly in PAAS-normalized REE pattern may be due to hydrothermal solution which originates in a deep sea environment (Worash and Valera 2002; Armstrong-Altrin et al. 2003) or due to diagenetic change (Tobia 2018; Abiding and Calagari 2015). The Narji limestones are deposited in a shallow marine carbonate platform; therefore, local enrichment of feldspar as well as diagenetic changes may lead to positive Eu anomaly for N3 sample. Negative Eu anomaly also indicates retention of the original marine water characteristics within the limestone samples.

Table 4 REE concentration (in ppm) studied within Narji limestones, Cuddapah Basin with the average value of PAAS (Taylor and McLennan 1985) and obtained values for the standard, JLS-1

Sample no.	La	Ce	Pr	Nd	Sm	Eu	Gd	Tb	Dy	Ho	Er	Tm	Yb	Lu	∑LREE/∑ HREE	∑REE
N-1	4.76	20.39	0.86	3.80	6.26	0.09	0.83	0.19	1.57	0.23	0.64	0.09	0.74	0.13	8.18	40.58
N-2	3.21	16.26	0.69	2.96	5.92	0.06	0.75	0.16	1.16	0.22	0.50	0.06	0.48	0.06	8.58	32.49
N-3	4.19	7.95	0.98	3.85	1.15	0.20	0.78	0.10	0.42	0.08	0.23	0.03	0.25	0.04	9.49	20.25
N-4	1.97	8.42	0.36	1.48	2.87	0.06	0.38	0.08	0.59	0.12	0.28	0.03	0.26	0.03	8.56	16.93
N-5	2.11	9.26	0.37	1.53	3.19	0.07	0.41	0.08	0.60	0.12	0.26	0.03	0.24	0.03	9.34	18.30
N-6	5.26	24.35	1.01	4.18	8.58	0.09	1.12	0.24	1.80	0.35	0.82	0.09	0.74	0.10	8.26	48.73
N-7	4.31	20.09	0.83	3.51	7.10	0.08	0.90	0.20	1.47	0.28	0.64	0.07	0.59	0.08	8.49	40.15
N-8	5.48	27.95	1.08	4.86	8.43	0.08	1.06	0.25	2.04	0.28	0.75	0.10	0.80	0.11	8.88	53.27
N-9	4.75	23.18	0.97	3.99	8.33	0.10	1.00	0.21	1.51	0.28	0.67	0.08	0.67	0.09	9.16	45.83
N-10	3.30	18.32	0.72	3.02	6.87	0.09	0.89	0.20	1.44	0.28	0.66	0.07	0.63	0.08	7.60	36.57
Average	3.94	17.62	0.79	3.32	5.87	0.09	0.81	0.17	1.26	0.22	0.54	0.06	0.54	0.08	8.60	35.31
PAAS	38.2	79.6	8.83	33.9	5.55	1.08	4.66	0.77	4.68	0.99	2.85	0.41	2.82	0.43	9.49	184.77
JLS-1	0.109	0.725	0.033	0.120	0.093	0.006	0.052	0.003	0.025	0.003	0.011	0.002	0.010	0.028	–	–

Table 5 Elemental ratios and anomalies of studied Narji limestones. $Ce/Ce^* = Ce_{SN}/(La_{SN} \times Pr_{SN})^{0.5}$; $Eu/Eu^* = Eu_{SN}/(Sm_{SN} \times Gd_{SN})^{0.5}$; $Pr/Pr^* = [Pr/(0.5Ce + 0.5Nd)]_{SN}$

Sample no.	Eu/Eu*	Ce/Ce*	Pr/Pr*	$(Nd/Yb)_{SN}$	$(La/Yb)_{SN}$	$(Dy/Yb)_{SN}$	Y/Ho	Er/Nd	V/(V + Ni)	U/Th
N-1	0.19	2.33	0.53	0.43	0.47	1.27	45.45	0.17	0.94	4.19
N-2	0.13	2.52	0.54	0.51	0.49	1.46	32.91	0.17	0.94	2.26
N-3	1.02	0.91	1.04	1.26	1.21	1.00	42.56	0.06	0.93	2.48
N-4	0.29	2.32	0.54	0.48	0.57	1.39	34.79	0.19	0.93	2.87
N-5	0.29	2.43	0.51	0.53	0.65	1.50	38.43	0.17	0.92	3.68
N-6	0.14	2.43	0.53	0.47	0.52	1.47	31.83	0.20	0.95	2.15
N-7	0.14	2.45	0.53	0.49	0.54	1.49	33.38	0.18	0.94	2.06
N-8	0.13	2.65	0.50	0.51	0.51	1.54	35.87	0.15	0.95	2.78
N-9	0.17	2.49	0.54	0.50	0.52	1.36	30.05	0.17	0.96	1.73
N-10	0.18	2.75	0.51	0.40	0.39	1.38	31.55	0.22	0.95	1.79
Average	0.27	2.33	0.58	0.56	0.59	1.39	35.68	0.17	0.94	2.60

Y/Ho ratio and seawater chemistry

Y/Ho ratio is treated as a proxy of marine environment (Bau 1996; Allwood et al. 2010; Tobia and Aqrawi 2016). In modern marine environment, Y/Ho ratio varies in between 40 and 90 (Bau 1999) whereas volcanic ash has chondritic Y/Ho ratio in between 26 and 28 (Kamber and Webb 2001). The Y/Ho ratios of the Narji limestones vary in between 30.05 and 45.45 (Table 5; Fig. 2) with an average value of 35.68. This suggests that the limestones were deposited in a marine environment, but due to the terrigenous input or due to diagenesis process, the average Y/Ho ratio of the limestones is decreased (Abiding and Calagari 2015; Tobia 2018). This Y/Ho ratio is also very much similar like other Neoproterozoic shallow marine platform carbonates, Bhima limestones, and Rhotas limestones (Table 6).

Ce anomaly–reflection on paleoredox condition

Real and apparent Ce anomalies can be differentiated among each other by using $Pr/Pr^* = [Pr/(0.5\ Ce + 0.5\ Nd)]_{SN}$ (Khelen et al. 2017). If $Pr/Pr^* = 1$, it indicates apparent Ce anomalies due to the over abundance of La. The Ce anomalies are indicated when Pr/Pr* ratio is > 1 or < 1. When Pr/Pr* are > 1, then the Ce anomalies are taken as negative whereas it becomes positive when Pr/Pr* < 1 (Bau and Dulski 1996). In this present study except N3, all the studied samples have Pr/Pr* < 1 (Table 5).

Several studies have been performed on the utilization of Ce anomaly in the marine phase for assuming the paleoceanographic situations (Nath et al. 1997; Hua et al. 2013; Khelen et al. 2017). To resolve the depositional redox condition, Ce anomalies are frequently applied because Ce

Table 6 Average geochemical values of the Narji Limestones compared to the other Proterozoic carbonate rocks of India showing seawater like REE patterns

Elements ratio	Narji Limestone[a]	Shallow marine platform carbonate[b]	Bhima Limestone[c]	Rohtas Limestone[d]
TREE (ppm)	32.81 ± 13.03	3.36 ± 2.55	32.2 ± 13.3	68.87 ± 9.25
Y/Ho	35.38 ± 5.03	35.90 ± 13.25	38.13 ± 21.35	33.30 ± 6.77
Er/Nd	0.16 ± 0.04	0.25 ± 0.17	0.15 ± 0.03	0.08 ± 0.02
Eu/Eu*	0.21 ± 0.27	–	1.51 ± 0.64	0.62 ± 0.05
Ce/Ce*	2.25 ± 0.52	–	0.57 ± 0.08	0.92 ± 0.04
$(La/Yb)_{SN}$	0.56 ± 0.23	0.68 ± 0.47	0.732 ± 0.12	1.31 ± 0.58
$(Nd/Yb)_{SN}$	0.53 ± 0.25	0.65 ± 0.39	0.64 ± 0.08	1.08 ± 0.35
$(Dy/Yb)_{SN}$	1.38 ± 0.16	1.10 ± 0.25	1.20 ± 0.13	1.19 ± 0.14

[a] Present study, $n = 10$

[b] Mazumdar et al. (2003), $n = 15$

[c] Nagarajan et al. (2011), $n = 18$

[d] Sen and Mishra (2015), $n = 7$

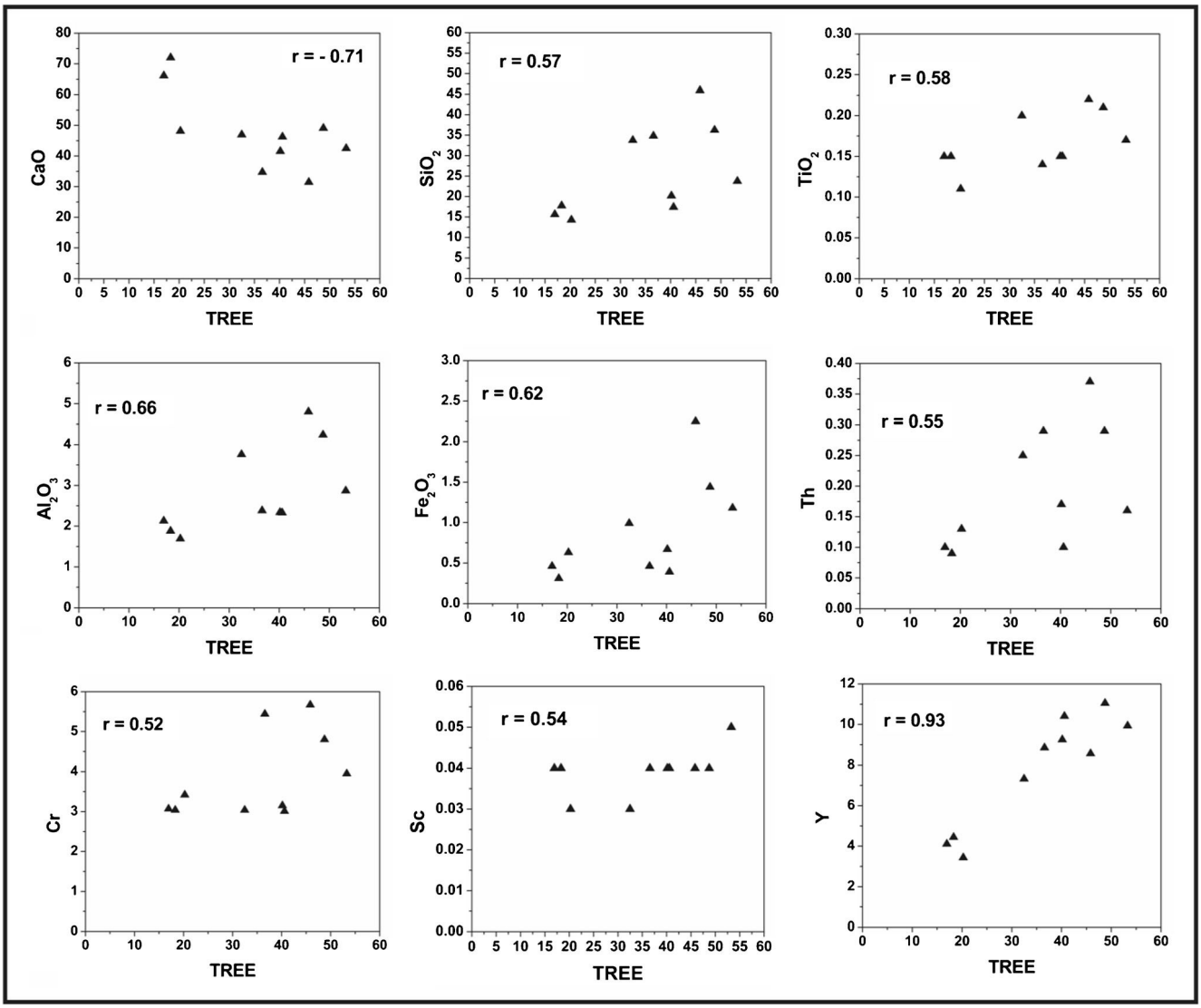

Fig. 7 Bivariate plots showing the relationship of the major oxides (in wt%) and trace elements (in ppm) of Narji limestones respect to ∑REE (in ppm)

valences and solubility vary based on redox condition. Under oxidized condition, Ce^{3+} oxidizes into Ce^{4+} and this results in Ce dissociate from the rest of the REEs. This leads to negative Ce anomaly (Bau and Dulski 1996; Hua et al. 2013). In our study, most of the Narji limestones (except N3) are showing positive Ce anomaly (Ce/Ce* > 1, Table 5) which indicates their deposition was in an anoxic condition.

Elemental ratios in Narji limestones–reflection on paleredox condition

Trace element concentration as well as elemental ratio is frequently used to identify the redox condition of carbonate deposits (Wright et al. 1984; Jones and Manning 1994; Armstrong-Altrin et al. 2015a). U/Th ratio higher than 1.25 indicates suboxic to anoxic depositional environment (Armstrong-Altrin et al. 2003). In this context, the U/Th ratios of the Narji limestones vary in between 1.73 and 4.19 (Table 5, Fig. 2) with an average of 2.60 and this clearly indicates their deposition in suboxic to anoxic environment.

V/(V + Ni) ratio has been also frequently applied by several workers to identify the paleoredox condition of carbonates (Rimmer 2004; Ramos-Vázquez et al. 2017). Carbonate samples whose V/(V + Ni) ratio is greater than 0.5 imply that their deposition is in dysoxic/anoxic condition. In this study, the Narji limestones show higher V/(V + Ni) ratio (0.92 to 0.96, Table 5) and therefore clearly indicates that deposition was in anoxic condition.

Conclusions

The geochemical signatures of the carbonate rocks from Neoproterozoic Narji Formation elucidate significant

knowledge regarding the depositional environment. Within the major oxides, a wide range of Cao (31.45 to 72.03 wt%) and SiO_2 (14.27 to 45.92 wt%) is recorded and the correlation between CaO and SiO_2 reflects negative correlation ($r = -0.62$) in between Ca and Si which clearly indicates that Ca and Si are from different modes of origin. Relatively higher concentration of SiO_2 within these limestones suggests clastic input within the limestones. PAAS normalized REE + Y pattern shows seawater like REE + Y pattern (depleted LREE and enriched to flat HREE) with negative Eu anomaly. The Er/Nd ratio varies from 0.06 to 0.22 with an average 0.17 and this points terrigenous input within the limestones. The Y/Ho ratios vary in between 30.05 and 45.45, and this also suggests that the limestones were deposited in a marine environment but due to the terrigenous input or contamination, the Y/Ho ratio is slightly decreased. Positive Ce anomaly, high U/Th (> 1.25), and V/(V + Ni) (> 0.5) ratios of Narji limestones clearly indicate that their deposition was in a dyoxic to anoxic condition.

Acknowledgements Analyses of the major oxides and trace, REE are carried out in National Centre for Earth Science Studies, Thiruvananthapuram, Kerala and National Geophysical Research Institute, Hyderabad, respectively. Sincere thanks are also being accorded to Dr. Faraj Habeeb Tobia and an anonymous reviewer for their constructive comments.

Funding information This work was financially supported by the Department of Science and Technology (DST), Government of India vide PURSE (Phase-II) program (No. F4/SC/20/15) and University Grants Commission (UGC), New Delhi for the scholarship (UGC Non-Net) given to the first author.

References

Abiding A, Calagari AA (2015) Rare earth element geochemistry of the upper Permian limestone: the Kanigorgeh mining district, NW Iran. Turk J Earth Sci 24:365–382

Allwood AC, Kamber BS, Walter MR, Burch IW, Kanik I (2010) Trace elements record depositional history of an early Archean stromatolitic carbonate platform. Chem Geol 270:148–163

Anand M, Gibson SA, Subbarao KV, Kelley SP, Dickin AP (2003) Early proterozoic melt generation processes beneath the intra cratonic Cuddapah basin. Southern India J Petrol 44:2139–2171

Anaya-Gregorio A, Armstrong-Altrin JS, Machain-Castillo ML, Montiel-Garcia PC, Ramos-Vazquez MA (2018) Textural and geochemical characteristics of late Pleistocene to Holocene fine-grained deep-sea sediment cores (GM6 and GM7), recovered from southwestern Gulf of Mexico. J Palaeogeogr 7:3

Armstrong-Altrin JS, Verma SP, Madhavaraju J, Lee YI, Ramsay S (2003) Geochemistry of Upper Miocene Kudankulam limestones, southern India. Int Geol Rev 45:16–26

Armstrong-Altrin JS, Lee YI, Verma SP, Worden RH (2009) Carbon, oxygen, and strontium isotope geochemistry of carbonate rocks of the Upper Miocene Kudankulam formation, southern India: implications for paleoenvironment and diagenesis. Chemie Erde-Geochem 69(1):45–60

Armstrong-Altrin JS, Madhavaraju J, Sial AN, Kasper-Zubillaga JJ, Nagarajan R, Flores-Castro K, Rodriguez JL (2011) Petrography and stable isotope geochemistry of the cretaceous El Abra limestone (Actopan), Mexico: implication on diagenesis. J Geol Soc India 77: 349–359

Armstrong-Altrin JS, Nagarajan R, Madhavaraju J, Rosales-Hoz L, Lee YI, Balaram V, Cruz-Martinez A, Avila-Ramirez G (2013) Geochemistry of the Jurassic and upper cretaceous shales from the Molango region, Hidalgo, eastern Mexico: implications for source-area weathering, provenance, and tectonic setting. Compt Rendus Geosci 345(4):185–202

Armstrong-Altrin JS, Machain-Castillo ML, Rosales-HoZ L, Carranza-Edwards A, Sanchaz Cabeza JA, Ruiz-Fernan AC (2015a) Provenance and depositional history of continental slope sediments in the South western Gulf of Mexico unraveled by geochemical analysis. Cont Shelf Res 95:15–26

Armstrong-Altrin JS, Nagarajan R, Balaram V, Natalhy-Pineda O (2015b) Petrography and geochemistry of sands from the Chachalacas and Veracruz beach areas Western Gulf of Mexico, Mexico: constraints on provenance and tectonic setting. J S Am Earth Sci 64:199–216

Bau M (1996) Controls on the fractionation of isovalent trace elements in magmatic and aqueous systems: evidence from Y/ho, Zr/Hf, and lanthanide tetrad effect. Contrib Mineral Petrol 123:323–333

Bau M (1999) Scavenging of dissolved yttrium and rare earths by precipitating Fe oxyhydroxide: experimental evidence for Ce oxidation, Y-ho fractionation, and lanthanide tetrad effect. Geochim Cosmochim Acta 63:67–77

Bau M, Dulski P (1996) Distribution of yttrium and rare-earth elements in the Penge and Kuruman iron-formations, Transvaal Supergroup, South Africa. Precambrian Res 79:37–55

Bertram CN (2012) Sedimentology, age and stable isotope evolution of the Kurnool group Cuddapah Basin. Dissertation, The University of Adelaide

Chakrabarti G, Shome D, Kumar S, Stephens GM III, Kah LC (2014) Carbonate platform development in a Paleoproterozoic extensional basin, Vempalle formation, Cuddapah basin, India. J Asian Earth Sci 91:263–279

Chen S, Gui H, Sun L (2014) Geochemical characteristics of REE in the late neo-proterozoic limestone from the northern Anhui Province ,China. Chin J Geochem 33:187–193

Condie KC (1991) Another look at rare earth elements in shales. Geochim Cosmochim Acta 55:2527–2531

Condie KC, Dengate J, Cullers RL (1995) Behavior of rare earth elements in a paleoweathering profile on granodiorite in the front range, Colorado, USA. Geochim Cosmochim Acta 59(2):279–294

Crawford AR, Compston W (1973) The age of the Cuddapah and Kurnool systems, southern India. J Geol Soc Austr 19:453–464

De Baar HJW, German CR, Elderfield H, Van Gaans P (1988) Rare earth element distributions in anoxic waters of the Cariaco trench. Geochim Cosmochim Acta 52:1203–1219

Devi KR, Duarah BP (2015) Geochemistry of Ukhrul limestone of Assam-Arakan subduction basin, Manipur, Northeast India. J Geol Soc India 85:367–337

Folk R (1965) Some aspects of recrystallization in an ancient limestone. In: Pray LC, Murrey RC (eds) Dolomitization and limestone diagenesis, Society of Economic Paleontology Mineralogy Special Publication, vol 13, pp 14–48

French JE, Heaman LM, Chacko T, Srivastava RK (2008) 1891–1883 ma southern Bastar–Cuddapah mafic igneous events India: a newly recognized large igneous province. Precambrian Res 160:308–322

Fu X, Wang J, Zeng Y, Tan F, He J (2011) Geochemistry and origin of rare earth elements (REEs) in the Shengli River oil shale, northern Tibet, China. Chem Erde 71(1):21–30

German CR, Elderfield H (1989) Rare earth elements in Saanich inlet, British Columbia, a seasonally anoxic basin. Geochim Cosmochim Acta 53:2561–2571

Hernández-Hinojosa V, Montiel-García PC, Armstrong-Altrin JS, Nagarajan R, Kasper-Zubillaga JJ (2018) Textural and geochemical

characteristics of beach sands along the western Gulf of Mexico, Mexico. Carpathian J Earth Environ Sci 13(1):161–174

Hua G, Yuansheng D, Lian Z, Jianghai Y, Hu H (2013) Trace and rare earth elemental geochemistry of carbonate succession in the middle Gaoyuzhuang formation, Pingquan section: implications for early Mesoproterozoic Ocean redox conditions. J Palaeogeogr 2(2):209–221

Jones B, Manning DC (1994) Comparison of geochemical indices used for the interpretation of paleo-redox conditions in ancient mudstones. Chem Geol 111(1–4):111–129

Kale V (2016) Proterozoic basins of Penninsular India status within the global Proterozoic system. Proc Indian Natl Sci Acad 82(3):461–477

Kamber BS, Webb GE (2001) The geochemistry of late Archaean microbial carbonate: implications for ocean chemistry and continental erosion history. Geochim Cosmochim Acta 65:2509–2525

Khelen AC, Manikyamba C, Ganguly S, Singh TD, Subramanyam KSV, Ahmad SM, Reddy MR (2017) Geochemical and stable isotope signatures of Proterozoic stromatolitic carbonates from the Vempalle and Tadpatri formations, Cuddapah Supergroup, India: implications on paleoenvironment and depositional conditions. Precambrian Res 298:365–384

Lokesh Bharani P (2015) Sedimentology provenance and depositional environments of Kurnool group palnad sub basin Andhra Pradesh South India. Ph.D. dissertation, University of Mysore, Karnataka, India

Madesh P, Lokesh Bharani P, Baby Shwetha S (2012) Study of microstylolite from carbonate rocks of Kurnool group, Andhra Pradesh, South India. Indian J Appl Res 1(2)

Madhavaraju J, Lee YI (2009) Geochemistry of the Dalmiapuram formation of the Uttatur group (early cretaceous), Cauvery Basin, southeastern India: implications on provenance and paleo-redox conditions. Rev Mex Cienc Geol 26:380–394

Madhavaraju J, Loser H, Lee YII, Santacruz RL, Pi-Puig T (2016) Geochemistry of lower cretaceous limestones of the Alisitos formation, Baja California, México: implications for REE source and paleo-redox conditions. J S Am Earth Sci 66:149–165

Mazumdar A, Tanaka K, Takahashi T, Kawabe I (2003) Characteristics of rare earth element abundances in shallow marine continental platform carbonates of late Neoproterozoic successions from India. Geochem J 37:277–289

Mitra R, Chakrabarti G, Shome D (2018) Geochemistry of the Palaeo-Mesoproterozoic Tadpatri shales, Cuddapah Basin, India: implications on provenance, paleoweathering and paleoredox conditions. Acta Geochem 37(5):715–733

Mouli Chandra A, Hanumanthu RC, Rao Jagadishwara R (2012) Conflicting Land-use Practises in the Narji Limestone Belt in YSR District,Andhra Pradesh (AP),India. Earth Sci India 5(3):1–9

Nagaraja Rao BK, Rajurkar ST, Ramalingaswami G, Ravindra BB (1987) Stratigraphy, structure and evolution of Cuddapah Basin. Purana basins of peninsular India. Geol Soc India Bangalore Bull 6:33–86

Nagarajan R, Madhavaraju J, Armstrong-Altrin JS, Nagendra R (2011) Geochemistry of Neoproterozoic limestones of the Shahabad formation, Bhima Basin, Karnataka, southern India. Geosci J 15(1):9–25

Nath BN, Bau M, Ramalingeswara Rao B, Rao CHM (1997) Trace and rare earth elemental variation in Arabian Sea sediments through a transect across the oxygen minimum zone. Geochim Cosmochim Acta 61(12):2375–2388

Patranabis-Deb S, Saha D, Tripathy V (2012) Basin stratigraphy, sea-level fluctuations and their global tectonic connections—evidence from the Proterozoic Cuddapah Basin. Geol J 47:263–283

Ramkumar M (2004) Lithology, petrography, microfacies, environmental history and hydrocarbon prospects of the Kallankurichchi formation (upper cretaceous, Ariyalur group, South India). Palaeont Stratigr. Facies 12:77–100

Ramos-Vázquez MA, Armstrong-Altrin JS, Rosales-Hoz L, Machain-Castillo ML, Carranza-Edwards A (2017) Geochemistry of deep-sea sediments in two cores retrieved at the mouth of the Coatzacoalcos River delta, western Gulf of Mexico, Mexico. Arab J Geosci 10(6):148

Rimmer SM (2004) Geochemical paleoredox indicators in Devonian-Mississippian black shales, central Appalachian Basin (USA). Chem Geol 206:373–391

Sen S, Mishra M (2015) Geochemistry of Rohtas limestone from Vindhyan Supergroup, Central India: evidences of detrital input from felsic source. Geochem Int 53(12):1107–1122

Shaltami OR (2015) Geochemistry of the Shahat marl member, Wadi Az Zad, Al Jabal Al Akhdar, NE Libya. Arab J Earth Sci 2(3):23–39

Sherman CE, Fletcherher CH, Rubin KH (1999) Marine and meteoric diagenesis of Pleistocene carbonates from a nearshore submarine terrace, Oahu, Hawaii. J Sediment Res 69(5):1083–1097

Sholkovitz ER (1990) Rare earth elements in marine sediments and geochemical standards. Chem Geol 88:333–347

Singh AK, Tewari VC, Sial AN, Khanna PP, Singh NI (2016) Rare earth elements and stable isotope geochemistry of carbonates from the mélange zone of Manipur ohiolitic complex, indo-Myanmar Orogenic Belt, northeastern India. Carbonates Evaporites 31(2): 139–151

Taylor SR, McLennan SM (1985) The continental crust: its composition and evolution. Blackwell Scientific, Oxford, p 312

Tobia FH (2018) Stable isotope and rare earth element geochemistry of the Baluti carbonates (Upper Triassic), Northern Iraq. Geosci J. https://doi.org/10.1007/s12303018-0005-4

Tobia FH, Aqrawi AM (2016) Geochemistry of rare earth elements in carbonate rocks of the Migra Mir formation (lower Triassic), Kurdistan region, Iraq. Arab J Geosci 9:259

Worash G, Valera R (2002) Rare earth element geochemistry of the Antalo Supersequence in the Mekele outlier (Tigray region, northern Ethiopia). Chem Geol 182:395–407

Wright J, Seymour RS, Shaw HF (1984) REE and Nd isotopes in conodont apatite: variations with geological age and depositional environment. Geol Soc Am Spec Pap 196:325–340

Zachariah JK, Bhaskar Rao YJ, Srinivasan R, Gopalan K (1999) Pb, Sr and Nd isotope systematics of uranium mineralised stromatolitic dolomites from the Proterozoic Cuddapah Supergroup, South India: constraints on age and provenance. Chem Geol 162:49–64

Original Article | Published: 03 November 2020

Neoproterozoic sedimentation and depositional environment: an example from Narji Formation, Cuddapah Basin, India

Adrika Roy ✉, Gopal Chakrabarti & Debasish Shome

Journal of Sedimentary Environments **5**, 559–574 (2020) | Cite this article

358 Accesses | **1** Citations | Metrics

Abstract

In the west-central part of Kurnool sub-basin of Cuddapah Basin, around Betamcherla–Bagannapali area, the Neoproterozoic Narji Formation rocks (Kurnool Group) of Cuddapah Supergroup are deposited. Sedimentary facies analysis including sedimentary structures and petrographic analysis of the studied samples have been carried out for understanding the depositional environment of the studied formation during Neoproterozoic time period. Sedimentological investigation of the studied formation rocks reveals intertidal-to-subtidal facies associations consisting of six lithofacies such as quartzite bearing massive purple limestone, laminated limestone, calcareous shale, heterolithic, massive whitish grey limestone and intra-formational conglomerate. Sedimentary deformation structures such as load structures and slump structures (micro-faults and folds) indicate perturbation and basin subsidence. Presence of pyrite (reducing condition) and glauconite also indicates shallow marine sediments (at depths of 50–300 m). Overall, the entire basin-fills are inferred to be deposited in shallow marine tidal flat area with occasional deep burial condition in an isolated basin with little clastic influx. Comparing with other coeval successions of Narji Formation lithology, it can be concluded that similar type of depositional milieu prevailed over the globe at early Neo-Proterozoic time during the formation of Rodinia.

Neoproterozoic sedimentation and depositional environment: an example from Narji Formation, Cuddapah Basin, India

Adrika Roy, Gopal Chakrabarti & Debasish Shome

Journal of Sedimentary Environments

ISSN 2662-5571
Volume 5
Number 4

J. Sediment. Environ. (2020) 5:559-574
DOI 10.1007/s43217-020-00035-2

Springer

Journal of Sedimentary Environments (2020) 5:559–574
https://doi.org/10.1007/s43217-020-00035-2

ORIGINAL ARTICLE

Neoproterozoic sedimentation and depositional environment: an example from Narji Formation, Cuddapah Basin, India

Adrika Roy[1] · Gopal Chakrabarti[2] · Debasish Shome[1]

Received: 10 August 2020 / Revised: 15 October 2020 / Accepted: 19 October 2020 / Published online: 3 November 2020

Abstract

In the west-central part of Kurnool sub-basin of Cuddapah Basin, around Betamcherla–Bagannapali area, the Neoproterozoic Narji Formation rocks (Kurnool Group) of Cuddapah Supergroup are deposited. Sedimentary facies analysis including sedimentary structures and petrographic analysis of the studied samples have been carried out for understanding the depositional environment of the studied formation during Neoproterozoic time period. Sedimentological investigation of the studied formation rocks reveals intertidal-to-subtidal facies associations consisting of six lithofacies such as quartzite bearing massive purple limestone, laminated limestone, calcareous shale, heterolithic, massive whitish grey limestone and intra-formational conglomerate. Sedimentary deformation structures such as load structures and slump structures (microfaults and folds) indicate perturbation and basin subsidence. Presence of pyrite (reducing condition) and glauconite also indicates shallow marine sediments (at depths of 50–300 m). Overall, the entire basin-fills are inferred to be deposited in shallow marine tidal flat area with occasional deep burial condition in an isolated basin with little clastic influx. Comparing with other coeval successions of Narji Formation lithology, it can be concluded that similar type of depositional milieu prevailed over the globe at early Neo-Proterozoic time during the formation of Rodinia.

Keywords Neoproterozoic · Facies · Diagenesis · Narji limestone · Depositional environment

1 Introduction

The Neoproterozoic Era (1000–541 Ma) connects the less oxygenated and impoverished fossil remains to the Mesoproterozoic times and the dominantly oxic and much diverse complex flora and fauna that dominated Phanerozoic Era. The earth experienced in this critical time climatic and environmental upheaval as manifested by the snowball earth, which is marked by two panglaciation: Sturtian (659–717 Ma) and Marinoan (635–645 Ma) with glacial interlude in between (Spence et al. 2016). The earth has also experienced a single cycle of supercontinental (Rodinia) rifting introducing protracted period of extreme climatic oscillation and subsequent reformation (Greater Gondwana or Pannotia; Young 2013). The early Neoproterozoic time (Tonian) is very important at this backdrop as it encompasses the assembly of the components and subsequent rifting of Rodinia and also the radical climate and environmental change leading to snowball earth as manifested by the subsequent Cryogenian glaciations.

The Cuddapah Basin of the southern India is considered as one of the largest Proterozoic intracratonic basin, which documented extensive development of mostly marine carbonates and clastic sediments. The Neo-Proterozoic time within Cuddapah Basin is represented by the Kurnool Group and the Narji Formation (early Neoproterozoic) is a part of this Kurnool Group. This lithology sits on over basal siliciclastic Banganapalli Formation (Table 1; Fig. 1a and b). The rifted Cuddapah Basin results from crustal doming, erosion and subsidence (Chakraborty 2000; Chakrabarti and Shome 2007) similar to other Proterozoic basins of Peninsular India. The Movement in the Central Indian Mobile Belt of Central Indian Tectonic Zone, leads to a complex deformation pattern, metamorphism, emplacement of igneous bodies, etc., resulting in development of intracratonic graben,

Communicated by M. V. Alves Martins

✉ Adrika Roy
adrika.geology@gmail.com

[1] Department of Geological Sciences, Jadavpur University, Kolkata 700032, India

[2] Education Directorate, Government of West Bengal, Kolkata 700091, India

Table 1 Stratigraphy of the Cuddapah Basin (Nagaraja Rao et al. 1987)

Group	Formation	Lithology	Age
Kurnool	Nandyal (50–100 m)	Shale/Limestone	Neoproterozoic
	Koilkuntala (15–50 m)	Limestone with shale	
	Paniam (10–35 m)	Quartzite	
	Owk (10-15 m)	Shale	
	Narji (100–200 m)	Massive Limestone, Flaggy Limestone	
	Banganapalli (10–15 m)	Quartzite with conglomerate	
Cuddapah supergroup			
	Unconformity		
	Srisailam (300 m)	Pebbly gritty Quartzite, Heterolithic Shales and stone	Mesoproterozoic
Nallamalai	Unconformity		
	Cumbum (~Pullampet Shale)	Shale, Dolomitic limestone, Quartzite	
	Bairenkonda (~Nagari Quartzite) (5500 m)	Pebbly and gritty Quartzite, Heterolithic Shales and stone	
Chitravati	Unconformity	(2000 m)	
	Gandikota (300 m)	Quartzite, Pebble beds	Mesoproterozoic
	Tadpatri (4600 m)	Shale, Quartzite, Stromatolitic dolomite with mafic flows, Sills and Dykes	
	Pulivendla (1–75 m)	Conglomerate, Quartzite	
Papaghni	Unconformity		
	Vempalle (1900 m)	Stromatolitic dolomite, Shale, Basic flows and intrusive	Palaeoproterozoic
	Gulcheru (30–210 m)	Conglomerate, Feldspathic sandstone and quartzite	
Dharwar craton	Unconformity		Archean

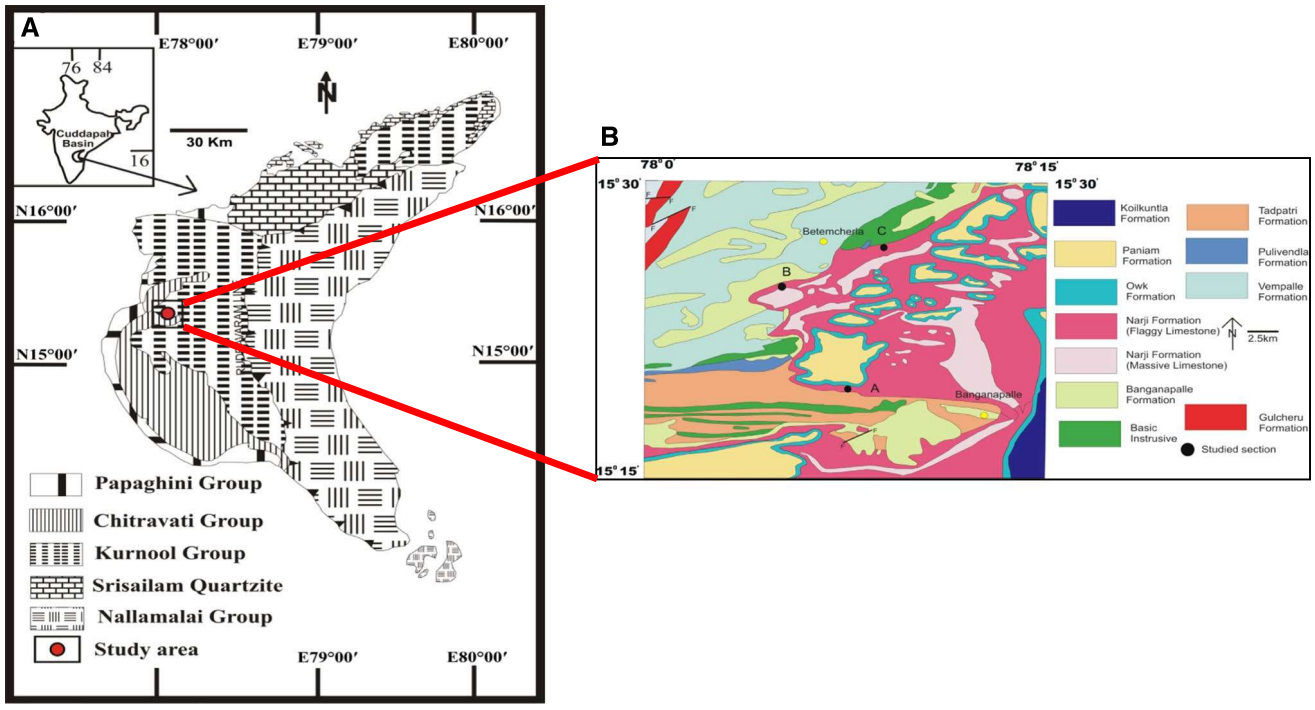

Fig. 1 Geological maps of the study area **a** Generalized geological map of the Cuddapah Basin (modified after Geological survey of India 1,2 million scale map, 1998); **b** Detail of the west -central Cuddapah Basin showing location of the measured section investigated in this study (modified after Survey of India Quadrangle map number 57I,1981; 1,250,000 scale)

which reactivated during sedimentation and accommodates huge thickness (~ 12 km) of Neo-Proterozoic sediments (Choudhuri et al. 2002; Chakrabarti and Shome 2007). The Neo-Proterozoic Narji Formation is mainly developed in a carbonate platform of marine environment and comprises a thick succession of massive to well-laminated limestone with minor siliciclastic layers mainly of calcareous shale (Patranabis Deb et al. 2012; Chakrabarti et al. 2014).

Previous works on this formation (Saha and Chakraborty 2003; Gupta et al. 2010; Chetty 2011; Perrin et al. 2011; Banerjee et al. 2012; Patranabis Deb et al. 2012; Saha and Tripathy 2012; Gopakumar and Waghmare 2016) are focused on sedimentations, tectonics and deformation. Detailed facies investigation leading to paleoenvironmental reconstruction of the Narji Formation was realized, which has not been studied until now. This paper describes reconstruction of paleoenvironment of the Narji sediments based on facies attributes as well as petrographic data to better visualize the development of a carbonate platform in a tectonically active early Neoproterozoic marine setting consequent to rifting to assembly and rifting of Rodinia, along with prevailing marine system during early Neoproterozoic time prior to the onset of Cryogenian glaciation.

2 Geologic setting of the Kurnool basin

In Peninsular India, there exist three large and six small sized Proterozoic intracratonic sedimentary basins (Kale 1991). Out of these nine, the crescent-shaped Cuddapah basin of the southern India is the second largest which is developed over the Eastern Dharwar Craton (Kale et al. 2020). The Kurnool sub-basin of Cuddapah Basin was formed due to gravity-induced block faulting which induced a formation of a basin depocentre (Singh and Mishra 2002). The basin-fills subsidence is controlled by deep faults (Meijerink et al. 1984; Chakraborty et al. 2010). After deposition, there has been eastward thrusting movement of deep faults, concomitant with epeirogenic movements, folding and metamorphism in the eastern part of the basin (Chakraborty et al. 2010).

The strata within Cuddapah Basin include the lower Cuddapah Supergroup and the unconformably overlying upper Kurnool Group (Table 1). The Cuddapah Supergroup of Palaeo- to Meso-proterozoic age is mainly comprised of three sub-groups namely Papaghni, Chitravati and Nallamalai groups (Nagaraja Rao et al. 1987) and onlaps the gneissic basement with a major unconformity that extends over the entire Papaghni Sub Basin (Table 1; Fig. 1a) (Saha et al. 2009; Mitra et al. 2018). The Kurnool Group of rocks of middle to late Proterozoic (980–520 Ma) is more than 500 m thick and is formed in two separate sub-basins namely Kurnool Sub-basin and the Palnad Sub-basin. The Kurnool sub-basin is situated in the western part in Kurnool districts (Fig. 1a and b), and the Palnad sub-basin in the northeast covering parts of Guntur, Nalgonda and Krishna districts (Nagaraja Rao et al. 1987). It is divided into six formations namely Banganapalle Quartzite, Narji Limestone, Owk Shale, Paniam Quartzite, Koilkuntla Limestone and Nandyal Shale; comprising two carbonate platform units and two intervals of sandstones and shales (Table 1). The eastern part of the basin is generally unmetamorphosed except few parts of Kurnool Group whereas the western part show deformation in the form of Nallamalai fold thrust belt (Meijerink 1984).

The Narji Limestone within the Kurnool Sub-Basin is deposited conformably over the clastic rocks of the Bagannapali Formation. The lower portion of the Narji Formation mainly consists of massive grey limestone with occasional development of siliceous-rich layers which are followed by siliceous pink and purple laminated limestone with thin lenticular lenses of gritty ferruginous sandstone (Patranabis Deb et al. 2012). The occurrence of pyrite and chert bearing bluish-grey to dark grey high-graded massive limestone along with alternating laminated siliceous limestone layer is also very common within the Narji Formation. The development of thin and discrete beds of intraformational conglomerate is also recorded within the Narji Limestone (Patranabis Deb et al. 2012). The massive and the laminated units show symmetrical distribution throughout the sections until they show a gradational contact with the yellowish Owk shale towards the top. The layers are mostly separated by paleokarstic surfaces.

3 Age of the Narji formation

There is no record to date about direct dating of Narji Formation sediment. The diamonds in the basal conglomerates of the Banganapalle Quartzite (Kurnool Group), are believed to be derived from 1050 Ma kimberlites, west of the Cuddapah Basin, or reports of a 980 Ma dolerite intruding the Kurnool rocks are interpreted to be of Neoproterozoic age (e.g. Ramakrishnan and Vaidyanadhan 2008; Saha and Tripathy 2012) reported the discovery of felsic tuff beds in the Owk Shale (Holland, 1913; Ramakrishnan and Vaidyanadhan 2008) in the mid-late Proterozoic Kurnool Group in the Cuddapah basin (Saha and Tripathy 2012). Combined, we can infer Narji Formation lying over Banganapalle Quartzite may be of early Neo-Proterozoic age.

4 Materials and methods

Three sections were chosen for sedimentological investigation (Fig. 1b) within the Narji Formation. The first section is along the road cut section (A) (15°18′ 45.00″ N,

78°07′ 35.76″ E) of Patapadu-Yaganti hills, located around 11Km from the town of Banaganapalle in Kurnool District. The second section is around Betamcherla hills (B) (15°25′18.49″ N, 78°05′6.20″ E) and the third section is the Kottala hills (C) (15°27′36.68″ N, 78°08′34.30″ E). The limestone quarry of Betamcherla section is about 21 km NW side and the road cut Kottala section is about 18 km NW from the town of Banaganapalle. Bed by bed measurement and field observation of the vertical sections gives us an idea of vertical lithological variation. About 150 rock samples are collected from these sections and analysed. Preparation of thin section is done from these samples. Then, these thin sections are further examined using standard polarized petrographic microscope. This area is mapped, logged and sampled accordingly. The diagenesis along with petrography is studied and is based on rock types, structural, and textural features (bedding type, texture, grain size and shape, primary sedimentary structures) of the basin. This gives an idea about the depositional environment. Measured sections (Fig. 2) provide critical information on the spatial and

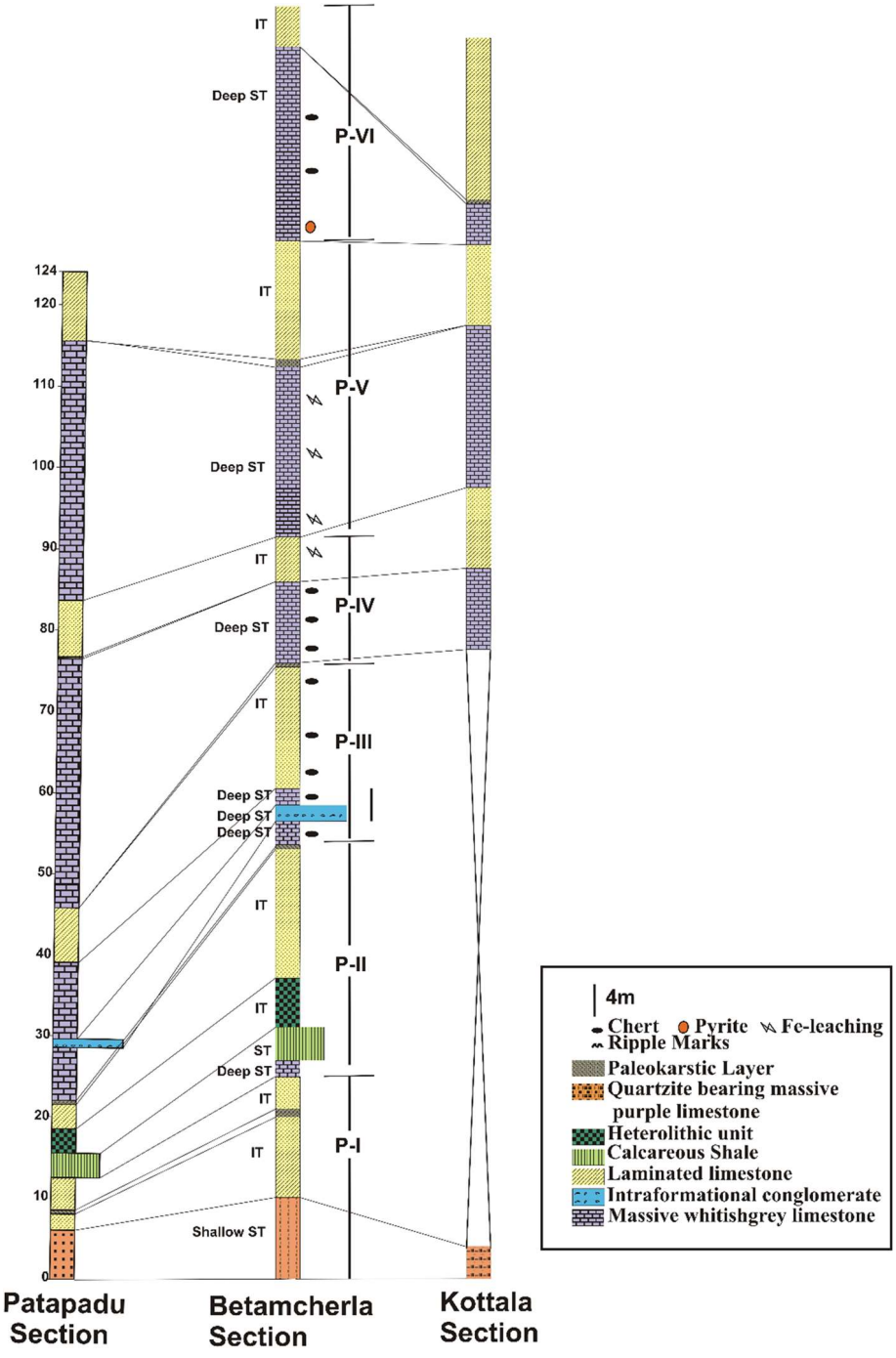

Fig. 2 Litholog showing measured stratigraphic section of the Narji Formation

vertical variation of lithofacies collected at regular intervals leading to characterisation of depositional setup. The geochemistry data of the Narji limestones obtained by Roy et al. (2018) are also used in this work to complement the interpretation of the new data of this work.

5 Results

5.1 Facies analysis

The sedimentological, mineralogical and petrographical analyses performed on the Narji rocks reveal the presence of six lithofacies, vis, quartzite bearing massive purple limestone, laminated limestone, calcareous shale, heterolithic, massive whitish grey limestone and intra-formational conglomerate (Table 2). The detailed descriptions of these facies with their indicative depositional environment are described below:

5.1.1 Quartzite-bearing massive purple limestone facies (N-1)

This is the lowermost facies resting on different underlying lithology at different places within the study area. At Betamcherla, it overlies the Banganapalli Quartzite with gradational contact. But in the Yaganti-Patapaduareathis facies (Fig. 3a) rests unconformably on the Tadpatri Shales. In the Kottala area, non-conformable contact with igneous dyke is observed. This coarse-grained facies is featured by bifurcating symmetrical ripple (R.I. = 5–8) (Fig. 3b) and syneresis cracks. At several places, thin lenses and stringers of sandstone (Fig. 3c) have been noted within the micritic matrix. The lower 3–4 m of the succession is quartzitic intercalation with gradually decreasing siliceous layers and increasing massive beds towards the top. The rocks are well jointed. This variety of limestone is commonly associated with numerous stylolitic structures in both macroscopic and microscopic levels. Some stylolites are filled with clay (Fig. 3d). Under microscope euhedral to subhedral calcite grains forms a hypidiotopic texture.

5.1.2 Interpretation

The overall presence of coarse-grained detrital material within this facies indicates deposition in moderate-to-high-energy environment. Bifurcating ripple marks are generated by to and from action of the water agitated by tides and waves, probably in shallow-marine condition (Chakrabarti and Shome 2007; Panja et al. 2017). The syneresis cracks frequently associated with calcareous sediment indicate a swelling in the soft substrate which is a result of salinity changes in the marine environment (Chakrabarti and Shome 2007). The development of this crack system may be due to shrinkage under sub aerial condition upon the loss of water in the subtidal zone (Chakrabarti and Shome 2007). Clay (clastic) lamination within the micrite indicates deposition in low-to-moderate energy shallow intertidal to subtidal environment (Flugel 2010; Ali et al. 2013; Hashmie et al. 2016).

5.1.3 Laminated limestone facies (N-2)

It is grey to dark grey-coloured laminated limestone with thickness ranging from 1 to 7 m (Fig. 4a) having undulatory contact with underlying and overlying lithology. The laminations are horizontal to slightly wavy (Fig. 4b), mostly lined with ferruginous and clayey material. They are less than 1 cm thick and are mostly parallel to sub-parallel. These laminations (Fig. 4c) have distinct colour and composition and can be easily distinguished from each other. The iron leaching is commonly observed on the surface. Planar (Fig. 4e), trough (Fig. 4e), hummocky cross-bedding

Table 2 Summarized table of the facies recognized in the studied sections of the Narji Formation, Cuddapah Basin

Facies code	Facies name	Lithology	Sedimentary structures	Trends
N-1	Quartzite bearing massive purple limestone	Massive Limestone with pockets of sandstone	Stylolites, ripples, synaeresis cracks	Laterally continuous
N-2	Laminated limestone	Limestone with lamination of fine grained terrigenous silt	Lamination, Planar and trough cross bed	Laterally continuous
N-3	Calcareous Shale	Clay with crudely laminated carbonate mud and some detrital quartz and sparite	Microstylolite	Laterally continuous
N-4	Heterolithic Facies	Mud and clay intermixed layer with detrital materials and associated with ferruginous and quartz vein	Veins, load and slump structure	Laterally continuous
N-5	Massive whitish grey limestone	Massive limestone	chert nodules, concretion	Laterally continuous
N-6	Intra-formational conglomerate facies	Clasts of micrite within sandstone	Crude alignment of tabular clasts	Laterally discontinuous

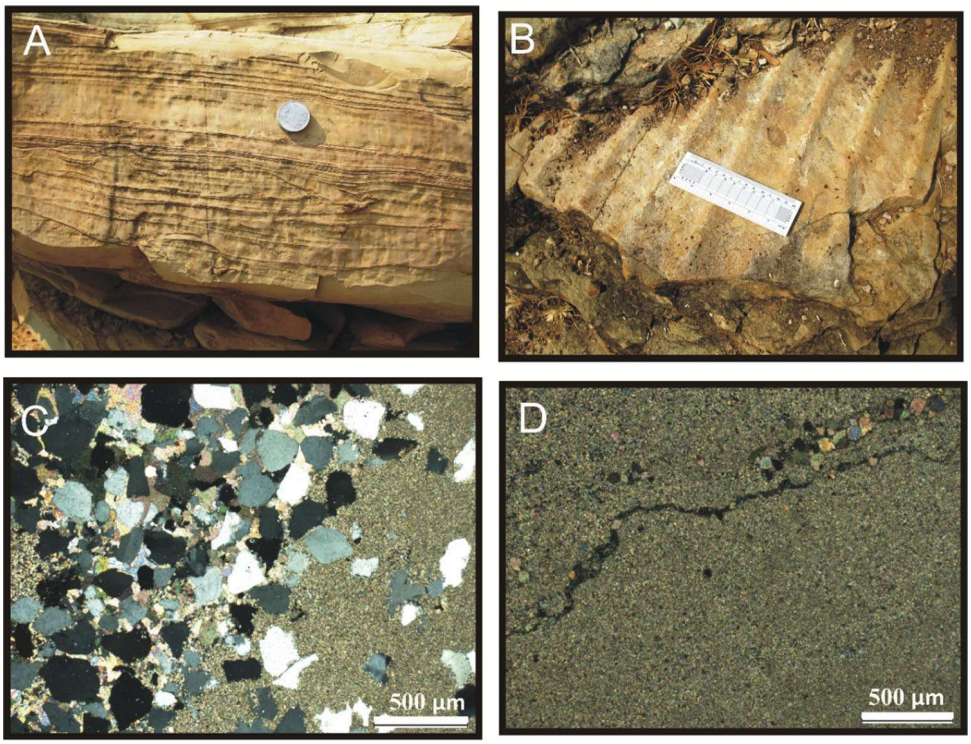

Fig. 3 Quartzite bearing massive purple limestone Quartz dominated limestone layer mostly present in the lower most part of the strata. **b** Symmetrical ripple mark in plan view **c** Pockets of sandstone within limestone encountered at the lower level **d** Clay lithified stylolite within the limestone indicating dewatering and tectonic disturbance

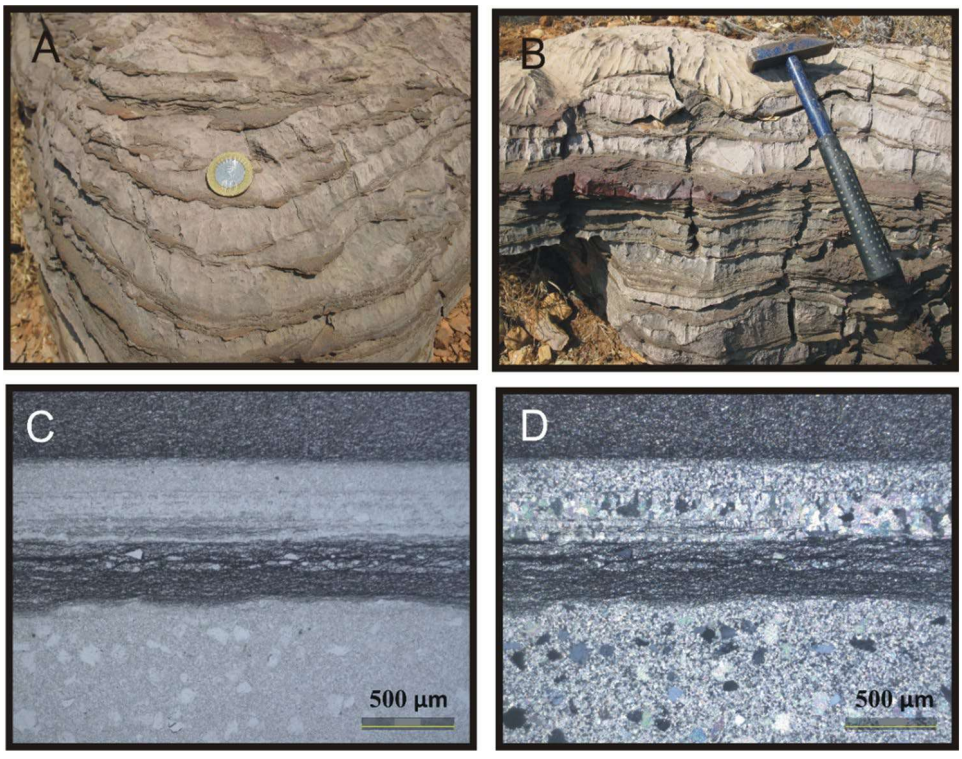

Fig. 4 laminated limestone: **a** Straight and wavy laminated limestone characterized by irregularly undulated layers. **b** Lamination of dark gray and light streaks of clay within massive micrite limestone characterized by alternating lamina couplets with elephant skin structure. **c** Alternate dark coloured clay and light coloured carbonate layer have distinct colour and composition and can be easily distinguished from each other. **d** Thin section showing course sparite grains and cement filling up the pore spaces

((Fig. 4f). and pinch and swell structure (Fig. 4g) are also observed. The height and length of individual trough ranges between 20 and 30 cm and 2 and 2.5 m, respectively. This facies has dominance of clay and micrite with coarse microsparitic mosaic of equant crystal in some samples observed under microscope. The lamination also contains glauconite along with minor amount of fine-grained terrigenous silt in the lowermost part. Veins of sparite within micrite are also identified in some samples under microscope. Some samples show coarse sparite grains (Fig. 4d) which are initially

replaced by micrite and patchy distribution of neomorphic cement filling up the inter-particle spaces.

5.1.4 Interpretation

High amount of suspension fall out along with carbonate precipitation indicate low-energy quiet environment. The trough cross-bedding indicates migrations of megaripples/sand waves. The troughs and hummocky were probably formed by oscillatory motion of storm waves affecting the bottom (Hamblin and Walker 1979; Ahmad et al. 2017). Pinch and swell structure is formed in layered, ductile rocks due to layer-parallel extension in which thickening takes place due to lateral contraction and thinning due to stretching (Knaust 2002). The thick units of limestone represent time of increased carbonate precipitation while clay indicates terrigenous influx (Chakrabarti et al. 2014; Hersi et al. 2015). The lamination may have been deposited from suspension by clay or colloidal particles or under the influence of tidal currents (Komatsu et al. 2014). Occurrence of glauconite indicates shallow marine environment (Naik et al. 2016). This interlaminated clay within limestone may be formed by tidal processes, possibly due to seasonally controlled fluctuations of sediment supply (Ahmad et al. 2015). Hence, this facies is probably deposited by suspension activity in shallow, quiet water with the periodic influx of the tidal currents and waves, in an intertidal environment (Patranabis Deb 2005).

5.1.5 Calcareous shale facies (N-3)

The calcareous shale facies is reddish-brown in colour, almost 3 m in thickness, brittle and micaceous in nature. It is positioned in the lowermost part of the studied sections having well defined fissility plane (Fig. 5a). Microstylolitic cracks are found (Fig. 5b). This facies is dominated mostly of calcareous clay with crudely laminated carbonate mud and some detrital quartz and sparite. The clay mineral shows crude schistosity wrapping around detrital quartz grains (Fig. 5c) and sparite (Fig. 5d).

5.1.6 Interpretation

Overall finer grain size indicates deposition of this lithology in comparatively low energy environment. Further mud and clay indicate deposition in low-energy anoxic environment through suspension and deposition (Srivastava and Singh 2017). Microstylolite reflects mechanical compaction with pressure dissolution processes (Garrison and Kenneday 1977; Bathurst 1987; Forte and Palma 2002). This facies seems to be mainly deposited in calm and low-energy environment of shallow subtidal environment (AI-Juboury et al. 2015).

5.1.7 Heterolithic facies (N-4)

This facies is laterally continuous, highly weathered (Fig. 6a) and found in association with mud and clay intermixed with

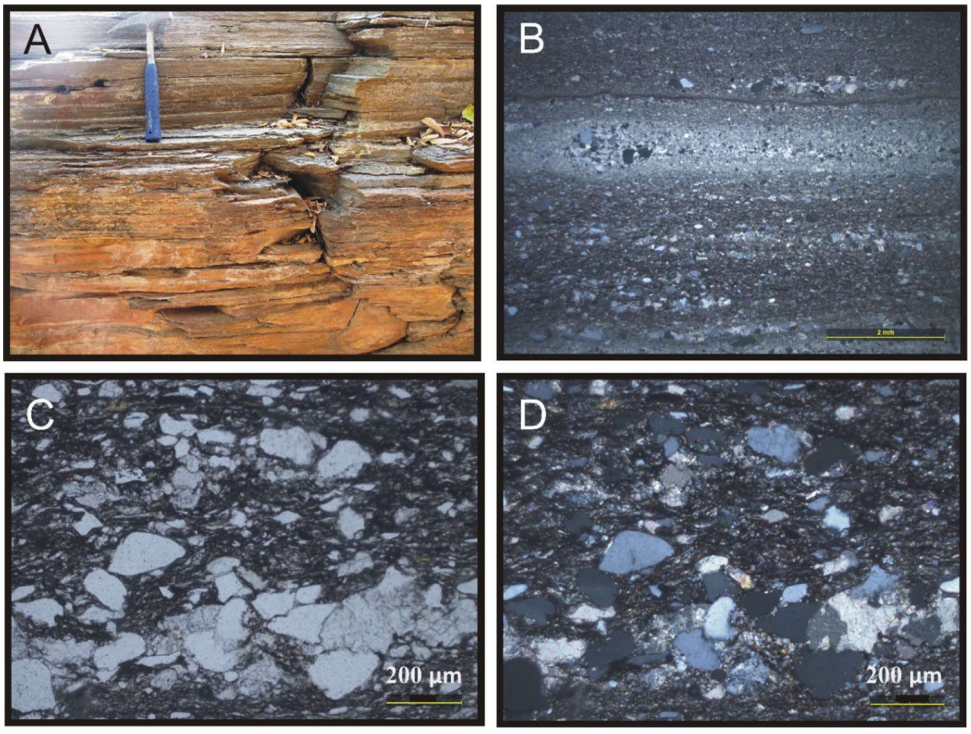

Fig. 5 calcareous shale: **a** thinly laminated calcareous shale within the lowermost part of the Narji Formation. **b** Very fine grained carbonate cemented calcareous shale. **c** The clay mineral show crude schistosity wrapping around detrital quartz grains and **d** sparite

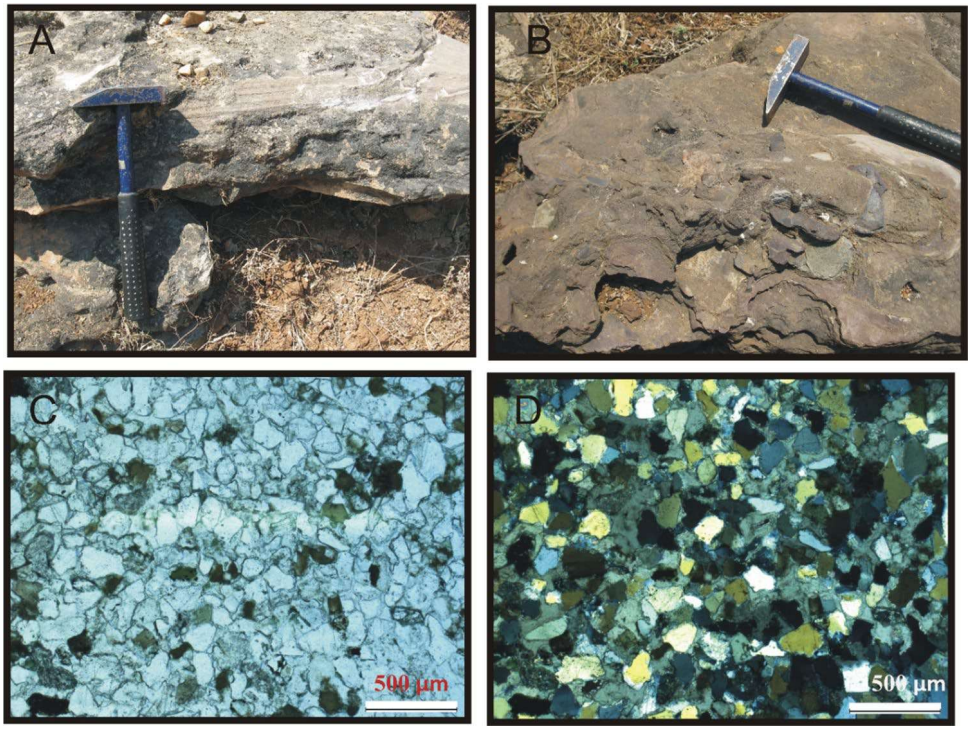

Fig. 6 Heterolithic facies **a** and **b** Intermixing of clay and mud without any distinct laminations. **c** and **d** the boundaries of the grains are mostly corroded by iron solutions

each other without any distinct lamination (Fig. 6b). Diagenetic concretion is present. A huge amount of detrital material of sand-sized particle is also observed. It is also found in association with glauconite (Fig. 6c) and ferruginous quartz veins. The clasts are sub-rounded with moderately sorted and cemented by carbonate material (Fig. 6d). Carbonate sometimes replaces quartz. Slump and load structures are also observed in this layer. Load structure is slight bulges and knobby bodies showing contorted laminations. Small-scale effect of slumping is observed within the layer like minor slippage along of sub-vertical beddings along sub-horizontal planes.

5.1.8 Interpretation

Presence of comparatively coarser material along with finer carbonates indicates a comparably high-energy environment. According to Dapples (1967), clay minerals with quartz and K-felspar give rise to glauconite indicating reducing environment in which small amount iron oxide may be present. Glauconite is deposited where rate of sedimentation is slow in partially restricted environment (Galliher 1935; Naik et al. 2016). Intermixing of layers of shale with clay pockets with little matrix indicate shallow marine set-up with storm erosion (Bertram 2012). Gravity, rapid deposition, difference in compaction, and density contrast between the layers play an important role for the formation of the slump and load structures (Collinson et al. 2006). Small-scale effect of slumping is caused by the down slope movement of sediment under gravity due to increase in pore pressure (Auchter et al. 2016; Panja et al. 2017). The heterolithic unit can be assumed to be deposited in intertidal set-up near to the shore (Grime and Cuthbert 1945; Bekker and Errickson 2003; Panja et al. 2019).

5.1.9 Massive whitish grey limestone facies (N-5)

This is the dominant among all facies having sharp contact with underlying and overlying unit. They have variable thickness of few metres to several metres (Fig. 7a). They are fine-grained, highly compact and very hard. Wavy, nodular, and lenticular chert units (Fig. 7b) are commonly present within the limestone. This facies is also associated with tepee structures, which are later filled by cement and sediments. The limestone is also found in association with rounded to sub-rounded pyrite grains (Fig. 7c), especially on the uppermost part of the succession. It appears opaque in transmitted light. There is evidence of iron leaching and partial replacement of micrite to sparite (Fig. 7d) along the boundary of the grains and occurrence of fenestral porosity. There is patchy distribution of clay minerals in some thin sections within this facies.

5.1.10 Interpretation

Presence of high amount of micrite and absence of any detrital input within this facies indicate deposition in low-energy environment. Presence of chert nodules and concretions are

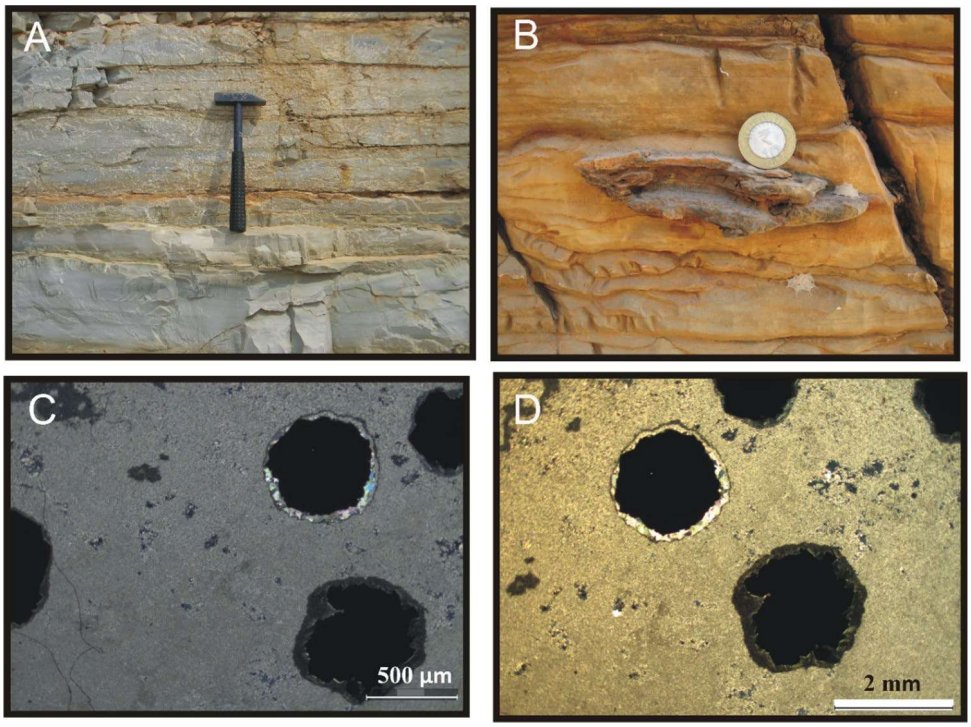

Fig.7 Massive whitish grey limestone **a** Massive white grey limestone showing macro stylolite and iron leaching. **b** Nodules and bands of chert within massive limestone. **c** Scattered crystals of pyrite within the limestone (under plane polarized light). **d** The margins of pyrite have been altered to sparite (under crossed polarized light)

probably formed during diagenesis. Decrease in the pH condition within the seawater led to the precipitation of chert nodules (Hesse 1988, 1989; Mathur et al. 2014). Presence of tepee structures points their formation in shallow carbonate saturated water where fractured and bedded marine limestone is bounded by micritic cements and undergoing diagenesis (Kendell and Warren 1987). Presence of pyrite in the upper part of this facies indicates euxinic and reducing condition. The deposition takes place through suspension and precipitation in restricted isolated basin mostly free from terrigenous influx depending on climate, sea level and tectonics (Srivastava and Singh 2017). Presence of high amount of micrite in this limestone demonstrates a low energy environment of deposition (Adachi et al. 2004). Therefore, it can be predicted that massive whitish grey limestone facies is mainly deposited in a low energy shallow subtidal environment (LaMaskin and Elrick 1997).

5.1.11 Intra-formational conglomerate facies (N-6)

This facies of Neoproterozoic Narji Limestone is narrow, laterally discontinuous facies, erratically distributed throughout the region but most commonly found in Yaganipalle area; rarely exceed 1 m lying over massive purple limestone. The facies, consisting of limestone clasts, are mostly tabular in nature (Fig. 8a) (long axes range from 12 to 30 cm), whereas few are sub-rounded to rounded pebbles/cobbles (long axes ranging from 5 to 15 cm). These lime clasts are poorly sorted with in micritic and coarse-grained siliceous matrix. This facies is devoid of any sedimentary structure except crude alignment of tabular clasts. The clasts are monomictic (Fig. 8b), and mostly composed of micrite (Fig. 8c and d) within sandstone. The lower and upper boundary is marked by undulatory surface and truncated abruptly by massive whitish grey limestone facies.

5.1.12 Interpretation

Presence of bimodal clasts within comparatively fine-grained matrix indicates that deposition is taken place in moderate to high-energy environment. The wavy bounding surface may indicate deposition from fluid-gravity flows in a standing mass of water where abrupt change in flow velocity has resulted in the deposition of conglomerate (Nemec and Steel 1984a, b; Chakrabarti and Shome 2007). This conglomerate seems to be the product of reworked sediments derived by subaqueous non-cohesive deep sub-tidal debris flow (Dasgupta et al. 2005; Chakrabarti et al. 2014) that have originated from a well-cemented platform rim by the storm currents or mild local seismic activity from the early lithified beds (Patranabis Deb et al. 2012). The bimodal size distribution indicates co-sedimentation of bedload and suspended load in fluctuating energy regime.

5.2 Karst features in the Narji limestone

The massive limestone is well karstified, present along the hill cut section of Narji. Karst features have developed under

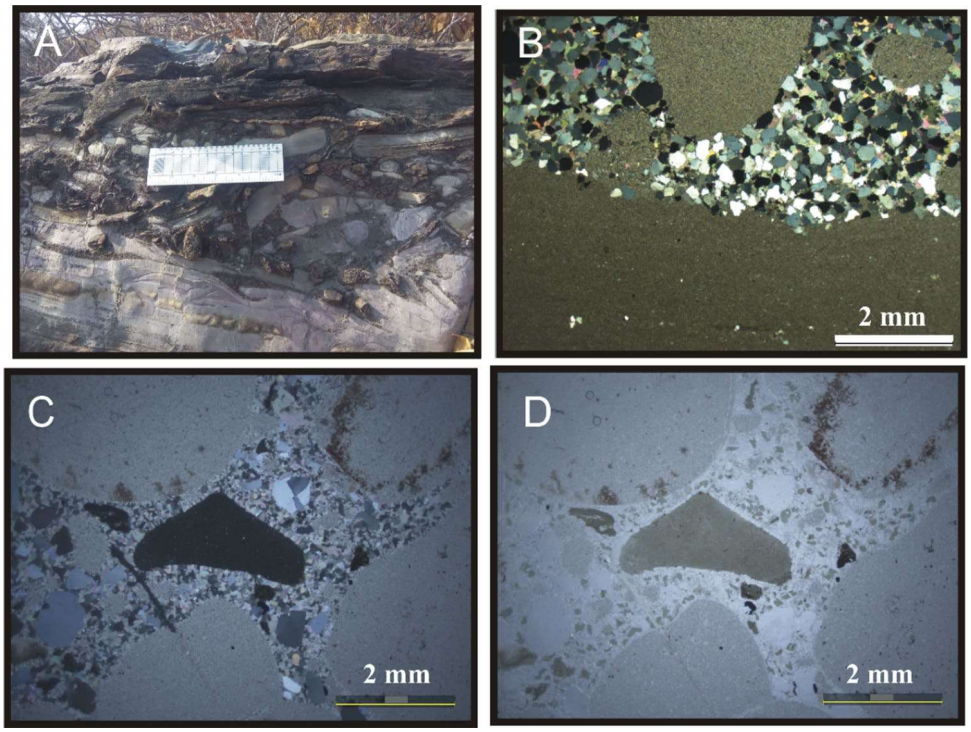

Fig. 8 Intra-formational conglomerate facie.s **a** Tabular and sub rounded micritic clasts within poorly sorted siliceous matrix mainly picked up by storm current from early lithified bed. **b** Mass flow conglomerate composed of clasts of grey micritic limestone floating within matrix of micrite and very coarse sand within Narji Limestone. **c** Intraformational conglomerate under plane polarized light. **d** Intraformational conglomerate under crossed polars.Sand grains are well cemented coarse sparitic cement and show well sorted and well rounded clast in calcareous matrix

more humid condition through dissolution processes, which were equally active due to location of carbonate aquifers in similar contexts than the Narji limestone aquifer. They have developed in a confined limestone aquifer setting where diffuse infiltration took place across quartzite and shale layers. Later, surface runoff and progressive erosion of the quartzite and shale resulted in the exposure of Narji limestone at the earth surface. It is fed by sinking streams issued from quartzite hills that diffuse infiltration through the limestone plateau. Also, because of high-intensity flashy rainfall resulted in runoff and karst formation (Dar et al. 2011).

5.3 Diagenesis of limestone

Narji limestone is well exposed in west-central part of Cuddapah Basin. It is deposited in carbonate platform mostly unmetamorphosed and undeformed marine carbonate with minor siliciclastic contamination. These limestones went through various digenetic changes which include compaction, cementation, authigenesis, micritization, neomorphism, silicification and dolomitization (Table 3). Carbonate diagenesis is primarily driven by the sediment–water interaction, which is most common within the marine, meteoric or deep burial environments. The other factors include depositional fabric of the rocks and the pressure conditions, which increases burial depth. The different carbonate component such as, micrite, cement, solution pore cement and inter-granular cement were observed within the facies. The carbonate samples are grouped into micro-sparite and micrite. Petrographic observation indicates that the limestone experienced different diagenetic alteration during the time span, which include early marine, meteoric, burial and uplift. Distinct type of diagenetic cement isopachous rim and syntaxial cement are formed in marine diagenetic stage. Dissolution, cementation (like equant mosaic, blocky, poikilotopic, syntaxial) physical compaction and neomorphism with inclusion of metasomatic fluid along the grain boundary (Fig. 9a), took place in meteoric environment. Also, physical and chemical compaction, pyritization, stylolite (Fig. 9b), large crystal of calcite (Fig. 9c), and dolomitization (Fig. 9d) are very common during burial stage of diagenesis. Finally, during the upliftment, precipitation of iron oxide cement (Fig. 9e) and silicification (Fig. 9f), took place within the vein fillings and fracture (Fig. 9g).

5.4 The geochemistry of Narji limestone

Recently, Roy et al. (2018) has worked on the geochemistry of the Narji Limestone. Eleven limestone samples which include laminated limestones, massive whitish grey limestones and quartzite-bearing massive purple limestone were analysed. Average SiO_2 (25.97), Al_2O_3/TiO_2 (16.67) and K_2O/Al_2O_3 (0.21) ratios of that study suggest clastic contamination in the Narji limestones. PAAS (Post-Archean Australian Shale) normalized REE + Y pattern of Narji limestones are showing seawater like REE + Y pattern.

The Er/Nd and Y/Ho ratios (average 0.17 and 35.68, respectively) of Narji limestones indicate the retention of

Table 3 Diagenetic sequence of the studied limestone. Straight lines indicate clearly observed processes; dash lines indicate minor processes

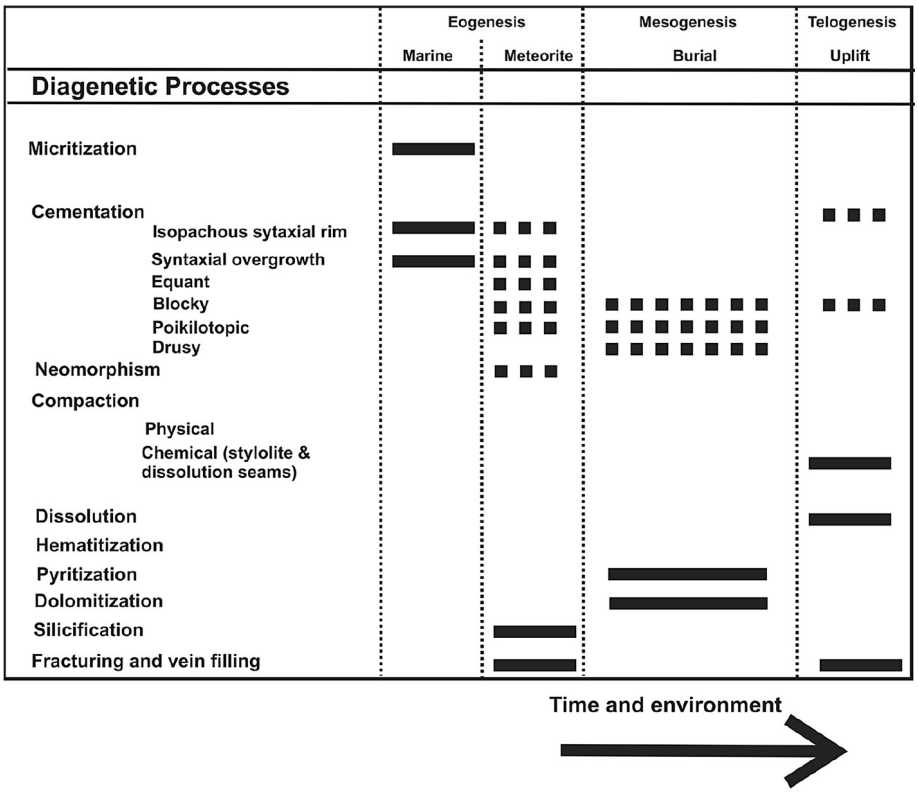

Fig. 9 Paleoenvironmental reconstruction of the Neoproterozoic NarjiFomrmation carbonate platform showing the distribution of facies

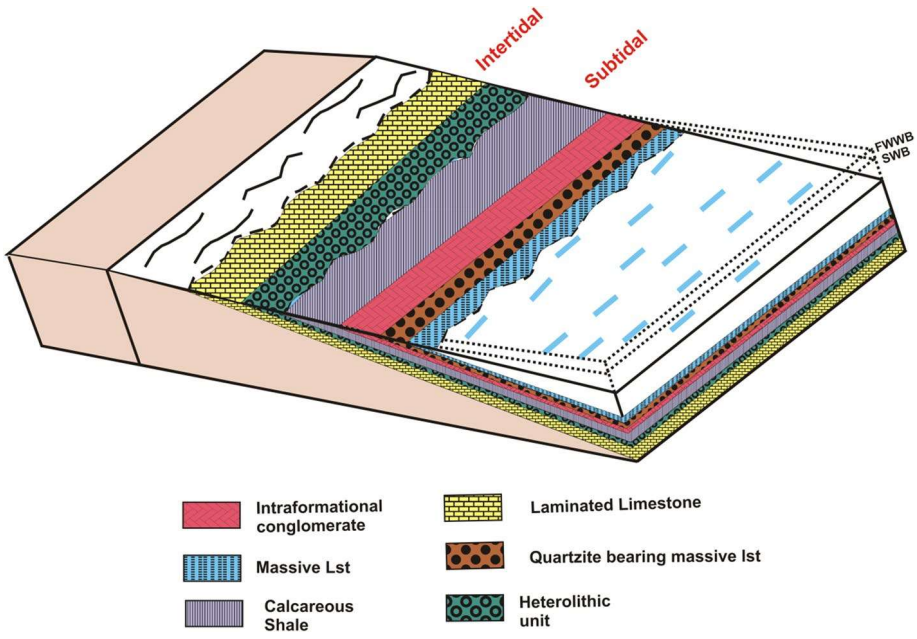

normal seawater character (De Baar et al. 1988; Abedini and Calagari 2015; Roy et al. 2018; Tobia 2018) with the signatures of terrigenous input and diagenesis process. Positive Ce anomaly, high U/Th (> 1.25) and V/(V + Ni) (> 0.5) ratios of Narji limestones clearly indicate their deposition in dysoxic to anoxic condition (Rimmer 2004; Ramos-Vázquez et al. 2017). Occurrence of pyrite also supports this, which is recorded in the Narji facies.

6 Discussion

Field observation including vertical facies variation, lateral facies transition, contacts of beds and various sedimentary structures with rest of the lithological data of the studied sections help us to depict the depositional environment of Narji Formation. A total number of six facies has been identified within the studied sections those are mainly deposited in a fluctuating condition of intertidal and subtidal environment. Broadly Narji deposits represent a transgressive phase where Narji carbonate platform is deposited on top of fan complex after attesting subsidence and then further transforming the basin into a large epicontinental sea (c.f. Patranabis Deb et al. 2012).

Identified six facies within the studied sections not only indicates hybrid depositional conditions but also signature with the features of periodic sub aerial exposure through paleokarstic layer, interpreting that deposition took place in intertidal—subtidal paleoenvironment.

he array of facies of Narji Formation may be grouped into two facies associations (FA-1) intertidal, and (FA-2) subtidal. Within the recorded facies, the laminated limestone and heterolithic facies are deposited in intertidal zone (below mean low-tide level but above fair weather wave base), the other facies which include quartzite-bearing massive purple limestone, calcareous shale, massive whitish grey limestone and intra-formational conglomerate facies are deposited in extended shallow subtidal environment (below the fair-weather wave base but above the storm wave base). The Narji formation starts with deposition in moderate to high-energy shallow subtidal environment. A list of studied facies associated with the intertidal and subtidal environment along with the probable interpretation has been listed in Table 4. A schematic profile of carbonate facies with minor clastic intercalation of Narji Formation with their depositional environment is shown in Fig. 10.

The initiation of Narji Formation begins with the deposition of quartzite bearing massive limestone probably deposited in a shallow subtidal environment over Banganapalli Formation that seems to be deposited in a fan-delta set-up (Patranabis Deb et al. 2012). These quartzites are the detrital materials derived from the underlying Banganapalli Quartzite formation. The grains are rounded to sub-rounded indicating a distal mode of transportation. The ripple marks indicate an oscillatory wave action and synaeresis cracks on the surface of the limestone indicate sub-areal exposure in near-shore to the beach setting. Presence of detrital material in the basal limestone indicates a link between the land and the carbonate platform. The heterolithic facies is deposited in intertidal tidal flat during the slack water phase of tide and/or after storm events (Panja et al. 2017). The occurrence of glauconite indicate slow rate of sedimentation during recession stage in shallow marine condition (Chattoraj et al. 2009; Srivastava and Singh 2017). The massive micrite dominated limestone seems to be deposited principally in subtidal regime within the framework of restricted carbonate platform (Patranabis Deb et al. 2012). Both tidal and storm influenced deposition of laminated limestone facies consisting of clay laminae of variable thickness. The irregular channels and fractures are formed in this limestone during early diagenesis and subaerial exposure (Srivastava and Singh 2017). Towards the end of deposition, the semi-consolidated lime mud is probably disturbed due to mild-tectonic activity resulting in intraformational conglomerate. Hummocks indicates sporadic storm event affecting the sea bed.

The horizontal distribution of these facies association, based on the distribution and genetic interpretation of facies helps to reconstruct an intertidal–subtidal depositional model (Fig. 10). This carbonate platform seems to have a low-gradient slope (Patranabis Deb et al. 2012). The shallowest of these facies in this carbonate platform is the laminated limestone and heterolithic facies of intertidal environment. The abrupt lithological transition from basal siliciclastic dominated strata to carbonate strata suggest sea-level rise or relation with regional denudation of the siliclastic source region. Overall, the Narji formation shows an aggradational pattern where majority of the intertidal facies are deposited in the lower part of the section, while majority of the subtidal facies are deposited in the upper part of the studied section with continued rise in sea level with moderate sedimentary influx and carbonate deposition that keeps pace with increased accommodation.

The Narji Formation is mainly dominated by limestone compared to the underlying Banaganaplle Quartzite and overlying Owk Shales of Kurnool Basin. This thick deposition of limestone is mainly due to chemical precipitation of

Table 4 Summarized table of the facies associations with their constituent facies and depositional environment, recognized in the studied sections of the Narji Formation, Cuddapah Basin

Facies associations	Constituent facies code	Depositional environment
FA-1	laminated limestone and heterolithic facies	Intertidal
FA-2	quartzite bearing massive purple limestone, intra-formational conglomerate, massive whitish grey limestone and calcareous shale facies	Subtidal

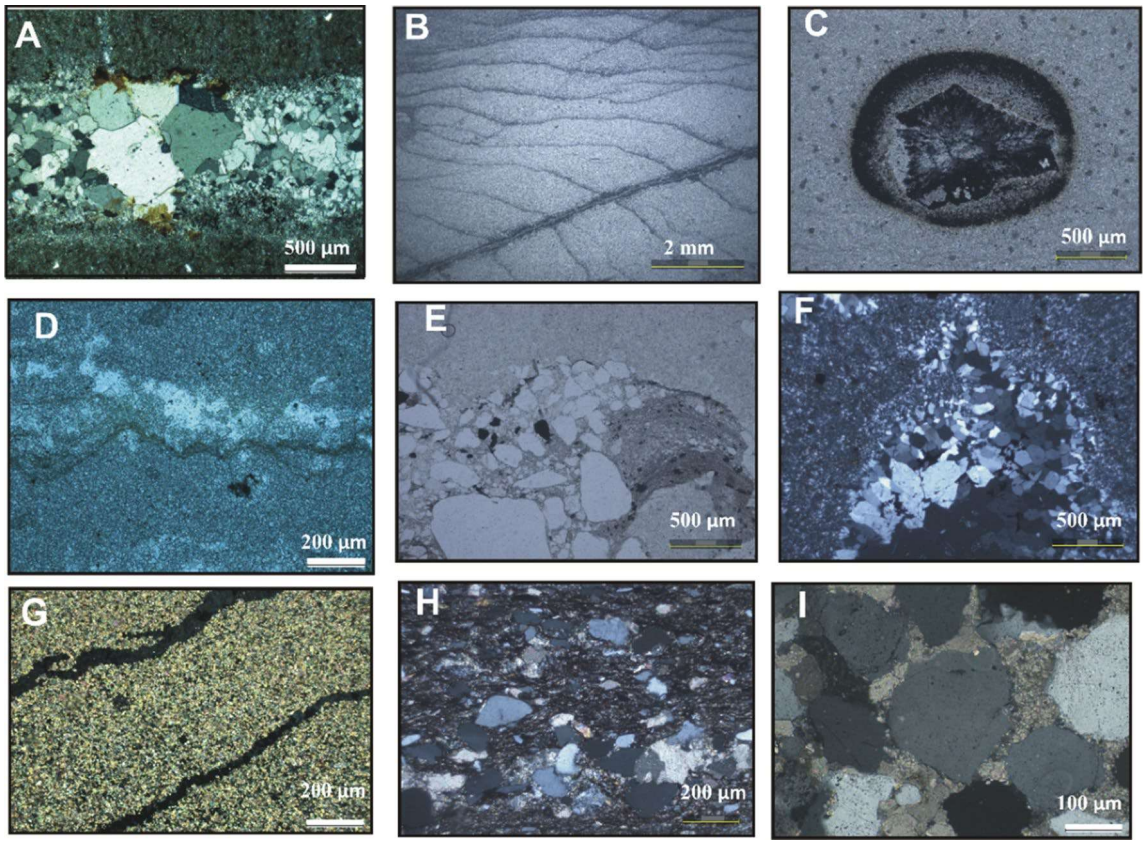

Fig. 10 Diagenesis in Narji Limestone. **a** Presence of altered neomorphic spar due to metasomatism along thegrainboundary. **b** Stylolite within carbonate rock. **c** Growth of large grain of calcite within massive micrite. **d** Growth of dolomite crystals towards fenestral porosity within micritic matrix of Narji Limestone. **e** Late stage of calcite cementation marked with the precipitation of ferroan calcite within pore spaces. **f** Silica replacement within Narji limestone during later stage of diagenesis. **g** Compaction producing fracture fabric in rocks. **h** Section showing crude schistosity and wrapping around detrital grains. **i** Authigenic overgrowth around the detrital quartz

carbonate into an intertidal–subtidal platformal depositional environment.

Formation of the supercontinent Rodinia took place at the end of Mesoproterozoic and beginning of the Neoproterozoic (Rogers and Santosh 2009). According to some authors Columbia may have converted to Rodinia without true dispersal (Piper 2013) and configuration of Pre-Gondwana continents. It is more correlated with the upper Riphean age (1000–650 M.A) of Lakhanda and Uy Group, and the Vendian Yocloma Group (Khudoley et al. 2001) occurring at the eastern margin of Siberian platform. Kurnool Formation lithology is deposited along with other coeval basin-fills around the globe during the formation of Rodinia. Hence, it is very interesting if we compare the Narji Formation lithology with other coeval successions during the critical time of formation of Rodinia.

The Jagdalpur Formation of Indravati Group, India, can be compared with Narji Formation as the depositional age of this formation is almost 700–1100 Ma (Mukherjee et al. 2012) which is very much similar with the depositional age of the Narji Formation. The Jagdalpur Formation is dominated by limestone with lesser amount of shale and this is very much similar with the Narji Formation. Development of stromatolites is well recorded in the upper part of the Jagdalpur Formation. However, occurrence of stromatolites is not reported in Narji Formation. This may be due to the anoxic environment prevailing during the deposition of the Narji Formation lithology (Roy et al. 2018).

Similarly, the Shahabad and Katamdevarahalli Formation of Bhima basin, India, are age equivalent with the Narji Formation. Shahabad and Katamdevarahalli Formation are dominated with massive, flaggy limestones with minor clastic inputs, pyrite and chert nodules. The succession is very much similar with the Narji Formation rocks and is inferred to be deposited in a shallow marine carbonate platform. Roy et al. (2018) have already performed a geochemical comparison between Bhima limestones and Narji limestones, which showed similar depositional conditions for both the formations. Hence, it may be concluded that depositional set-up of the limestone dominated formations during this particular time period is almost identical with some local variation in oxic/anoxic

condition which further leads/perturbs the development of algal bodies like stromatolites.

Globally, there are some reports of coeval successions of Narji Formation. Within these, the early Neoproterozoic Beck Spring Dolomite of California, USA (Tucker 1982) is very much identical with the Narji Formation. Both the formations deposited in a carbonate platform with similar type of marine diagenetic history. Beck Spring Dolomite is dominantly consisting of carbonate which is precipitated from anoxic, ferruginous seawater. Therefore, the depositional environment is also similar for both the formations. Facies analysis with recorded sedimentary structures depict that the Beck Spring Dolomite is deposited in a shallow subtidal to upper intertidal marine environments (Shafer 1983; Tucker 1983; Marian and Osborne 1992; Harwood and Sumner 2012) similar to the Narji Formation.

Comparing with these all formations, it can be attributed that they are the ancient analogues of Narji Formations. Hence, we can conclude that all the coeval successions of Narji Formation rocks throughout the globe indicate a similar type of depositional pattern during this time interval (early Neo-proterozoic) especially during the breaking and amalgamation of Rodinia.

7 Conclusion

The study of the facies association within the Narji Formation lead to the understanding of Cuddapah Basin's sedimentation during Neoproterozoic time period, which can be conclusive as below.

For detailed sedimentological investigation within the Narji Formation, three sections were studied. The first section is along the road cut section (A) (15°18′45.00″ N, 78°07′35.76″ E) of Patapadu-Yaganti hills, located around 11 km from the town of Banaganapalle in Kurnool District. The second section is around Betamcherla hills (B) (15°25′18.49″ N, 78°05′6.20″ E) and the third section is the Kottala hills (C) (15°27′36.68″ N, 78°08′34.30″ E).

Lithologically of Narji Formation is mainly dominated by limestone with minor amount of shale. Sedimentological facies analysis from the study area of the Narji Formation indicates occurrence of six different lithofacies, namely, quartzite bearing massive purple limestone, laminated limestone, calcareous shale, heterolithic facies, massive whitish grey limestone and intra-formational conglomerate are delineated in the study area. The cyclic repetition of facies indicates short-term alternate marine transgression and regression together with shallow marine, tidal flat to comparatively deep burial (intertidal to subtidal) depositional environment. This depositional environment provides the mixed influence of waves and tides, episodic emergence and subsidence, intermittent sheet flood, and storm-dominated depositional processes. A reducing condition is also suggested during the sedimentation, based on the presence of pyrite granules and glauconite and by the geochemical analysis of the sediments of Narji Formation. From the geochemistry point of view, it is also clear that Narji deposited in dysoxic/anoxic environment. Based on depositional environment the array of facies of Narji Formation are further grouped into two facies associations (FA-1) intertidal and (FA-2) subtidal.

Based on facies association, related sedimentary structures, and limited geochemical analysis of the carbonates, it can be concluded that the deposition of the Narji Formation, Cuddapah Basin, sediments mainly takes place in a carbonate dominated intertidal–subtidal environment with reducing dysoxic/anoxic condition. Comparative study of the Narji Formation with coeval successions throughout the globe shows an almost similar type of depositional regime during early Neoproterozoic time, especially during the breaking and amalgamation of Rodinia.

Acknowledgements The authors are grateful to the Department of Science and Technology, Government of India for financial support vide PURSE (Phase-II) program (No. F4/SC/20/15) and State Fellowship of West Bengal Government. Sincere thanks are also being accorded to Jadavpur University, Kolkata for providing infrastructural support. The second author is also grateful to Late Dr. P.K. Dasgupta, Emeritus Professor of Geology, University of Calcutta for introducing him to the Cuddapah Basin and sharing his experience and insights about the rocks.

Compliance with ethical standards

Conflict of interest On behalf of all authors, the corresponding author states that there is no conflict of interest.

References

Abedini, A., & Calagari, A. A. (2015). Rare earth element geochemistry of the Upper Permian limestone: the Kanigorgeh mining district, NW Iran. *Turkish Journal of Earth Sciences, 24,* 365–382.

Adachi, N., Ezaki, Y., & Liu, J. B. (2004). The fabrics and origins of peloids immediately after the end-Permian extinction, Guizhou Province, South China. *Sedimentary Geology, 164*(1–2), 161–178.

Ahmad, A. H. M., Irshad, R., & Bhat, G. M. (2015). Facies and diagenetic evolution of the Bathonian-Oxfordian mixed siliciclastic-carbonate sediments of the Habo Dome, Kachchh Basin, India. *Volumina Jurassica, XII, I*(1), 83–104.

Ahmad, F., Quasim, M. A., Ghaznavi, A. A., Khan, Z., & Ahmand, A. H. M. (2017). Depositional environment of the Fort Member of the Jurassic Jaisalmer Formation (western Rajasthan, India), as revealed from lithofacies and grain-size analysis. *Geologica Acta, 15*(3), 153–167.

Ali, C. A., & Mohammad, K. R. (2013). Microfacies and diagenesis in the Setul Limestone on Langkawi and Perlis. *Bulletin of the Geological Society of Malaysia, 59,* 59–66.

Al-Juboury, A. I., Al-Haj, A. M., & Jabbar, J. W. (2015). Facies analysis and depositional environment of gelikhana formation (Middle

Triassic) Northern Iraq. *Arabian Journal of Geosciences, 8*(7), 4765–4777.

Auchter, N. C., Romans Brian, W., & Hubbard, S. M. (2016). Influence of deposit architecture on intrastratal deformation, slope deposits of the Tres Pasos Formation, Chile. *Sedimentary Geology, 341,* 13–26.

Banerjee, R., Bahukhandi, N. K., Rahman, M., Achar, K. K., Babu Ramesh, P. V., & Umamaheswara, K. (2012). Lithostartighraphic and radiometric appraisal of deeper parts of Srisailam and Palnad sub-basins in Kottapullareddipuram-Achchammagunta-Rachchamallepaduarea, Guntur district. *Exploration and research for Atomic Minerals, 22*((special issue)), 55–69.

Bathrust, G. C. R. (1987). Diagenetically enhanced bedding in argillaceous platform limestones: stratified cementation and selective compaction. *Sedimentology, 34*(5), 749–778.

Bekker, A., & Eriksson, K. A. (2003). A Paleoproterozoic drowned carbonate platform on the southeastern margin of the Wyoming Craton: a record of the Kenorland breakup. *Precambrian Research, 120,* 327–364.

Bertram, T. (2012). Seismic and sequence stratigraphic analysis. *Regional Geology and tectonics: Principles of Geologic Analysis, 1,* 864.

Chakrabarti, G., & Shome, D. (2007). Reworked Diamictite accumulation as debris flow in aqueous medium–an example from late Paleoproterozoic basal Gulcheru Formation Cuddapah Basin India. *Himalayan Geology, 28*(1), 87–98.

Chakrabarti, G., Shome, D., Kumar, S., Stephens, G. M., III., & Kah, L. C. (2014). Carbonate platform development in a Palaeoproterozoic extensional basin, Vempalle Formation, Cuddapah Basin, India. *Journal of Asian Earth Sciences, 91,* 263–279.

Chakraborty, B. K. (2000). Precambrian geology of India—a synoptic view. *Geological Survey of India, Special Publication, 55,* 1–12.

Chakraborty, P. P., Dey, S., & Mohant, S. (2010). Proterozoic platform sequences of Peninsular India, implications towards basin evolution and supercontinent assembly. *Journal of Asian Earth Sciences, 39,* 589–607.

Chattoraj, S. L., Banerjee, S., & Saraswati, P. K. (2009). Glauconites from the Late Palaeocenee Early Eocene Naredi Formation, western Kutch and their genetic implications. *Journal of the Geological Society of India, 73,* 567–574.

Chetty, T. (2011). Tectonics of Proterozoic Cuddapah basin, Southern India: a conceptual model. *Journal of Geological Society of India, 78*(5), 446–456.

Choudhuri, A. K., Deb, G. K., Deb, S. P., Mukherjee, M. K., & Ghosh, G. (2002). The Purana Basins of Southern Cratonic Province of India—a case for Mesoproterozoic FossilRifts. *Gondwana Research, 5,* 23–33.

Collinson, J. D., Mountney, N., & Thompson, D. (2006). *Sedimentary structures* (3rd ed.). England: Terra Publishing.

Dapples, C. E. (1967). Silica as an agent in Diagenesis. *Development in sedimentology, 8*(3), 23–342.

Dar, F. A., Perrin, J., Riotte, J., Gebauer, H. D., Narayana, A. C., & Ahmed, S. (2011). Karstification in the Cuddapah Sedimentary Basin, Southern India Implications for Groundwater Resources. *Acta Carsologica, 40*(3), 457–472.

Dasgupta, P. K, Biswas, A., & Mukherjee, R. (2005). Cyclicity in Paleoproterozoic to Neoproterozoic Cuddapah Supergroup and its significance in basinal evolution in, *Mabesoone, J.M., Neuman, VH (Eds.), Cyclic Development of Sedimentary Basins*. Elsevier. 313–345.

De Baar, H. J. W., German, C. R., Elderfield, H., & Van Gaans, P. (1988). Rare earth element distributions in anoxic waters of the Cariaco Trench. *Geochimica et Cosmochimica Acta, 52,* 1203–1219.

Flugel, E. (2010). *Microfacies of carbonate rocks, analysis, interpretation and application*. Berlin: Springer.

Forte, L. L. G., & Palma, R. R. (2002). Facies, Microfacies, and diagenesis of late Calovian–early Oxfordian carbonates (La Manga Formation) in the east central Argentinean high Andes. *Carbonates and evaporates*, 17(1), 1.

Galliher, E. W. (1935). Geology of glauconite. *Bulletin of the American Association of Petroleum Geologists, 19,* 1569–1601.

Garrison, E. R., & Kennedy, W. J. (1977). Origin of solution seams and Flaser structures in Upper Cretaceous chalks of southern England. *Sedimentary Geology, 17,* 107–137.

Gopakumar, B., & Waghmare, M. (2016). Nature of occurrence of phosphatic bands in Owk Formation, Neoproterozoic Kurnool basin, Andhra Pradesh. *Journal of Geological Society of India, 88*(2), 212–221.

Grime, R., & Cuthbert, L. F. (1945). Some clay-water properties of certain clay minerals. *Journal of American Ceramic Society, 8*(3), 90–95.

Gupta, S., Vimal, R., Banerjee, R., Ramesh Babu, P. V., & Maithani, P. B. (2010). Sedimentation pattern and the depositional environment of banganapalle formation in the Southwestern Part of the Palnad Sub-Basin, Guntur District, Andhra Pradesh. *Gondwana Geological Magazine, 12,* 59–70.

Hamblin, P. A., & Walker, G. R. (1979). Storm–dominated shallow marine: The Fernie-Kooteney (Jurassic) transition, southern Rocky Mountains. *Canadian Journal of Earth Sciences, 16*(9), 1673–1690.

Harwood, C. L., & Summer, D. Y. (2012). Origins of microbial microstructures in the neoproterozoic beck spring dolomite: variations in microbial community and timing of lithification. *Journal of Sedimentary Research, 82*(9), 709–722.

Hashmie, A., Rostamnejad, A., Nikbakht, F., Ghorbanie, M., Rezaie, P., & Gholamalian, H. (2016). Depositional environments and sequence stratigraphy of the Bahram formation (middle-late Devonian) in north of Kerman, south-central Iran. *Geoscience Frontiers, 7,* 821–834.

Hersi, O., Salad, A. I. A., & Harthyl, A. A. L. (2015). Sedimentology, rhythmicity and basin-fill architecture of a carbonate ramp depositional system with intermittent terrigenous influx: The Albian Kharfot Formation of the Jeza-Qamar Basin, Dhofar, Southern Oman. *Sedimentary Geology, 331,* 114–131.

Hesse, R. (1988). Origin of chert: diagenesis of biogenic siliceous sediments. *Geoscience Canadas, 15*(3), 171–192.

Hesse, R. (1989). "Drainage system" associated with mid ocean channels and submarine yazoos: Alternative to submarine fan depositional systems. *Geology, 17*(12), 1148–1151.

Holland, T. H. (1913). Indian geological terminology. *Geological Survey of India, 6,* 204.

Kale, V. S. (1991). Constraints on the evolution of the Purana basins of Peninsular India. *Indian Journal of Geology, 38,* 231–252.

Kale, V. S., Saha, D., Patrabnis-Deb, S., Sai, V. S. S., Tripathy, V., & Pillai, S. P. (2020). Cuddapah Basin, India: A Collage of proterozoic subbasins and terranes. *Proc Indian National Science Academy., 86,* 137–166.

Kendell, G. S. T. C., & Christopher, W. J. (1987). A review of the origin and settings of tepees and their associated fabrics. *Sedimentology, 34,* 1007–1027.

Khudoley, A. K., Rainbird, R. H., Stern, R. A., Kropachev, A. P., Heaman, L. M., Zanin, A. M., et al. (2001). Sedimentary evolution of the Riphean Vendian basin of southeastern Siberia. *Precambrian Reserch, 111,* 129–163.

Knaust, D. (2002). Pinch-and-swell structures at the Middle/Upper Muschelkalk boundary (Triassic): evidence of earthquake effects (seismites) in the Germanic Basin. *International Journal of Earth Sciences, 91,* 291–303.

Komatsu, T., Naruse, H., Shigeta, Y., Takashima, R., Maekawa, T., Dang, H. T., et al. (2014). Lower Triassic mixed carbonate and siliciclastic setting with Smithian-Spathian anoxic to dysoxic

facies, An Chau basin, northeastern Vietnam. *Sedimentary Geology, 300,* 28–48.

LaMaskin, T. A., & Elrick, M. (1997). *Sequence stratigraphy of the Middle to Upper Devonian Guilmette Formation, southern Egan and Schell Creek ranges* (p. 321). Nevada: Special Paper of the Geological Society of America.

Marian, M.L., & Osborne, R.H. (1992). Petrology, petrochemistry, and stromatolites of the middle to late Proterozoic Beck Spring Dolomite, eastern Mojave Desert, California: *Canadian Journal of Earth Sciences*, 29, 2595–2609.

Mathur, R., Udai, R., & Balaram, V. (2014). Petrographic characteristics of the Proterozoic Vempalle carbonates, Cuddapah Basin, India and their implications. *Journal of the Geological Society of India, 84,* 267–280.

Meijerink, A. M. J., Rao, D. P., & Rupke, J. (1984). Stratigraphic and structural development of the Precambrian Cuddapah Basin. S.E India. *Precambrian Research, 26,* 57–104.

Mitra, R., Chakrabarti, G., & Shome, D. (2018). Geochemistry of the Palaeo-Mesoproterozoic Tadpatri shales, Cuddapah Basin, India, implications on provenance, paleoweathering and paleoredox conditions. *Acta Geochimica, 37*(5), 715–733.

Mukherjee, A., Bickford, M. E., Hietpas, J., Schieber, J., & Basu, A. (2012). Implications of a newly dated ca. 1000 Ma rhyolitic tuff in the Indravati basin, Bastar craton India. *Journal of Geology120,* 477–485.

Nagaraja Rao, B. K., Rajurkar, S.T., Ramalingaswami, G., & Ravindra, B., B. (1987). Stratigraphy, structure and evolution of Cuddapah Basin. In, Radhakrishna, B.P. (Ed.) Purana Basins of Peninsular India. *Geol. Soc. India Bangalore Bull*, 6, 33−86.

Naik Gope, V., Suresh, U. K., & Sunil, K. (2016). Diagenesis of Glauconite Bearing Quartzite of the Cuddapah Basin, Andhra Pradesh, India. *International Journal of Geology and Earth Sciences,* 4.

Nemec, W., & Steel, R.J. (1984). Alluvial and coastal conglomerates: their significant features and some comments on gravelly mass-flow deposits. In: Koster, E.H., Steel, R.J. (Eds.), Sedimentology of Gravels and Conglomerates. *Mem Can. Soc. Pet. Geol.,* l, 10, 1–31.

Nemec, W., & Steel, R. J. (1984). Alluvial and coastal conglomerates: their significant features and some components on gravelly mass-flow deposits. *Canadian Society of Petroleum Geologists, Memoir, 10,* 1–31.

Panja, M., Chakrabarti, G., & Shome, D. (2017). Depositional system of an open coast Tidal flat—an example from Paleoproterozoic Vempalle Formation, Cuddapah Basin, India. *Carpathanian Journal of Earth and Environment Sciences, 12*(1), 269–282.

Panja, M., Chakrabarti, G., & Shome, D. (2019). Earthquake induced soft sediment deformation structures in the Paleoproterozoic Vempalle Formation (Cuddapah basin, India). *Carbonates and Evaporites, 34*(3), 491–505.

Patranabis-Deb, S. (2005). Tidal shelf sedimentation in the Neoproterozoic Chattisgarh succession of central India. *Journal of Earth System Science, 114,* 211–226.

Patranabis-Deb, S., Saha, D., & Tripathy, V. (2012). Basin stratigraphy, sea-level fluctuations and their global tectonic connections—evidence from the Proterozoic Cuddapah Basin. *Geological Journal, 47,* 263–283.

Perrin, J., & Dar, F. A. (2011). Karstification in the Cuddapah Sedimentary Basin, Southern India: Implications for Groundwater Resources. *Acta Carsologica, 40*(3), 457–472.

Piper, J. D. A. (2013). A planetary perspective on Earth evolution: Lid Tectonics before Plate Tectonics. *Tectonophysics, 589,* 44–56.

Ramakrishnan, M., & Vaidyanadhan, R. (2008). Geology of India, vols. 1 and 2. *Geological Society of India. Text Book Series*, 994 p.

Ramos-Vázquez, M. A., Armstrong-Altrin, J. S., Rosales-Hoz, L., Machain-Castillo, M. L., & Carranza-Edwards, A. (2017). Geochemistry of deep-sea sediments in two cores retrieved at the mouth of the Coatzacoalcos River delta, western Gulf of Mexico Mexico. *Arabian Journal of Geosciences, 10*(6), 148.

Rimmer, S. M. (2004). Geochemical paleoredox indicators in Devonian-Mississippian black shales, Central Appalachian Basin (USA). *Chemical Geology, 206,* 373–391.

Rogers, J. J. W., & Santosh, M. (2009). Tectonics and surface effects of the supercontinent Columbia. *Gondwana Research, 15,* 373–380.

Roy, A., Chakrabarti, G., & Shome, D. (2018). Geochemistry of the Neoproterozoic Narji limestone, Cuddapah Basin, Andhra Pradesh, India: implication on palaeoenvironment. *Arabian Journal of Geosciences, 11,* 784.

Saha, D., & Chakraborty, S. (2003). Deformation pattern in the Kurnool and Nallamalai Group in the northeastern part (Palnad area) of the Cuddapah Basin, South India and its implication on Rodinia/Gondwana. *Gondwana Research, 6*(4), 573–583.

Saha, D., Ghosh, G., Chakraborty, A. K., & Chakraborty, S. (2009). Comparable Neoproterozoic sedimentary sequences in Palnad and Kurnool subbasins and their palaeogeographic and tectonic implications. *Journal of the Geological Society of India, 78,* 175–192.

Saha, D., & Tripathy, V. (2012). Paleoproterozoic sedimentation in the CuddapahBasin, South India and regional tectonics: a review. *Geological Society, London, Special Publication, 365*(1), 161–184.

Shafer, D.C. (1983). Petrology and depositional environments of the Beck Spring Dolomite, southern Death Valley region [M.S. Thesis]: Davis, University of California, 195 p.

Singh, A. P., & Mishra, D. C. (2002). Tectono sedimentary evolution of Cuddapah Basin and Eastern Ghat mobile belt (India) as Proterozoic Collision, gravity, seismic and geodynamic Constrains. *Journal of Geodynamic, 33,* 249–267.

Spence, G. H., Le Heron, D. P., & Fairchild, I. J. (2016). Sedimentological perspectives on climatic, atmospheric and environmental change in the Neoproterozoic Era. *Sedimentology, 63*(2), 253–306.

Srivastava, V. K., & Singh, B. P. (2017). Facies analysis and depositional environment of the early Eocene Naredi Formation (Nareda locality) Kutch, Western India. *Carbonate Evaporites, 32,* 279–293.

Tobia, F. H. (2018). Stable isotope and rare earth element geochemistry of the Baluti carbonates (Upper Triassic), Northern Iraq. *Geosciences Journal, 22,* 975–987.

Tucker, M. E. (1982). Precambrian dolomites: petrographic and isotopic evidence that they differ from Phanerozoic dolomites. *Geology, 10,* 7–12.

Tucker, M. E. (1983). Diagenesis, geochemistry, and origin of a Precambrian dolomite: the Beck Spring Dolomite of eastern California. *Journal of Sedimentary Petrology, 53,* 1097–1119.

Young, G. M. (2013). Secular changes at the Earth's surface; evidence from paleosols, some sedimentary rocks, and paleoclimatic perturbations of the Proterozoic Eon. *Gondwana Research, 24*(2), 453–467.

Study of Micro-Stylolite based on Geometry and Bedding Relationship Pattern in Neo-Proterozoic Narji Limestone from Betamcherla – BanganapalleArea of Kurnool Sub-Basin, Andhra Pradesh, South India

Adrika Roy* & Gopal Chakrabarti[2] & Debasish Shome[1]
[1]Department of Geological Sciences, Jadavpur University, Kolkata 700032, India
[2] Education Directorate, Government of West Bengal, Kolkata 700091, India

Received: May 14, 2018 Accepted: June 23, 2018

ABSTRACT *Microstyololites within the Neo-Proterozoic Narji Limestone inBetamcherla–Banganapallearea are very well developed. They commonly occur within fine grained micritic limestone and mostly contain clayey material within them. Different types of microstylolites are recorded and described on the basis of the geometry and the bedding plane relationship. On the basis of the geometry the microstylolites are wavy and simple suture in nature.Whereas based on their bedding plane relationship they are horizontal, inclined as well as vertical in attitude. Their relationship with the host rock clearlyindicates that they are formed from the action of pressure solution process during lithification and diagenesis.*

Keywords: *Kurnool sub-basin,Narji,Pressure solution,microstylolite.*

1. INTRODUCTION

Stylolites have been derived from Greek word means stylos or pillar; and lithos means stone. These are zigzag surfaces within a rock mass at which mineral material within the rock has been removed by pressure dissolution due to diagenesis and/or tectonic features (Kerrich, 1978; Robin, 1978 and others). This results in a process that decreases the total volume of rock. They are recognized from there irregular planes of discontinuity between two rock units in the shape of columns and pyramids. The two rock units appear to be interlocked or mutually interpenetrating. Well-developed macro and micro stylolites are seen within in the carbonate rocks of Kurnool group, Andhra Pradesh. Earlier Vijayam and Reddy (1973), Malur and Nagendra (1988) and Madesh et al (2012) reported microstylolites from Precambrian carbonate rocks. The occurrence of macro and micro stylolite in Kurnool group was reported first by Vijayam and Reddy (1973). Stylolite study from Narji Limestone was carried by Natarajan and Rajagopalan Nair (1977) and Harish (1995). Our present work mainly focuses on the the classification and origin of microstylolites within the Narji Limestone reflecting the probable effect on sedimentological, diagenetic process and tectonic influence or disturbance in the area.

2. LOCATION OF THE STUDY AREA

LithostratigraphicallyCuddapah Basin is subdivided into older CuddapahSupergroup and relatively younger Kurnool Group (Table. 1). The Kurnool Group of rocks is well exposed in two sub basin namely the Kurnool sub basin in the west central part and the Palnad sub basin in the north eastern part of the Cuddapah. The two sub basins are separated by the distance of 75km, with the Srisailam Quartzite covering the gap. The NarjiLimestone within the Kurnool Sub-basin was deposited conformably on top of the clastic rock of the BanganapalleFormation.

Table 1. Stratigraphy of the Cuddapah Basin (after NagarajaRao et al., 1987)

GROUP	FORMATION	LITHOLOGY	AGE
KURNOOL	Nandyal (50-100 m)	Shale/ Limestone	Neoproterozoic
	Koilkuntala (15-50 m)	Limestone with shale	
	Paniam (10-35 m)	Quartzite	
	Owk (10-15 m)	Shale	
	Narji (100-200 m)	Massive Limestone, Flaggy Limestone	
	Banganapalli (10-15 m)	Quartzite with conglomerate	

------Unconformity------				
CUDDAPAH SUPERGROUP		Srisailam (300 m)	Pebbly grit, Quartzite, HeterolithicShales and stone	Mesoproterozoic
	------Unconformity------			
	NALLAMALAI	Cumbum (~ Pullampet Shale) (2000 m)	Shale, Dolomitic limestone, Quartzite	
		Bairenkonda (~ Nagari Quartzite) (5500 m)	Pebbly grit, Quartzite, HeterolithicShales and stone	
	------Unconformity------			
	CHITRAVATI	Gandikota (300 m)	Quartzite, Pebble beds	Mesoproterozoic
		Tadpatri (4600 m)	Shale, Quartzite, Stromatolitic dolomite with mafic flows, Sills and Dykes	
		Pulivendla (1-75 m)	Conglomerate, Quartzite	
	------Unconformity------			
	PAPAGHNI	Vempalle (1900m)	Stromatolitic dolomite, Shale, Basic flows and intrusive	Palaeoproterozoic
		Gulcheru (30-210 m)	Conglomerate, Feldspathic sandstone and quartzite	
------Unconformity------				
DHARWAR CRATON				Archean

The three sections were chosen for investigation. The first sections is along the road cut section (15°18'45.00"N, 78°07'35.76"E) of Patapadu-Yaganti hills located around 11Km from the town of Banaganapalle in Kurnool District. The second section is around Betamcherla hills (15°25'18.49'' N, 78°05'6.20'' E) and the third section is the Kottala hills (15°27'36.68'' N, 78°08'34.30'' E). These sections are located about 20km from the town Banaganapalle in Kurnool District, Andhra Pradesh. The micritedominatedNarji Formation starts with quartzite bearing massive purple limestone followed by siliceous pink and purple laminated limestone with thin lenticular lenses of gritty ferruginous sandstone (Patranabis Deb et al; 2012). These siliceous rich layers are mostly dominated towards the base of the formation (Patranabis Deb et al; 2012).These layers grade into pyrite and chert bearing massive whitish-grey limestone along with alternating laminated limestone layer. Thin and discrete beds of intraformational conglomerate occur within the Narji limestone (Patranabis Deb et al; 2012). The massive and the laminated units show symmetrical distribution throughout the sections till it show a gradational contact with the yellowish Owk shale towards the top. The layers are mostly separated by paleokarstic surfaces.

3. CLASSIFICATION OF MICROSTYLOLITES

Microstylolites occurring in the Narji Limestone are mostly parallel, inclined and vertical with respect to bedding plane. They are identified by their irregular nature. Their penetrative columns contains insoluble residue within them. These residues sometimes vary within their individual crest and trough regions. These structures have varied in

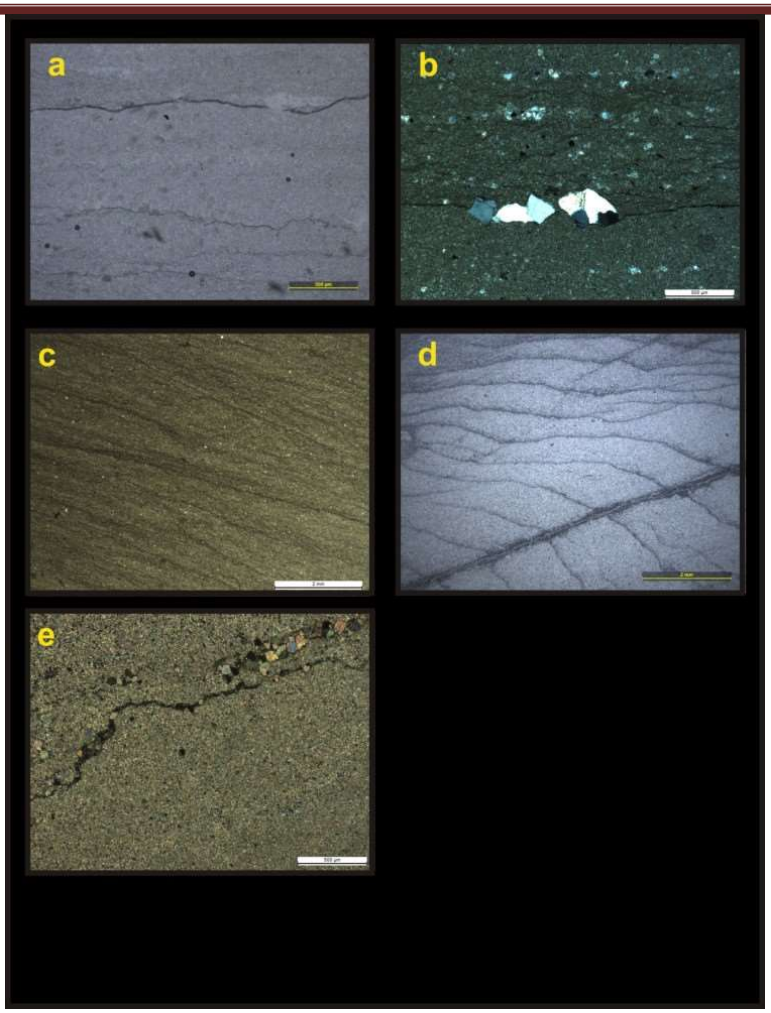

Fig. 1.Geometrical classification of microstylolites;aand**b**: stylolite of simple wavy parallel type-smooth and parallel to the bedding; **c**and**d**: stylolite of simple wavy non- parallel type-non parallel and interconnecting with each other; **e**: stylolite of suture type-simple suture likes projections on both sides.
amplitude, wavelength and shape result in different geometric pattern. Their classification is based on their (a) Geometrical classification and (b) attitude with respect to bedding.

(a) Geometrical classification:

Earlier geometric classification was given by Park and Schot (1968) into six different types. Malur et al., (1988 and 1992) classified microstylolites from Bhima Basin based on the pure geometry and bedding orientation. The microstylolite patterns within the Narji Limestone are mostly wavy while some are simple suture types that are both parallel and non-parallel types (Fig.1). Wavy microstylolites have small and gentle undulation with small amplitude (Malur and Nagendra 1988, Madesh et al 2012). Their crest and trough are mostly smooth, gentle and wavy (Fig.1 a-d). They run parallel or non-parallel to the bedding surface. The non-parallel types are mostly interconnecting and branching types. Mostly found in layered sedimentary rocks like carbonates. The residual clay materials are irregularly distributed within the stylolites (Fig.1 a-d). The simple suture type resemble like ammonoid suture pattern (Fig. 1e). Their anticline and synclinal patter of suture are symmetrically distributed. They are mostly non-parallel and asymmetrically distributed. They have interlocking project ions in either side. They are formed due to differential pressure solution phenomena forming suture of various amplitude (Fig. 1e).They mostly occur in quartz bearing limestone.

(b) Attitude with respect to bedding*:*

With respect to the bedding plane they are generally horizontal, inclined and vertical in attitude. Horizontal microstylolites (Fig. 2a) are developed parallel to bedding plane and it is common in almost all carbonate rocks. Vertical microstylolites are formed perpendicular to the bedding (Fig. 2b), and generally found along fracture planes. They are formed when the pressure act at right angle to the bedding. Inclined or oblique types have different inclination with respect to bedding. The rocks which they occur may be affected and unaffected by structural activity.

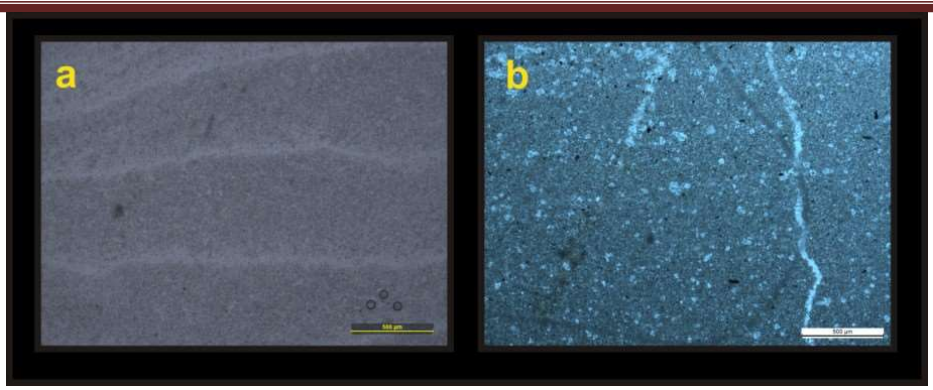

Fig. 2: Attitude with respect to bedding a: horizontal microstylolite parallel to bedding plane; **b**: Vertical microstylolitesareformed perpendicular to the bedding;

4. ORIGIN OF MICROSTYLOLITES

The three different theories based on the origin and formation of stylolite have been proposed by Wagner (1913) and Stockdale (1922) which is based on solution pressure theory, Rothpletz (1900) based on contraction pressure and finally by Rothpletz (1900), Shaub (1939), Marsh (1968), and Prokopovich's (1952) based on subaqueous solution theory.

During our study it is observed that some microstylolites are initially inclined which branches later (Fig.3a). It is caused by action of two successive differential pressure phenomena. It may be due to disturbance acting in different direction forming microstylolite of low amplitude. Some thin sections indicate diagenesis like presence of dolomite grains (Fig.3b) while other indicates micro faulting. These micro faults lack significant continuity within the host rocks (Fig.3c). Along stylolite, symbol of pre-lithification, pressure solution during compaction are identified. All these are well supported by the presence of residual seam having insoluble residual material along stylolite surface. Initially there is deposition of sediment which may be associated with water. The fine grained carbonate sediment mostly occurs with pyrite and clay. Due to dynamic

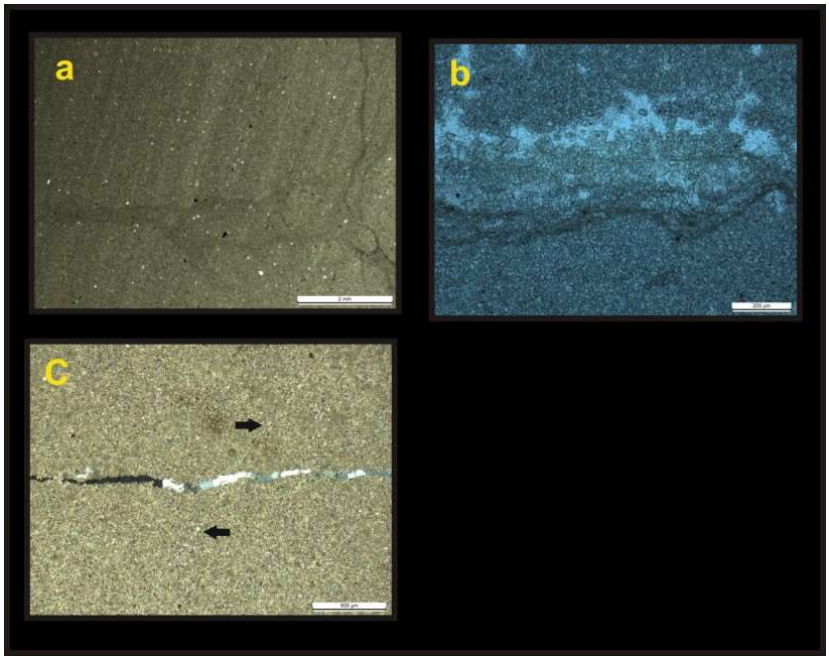

Fig. 3: a: stylolite of interconnecting branching type; **b:** presence of dolomite grains along the stylolite, **c:** micro faultwihin host rock

pressure effect during lithification the stylolite layers becomes mostly parallel or horizontal with respect to bedding plane. The pressure is generated by overlying rocks or due to tectonic influence (Madesh et al; 2012) during compaction and dewatering of sediments. During this process there is volume contraction and differential pressure due to loss of water. The soluble materials are pressed out of the rocks and the insoluble materials at the contacts remain intact as relicts forming stylolite seams.

5. MICROSTYLOLITE AND HOST ROCK RELATIONSHIP

The Narji limestone are mostly fine grained contains both micro and macro stylolites. Other accessory minerals are quartz and pyrite. The quartz grains are mostly subhedral and euhedral. The microstylolites have their distinct geometric forms and structure. Insoluble minerals, like clays, pyrite and calcite, occur within the stylolites and are fairly visible in some samples. The stylolite seams can be easily distinguishable from the material and the composition of the host rock which it contains. Due to cryptocrystalline nature of the carbonate rocks the identification of individual minerals under the petrological microscope is very difficult. The stylolites give evidence of probable disturbance in the area.

6. CONCLUSION

The microstylolites within Narjilimestones help to depict the sedimentological, diagenetic process and tectonic disturbance within the study area. The wavy and simple suture types reveal many features which can be explained by the pressure solution theories. Presence of dolomite grains along the microstylolite indicates diagenesis. The pre lithification process was identified by the presence of residual seam, insoluble material, micro faults and suture type stylolites. The presence of residual clay capping in the stylolite indicate the solution pressure theory or origin .The horizontal, vertical and inclined stylolite evidence from the successive pressure system indicate local disturbance and tectonic activity in this area with varied direction of action of these forces.

Acknowledgements:

The first author is thankful to the UGC for the fellowship vide UGC Non-Net scheme. The authors are also grateful to Department of Science and Technology, Government of India for financial support vide PURSE (Phase-II) program (No. F4/SC/20/15). Sincere thanks are also being accorded to Jadavpur University, Kolkata for providing infrastructural support.

References

1. Harish, V. (1995).Unpublished Ph.D thesis, Univ.of Mysore,
2. Kerrich, R.(1978).An historical review and synthesis of research on pressure solution.Zentralbl. Geol. Palaeontol., Teil I, 5/6:512-550.
3. Madesh, P., LokeshBharani, P. and Baby Shwetha, S. (2012). Study of Microstylolite from Carbonate Rocks of Kurnool Group,Andhra Pradesh, South India. Indian Journal of applied Research, 1: 2.
4. Malur, M.N. and Nagendra, R. (1988).Microstylolite in late Precambrian carbonate rocks, Karnataka, South India. Jour. Geol. Soc. India, 32: 430-432.
5. Malur, M,N., Rudraiah, M. and Nagendra, R. (1992).Microstylolites from Kurkunta Formation, Bhima Group (Eastern Part), Karnataka, Southern India.Jour. Mys. Univ., 32(B): 188-190.
6. Marsh, O.C. (1868).In the origin of the so called lignites or epsomites.Amer. Assoc. Adv. Sci. Proc., 16: 135-143.
7. Natarajan, V. and Rajagopalan Nair, S. (1977).Stylolites in the NarjiLimestones from Jaggayyapeta area, Krishna district, Andhra Pradesh. Ind. Miner., 30(1): 50-54.
8. Park, W.C. and Schot, E.H.(1968).Stylolites; their nature and origin.Jour.Sed.Petrol., 38(1): 175-191.
9. Patranabis-Deb, S., Saha, D. and Tripathy, V. (2012). Basin stratigraphy, sea-level fluctuations and their global tectonic connections—evidence from the Proterozoic Cuddapah Basin. Geological Journal, 47: 263–283.
10. Prokopovich, N. (1952).The origin of stylolites.Jour. Sed. Pet., 22: 212-220.
11. Robin, P.Y.F. (1978).Pressure solution at grain-to-grain contacts.Geochim.Cosmochim.Acta, 42: 1383-1389.
12. Rothpletz,A.,(1900). UbereigenthumlicheDeformationenJurassicher Ammoniten durch Drucksuturen and derenBeziehungenZu den Stylolithen. Sitz-Ber.Math.- Phys. Kl. Bayer Akad. Wiss., 30: 3-32.
13. Shaub, B.M. (1939).The origin of stylolites.Jour. Sed. Petrol., 9: 47-61.
14. Stockdale, P.B. (1922).Stylolites; the nature and origin, Indiana Univ. Studies, 11: 1-97.
15. Vijayam, B.E. and Reddy, G.V. (1973).Microstylolites in NarjiLimestones from Kurnool district, Andhra Pradesh. Jour.Ind. Acad. Geosc.,16: 2.
16. Wagner, G. (1913).Stylolithen and Drucksuturen, Geol. Palaeont. Abhandlungen, 11: 101-128.